

281



EANDC (E) 115 "U"

INDC-281

INDC(EUR)-2/E

PROGRESS REPORT

ON NUCLEAR DATA RESEARCH IN THE EURATOM COMMUNITY

for the period January 1 to December 31, 1968

Submitted by the Joint Euratom Nuclear Data
and Reactor Physics Committee

(Secretariat : Central Bureau for Nuclear
Measurements, Euratom, Geel, Belgium)

March 1968

EUROPEAN AMERICAN NUCLEAR DATA COMMITTEE

EANDC (E) 115 "U"

PROGRESS REPORT
ON NUCLEAR DATA RESEARCH IN THE EURATOM COMMUNITY
for the period January 1 to December 31, 1968

Submitted by the Joint Euratom Nuclear Data
and Reactor Physics Committee

(Secretariat : Central Bureau for Nuclear
Measurements, Euratom, Geel, Belgium)

March 1968

EUROPEAN AMERICAN NUCLEAR DATA COMMITTEE

LEGAL NOTICE :

The information contained in this progress report has a preliminary character.

No data contained in this report may be used without the permission of the responsible authorities.

It is suggested that experimentators should be contacted in this respect.

I N D E X

I.	Kernforschungszentrum Karlsruhe (Germany) Institut für Angewandte Kernphysik	1
II.	Kernforschungszentrum Karlsruhe (Germany) Institut für Neutronenphysik und Reaktortechnik	18
III.	Physikalisches Institut der Universität Giessen und Physik-Department, Technische Hochschule München (Germany)	21
IV.	Physik-Department, Technische Hochschule München (Germany)	30
V.	Physik-Department der Th. München und Institut für Festkörper- und Neutronenphysik der Kernforschungs- Anlage Jülich	43
VI.	Institut für Festkörper- und Neutronenphysik, KFA - Jülich	45
VII.	Institut für Kernphysik, University of Frankfurt/ Main (Germany)	63
VIII.	Physikalisches Staatsinstitut, I. Institut für Experimentalphysik, Hamburg (Germany)	66
IX.	Institut für Reine und Angewandte Kernphysik der Universität Kiel (IKK), Geesthacht	70
X.	Laboratorio di Fisica Nucleare Applicata, Centro di Studi Nucleari del C.N.E.N., Casaccia (Roma) (Italy)	80
XI.	Centro Siciliano di Fisica Nucleare e di Strut- tura della materia, Istituto Nazionale Fisica Nu- cleare - Sezione Siciliana, Istituto di Fisica dell'Universita' Catania (Italy)	83

V	XII. Gruppo di Ispra per le Misure di Sezioni d'Urto del CNEN- Ispra (Varese), (Italy)	90
V	XIII. Gruppo di Ricerca I.N.F.N. delle Basse Energie dell'Istituto di Fisica Nucleare dell'Universita' Pavia, (Italy)	91
N	XIV. Gruppo di Ricerca I.N.F.N. - Istituto di Fisica dell'Universita' Padova (Italy)	94
V	XV. Sottosezione di Firenze dell'Istituto Nazionale di Fisica Nucleare - Istituto di Fisica dell' Universita', Firenze (Italy)	97
V	XVI. Gruppo di Ricerca del contratto EURATOM-CNEN-INFN Istituto di Fisica dell'Universita', Bologna (Italy)	101
V	XVII. Laboratorio dati Nucleari, Centro di Calcolo del C.N.E.N., Bologna (Italy)	109
V	XVIII. Gruppo di Ricerca del Contratto EURATOM-CNEN-INFN, Istituto di Fisica dell'Universita' Torino (Italy)	134
	XIX. Service des Mesures Neutroniques Fondamentales CEA Saclay (France)	139
	XX. Service de Physique Experimentale - Centre d'Etudes de Bruyeres-le-Chatel - C.E.A. (France)	165
	XXI. Section Mesures Nucléaires - Centre d'Etudes de Limeil - C.E.A. France	180
	XXII. Laboratoire de Physique Nucléaire - C.E.A. Grenoble (France)	184

XXIII. Service d'Etudes de Protection de piles - C.E.A. Fontenay-aux-Roses (France)	186
XXIV. Centre de Physique Nucléaire de l'Université de Louvain (Belgium)	187
XXV. Centre d'Etude de l'Energie Nucléaire (C.E.N.-S.C.K.) Mol (Belgium)	188
XXVI. Reactor Centrum Nederland Petten	201
XXVII. Central Bureau for Nuclear Measurements	208

KERNFORSCHUNGSZENTRUM KARLSRUHE (GERMANY)

INSTITUT FÜR ANGEWANDTE KERNPHYSIK

1. 3 MeV Van de Graaff

1.1 High Resolution Resonance Spectroscopy

G. Rohr, K.-N. Müller, M. A. Kazerouni

Measurements of total neutron cross sections were continued with ^{45}Sc in the energy range from 20 to 300 keV using an improved energy resolution of $< 0.2 \text{ n sec/m}$ with a flight path of 22 m. In Fig. 1 part of the experimental cross section is shown.

Analysis of data on ^{57}Fe and ^{53}Cr is not yet completely finished. In the case of ^{57}Fe inelastic scattering above 14.4 keV is possible for compound resonances with spin 1 and one has to use two channel multilevel formula to find the resonance parameters. The existence of the $(n, n'\gamma)$ reaction was proved by detecting the 14.4 keV γ -energy with a NaI(Tl)-detector. Inelastic scattering is a possible method not yet used for the population of the Mößbauer level.

Starting from a set of single particle levels within the shell model level densities in the region of neutron binding energies were calculated for nuclei between $A \approx 40$ and $A \approx 70$. To improve the model pair correlations were taken into account. Similar to an approximation of Block and Feshbach a relation was assumed between the strength function and the density of doorway-states evaluated in our model. Fig. 2 shows a comparison between experimental and preliminary theoretical results.

1.2 Radiative Capture Cross Sections

D. Kompe, A. Ernst

In 1968 the computer program for the extraction of strength functions from average capture cross section data were extended so that now open inelastic exit channels can be treated adequately. With the modified code we obtain p- and d-wave strength functions which differ in some cases, especially for the d-wave, from our preliminary results where

inelastic scattering had been neglected [1]. The revised values are given in Table 1 [2].

The linearity and count rate independence of the electronic equipment associated with the 800 l liquid scintillation detector were improved. Capture cross sections measurements on a number of separated isotopes are being prepared.

Table 1

Element	$S_0 \cdot 10^4$ *	$S_1 \cdot 10^4$	$S_2 \cdot 10^4$
Nb	0.4	11 \pm 3.2	0.4 \pm 0.3
Ag	0.45	7.5 \pm 1.3	3.1 \pm 1.3
Cs	0.7	3.9 \pm 1.0	2.4 \pm 1.5
Hf	2.5	0.13 \pm 0.06	2.1 \pm 0.7
Ta	2.1	0.1 \pm 0.04	2.2 \pm 0.5
W	2.1	0.32 \pm 0.09	0.7 \pm 0.15
Re	2.4	0.1	6.3 \pm 1.0
Au	1.6	0.19 \pm 0.04	1.4 \pm 0.4

* values from [3]

[1] EANDC Progress Report (E) 89 "U" (1968)

[2] D. Kompe, Nucl. Phys., to be published

[3] K.K. Seth, Nuclear Data A 2/3 (1966)

1.3 High-Precision Measurements of Pu²³⁹ and U²³³ Fission Cross Sections Relative to U²³⁵ Between 5 keV and 1 MeV

E. Pfletschinger and F. Käppeler

Relative fission cross sections of Pu²³⁹ and U²³³ were measured, with U²³⁵ as the reference nuclide, in the neutron energy range between 5 keV and 1 MeV. Neutrons were produced via the Li⁷ (p, n) reaction. Below 30 keV the time-of-flight method was used, above 30 keV we worked with monoenergetic neutrons. In order to increase the precision all corrections were reduced as far as possible. Background was minimized by simultaneous registration of both fission fragments in the two halves of a gas scintillation detector. Two such scintillation detectors were used in each run in symmetrical positions with respect to the beam, one containing the sample, the other containing the reference foil (U²³⁵). With this technique practically all fission events occurring are detected with very small background. The corrections which had to be applied to the raw data were smaller than 2 % and the ratio values are believed to be accurate to 2,5 % or better. Our data shown in Figs. 3 and 4 are preliminary in the sense that we do not know yet the exact sample thicknesses. This means that only the curve shapes are final, but not the absolute values. (The error bars shown do not include the foil thickness uncertainties). The shapes are seen to agree quite well with Davey's recommended values [1]. The thickness of the foils is being determined accurately at CBNM (Geel).

1.4 Pu²³⁹ - α - Measurement

H. Meißner, R. E. Bandl

Detectors have been prepared for a measurement of α , the capture to fission ratio, for Pu²³⁹ in the energy range 7 - 60 keV. Here α will be determined by a measurement of the transmission of a metallic Pu sample, the flux of neutrons scattered in the sample and the number of fission neutrons. The measurement will begin in the near future.

1.5 Operation of the Machine

H. Mießner

The pulsed 3 MeV Van-de-Graaff Generator could be operated without any serious breakdowns during the last year and only routine repairs were necessary. The total weekly operations time of the machine was about 120 hours, 80 % of this time was effectively used as measuring time.

Some improvements of the ion source system led to a reduction of the amplitude of satellite pulses from $\sim 3 \times 10^{-3}$ (relative to that of the main pulse) to less than 10^{-4} . Furthermore the beam current of the machine could be increased by 30 - 50 % for measuring periods of several days.

2. Neutron Capture Gamma Ray Spectroscopy

W. Michaelis, U. Fanger, G. Markus, H. Ottmar, H. Schmidt, F. Weller

At the Karlsruhe research reactor FR2 the excited states of several nuclei in the mass regions $50 < A < 100$ and $150 < A < 190$ have been investigated using radiative capture of thermal neutrons. The nuclei studied are Fe⁵⁸, Ni⁶², Zn⁶⁸, Sr⁸⁸, Mo⁹⁸, Dy¹⁶⁵, Er¹⁶⁷, Er¹⁶⁸ and Yb¹⁶⁹. High resolution measurements of the gamma-ray spectra have been performed utilizing a Ge(Li) anti-Compton spectrometer [1] in the low-energy region (< 3 MeV) and a Ge(Li) pair spectrometer [2] for the high-energy transitions (> 2.5 MeV). Up to 400 gamma lines per sample have been detected in the spectra. The high accuracy of the data [3] allows the application of Ritz's combination principle to excitation energies up to 5 MeV in the case of spherical even nuclei and up to 1.5 MeV for deformed odd nuclei. Cascade relationships have been found by two-parameter measurements using both a 34 cm^3 Ge(Li)- $3" \times 3"$ NaI(Tl) coincidence apparatus [4] and a system with two $4" \times 5"$ NaI(Tl) detectors. Level spins and multipole mixing ratios have been determined by means of an angular correlation spectrometer [5] consisting of two $4" \times 5"$ NaI(Tl) crystals. In both the coincidence and the angular correlation experiments extensive use is made of the capabilities of an on-line computer. For

instance, more than 30 gamma-gamma angular correlations can now be measured simultaneously.

For a detailed discussion of the results on Fe⁵⁸ and Yb¹⁶⁹ see refs. 6 - 87. An extensive analysis of the data on Ni⁶², Er¹⁶⁷ and Er¹⁶⁸ will be published in the near future 9, 107. In summary, the results on spherical nuclei show that the excitation spectrum is described with only little success in the framework of vibrational models whereas shell model calculations which take into account residual interactions give quite good agreement 6, 97. A comparison of the data on deformed odd nuclei with own theoretical calculations shows that the experimental results can be well interpreted within a model which takes into account pair correlations, quasiparticle-phonon interaction, rotation-vibration interaction and Coriolis coupling 8, 107. The calculations performed predict the energy and structure of individual levels, the ratios of intensities for gamma-ray transitions, absolute level half-lives and multipolarity admixtures.

- 17 W. Michaelis and H. Kipfer, Nuclear Instr. and Meth. 56 (1967) 181
- 27 G. Markus, W. Michaelis, H. Schmidt and C. Weitkamp
Z. Physik 206 (1967) 84
- 37 F. Horsch, O. Meyer and W. Michaelis, Proc. Int. Symp. on Nuclear Electronics, Paris, September 1968; KFK 778 (1968)
- 47 U. Fanger, KFK 887 (1968)
- 57 H. Schmidt, KFK 877 (1968)
- 67 U. Fanger, W. Michaelis, H. Schmidt and H. Ottmar
Nuclear Physics (in press)
- 77 H. Schmidt, Nuclear Physics (in press)
- 87 W. Michaelis, F. Weller, H. Schmidt, G. Markus and U. Fanger,
Nuclear Physics A 119 (1968) 609
- 97 U. Fanger, R. Gaeta, W. Michaelis, H. Ottmar and H. Schmidt
Nuclear Physics, to be published
- 107 W. Michaelis, F. Weller, R. Gaeta, H. Schmidt, G. Markus and U. Fanger,
Nuclear Physics, to be published

3. Slow Neutron Inelastic Scattering

3.1 Scattering Law Measurements

W. Gläser, K. B. Renker, W. Schott

A full account of scattering law data for reactor moderator materials measured and evaluated at Karlsruhe has been given recently [17], also a detailed report on graphite scattering law data was published [27].

Measurements on solid H_2O were completed. The derived generalized frequency distribution showed reasonable agreement with calculations for a simple dynamical model for ice [37].

Experiments dedicated towards an understanding of the molecular dynamics of solid hydrogen were completed [47]. A generalized frequency distribution was derived from the scattering law data.

3.2 Chemical Binding Effects on the Line Shape of the 6.68 eV Resonanz in ^{238}U

E. Alböld

The line shape measurements of the 6.68 eV resonance in ^{238}U as a function of temperature using a high resolution crystal spectrometer and the analysis of data using the scattering law formalism have been completed. The results indicate that Lamb's condition of weak binding is not satisfied in this case. Therefore it is not possible to calculate the line width and its temperature dependence using simple models and a fixed Debye temperature.

3.3 Phonon Dispersions in Metals

W. Drexel, W. Gläser, R. Orlich

Phonon dispersion measurements in platinum at room temperature have been completed [57]. The study of phonon dispersion in silver has been started. [67]

3.4 New Techniques

F. Gompf, W. Drexel

A new technique for time-of-flight experiments in slow neutron elastic and inelastic scattering work has been developed and successfully tested in the reported period. This technique replaces the conventional beam pulsing by pseudostatistical pulsing and the cross correlation technique

for analysis.

A time utilization of the continuous beam of 50 % is realized in this way [7]. For increasing the reactor neutron intensity in the 0.2 - 0.3 eV range a "hot neutron source" has been constructed and tested [8].

Literature

- [1] W. Gläser, Nukleonik 11 (1968) 282
- [2] F. Carvalho, Nucl. Sci. Engng. 34 (1968) 224
- [3] K. B. Renker and P. v. Blanckenhagen, "Intern. Symp. on Physics of Ice", München 1968
- [4] W. Schott et al., Phys. Let. 27 A (1968) 566
- [5] R. Orlich and W. Drexel, "Neutron Inelastic Scattering", Vol. I, IAEA Vienna 1968, 203
- [6] W. Drexel et al., Phys.Let., in print
- [7] F. Gompf et al., "Neutron Inelastic Scattering", Vol. II, IAEA Vienna 1968, 417
- [8] O. Abeln et al., "Neutron Inelastic Scattering", Vol. II, IAEA Vienna 1968, 331

4. Isochronous Cyclotron

S. Cierjacks, P. Forti, D. Kopsch, L. Kropp, J. Nebe, H. Unseld

4.1 Development of the Time-of-Flight Spectrometer

During the period covered by this report the new flight path with a total length of 190 m was completed. First test runs have been performed with the system. For the long flight path a neutron detector with 25 cm dia. and 1 cm thickness is now available.

For applications in resonance spectroscopy of separated isotopes a new collimator system has been designed capable to study total neutron cross sections for small sample applications (3 cm^2 sample area at minimum). The development of the new outer deflector plates for use as stripe-lines has been finished. The result is a system with 100Ω impedance and a reflection coefficient of smaller than 2 %. First runs with 200 kc repetition rates are expected to be done early in 1969.

17 S. Cierjacks, B. Duelli, P. Forti, D. Kopsch, L. Kropp, M. Lösel, J. Nebe, M. Schweikert, H. Unseld

Rev. Sci. Instr. 39 (1968) 1279 - 89

18 S. Cierjacks, B. Duelli, P. Forti, D. Kopsch, L. Kropp, M. Lösel, J. Nebe, M. Schweikert, H. Unseld.

KFK-Report 959 (1968)

4.2 Total Cross Section Measurements

Total neutron cross sections of F, Si, Cl, K, V, Cr, Co, Ni and Mn were measured from about 0,5 to 30 MeV with 1 nsec channel width. The energy resolution has been determined to be about 2 channels at all energies. The statistical uncertainties in most of the data points are $\leq 2 \%$. Absolute uncertainties are less than 3 %. The data had been compared with selected published data from various laboratories and are, in general, in good agreement with the previous measurements. In several energy regions our data exhibit more structures than was observed in the earlier studies.

17 S. Cierjacks, P. Forti, D. Kopsch, L. Kropp, J. Nebe, H. Unseld
KFK-Report 1000
EANDC (E) - "U" 111
EUR 3963 e

18 S. Cierjacks, P. Forti, D. Kopsch, L. Kropp, J. Nebe, H. Unseld
KFK-Report 1000
EANDC (E) - "U" 111
EUR 3963 e

I. Supplement, to be published

19 S. Cierjacks, P. Forti, D. Kopsch, L. Kropp, J. Nebe, H. Unseld
KFK-Report 1000
EANDC (E)-"U" 111
EUR 3963 e

II. Supplement to be published

4.3 Partial Cross Sections Measurements

In the energy range $5 \text{ MeV} \leq E_n \leq 30 \text{ MeV}$ the charged particles emitted from fast neutron interactions with Be^9 nuclei have been measured with semiconductor counter telescopes. The evaluation of energy and angular distributions of the charged particles p, d, t, and α is underway.

The experimental set-up for the $(n, n'\gamma)$ reaction measurements has been completed. First measurements of these reactions on light nuclei with $\text{Ge}(\text{Li})$ detectors will be done with the time-of-flight spectrometer in spring 1969.

4.4 Subthreshold Fission Cross Sections of U^{238}

S. Cierjacks, P. Forti, F. Käppeler, D. Kopsch, L. Kropp, J. Nebe
E. Pfletschinger

Preliminary measurements of the fission cross section of U^{238} were performed in the energy range from $\sim 0.5 - 30 \text{ MeV}$ with

argon gas scintillation detectors. The result of subthreshold fission below ~ 1.0 MeV is of special interest with respect to the theory of fission processes. The first results were obtained with poor statistical accuracy and are not yet conclusive as to a periodical appearance of clusters of resonances as was found in the subthreshold fission cross sections of Pu^{240} , Np^{237} and U^{234} .

For the fission cross sections of U^{238} in the energy range from 0.5 - 30 MeV the well known n-p scattering data will be used as a standard. New measurements with 0.01 ns/m resolution, higher neutron intensity, and more fission detectors were prepared, which allow to observe also narrow resonances.

4.5 Resonance Spectroscopy and Fluctuation Analysis

The extremely complicated structure of the total cross sections in the fast neutron energy region for intermediate and heavy weight nuclei can be assumed mainly to be caused by isolated compound nuclear levels, Ericson fluctuations, fluctuations in spacings and widths of the compound nuclear levels and possibly intermediate structure in the sense of Block and Feshbach.

A microscopic resonance analysis for s-, p- and d-waves has been performed with the least squares method for the calcium data in the .5 - 1 MeV region. The underlying theory is based on the multilevel R-matrix formalism.

To investigate the broad structure as well as the fine structure in the region of overlapping levels a statistical analysis was performed for Al, Na, Ca, Fe and S. For the intermediate structure occurring mainly below 4 MeV incident neutron energy widths of about 200 keV were deduced. Further investigations of the fluctuations in the total and partial cross section data are in progress.

/1/ S. Cierjacks, P. Forti, D. Kopsch, L. Kropp, J. Nebe
Proc. of a Conference on Neutron Cross Sections and Technology,
Washington D.C., March 68, NBS Spec. Publ. 299, p 743

/2/ S. Cierjacks, P. Forti, D. Kopsch, L. Kropp, J. Nebe
KFK-Report 840 (1968)

5. New Developments in Instrumentation

5.1 On-Line Computers

G. Ehret and H. Hanak

The operation of MIDAS (Multiple Input Data Acquisition System) as an on-line real-time multichannel analyzer with a total capacity of about 262.000 channels has been proven very useful during routine operation round the clock in the reported period. An efficiency of more than 97 % was achieved. The main effort in programming was in optimizing the system routines. The library of the experiment-oriented measuring subroutines has been considerably extended.

Several new programs for the time-of-flight experiments at the isochronous cyclotron using the CDC 3100 were designed and tested. The maximum input rate could be increased from 8000 to 16000 events per sec. Studies aiming at a further increase resulted in a direct-access concept allowing program-controlled on-line correction of linear drifts of time-of-flight spectra at a rate of more than 100000 events per sec. The construction of the necessary units is in progress. The CAE 510 installed at the 3 MeV van de Graaff was running in routine operation.

5.2 Semiconductor Spectrometers

W. Michaelis, F. Horsch, D. Lange, O. Meyer, U. Tamm

5.2.1 Detector Technology

The main activities were concentrated on a through study of ion implantation techniques [1 - 6]. The thickness of the entrance window of ion-implanted semiconductor counters was investigated by pulse-height defect measurements. The dependence of window thickness D on reverse voltage U_A may be described by the function $U_A = F(D)^{-\eta}$. The influence of the following parameters on the constants F and η was measured: doping concentration of the base material, energy of the implanted ions, total number of implanted ions, annealing temperature and crystal orientation [5].

For boron-implanted contacts a formula was found that describes the experimental results within 20 %. An analytical treatment of detector characteristics [6] allows the calculation of the depth concentration of electrically active centers starting from the measured dependence of the window thickness on reverse voltage. The influence of the above parameters on the depth distribution was studied. By variation of the doping concentration of the base material it was possible to determine the concentration distribution over several orders of magnitude.

A large number of silicon detectors has been fabricated by ion implantation. These counters proved to be less sensitive to changes of ambient atmosphere and to mechanical touching than surface barrier detectors. In collaboration with the "Centre de Recherches Nucleaires" at Strassburg thin-window germanium counters with ion-implanted contacts were fabricated using material in which electrically active defect centers had been produced by gamma irradiation. These detectors show a poorer energy resolution than Li-drifted diodes. They can, however, be stored at room temperature.

The response characteristics of Ge(Li) detectors has been studied experimentally for counters ranging in size between 3.8 and 28 cm^3 [7, 8].

5.2.2 Electronic Instrumentation and New Spectrometers

In order to make full use of the resolution capabilities of semiconductor counters it is necessary to stabilize digitally gain and zero drift of the spectrometer system and to correct the channel-energy relationship for nonlinearities. For these purposes a ultra-high precision pulse generator has been designed which has an instability of $< 10 \text{ ppm}/^\circ\text{C}$ and a nonlinearity of $\leq \pm 10 \text{ ppm}$ [9]. For applications where optimum energy resolution is of utmost importance in coincidence experiments a timing unit has been developed which is connected between preamplifier and shaping amplifier and which provides reasonable time information even for unfavourable bandwidth performance of the charge-sensitive preamplifier [10].

The performance of the anti-compton spectrometer [11] has been further improved. Accuracies in the energy determination between 50 and 100 eV are now achieved in the MeV region [3]. Theoretical studies on the new internal pair formation spectrometer [12] show that the response characteristics of the system can be improved by orders of magnitude if a superconducting magnet is used for focusing the position-electron pairs on the semiconductor telescope.

- [1] O. Meyer, Frühjahrstagung DPG Halbleiterphysik, Metallphysik, Tiefe Temperaturen, Thermodynamik; Berlin, März 1968
- [2] O. Meyer, Semiconductor Counters with Thin Window n⁺ and p⁺ Contacts Produced by Ion-Implantation; IEEE Trans. NS-15 (1968) 232
- [3] F. Horsch, O. Meyer and W. Michaelis, Proc. Int. Symp. on Nuclear Electronics, Paris, Sept. 1968; KFK 778 (1968)
- [4] O. Meyer, Meeting on Special Techniques and Materials for Semiconductor Detectors, Ispra, Oct. 1968
- [5] O. Meyer, Nucl. Instr. and Meth. (in press)
- [6] O. Meyer, Nucl. Instr. and Meth. (in press)
- [7] W. Michaelis, Nucl. Instr. and Meth. (in press)
- [8] W. Michaelis, KFK 865 (1968)
- [9] F. Horsch, KFK 558 (1968)
- [10] W. Michaelis, Nucl. Instr. and Meth. 61 (1968) 109
- [11] W. Michaelis and H. Küpfer, Nucl. Instr. and Meth. 56 (1967) 181
- [12] W. Michaelis and D. Lange, Nucl. Instr. and Meth. 58 (1968) 349

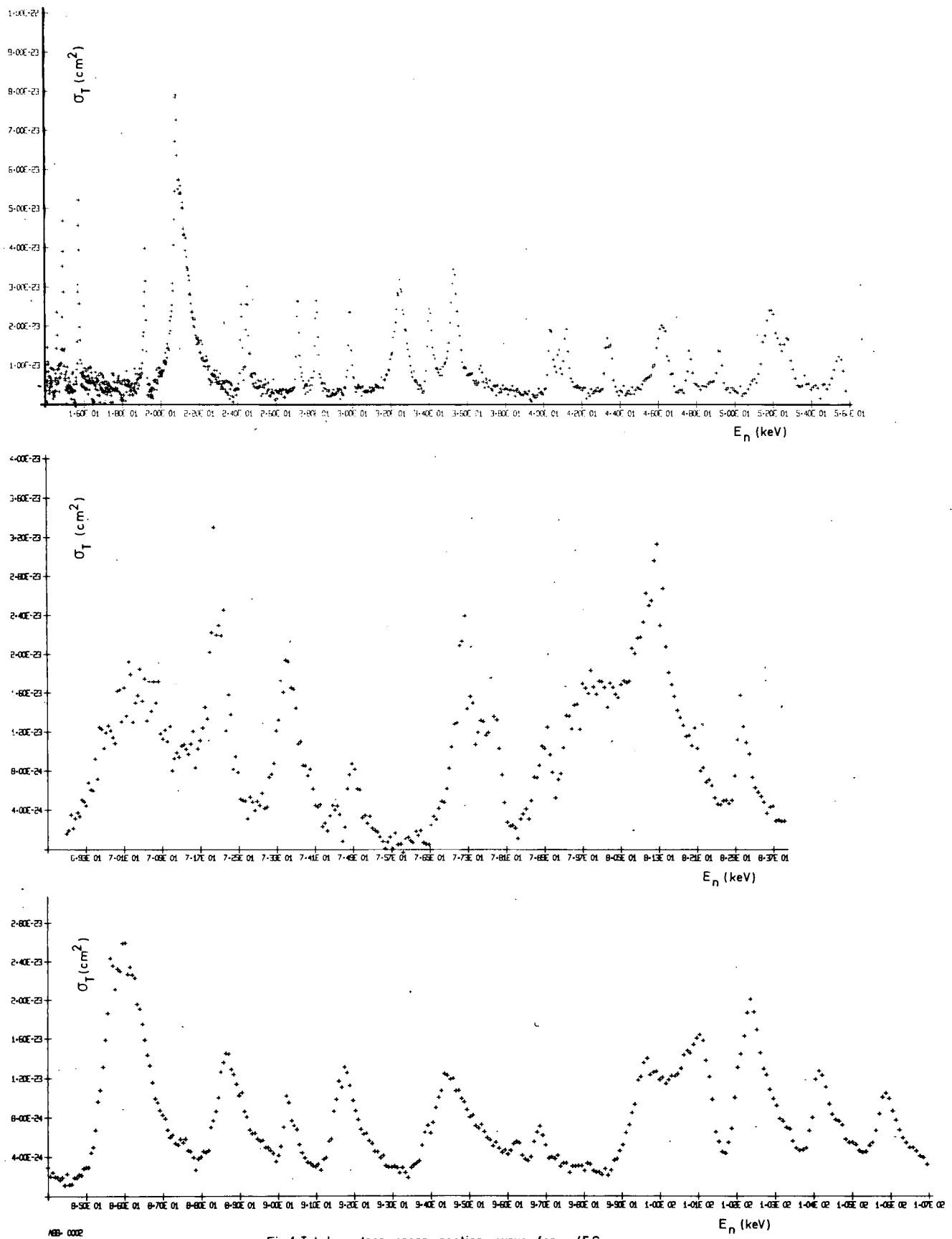


Fig.1 Total neutron cross section curve for ^{45}Sc

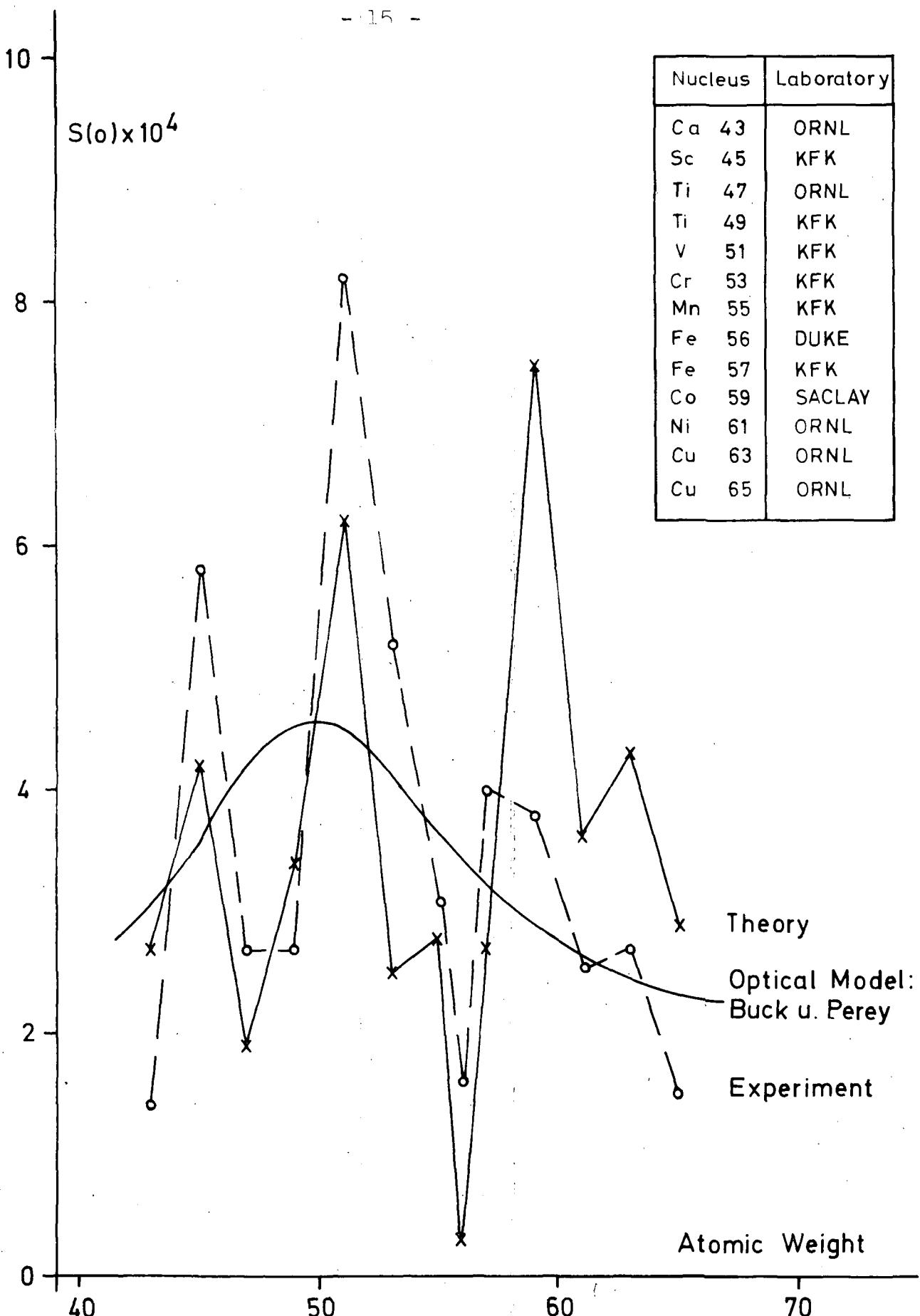


Fig. 2 S-Wave Neutron strength function plotted against atomic weight.

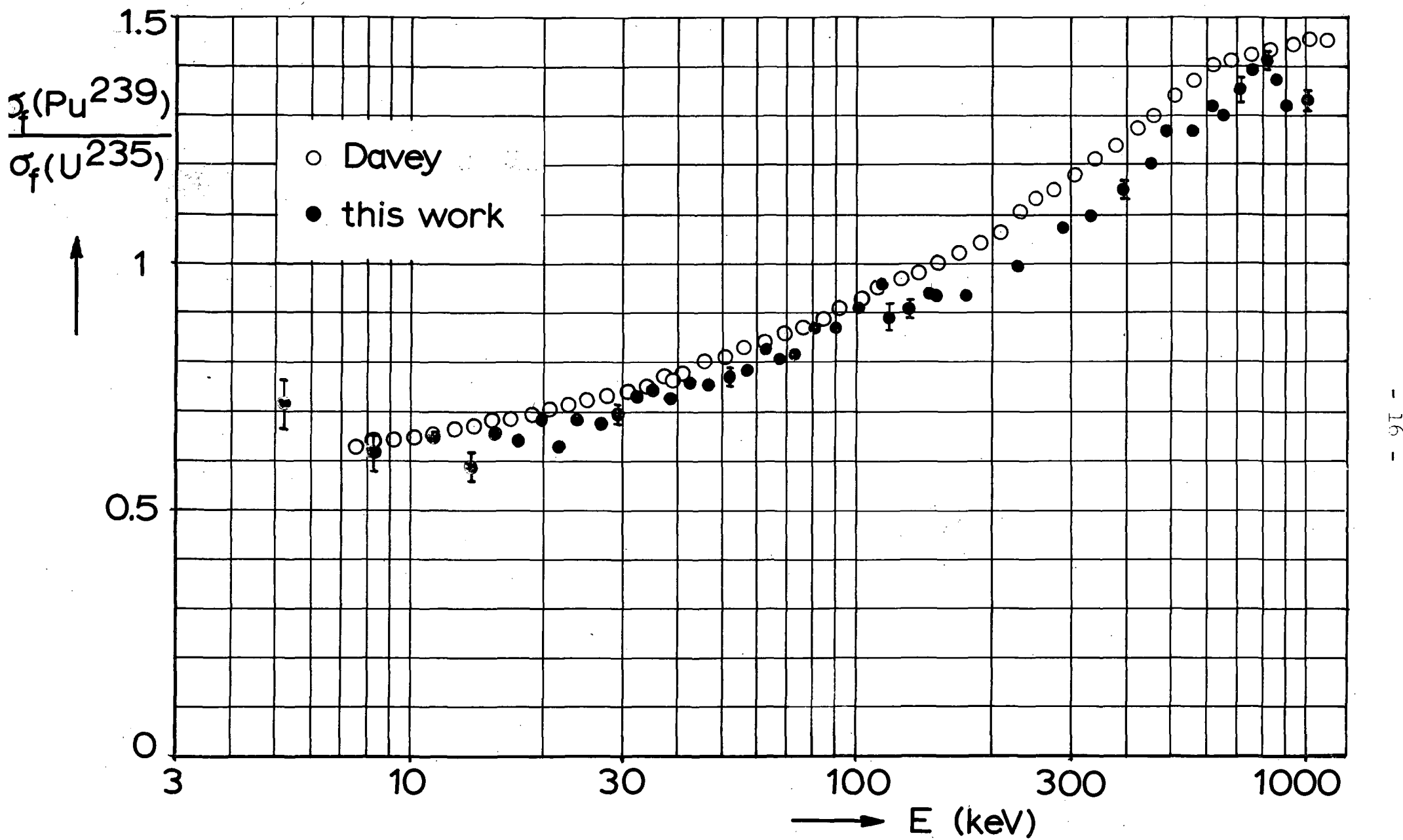


Fig. 3 Preliminary fission cross section ratios ($\text{Pu}^{239}/\text{U}^{235}$). Error bars do not include sample thickness uncertainties and our data will be subject to renormalization as soon as samples are assayed more

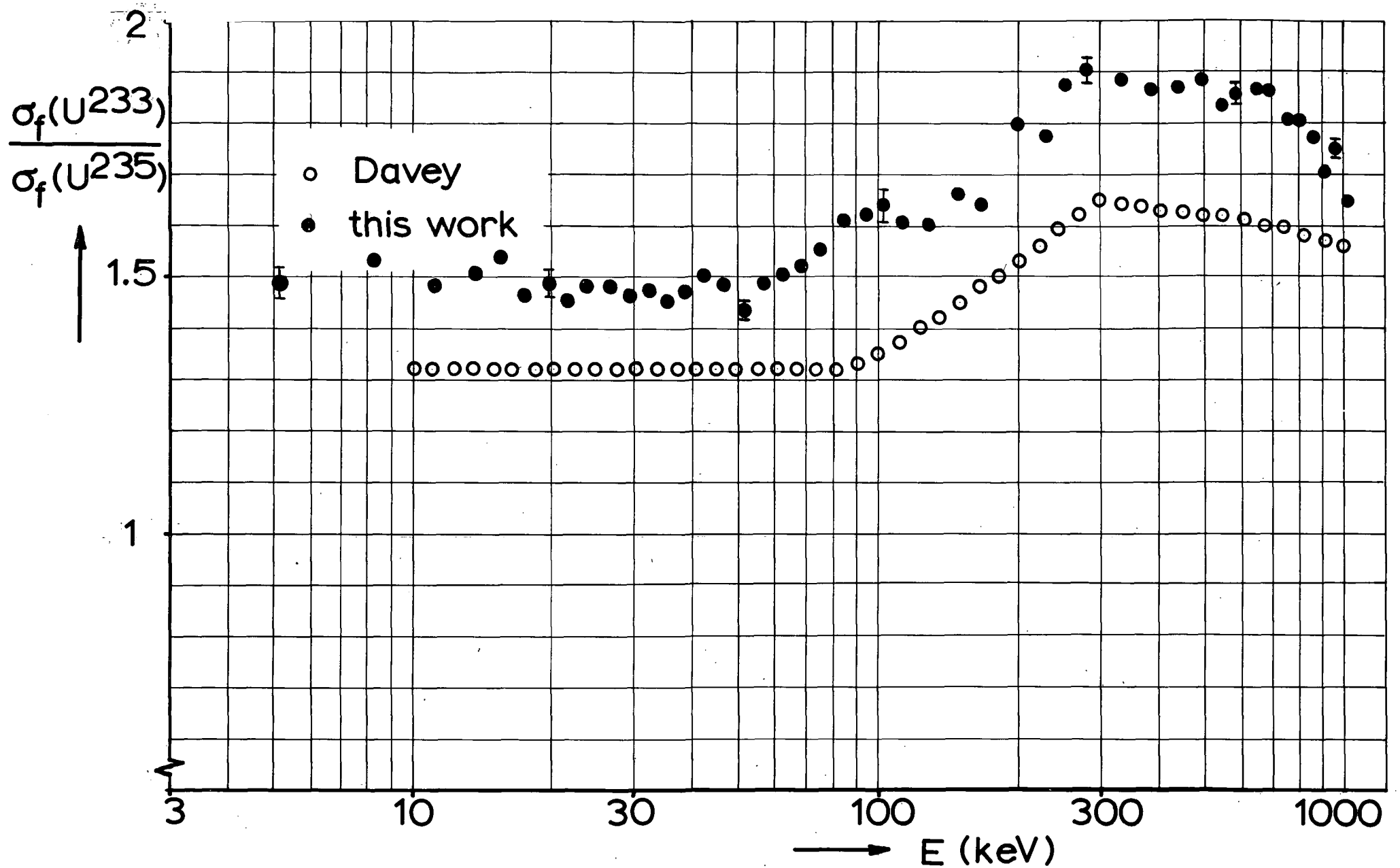


Fig. 4 Preliminary fission cross section ratios ($\text{U}^{233}/\text{U}^{235}$). Error bars do not include sample thickness uncertainties and our data will be subject to renormalization as soon as samples are assayed more accurately. Open circles are Davey's recommended values [1].

II. KERNFORSCHUNGSZENTRUM KARLSRUHE (GERMANY)

INSTITUT FÜR NEUTRONENPHYSIK UND REAKTORTECHNIK

Neutron Nuclear Data Evaluation

B. Hinkelmann, B. Krieg, I. Langner, J.J. Schmidt, F. Siep, D. Woll.

In addition to KFK 120 / part I a new (compared to the first edition, KFK 120 / part II in 1962) much improved and enlarged volume with tables of evaluated "best" microscopic cross sections and related nuclear data for the most important reactor materials was edited /^1_7. Being essentially a copied print-out of the Karlsruhe evaluated nuclear data file KEDAK it simultaneously serves as documentation of the content of KEDAK.

The first phase of the evaluation of all microscopic cross sections and related nuclear data needed in reactor calculations for the higher Pu isotopes Pu^{240} , Pu^{241} and Pu^{242} performed by the group of Prof. Yiftah in collaboration with Karlsruhe as part of a contract between the TECHNION, Haifa, and the Gesellschaft für Kernforschung Karlsruhe is finished /^2_7.

Before entering these data into the KEDAK file capture cross sections and resonance parameters for Pu^{240} were still improved by taking into account the recent comprehensive resonance results obtained at Geel. As part of a new two years contract the present evaluations for Pu^{240} , Pu^{241} and Pu^{242} will be still improved particularly regarding fission, capture and inelastic scattering cross sections.

For Cd an existing GGA evaluation has been improved and incorporated into KEDAK. 26-group cross section sets (ABN-group structure) have been calculated from these data with ABN and Na prototype reactor spectrum weighting, respectively.

In order to enable the transfer of the KEDAK file to the IBM-360/65 recently installed at Karlsruhe and to the Saclay CCDN computer, a card image format has been developed for KEDAK /^3_7. Very shortly the KEDAK file in this

format will be sent to the Saclay CCDN together with the necessary documentation of its present content.

As one of the main points of the Karlsruhe evaluation work a systematic comparison and evaluation of recent discrepant absorption and fission cross section measurements particularly for U^{238} and Pu^{239} has been started, in close interaction with integral experimental results obtained at the Karlsruhe facilities SNEAK and SUAK. First results of these investigations together with the feedback on reactor physics calculations were reported at the International Winter Meeting of the American Nuclear Society at Washington, November 1968 174_7.

The treatment of inelastic scattering within the reactor physics computer programs was improved over the hitherto used ABN scattering matrices by making use of the evaluated excitation cross section data from KEDAK in the region of resolved rest nucleus levels and of the evaporation model in the so-called "continuum" range.

In the framework of theoretical safeguard investigations the methodically still simple derivation of five-group cross section sets for σ_γ , σ_f , σ_{2n} and $\bar{\nu}$ for a series of Pa, U, Np, Pu, Am and Cm isotopes was started.

As one of the main users the Karlsruhe nuclear data evaluation group participates extensively in the principal considerations and efforts of the four international data centres for the creation of an advanced international neutron data storage and retrieval system (SCISRS-II) 175_7. At several occasions reviews were given on the technical principles and the organizational aspects in the field of neutron nuclear data evaluation 176,7_7.

Table of Literature

1. I. Langner, J.J. Schmidt, D. Woll, "Tables of evaluated neutron cross sections for fast reactor materials", KFK 750 (EANDC(E)-88"U", EUR-3715e), 1968.
2. S. Yiftah, J.J. Schmidt, M. Caner, M. Segev, "Basic nuclear data for the higher Pu isotopes", IAEA Symposium on Fast Reactor Physics, Karlsruhe, 1968, Proceed. Vol. I, p. 123, see also IA-1152, 1968.
3. D. Woll, "Card image format of the Karlsruhe evaluated nuclear data file KEDAK", KFK 880 (EANDC(E)-112"U", EUR 4160e).
4. H. Küsters, J.J. Schmidt, E. Eisemann, M. Metzenroth, K.E. Schroeter, D. Thiem, "Analysis of fast critical assemblies and large fast power reactors with group-constant sets recently evaluated at Karlsruhe", Proceed. of the International Winter Meeting, American Nuclear Society, Washington D.C., November 1968; see also KFK 793 (EUR 3962e), 1968.
5. J.J. Schmidt, "Karlsruhe comments on SCISRS-II", 1968, restricted distribution.
6. J.J. Schmidt, "Principles of cross section evaluation", Second Conf. on Neutron Cross Sections and Technology, Washington D.C., March 1968, Proceed. Vol. II, p. 1067; see also KFK 772, 1968.
7. J.J. Schmidt, "Organizational and technical aspects in the field of neutron nuclear data evaluation", First International CODATA Conference at Evangelische Akademie Arnoldshain/Taunus/Frankfurt, July 1968; see also KFK 791, 1968.

III. PHYSIKALISCHES INSTITUT DER UNIVERSITÄT GIESSEN UND
PHYSIK-DEPARTMENT, TECHNISCHE HOCHSCHULE MÜNCHEN (GERMANY)

1. Fine structure in fission fragment charge distributions.

E.Konecny, H.Gunther, H.Rösler, G.Siegert

1.1 Introduction

A reliable determination of the charge split in a fission process on the two fragments as a function of fragments mass requires a fast separation of the fragments, since the charge changes with time within each mass chain due to beta decay. For the determination of the nuclear charge, the number of emitted beta fragments was used. The main purpose of the measurements reported here was to investigate, whether closure of nuclear shells and the pairing effect cause fine structures in the charge distributions.

1.2 Experimental method

Fission fragments from a thin ^{235}U foil, which is located near the core of a reactor, are separated with their initial kinetic energies with respect to mass, energy and ionic charge state by a large mass spectrometer which consists of a electrostatic and a magnetic field in succession. (1,2). A schematic diagram of the set-up is shown in fig 1. In the focal plane of the spectrometer which coincides with the exit boundary of the magnet, particles with known energies and ionic charge states can be spatially separated according to their mass number, as is shown in fig 2. Fission fragments of the mass to be investigated are separated by a slit and caught either in a photographic nuclear emulsion or in a stopping foil within a 4N-proportional counter. With both methods the number of emitted beta particles per fission fragments is measured.

The nuclear emulsion is stored for a sufficiently long time to allow for beta decays and is afterwards processed and scanned for beta-track emerging from the end of each individual fragment track. Since each β -decay increases the nuclear charge by one elementary charge unit,

the primary charge of a fission fragment, Z_{pr} , can be immediately concluded from the number of beta-particles by $Z_p = Z_{st} - n$, where Z_{st} is the stable (within the time which was allowed for beta decays) charge number of the mass chain investigated, which is known from the nuclear chart. Statistics of the number $N(n)$ of fragments associated with n beta-tracks therefore represents the charge distribution of the mass chain. The share of conversion electrons, which are registered as well in the emulsion and may induce some error in the charge distribution, can be approximately estimated to be small. They can be discriminated against only roughly by their low energy. To avoid this problem which is inherent to the emulsion method, another series of experiments was performed using the 4π-proportional counter. In the counter the conversions electrons following the preceding beta particle within the large coincidence time of 5msec are scaled just as one event. By this method clearly not the whole distribution of charge, just its average value can be deduced.

1.3 Results

Fig 3 shows the average primary charge of the heavy fragments from our measurements as compared to the best fit of corresponding radiochemical data as given by Wahl (3). The observed dip at mass number 132 to $Z = 50$ (corresponding to the doubly magic nucleus ^{32}Sn) is in contradiction to radiochemical measurements (4).

The electromagnetic mass separation used allows to separate fragments of specific mass as a function of fragments kinetic energy. On general reasons (5,6) it can be expected that fine structure effects are increased when particles of higher than average kinetic energy are selected. Fig 4 shows the charge distribution of the mass chain $A=138$ as a function of fragment kinetic energy. The increase in the yield of the doubly even nucleus $^{138}_{54}\text{Xe}$ with increasing fragment kinetic energy can be read from the figure. Neighbouring odd mass chains ($A=137,139$) do not show this effect, as is more explicitly indicated in fig 5.

References

- (1) H.Ewald, E.Konecny, H.Opower, H.Rösler, Z.Naturforschg 19a (1964) 194
- (2) E.Konecny, H.Opower, H.Ewald, Z.Naturforschg 19a (1964) 200
- (3) A.C.Wahl, R.L.Ferguson, D.R.Nethaway, D.E.Trotner, K.Wolfsberg, Phys.Rev 126 (1962) 1112
- (4) P.Strom, D.L.Love, A.E.Creedale, A.E.Delucchi, D.Sam, N.E.Ballon, Phys.Rev. 144 (1966) 984
- (5) E.Konecny, H.Gunther, G.Siegert, L.Winter, Nucl.Phys. A100 (1967) 465
- (6) H.Gunther, G.Siegert, R.Gebert, D.Kerr, E.Konecny, Z.Naturf. 22a (1967) 1808

2. Ionic charge states of fission fragments.

E. Konecny, G. Siegert.

Fission fragments represent a natural source of fast heavy ions with a large range of mass and kinetic energy. Already within the target foil they assume an equilibrium charge state which is dependent on the fragment mass and nuclear charge, its velocity and the target material. The distribution of fission fragment ionic charge states has been investigated with the fission fragment mass spectrometer described in the preceding article (1, 2).

Fig. 6 gives the charge distribution of heavy fission fragments leaving a thin uranium foil with mass numbers $A=132$ to $A=137$. The charge distribution obtained by summing over all heavy and light fragments, respectively, is given in fig 7 and compared to older measurements of Lassen (3). Fig 8 shows the average ionic charge of fragments with $A = 134$ as a function of energy (lower scale) and velocity (upper scale). A detailed analysis is given in refs (4,5).

In collisions with gas atoms the fission fragment ions change their charge state by electron loss and pick-up. The cross section for electron pick-up for fission fragments of mass number $A = 133$, kinetic energy $E = 78,5$ MeV and ionic charge state $e = 23$ elementary units is given in Tab. I for several gases (5).

Table I

Cross sections for electron pick-up

N_2, O_2 (air)	$6.4 \cdot 10^{-16} \text{ cm}^2/\text{atom}$
He	$3.1 \cdot 10^{-16} \text{ cm}^2/\text{atom}$
CH_4	$8.5 \cdot 10^{-16} \text{ cm}^2/\text{molecule}$

References

- (1) H.Ewald, E.Konecny, H.Opower, H.Rösler, Z.Naturforschg 19a (1964) 194
- (2) E.Konecny, H.Opower, H.Ewald, Z.Naturforschg 19a (1964) 200
- (3) N.O.Lassen, Kgl. Danske Vidensk. Selskab, Mat.Fys.Medd 26 (1951) No5
- (4) H.Opower, E.Konecny, G.Siegert, Z.Naturforschg 20a (1965) 131
- (5) E.Konecny, G.Siegert, Z.Naturforschg 21a (1966) 192
- (6) G.Siegert, H.Gunther, E.Konecny, Z.Naturforschg 22a (1967) 979

3. Multiple scattering of fission fragments

D.Kerr, G.Siegert, E.Konecny

In scattering fission fragments the value of the Born parameter $a = Z_1 Z_2 / 137 \cdot \beta$ is one to two order of magnitude larger than values that have been previously involved in such measurements. The theories of G.Molière (1) and of Nigam, Sundaresan and Wu (NSW) (2) predict different angular distributions for the scattered particles. No direct comparison with the experimental results is possible, because the fission particles are not fully ionized. Two approximations were made to account for the additional electronic screening. The first and very simple one is, that the value of the effective charge for scattering must lie between the ionic and the nuclear charge of the scattered fission fragments. The second approximation was to introduce a screening term in the theories of Molière and NSW and carry it through the calculation. This physically more significant approximation has the advantage that a variation in the screening potential influences the resulting width of the distribution much less than a variation in the effective charge does in first approximation. The present work shows for both approximations applied that Molière's theory still predicts reasonable results for values of the scattering parameter as large as 850, while the predictions of the NSW theory and the experimental results diverge (3).

References

- (1) G.Molière, Z.Naturforschg 2a (1947) 153; 3a (1948) 78
- (2) B.P.Nigam, M.K.Sundaresan, T.Y.Wu, Phys.Rev. 115 (1959) 491
- (3) D.Kerr, G.Siegert, K.Kürzinger, E.Konecny, H.Ewald, Z.Naturforschg 22a (1967) 1799

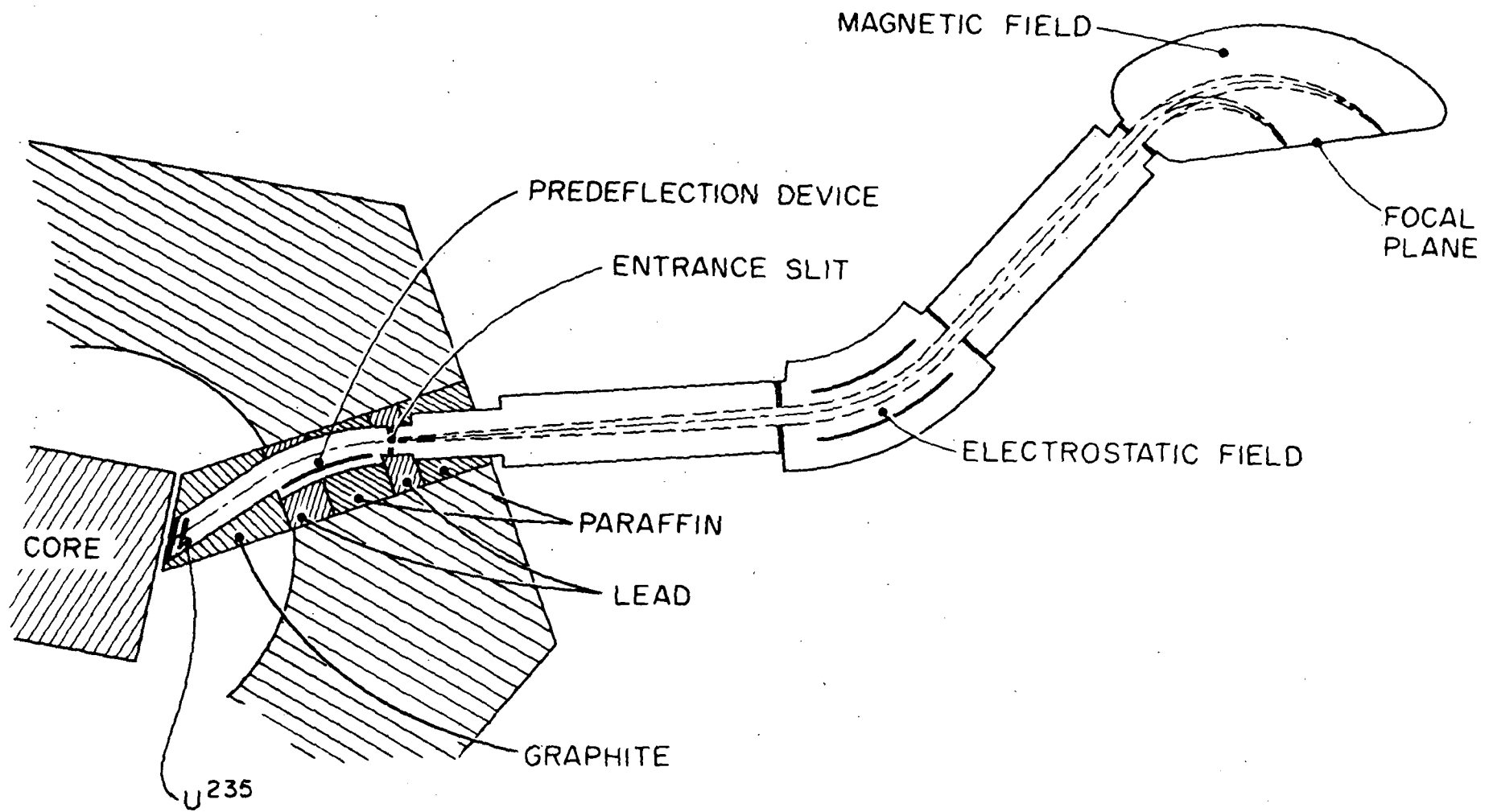


Fig.1 Scheme of the Mass Spectrometer

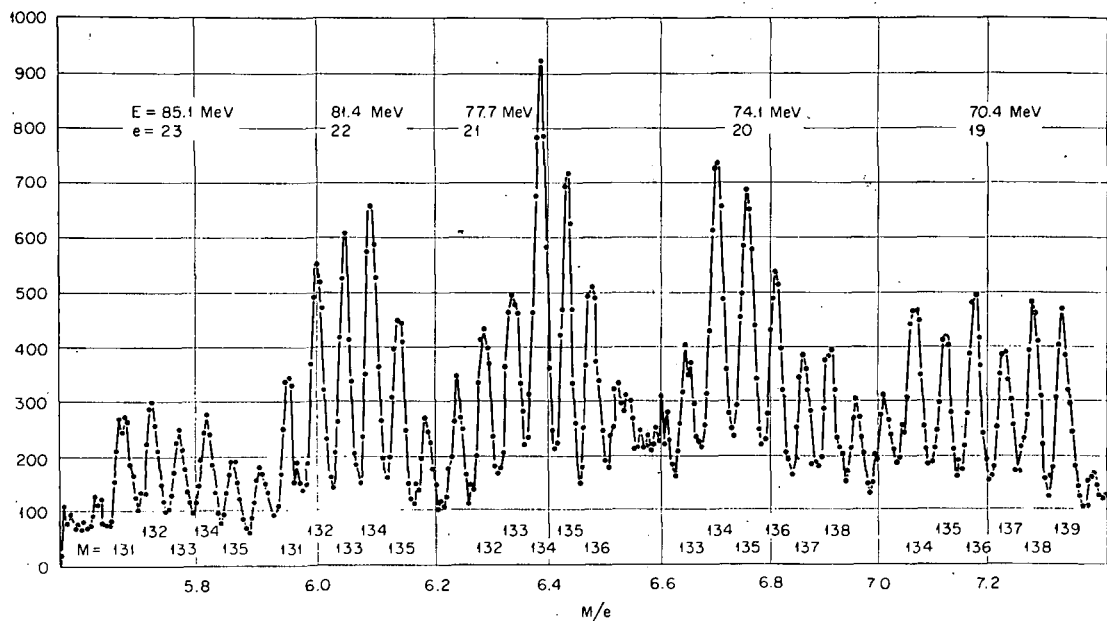


Fig 2 Fission particle spectrum in the focal plane of the spectrometer.

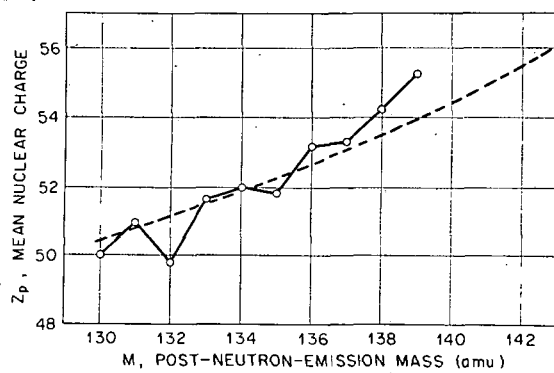


Fig 3 Mean nuclear charges compared to the best fit to radiochemical data as obtained by Wahl (dotted line).

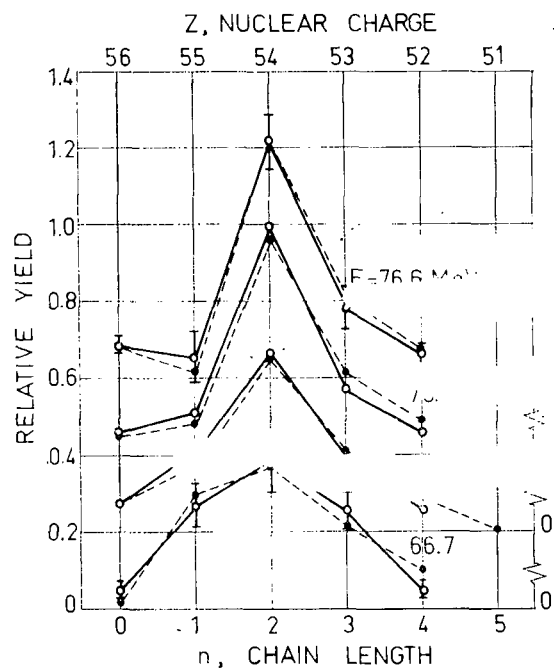


Fig 4 $A = 138$ charge distributions as a function of fragment kinetic energy.

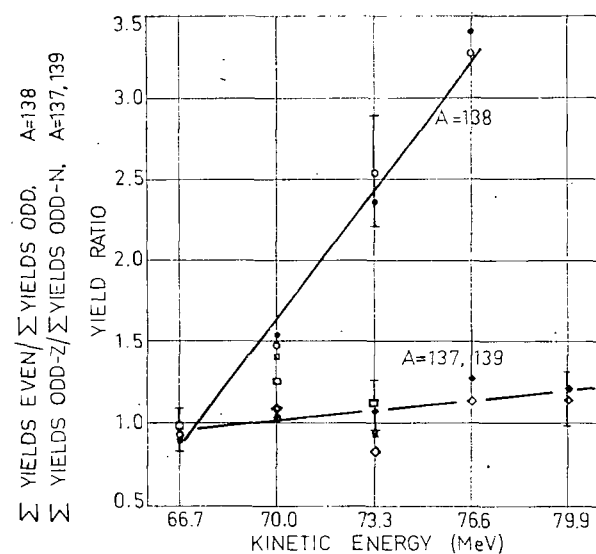


Fig 5 Yield ratio of even-even to odd-odd yields for $A=138$ fission fragments and yield ratio of odd-Z to odd-N nuclei for $A=137$ and 139 fragments as a function of fragment kinetic energy.

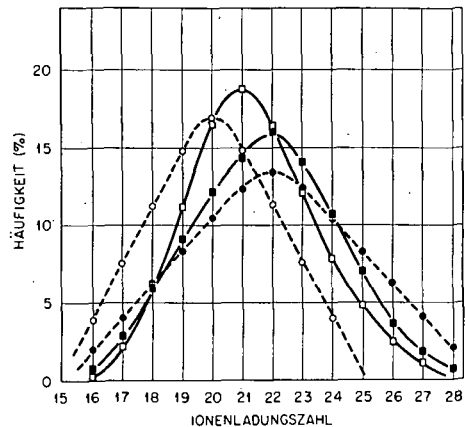


Fig 6 Ionic charge distributions for heavy (full points) and light (open points) fission fragments. The dotted lines refer to older measurements of Lassen.

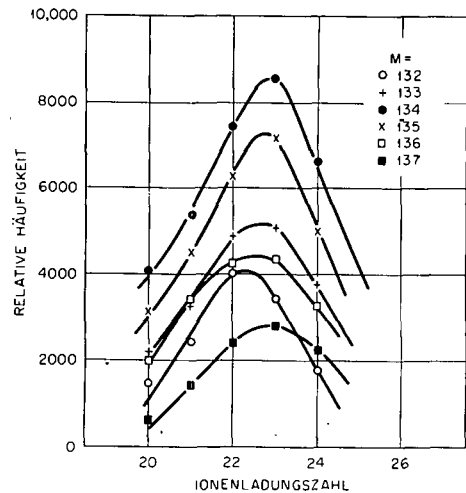


Fig 7 Ionic charge distributions for mass selected fission fragments.

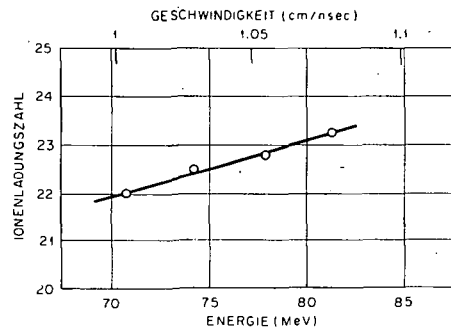


Fig 8 Mean ionic charge for $A=134$ fission fragments as a function of kinetic energy (lower scale) and velocity (upper scale).

IV. PHYSIK-DEPARTMENT, TECHNISCHE HOCHSCHULE MÜNCHEN (GERMANY)

1. γ -rays and conversion electrons following neutron capture.

T.v.Egidy, W.Kaiser and W.Mampe.

H.R.Koch, H.Baader, D.Breitig, K.Mühlbauer, A.Wimmer and O.W.B.Schulte.

1.1 $^{152}\text{Sm}(\text{n},\text{e})^{153}\text{Sm}$

35 conversion electron lines have been measured in the $^{152}\text{Sm}(\text{n},\text{e})^{153}\text{Sm}$ reaction between 0keV and 500keV with the beta spectrometer at the FRM reactor (1). Multipolarities for 33 transitions were deduced using gamma intensities measured with the bent crystal spectrometer at Argonne. A level scheme of ^{153}Sm was constructed in cooperation with R.K.Smither, E.Bieber (Argonne National Laboratory) and K.Wien (Technische Hochschule Darmstadt) who measured beta decay of ^{153}Pm to ^{153}Sm (2). Two rotational bands with $K=3/2^-$ were found: $3/2^-$: 35.843, $5/2^-$: 90.874, $7/2^-$: 174.17 and $3/2^-$: 127.298, $5/2^-$: 182.90, $7/2^-$: 265.93 .(Energies in keV). The levels at 0.0 ($3/2^+$), 7.535 ($5/2^+$), 53.533 ($7/2^+$) and 112.954 ($9/2^+?$) may be members of a disturbed $K=3/2^+$ band. (Fig.1)

1.2 $^{199}\text{Hg}(\text{n},\text{e})^{200}\text{Hg}$

The conversion electron spectrum of the $^{199}\text{Hg}(\text{n},\text{e})^{200}\text{Hg}$ reaction showed 98 lines between 100 and 2300 keV (3). 63 Multipolarities were determined in combination with bent crystal spectrometer gamma data from Risø (4) and Ge(Li) gamma data (5). The level scheme of Schult et.al. (5) was confirmed especially the 0^+ character of the 1029keV level. Branching ratios are discussed and compared with theoretical predictions. Spin and parity was determined to some levels the first time. It is interesting to note that no E1 transition was detected so that all known parities of levels are positive. (Fig.2)

1.3 $^{151}\text{Eu}(\text{n},\gamma)^{152}\text{Eu}$; $^{151}\text{Eu}(\text{n},\text{e})^{152}\text{Eu}$

The capture gamma ray spectrum has been studied with the Risø bent crystal spectrometer over the energy range of 20 to 1000keV. 2600

gamma lines were found. About 500 conversion lines have been observed with the beta spectrometer at the FRM reactor between 0 and 350 keV. A level scheme of ^{152}Eu is going to be constructed. The present results show that some levels at the scheme proposed by Borovikov, Grozdev and Porsev (6) cannot be confirmed.

1.4 ^{142}Pr

Low lying levels of ^{142}Pr have been studied by groups of the University of Fribourg, Switzerland, of the Florida State University, Tallahassee, of the University of California, Berkeley and Los Alamos, of the Technical University, Munich, and of the Research Establishment, Risø, Denmark. A combination of (d,p)- and (n,γ)-reaction spectroscopic data and their theoretical analysis has revealed the following states: $E\gamma(I\pi) = 0 \text{keV}(2^-)$, $3.683 \text{ keV}(5^-)$, $17.740 \text{ keV}(3^-)$, $63.746 \text{ keV}(6^-)$, $72.294 \text{ keV}(4^-)$, $84.998 \text{ keV}(1^-)$, $128.251 \text{ keV}(5^-)$, $144.587 \text{ keV}(4^-)$, $176.863 \text{ keV}(3^-)$, and $200.525 \text{ keV}(2^-)$. These levels are interpreted as arising from the configurations $p(d5/2)n(f7/2)$ and $p(g7/2)n(f7/2)$ and their mixture. Several higher lying states are indicated (7).

1.5 ^{186}Re

Levels of ^{186}Re have been studied through (d,p)-, (d,t)-, (n,e^-)-, and (n,γ)-spectroscopy by groups of the Florida State University, Tallahassee, the Technical University, Munich, the Research Establishment, Risø, Denmark, and the University of California, Los Alamos. Excited states were identified at 59.009 keV , 99.361 keV , 146.275 keV , 173.929 keV , 186 keV , 210.696 keV , 268.796 keV , 273.629 keV , 316.463 keV , 322.391 keV , 378.383 keV , and others are indicated at higher excitation energies. The 314 keV level does probably arise from the coupling of the $[514\uparrow]$ proton and the $[512\uparrow]$ neutron. The other states have been interpreted as the $[402\uparrow]$ proton orbital coupled with the $[512\uparrow]$, $[510\uparrow]$, and $[503\uparrow]$ neutron orbitals. Several of the observed levels appear to be strongly mixed (8).

1.6 ^{158}Gd

The low-energy γ -spectrum from slow neutron capture in ^{157}Gd has been measured with the Risø - curved crystal spectrometer. Strong γ -lines were recorded with a resolution as good as $\Delta E/E \approx 8 \times 10^{-4}$ $E_\gamma(\text{MeV})$. The data are being evaluated at the present time. They will be combined with (n, e^-) -data from Studsvik and high energy (n, γ) -data from Idaho.

1.7 ^{156}Gd

The low energy part of the ^{155}Gd (n, γ) -spectrum has also been measured with the spectrometer at Risø. The resolution was not quite as good as during the ^{157}Gd (n, γ) -run. It is intended to interpret the data in combination with (n, e^-) - and high energy (n, γ) -data from the groups at Studsvik and Idaho.

1.8 ^{169}Yb

The Risø-spectrometer has also been used for the measurement of the low-energy γ -spectrum from neutron capture in ^{168}Yb . The experiment was performed as part of a cooperative work with the groups in Idaho and Studsvik in order to complete the information on low lying levels in ^{169}Yb which has been studied rather carefully by several other groups.(9-11)

1.9 ^{153}Eu

Gamma transitions in ^{153}Eu have been measured after slow neutron capture of the 3^- isomer of ^{152}Eu which was produced through the $^{151}\text{Eu}(n, \gamma)$ reaction. A great number of γ -transitions were observed and about 40 of these were assigned to ^{153}Eu . Most of these transitions could be located in the ^{153}Eu level scheme through the application of the Ritz combination principle to the very precisely determined transition energies. The $I^\pi = 5/2^+, \dots, 1-5/2^+$ levels of the [413 \dagger] ground state rotational band were obtained. The states of the [532 \ddagger] band were established up to the $13/2^-$ member and levels of the [411 \ddagger] band were obtained up to the $11/2^+$ state (12). The energies

of the levels of the $K=5/2^-$ band were found to strongly deviate from the simple rotational sequence. The decay of all of these levels has been established through intra band and several inter band transitions.

References

- (1) T.v.Egidy, W.Kaiser, Z.Physik 201 (1967) 378
- (2) R.K.Smith, E.Bieber, T.v.Egidy, W.Kaiser, K.Wien, Bull.Am. Phys.Soc.Ser. 11, 12 (1967) 1065
- (3) O.W.B.Schult, W.Kaiser, W.Mampe, T.v.Egidy, Z.Physik 218 (1969) 95
- (4) B.P.Maier, U.Gruber, H.R.Koch, O.W.B.Schult, Z.Physik 185 (1965) 478
- (5) O.W.B.Schult, W.R.Kane, M.A.J. Mariscotti, J.M.Simic, Phys.Rev. 164 (1968) 1548
- (6) A.V.Borovikov, V.S.Grozdev, G.D.Porsev, Program of the 18th conference on nuclear structure, Acad.sci. USSR, Riga (1968) 73
- (7) J.Kern, G.L.Struble, R.K.Sheline, E.T.Jurney, H.R.Koch, B.P.K.Maier, U.Gruber, and O.W.B.Schult, Phys.Rev. 173 (1968) 1133
- (8) R.G.Lanier, R.K.Sheline, H.F.Maklein, T.v.Egidy, W.Kaiser, H.R.Koch, U.Gruber, B.P.K.Maier, O.W.B.Schult, D.W.Hafemeister, and E.B.Shera, Phys.Rev. (1969) in press
- (9) D.G.Burke, B.Zeidman, B.Elbok, B.Herskind, and M.Olesen, Mat.Fys.Medd.Dan.Vid.Selsk. 35 Nr.2 (1966)
- (10) E.B.Shera, M.E.Bunker, R.K.Sheline and S.H.Vegors, Phys.Rev. 170 (1968) 1108.
- (11) W.Michaelis, F.Weller, H.Schmidt, G.Markus, and U.Fanger, Nucl.Phys. 119 (1968) 609
- (12) K.Mühlbauer, Thesis, Physics-Department of the Technical University, Munich, 1969.

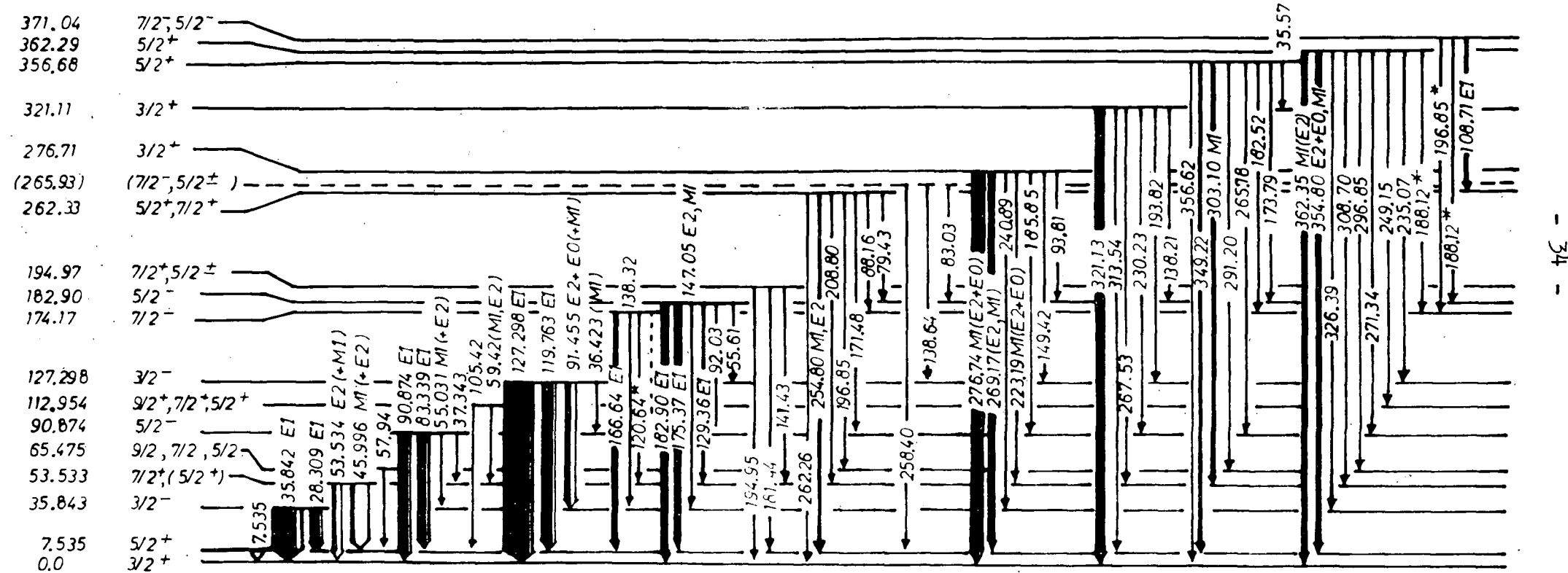
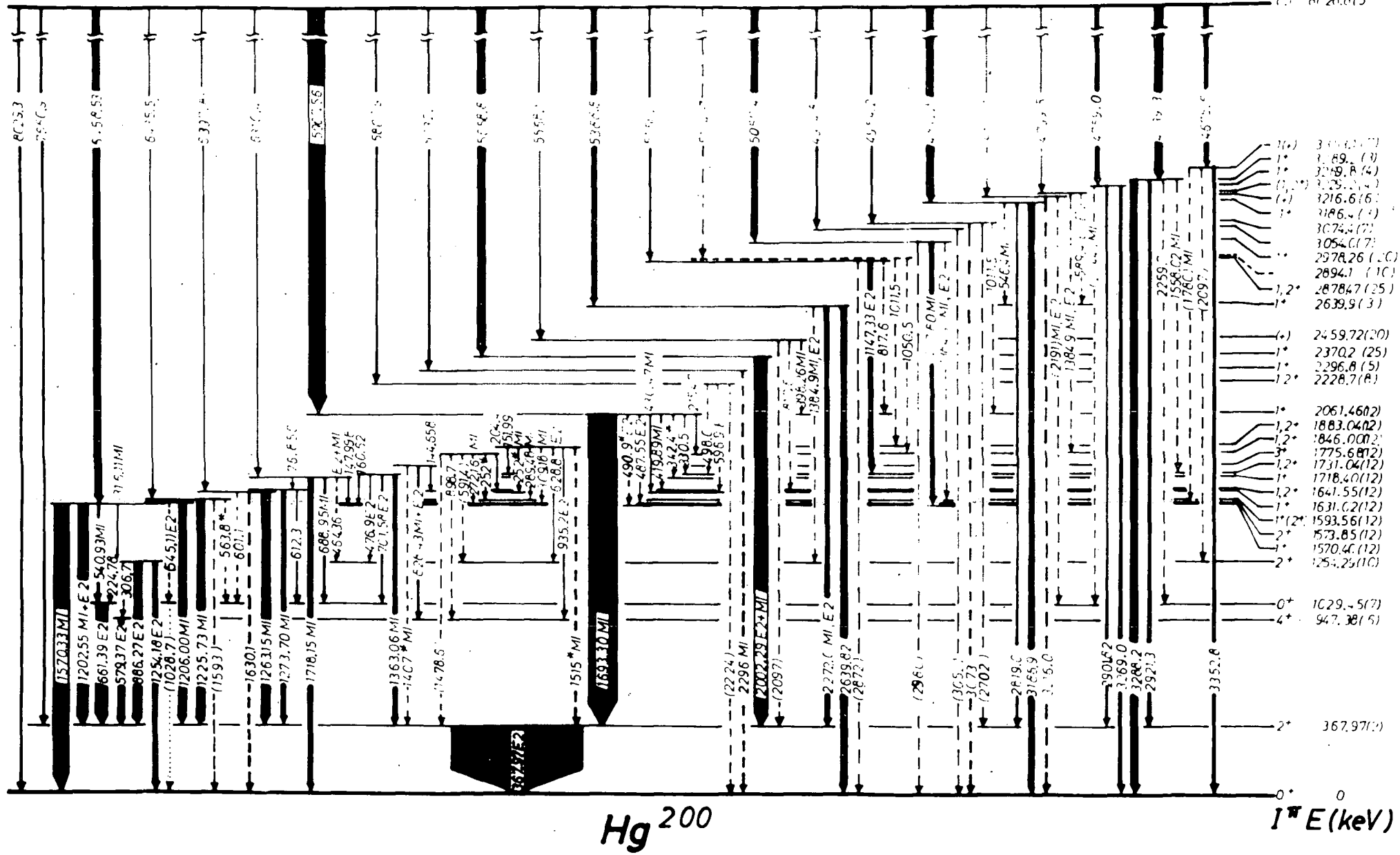


Fig. 7 Niveauschema von Sm^{153}

- $\frac{1}{2}\Xi^-$ -

Fig. 2 Niveauschema von Hg^{200}

2. Coincidence measurements after neutron capture.

K.E.G.Löbner, A.Gerl, J.Klöckner, H.Schimmer and P.Sperr

Gamma-gamma prompt and delayed coincidence measurements have been performed after neutron capture with Ge(Li) and NaI(Tl) detectors at the external neutron beam of the reactor near Munich (FRM). With a cooled bismuthfilter a neutron flux of $\approx 5 \times 10^6$ neutrons/cm²sec is obtained at the position of the target.

2.1 ¹⁵²Eu:

The half-life of the 89.83 keV level in ¹⁵²Eu was measured with a time-to-amplitude converter to be 381 ± 19 ns. This value is much more accurate than earlier measurements:

$T_{1/2} = 650 \pm 350$ ns (1) and $T_{1/2} = 400 \pm 100$ ns (2). The 89.83 keV level is only depopulated by a mixed E1-M2 transition to the ground state. The following hindrance factors are obtained relative to the Weisskopf estimate

$$F_W(E1) = (2.3 \pm 0.4) \times 10^6 \text{ and } F_W(M2) = (2.0 \pm 0.8) \times 10^{-1}.$$

The low energy gamma-ray spectrum populating the 89.83 keV level was measured by the delayed gating technique with a Ge(Li) detector. This spectrum is rather complex with strong peaks at approximately 50, 72.5, 99.5, 104, 108, 122.5 and 140 keV.

2.2 ¹⁶⁰Tb

The half-lives of two excited levels in ¹⁶⁰Tb have been measured after neutron capture ¹⁵⁹Tb(n,γ) with a time-to-amplitude converter to be 59.0 ± 1.2 ns and 3.5 ± 0.8 ns, respectively. Using the delayed gating technique it was shown, that the level with the half-life of 59 ns is only depopulated by a gamma-ray of 64 ± 1 keV. This transition probably corresponds to an E2 transition to the ground state

$3^- \{ p\ 3/2^+ [411] + n\ 3/2^- [521] \}$ from the 1^- state $\{ p\ 3/2^+ [411] - n\ 5/2^- [523] \}$. The hindrance factor relative to the Weisskopf estimate for this transition $F_W \approx 10^{-1}$ lies in the range of other E2, K = 2 transitions (3). The measured half-life of 3.5 ± 0.8 ns probably belongs to the 78.86 keV level.

2.3 ^{198}Au (Fig.3):

Low energy gamma-gamma coincidence measurements after neutron capture $^{197}\text{Au}(n,\gamma) ^{198}\text{Au}$ with two Ge(Li) detectors have been performed. These measurements confirm the main parts of the level scheme constructed by von Egidy et. al. (4) but in several aspects it has to be modified. By measuring delayed coincidences the half-life of the 367.29 keV level was determined to be ≈ 110 ns. This half-life probably corresponds to the unassigned half-life of $T_{1/2} = 128 \pm 15$ ns measured by Bonitz (5) in the $^{197}\text{Au}(d,p) ^{198}\text{Au}$ reaction. The 367.29 keV level is mainly depopulated by a 97.21 (E1), 214.89, 55.188 keV cascade according to our coincidence and delayed coincidence measurements and the data of von Egidy et.al. (4). The 97.21 keV E1 transition is hindered relative to the Weisskopf estimate by a factor $\approx 8 \times 10^5$.

References:

- 1) A.M. Berestovoi et. al., Nucl. Sci. Abstr. 18 (1964) 843, No. 6259
- 2) K.Takahashi, M. McKeown and G.Scharff-Goldhaber, Phys. Rev. 137B (1965) 763
- 3) K.E.G.Löbner, Phys. Letters 26B (1928) 369
- 4) T. von Egidy, E.Bieber and Th.W.Elze, Z. Physik 195 (1966) 489
- 5) M. Bonitz, Nucl. Phys. A118 (1968) 478

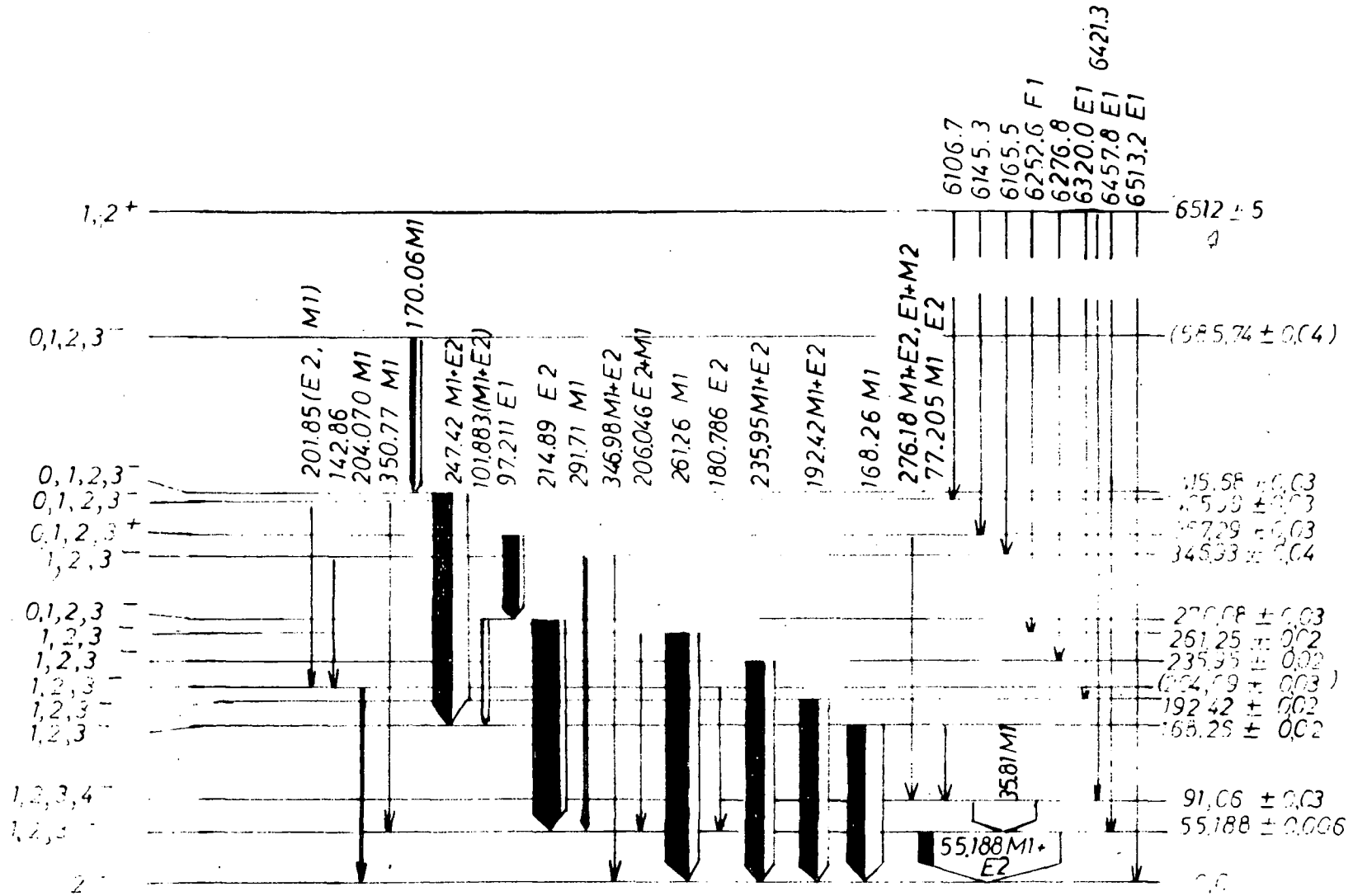


Fig. 3 Niveauschema von Au^{198}

3. K - forbidden gamma-ray transitions.

K.E.G.Löbner

All available experimentally determined absolute gamma-ray transition probabilities between different intrinsic states in odd-and even-mass nuclei of the rare earth region (with neutron numbers $89 \leq N \leq 114$ and proton numbers $62 \leq Z \leq 78$) and of the actinide region ($N \geq 134$) are compared to the Weisskopf estimate for different $|\Delta K|$ values. For all multipolarities a systematic decrease of the reduced transition probabilities by approximately a factor of 100 per degree of K-forbiddenness is found, but the frequently used "empirical" rule $\log F_W = 2(|\Delta K| - L)$ is not true in general, [where F_W is the hindrance factor relative to the Weisskopf estimate and L is the multipolarity of the gamma-ray transition].

Reference:

K.E.G.Löbner, Physics Letters 26B (1968) 369

4. Decay scheme study

K.E.G.Löbner

^{234}U

The half-life of the 1552 keV level in ^{234}U was measured in the decay of 6.7 h ^{234}Pa by delayed coincidences with a time-to-amplitude converter to be 2.20 ± 0.25 ns(1). This half-life determines the transition probability of the 131 keV E1 transition between the two neutron states $5^+ \{ 5/2^+ [622]\uparrow + 5/2^+ [633]\downarrow \}$ and $6^- \{ 7/2^- [743]\uparrow + 5/2^+ [633]\downarrow \}$. The hindrance factors ($F_W = 3.5 \times 10^4$ and $F_N = 0.27$) are compared to those of the E1 transition between the same Nilsson states in the odd-mass nucleus ^{239}Pu ($F_W = 2.2 \times 10^6$ and $F_N = 13$). The difference of the reduced transition probabilities is discussed in terms of pairing interactions. It was confirmed that the 1552 keV level is only depopulated by the 131 keV E1 transition.

Reference :

- (1) K.E.G. Löbner, O.F.A. Goudsmit, J.Konijn, E.W.A. Lingeman and P.Polak, Nuclear Physics A122 (1968) 214.

5. Coherent scattering length measured by total reflection and by small angle scattering of slow neutrons.

L.Koester, N.Nücker, W.Nistler, D.Trustedt, H.Ungerer

The list of scattering length measured using the neutron gravitation refractometer at the FRM has been completed by further substances. The scattering length of some substances published up to now had to be corrected by about 0.1% or less on account of a more precise theory of the refractometer.

The scattering length of the bound atoms determined are:

Hydrogen:	$a = -(3.723 \pm 0.003) F$
Deuteron:	$a = +(6.73 \pm 0.05) F$ a)
Carbon:	$a = +(6.626 \pm 0.003) F$
Oxygen:	$a = +(5.75 \pm 0.04) F$ b)
Fluorine:	$a = +(5.74 \pm 0.03) F$ b)
	$\dots = +(2.852 \pm 0.006) F$ b)
Chlorine:	$a = +(9.584 \pm 0.002) F$
Bromine:	$a = +(6.85 \pm 0.04) F$ b)
Tungsten:	$a = +(4.77 \pm 0.05) F$ a)
Mercury:	$a = +(12.66 \pm 0.02) F$
Lead:	$a = +(9.40 \pm 0.01) F$ b)
Bismuth:	$a = +(8.5234 \pm 0.0014) F$

a) small angle scattering result

b) preliminary value

The values for Hydrogen, Carbon, Oxygen, Fluorine, Chlorine and Bromine were calculated from measured scattering length of organic liquids. The deuteron value was determined from a measurement of heavy water relative to light water. The measured scattering length of the liquids used for the determination of the scattering length of the elements are:

$C_8 H_{10}$ (Xylene)	: $a = +(15.784 \pm 0.008) F$
$C_{13} H_{12}$ (Ditan)	: $a = +(41.460 \pm 0.013) F$
$C_7 H_8$ (Toluene)	: $a = +(16.590 \pm 0.007) F$
$C_4 Cl_4$: $a = +(44.960 \pm 0.010) F$
$C_2 Cl_4$: $a = +(51.590 \pm 0.010) F$
$C_6 H_5 F$: $a = +(26.879 \pm 0.008) F$
$C_6 H_5 Cl$: $a = +(30.723 \pm 0.007) F$

C ₆ H ₅ Br	: a = +(27.987 ± 0.006) F
C ₇ H ₁₂ O ₄	: a = +(24.707 ± 0.020) F
D ₂ O	: a = +(19.20 ± 0.08) F

Measurements on high purity lead and on heavy and light water mixtures are in preparation.

6. Nuclear spectroscopy of short-lived fission products Nb, Mo and Tc.

G. Zicha, P. Maier-Komor, J. Maul, U. Zahn, H.J. Körner, K.E.G. Löbner,
P. Kienle.

The decay of neutron-rich Tc fission products ($A=103-108$) was investigated by measuring γ -spectra and prompt and delayed $\gamma-\gamma$ -coincidences using Ge(Li)-detectors. It was possible to separate the fission products radiochemically within 4s after neutron irradiation of ^{235}U .

In ^{106}Ru a ground state rotational band has been found with $\hbar^2/2J = 15,7$ keV. A deformation parameter $B \approx 0.64$ can be estimated from the lifetime of the 94 keV 2^+ state. Investigation of the excited states of ^{105}Ru , ^{107}Ru and ^{108}Ru indicate strong deformation of these nuclei.

In ^{103}Tc an isomer with a half-life of 15s has been found, the decay of which may be explained by a M4-transition between $p_{1/2}$ and $g_{1/2}$ shell model states.

An upper limit for the half-life of the still unknown isotopes ^{103}Nb and ^{104}Nb has been determined as 1s and 2s, respectively, by variation of the separation time.

V. PHYSIK-DEPARTMENT DER TH. MÜNCHEN UND

INSTITUT FÜR FESTKÖRPER- UND NEUTRONENPHYSIK DER KERNFORSCHUNGS-

ANLAGE JÜLICH

Total neutron scattering cross sections for the rare earth elements

Tb, Dy, Ho, Er, Tb and Lu in the subthermal energy range

A. Knorr and W. Schmatz

Total cross sections σ_{tot} are measured with a mechanical velocity selector. The results are given in the table. The error F for the neutron energy E is due to the calibration accuracy, the error for σ_{tot} due to counting statistics. σ_{tot} is already corrected for rare earth impurities of high absorption cross sections like Gd and Eu. The absorption cross section σ_a is reduced from σ_{tot} by correction for paramagnetic scattering (metal foils at room temperature have been used). Other scattering contributions are of minor importance and are also considered. Experimental procedure and data handling will be discussed in detail in Nukleonik (1969). The systematic errors F_{syst} are mainly due to that of the total cross section, to the correction for impurities (σ_{tot}) and to the paramagnetic scattering cross section.

T e r b i u m

D y s p r o s i u m

$E[\text{meV}]$	$F_{\text{in}}\%$	$\bar{\sigma}_t [\text{barn}]$	$F_{\text{in}}\%$	$\bar{\sigma}_\alpha [\text{barn}]$	$E[\text{meV}]$	$F_{\text{in}}\%$	$\bar{\sigma}_{\text{in}} [\text{barn}]$	$F_{\text{in}}\%$	$\bar{\sigma}_\alpha [\text{barn}]$
3,164	0,4	113,3	0,2	59 \pm 8	3,207	0,2	3057	0,1	2900 \pm 70
2,298	0,4	126,8	0,2	73,5 \pm 8,5	2,416	0,2	3531	0,1	3380 \pm 70
1,635	0,4	140,7	0,2	89 \pm 8,5	1,730	0,2	4109	0,1	3950 \pm 60
1,154	0,4	162,2	0,2	120 \pm 9	1,261	0,2	4795	0,1	4680 \pm 50
0,683	0,4	208,6	0,2	152 \pm 9,5	0,720	0,2	6233	0,1	6115 \pm 50
0,346	0,4	289,1	0,2	212,5 \pm 13	0,391	0,2	8484	0,1	8345 \pm 60
0,214	0,4	368,9	0,3	260 \pm 18	0,257	0,3	10330	0,2	10165 \pm 70
0,131	0,8	460,5	0,5	331 \pm 22					
$F_{\text{syst}} \rightarrow$		$\pm 1,2\%$		$\pm 2,1\%$		$\pm 2,8\%$		$\pm 1,2\%$	
								$\pm 2,2\%$	
								$\pm 2,2\%$	

H o l m i u m

E r b i u m

T h u l i u m

L u t e t i u m

$E[\text{meV}]$	$F_{\text{in}}\%$	$\bar{\sigma}_t [\text{barn}]$	$F_{\text{in}}\%$	$\bar{\sigma}_\alpha [\text{barn}]$	$\bar{\sigma}_{\text{tot}} [\text{barn}]$	$F_{\text{in}}\%$	$\bar{\sigma}_t [\text{barn}]$	$F_{\text{in}}\%$	$\bar{\sigma}_\alpha [\text{barn}]$	$\bar{\sigma}_{\text{tot}} [\text{barn}]$	$F_{\text{in}}\%$	$\bar{\sigma}_\alpha [\text{barn}]$
3.168	0,3	241,5	0,2	184 \pm 12	435,5	0,2	382 \pm 18	0,2	306 \pm 12	195,0	0,4	187,5 \pm 40
2.301	0,3	273,0	0,2	218 \pm 13	504,5	0,2	452 \pm 19	0,2	367 \pm 12	226,5	0,4	221,5 \pm 4,0
1,663	0,3	311,0	0,2	259 \pm 13	581,5	0,1	530 \pm 18	0,2	430 \pm 12	256,5	0,3	253,5 \pm 2,5
1,282	0,2	348,0	0,1	296 \pm 14	661,5	0,1	612 \pm 17	0,2	492 \pm 11	294,0	0,3	291,0 \pm 3,0
0,688	0,2	464,0	0,1	406 \pm 14	890,0	0,1	836 \pm 19	0,2	687 \pm 12	399,0	0,3	397,0 \pm 3,0
0,345	0,3	640,5	0,2	562 \pm 19	1250,0	0,2	1177 \pm 24	0,2	954 \pm 16	554,5	0,3	552,5 \pm 3,5
0,217	0,3	805,0	0,2	702 \pm 25	1570,0	0,2	1476 \pm 30	0,5	1208 \pm 18	711,5	0,3	709,5 \pm 4,
0,137	0,8	992,0	0,4	860 \pm 35	1955,0	0,3	1834 \pm 40	0,5	1497 \pm 30	887,0	0,7	884,5 \pm 8
$F_{\text{syst}} \rightarrow$		$\pm 1,2\%$		$\pm 0,8\%$		$\pm 1,0\%$		$\pm 0,6\%$		$\pm 0,7\%$		$\pm 1,8\%$
								$\pm 0,8\%$		$\pm 0,8\%$		$\pm 1,8\%$
												$\pm 1,8\%$

VI. INSTITUT FÜR FESTKÖRPER- UND NEUTRONENPHYSIK, KFA JÜLICH

1. Measurement of Mass- and Time-Dependence of Delayed Fission Neutrons

(E.Roeckl, J. Eidens, and P.Armbruster)

Delayed neutron emission for thermal neutron fission of ^{235}U is investigated by means of a helium-filled mass separator. At the focus of the separator, the neutron activity is detected in coincidence with the β decay preceding the neutron emission. Measurements of the activity build-up give the total delayed neutron yield and the yields for different times after fission. Measurements of the activity decay give the half-life distribution.

The mass-dependence of yield and half-life was investigated for the whole fission product mass region. The splitting of the total yield of delayed neutrons between light and heavy fission products has been determined (table I). Based on KEEPIN's value of the total number of delayed neutrons per fission, a yield of 1.05 and 0.53 neutrons per 100 fissions has been obtained for light and heavy fission products, respectively. The experimentally determined mass- and time-dependence of delayed neutron emission are compared with those calculated from the known precursors. Unidentified neutron activities rest in the mass regions 85 - 88 (half-life 1 sec, yield 0.10 n/100 f) and 96 - 100 (half-life 1.5 sec, yield 0.24 n/100 f). By means of theoretical considerations the yield difference for delayed neutrons between light and heavy fission products is interpreted and the new neutron activity is assigned to the precursors ^{98}Y or ^{99}Y (fig. 1).

Table I

Identified and unidentified fraction of delayed neutron yield

	Light fission products		Heavy fission products	
	Fraction of total yield (%)	Absolut yield (n/100 f)	Fraction of total yield (%)	Absolut yield (n/100 f)
Delayed neutron yield (total: 1.58 ± 0.05 n/100 f)	67 ± 3	1.05 ± 0.06	33 ± 3	0.53 ± 0.04
Identified fraction	51 ± 10	0.79 ± 0.15	25 ± 6	0.40 ± 0.10
Not identified fraction	16 ± 7	0.26 ± 0.10	8 ± 7	0.12 ± 0.11

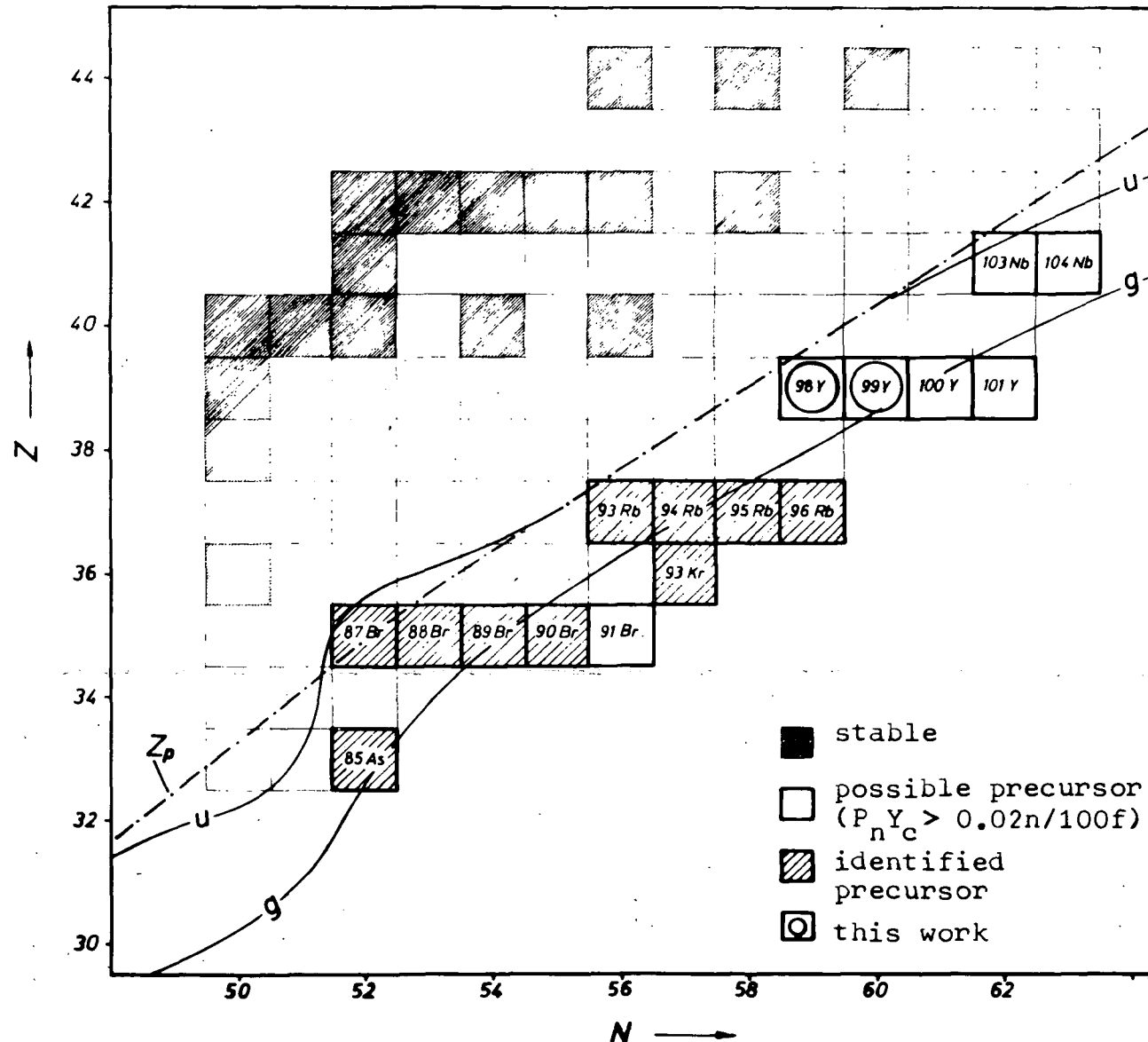


Fig. 1. Delayed neutron precursors among light fission products. - \cdots - Z_p of the primary charge distribution. -o- Neutron emission threshold for odd Z precursors. -e- Neutron emission threshold for even Z .

2. Identification and Decay Investigation of Several Short-Lived Fission Products by an On-Line Mass Separator

(J. Eidens, E. Roeckl, P. Armbruster)

A device for nuclear spectroscopy on short-lived fission products has been operated at the focus of the gas-filled on-line mass separator at the FRJ-2 reactor. By the known γ -lines of long-lived fission products, a mass calibration of the separator was carried out. Several unknown short-lived fission products could be identified by investigating some very intense γ -lines. For these lines, the decay curves were measured and β - γ -coincidence spectra as well as γ - γ -coincidence spectra were recorded. The data were assigned to 8 nucleides. Their half-lives, β decay Q-values, and γ -lines are given in table I, coincident γ -lines are separated by a comma, non coincident ones by a semicolon. In 3 of the 8 cases the decay curves permitted the following estimates for the half-lives of the precursors: ^{97}Sr (0.4 ± 0.3) sec; ^{99}Y (0.8 ± 0.7) sec; ^{100}Zr (1.0 ± 0.9) sec. Using the data obtained in this investigation a proposal for decay schemes of the 8 nucleides could be made. Here, in a few cases, published data from earlier β decay or nuclear reaction measurements have been taken into account.

Table I

Data on new short-lived fission products

Nucleide	$T_{1/2}$ (sec)	Q_β (MeV)	E_γ (keV)
^{84}Se	210 ± 5	1.8 ± 0.1	406 ± 3
^{91}Kr	7.9 ± 0.5	5.7 ± 0.4	$111 \pm 3, 630 \pm 20$
^{97}Y	1.11 ± 0.03	5.7 ± 0.2	$125 \pm 3, 810 \pm 3$
^{99}Nb	14.3 ± 0.06	3.7 ± 0.2	137 ± 3
^{99}Zr	2.4 ± 0.1	4.5 ± 0.2	$468 \pm 3, 548 \pm 3;$ $595 \pm 3, 430 \pm 20$
^{100}Nb	6.6 ± 0.2	6.5 ± 0.3	$159 \pm 3, 533 \pm 3$
^{101}Nb	7.0 ± 0.2	4.6 ± 0.2	$273 \pm 3; 399 \pm 3$
^{101}Zr	3.3 ± 0.6	6.5 ± 0.7	$293 \pm 3, 400 \pm 20$

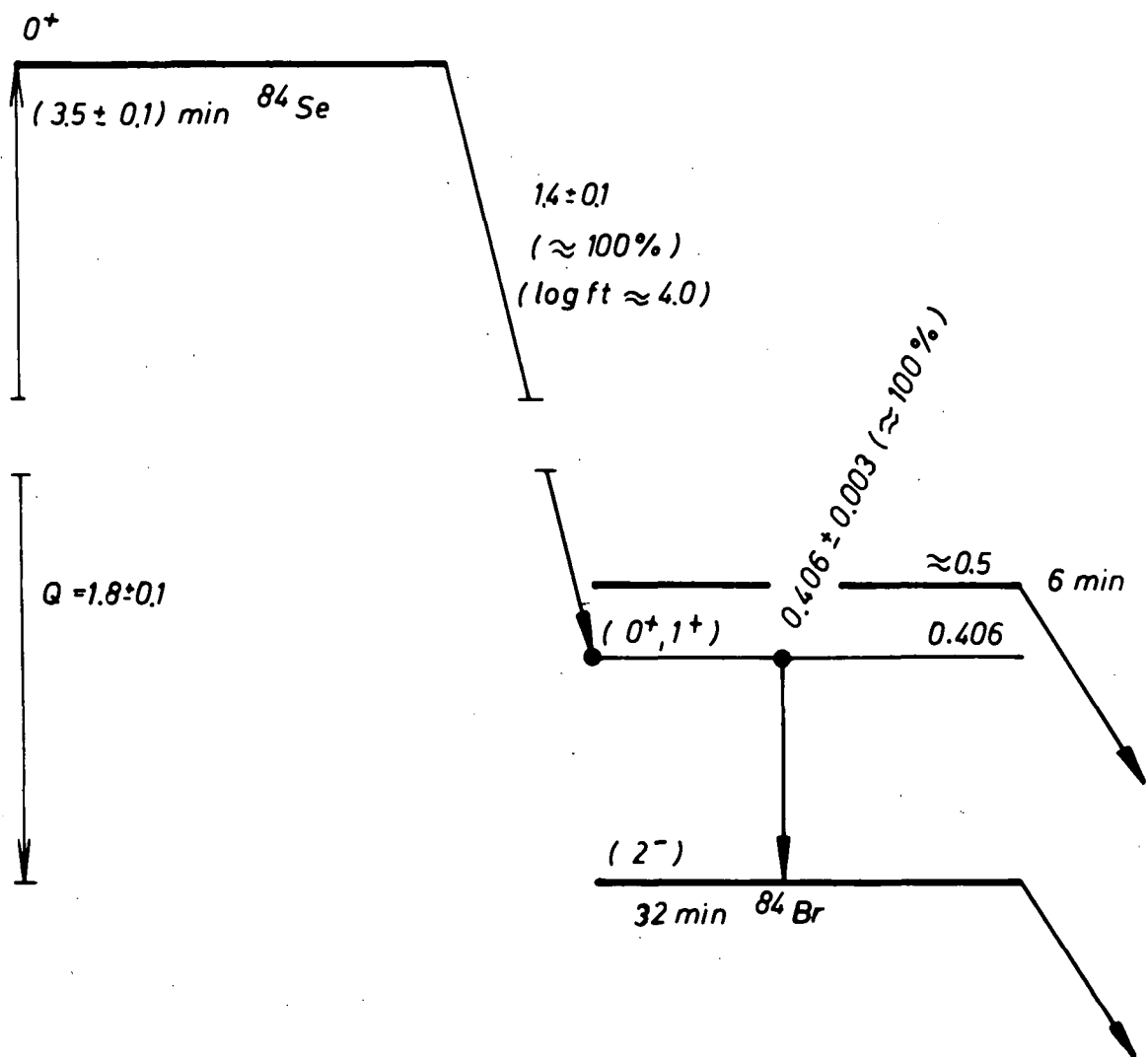


Fig. 1. Proposed decay scheme for ^{84}Se

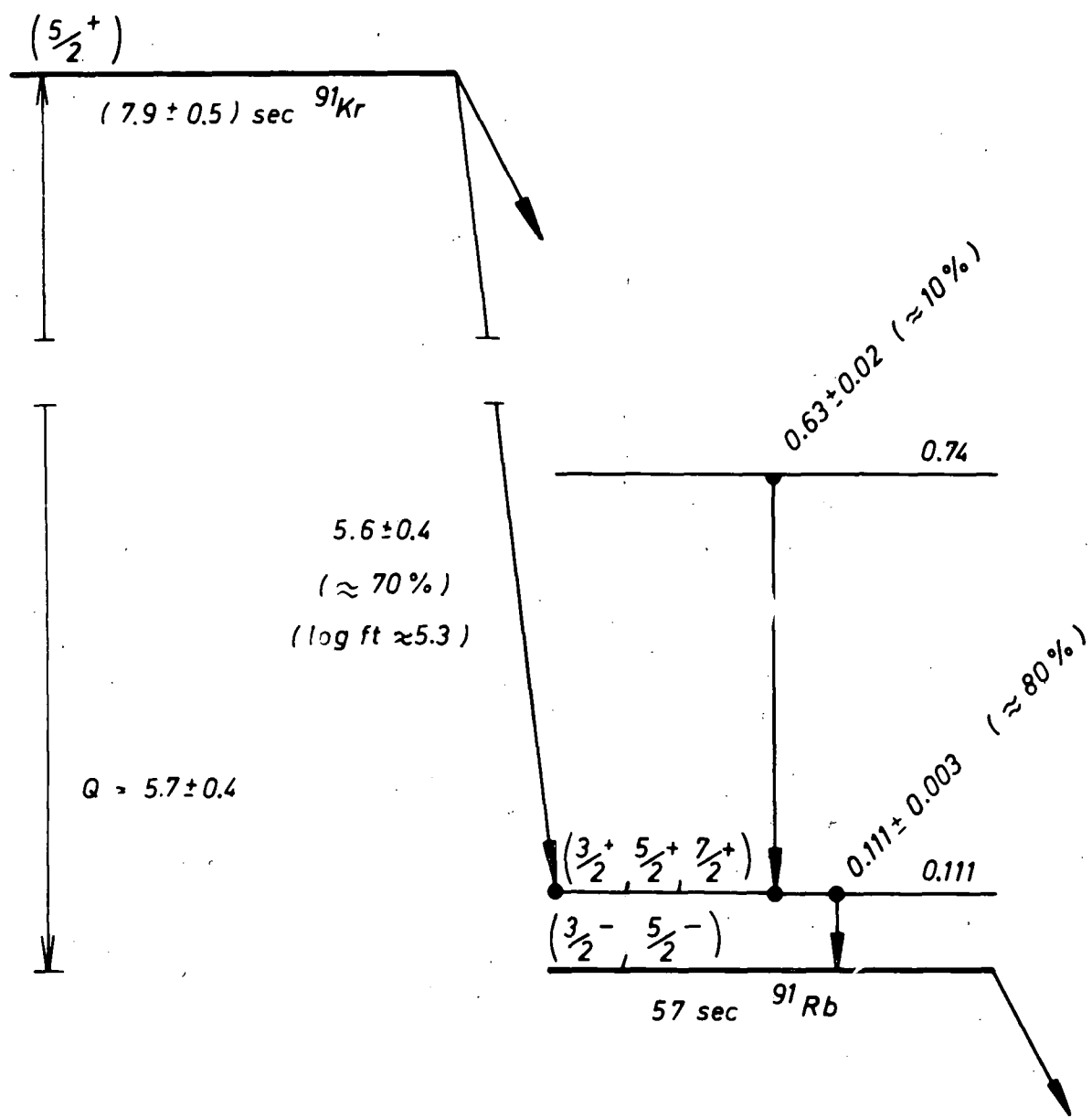


Fig. 2. Proposed decay scheme for ^{91}Kr

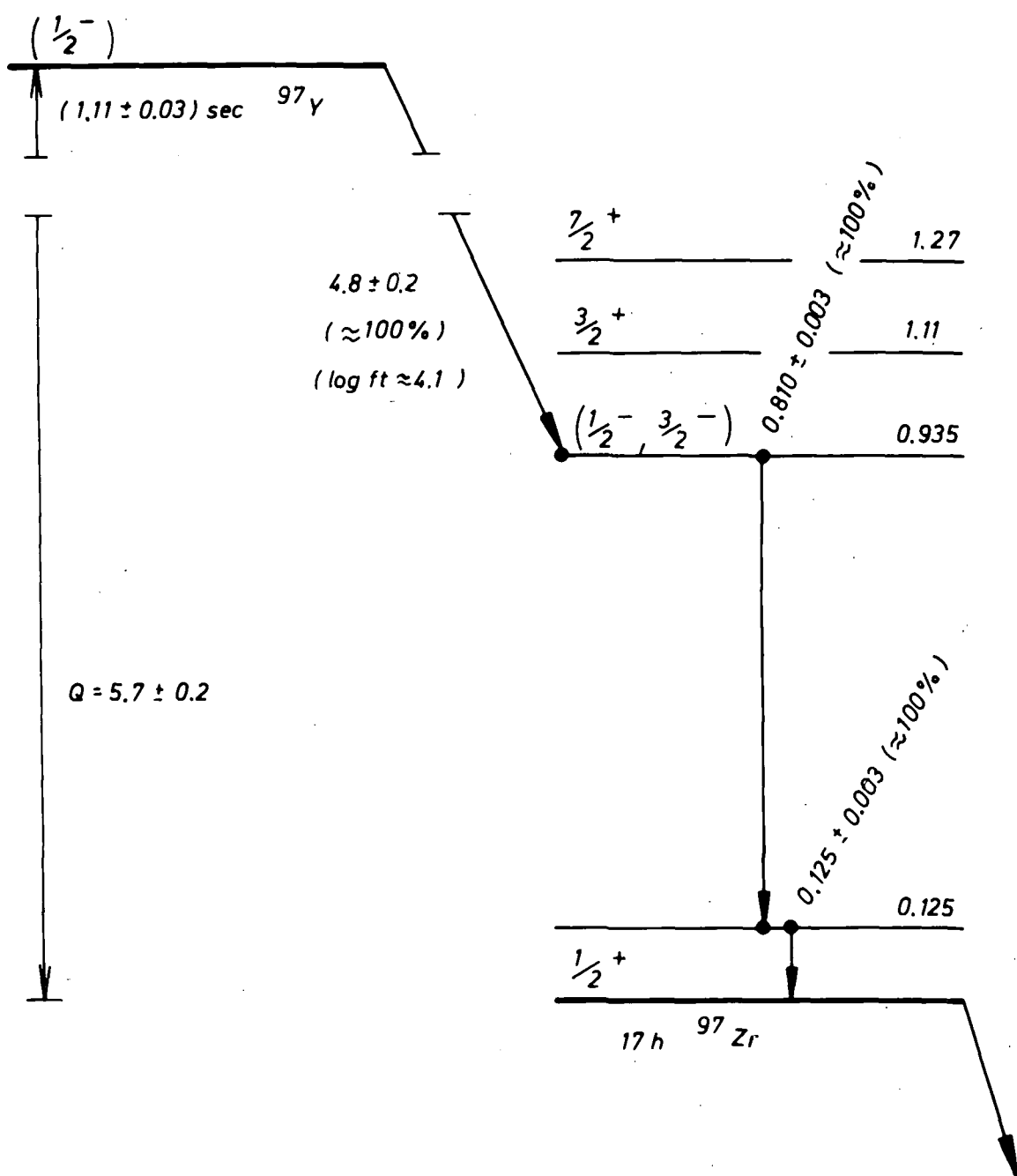


Fig. 3. Proposed decay scheme for ^{97}Y

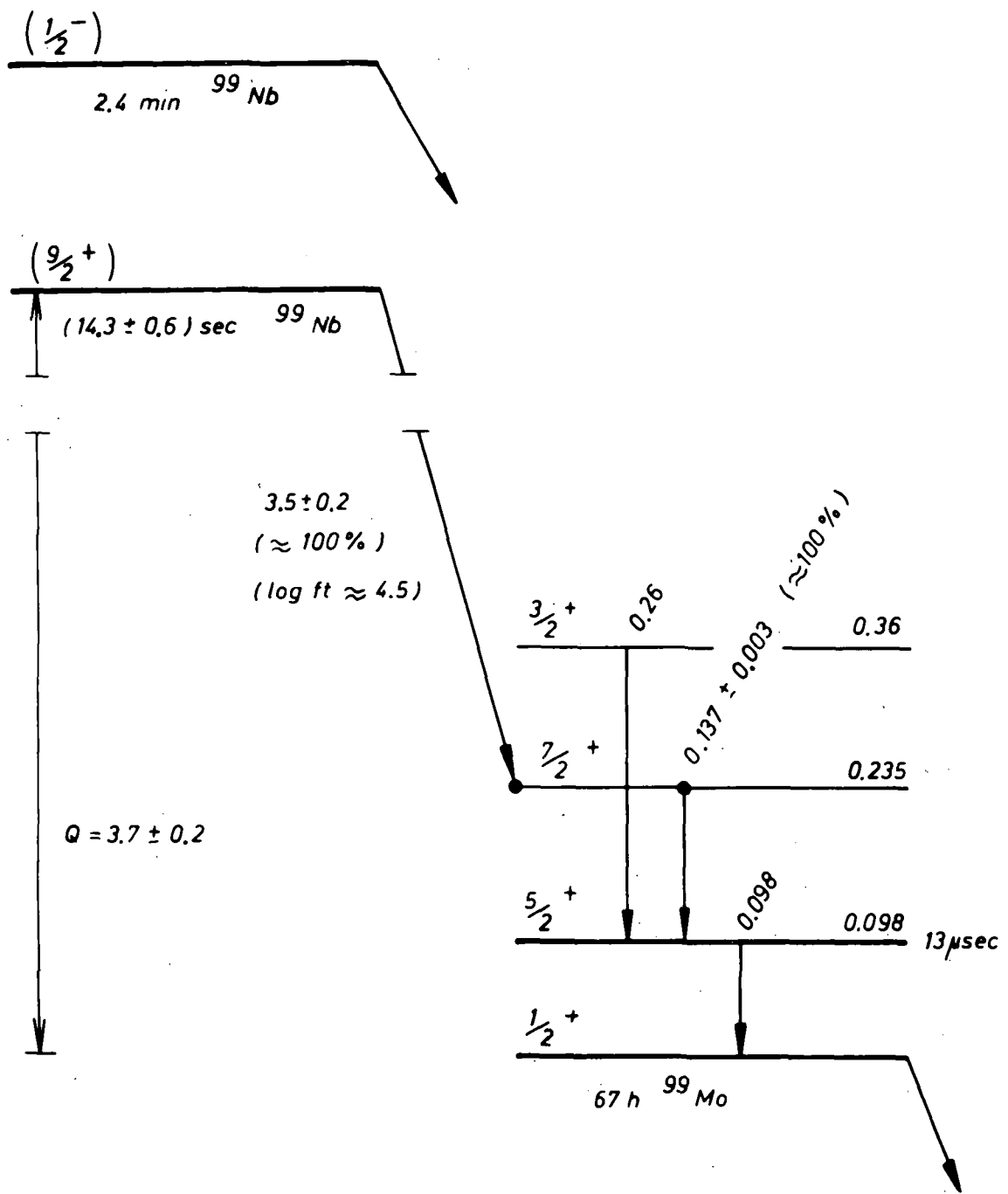


Fig. 4. Proposed decay scheme for ^{99}Nb

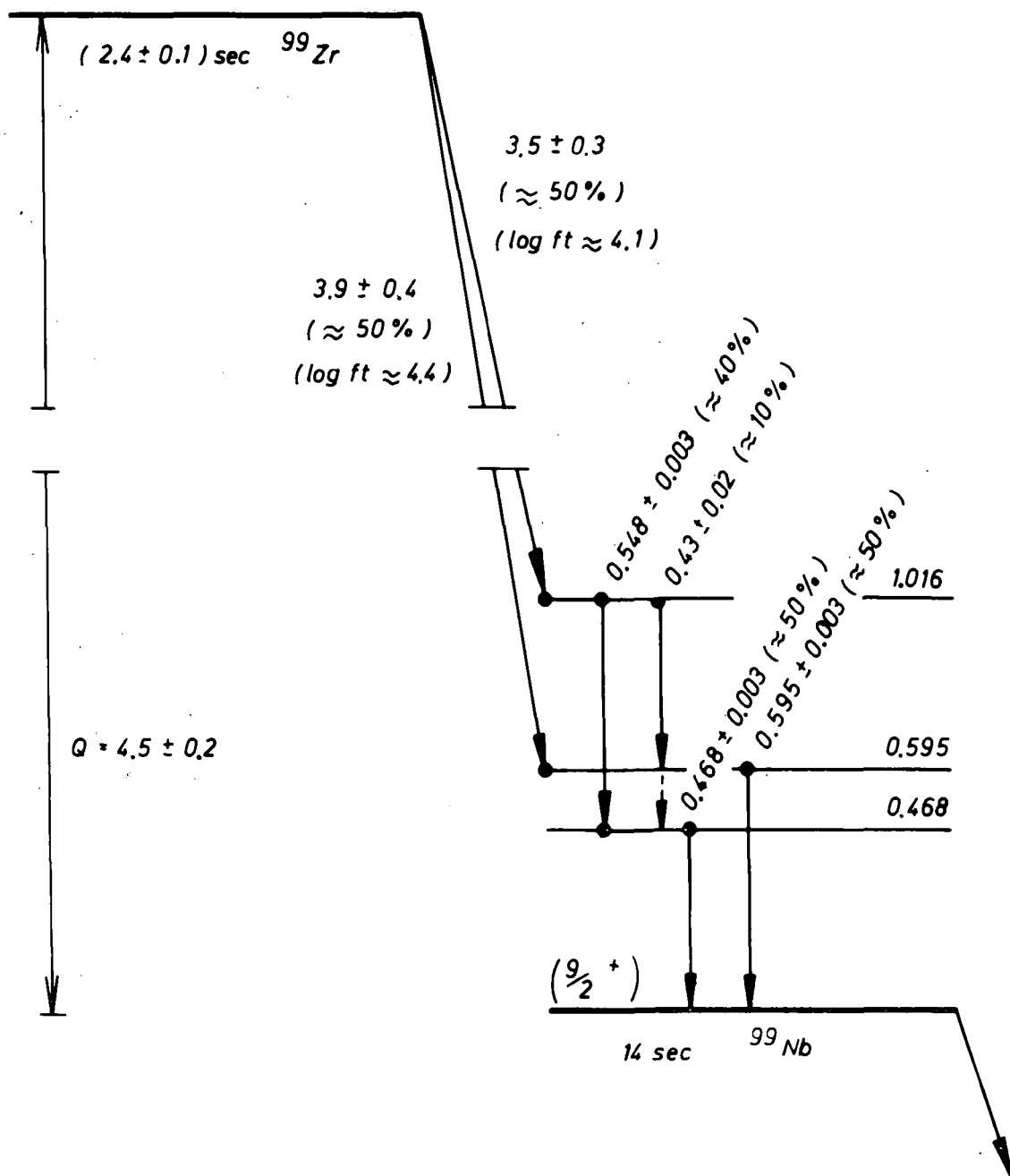


Fig. 5. Proposed decay scheme for ^{99}Zr

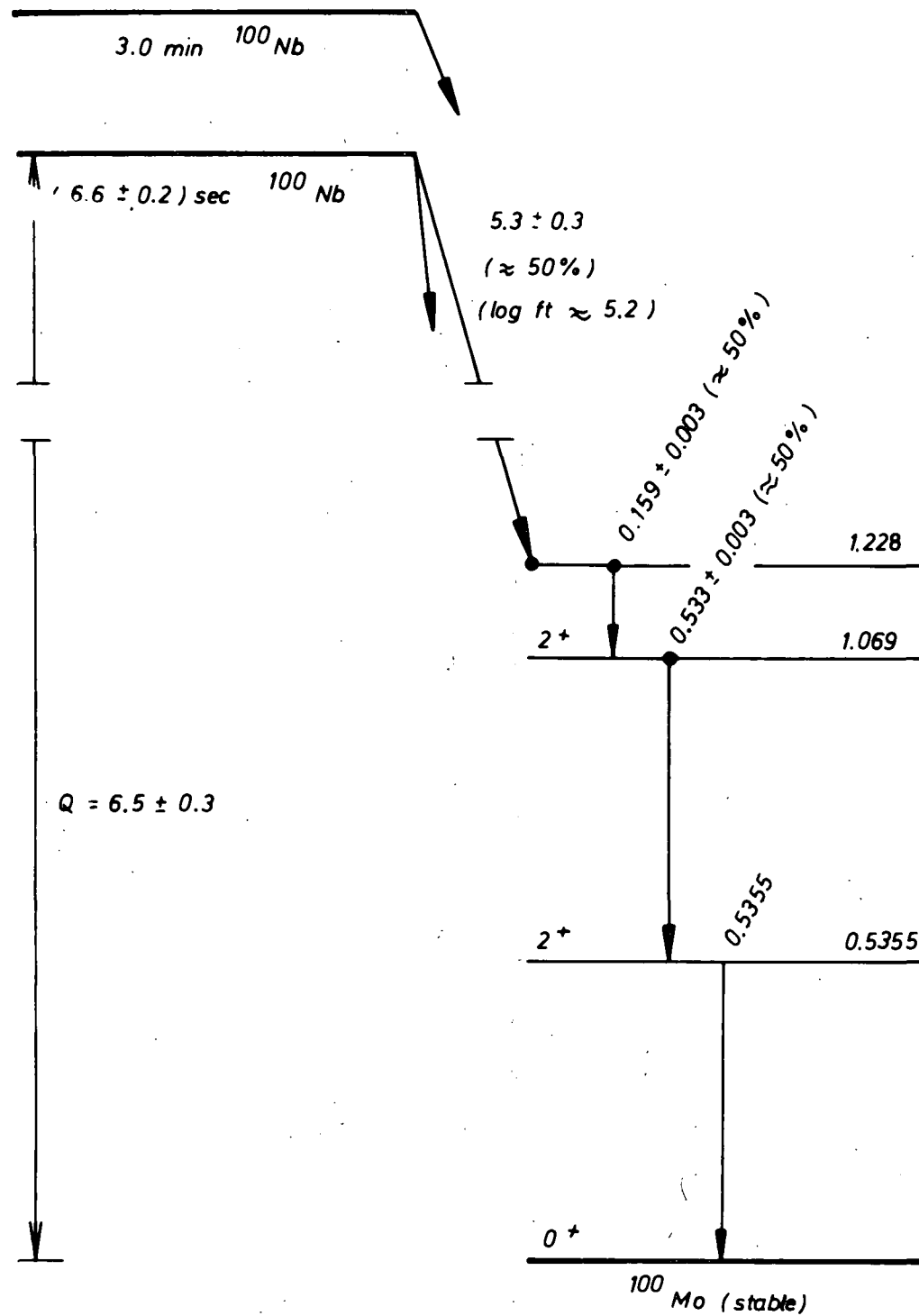


Fig. 6. Proposed decay scheme for ^{100}Nb

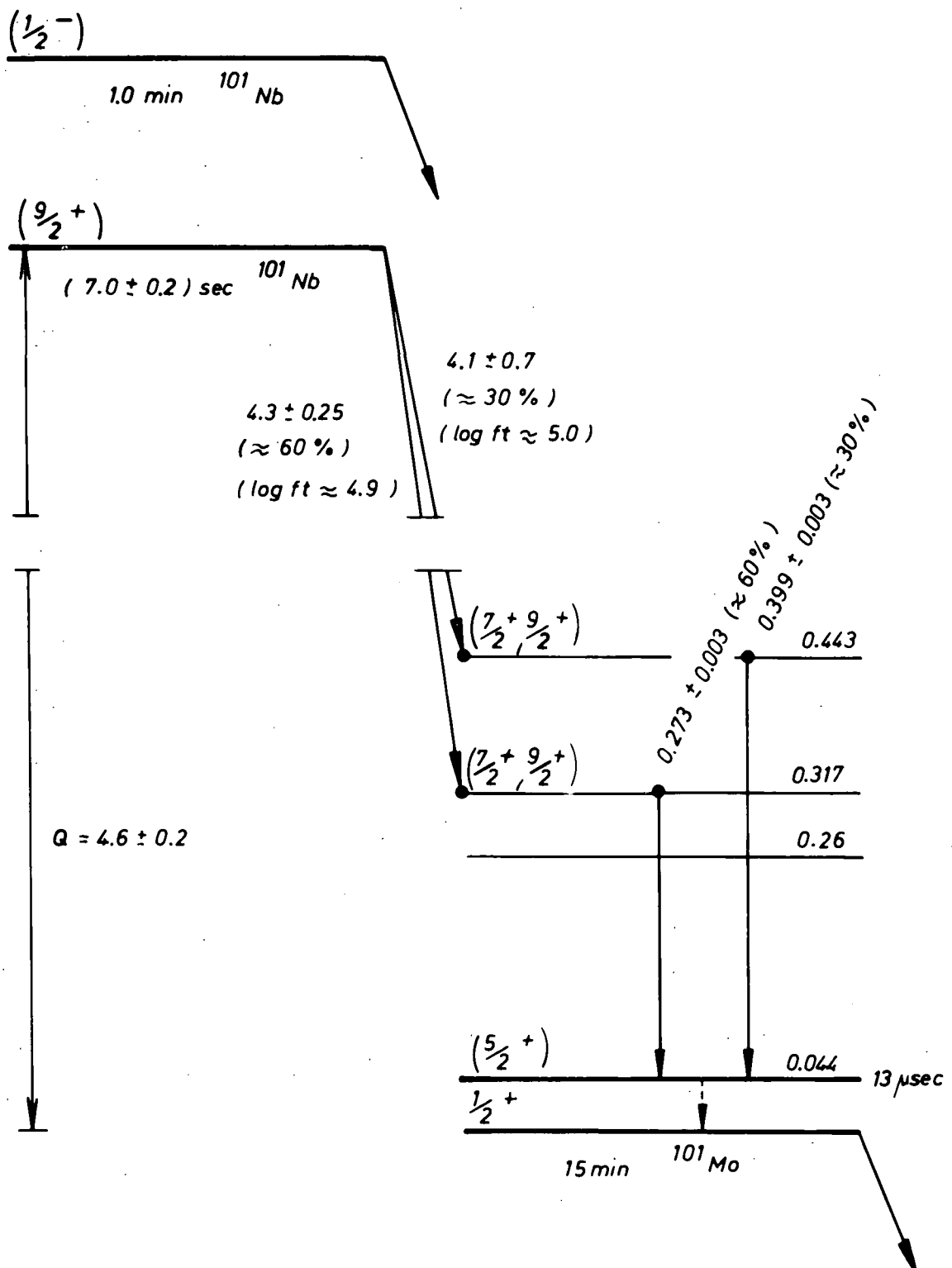


Fig.7. Proposed decay scheme for ^{101}Nb

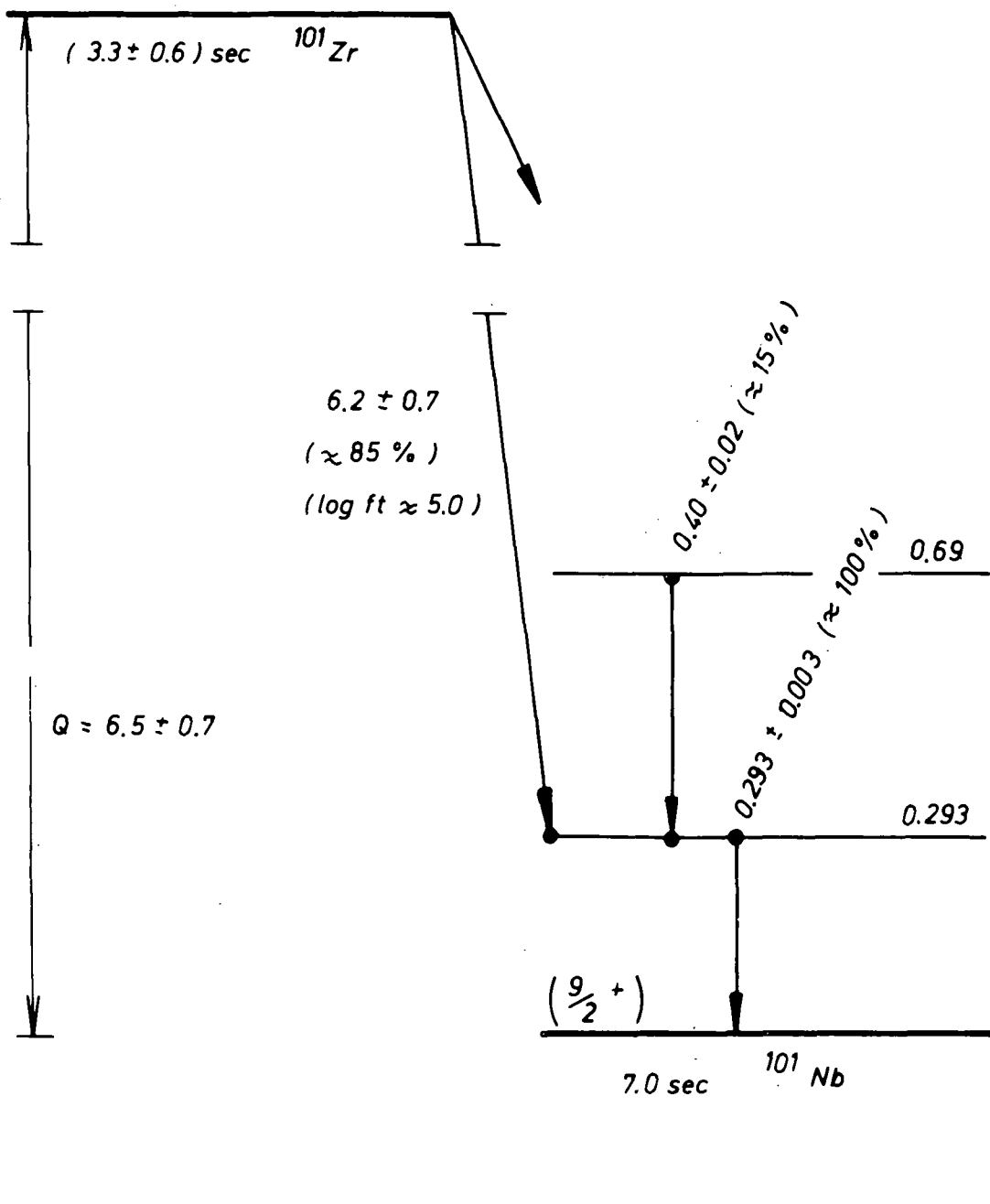


Fig. 8. Proposed decay scheme for ^{101}Zr

3. Mass Dependence of the Average Nuclear Charge of Primary Fission Products in the Thermal Fission of ^{235}U

(K. Sistemich, P. Armbruster)

The gas filled on-line separator for fission products at the reactor FRJ-2 has been used to remeasure primary charge values by absolute β -counting. The activity build-up technique combined with 4π -counting gives the number of β decays up to a time of 3000 sec after fission. From this measured quantity and the charge values of the fission products 3000 sec after fission which are calculated from the stable charge and the known long half-lives, the primary charge value has been obtained, (fig. 1). Using a new compilation of prompt neutron data (fig. 2) a Wahl diagram for thermal fission of ^{235}U has been plotted, (fig. 3). A comparison to a X-ray measurement of Reisdorf and Armbruster (1) and to a fit through all available radiochemical data is given in fig. 4. The discrepancy between the different measurements are never larger than 0.3 charge units, the average quadratic deviation between the measurements are 0.1 charge units. Nevertheless there seem to be still some systematic deviations between radiochemical and physical measurements.

- (1) W.Reisdorf, P.Armbruster: Phys. Lett. 24 B (1967) 501
- (2) J.C.D.Milton, J.S. Fraser: in "Physics and Chemistry of Fission", Proc. of the Salzburg Symposium (1965), IAEA Vienna Vol. II, p. 39
- (3) V.F.Apalin, Yu.N.Gritsyuk, I.E.Krutikov, V.I.Lebedev, L.A.Mikaelyan: Nucl.Phys. 55 (1964) 249
- (4) E.E. Maslin, A.L. Rodgers, W.G.F. Core: Phys Rev. 164 (1967) 1520
- (5) J.Terrell: Phys. Rev. 127 (1962) 880

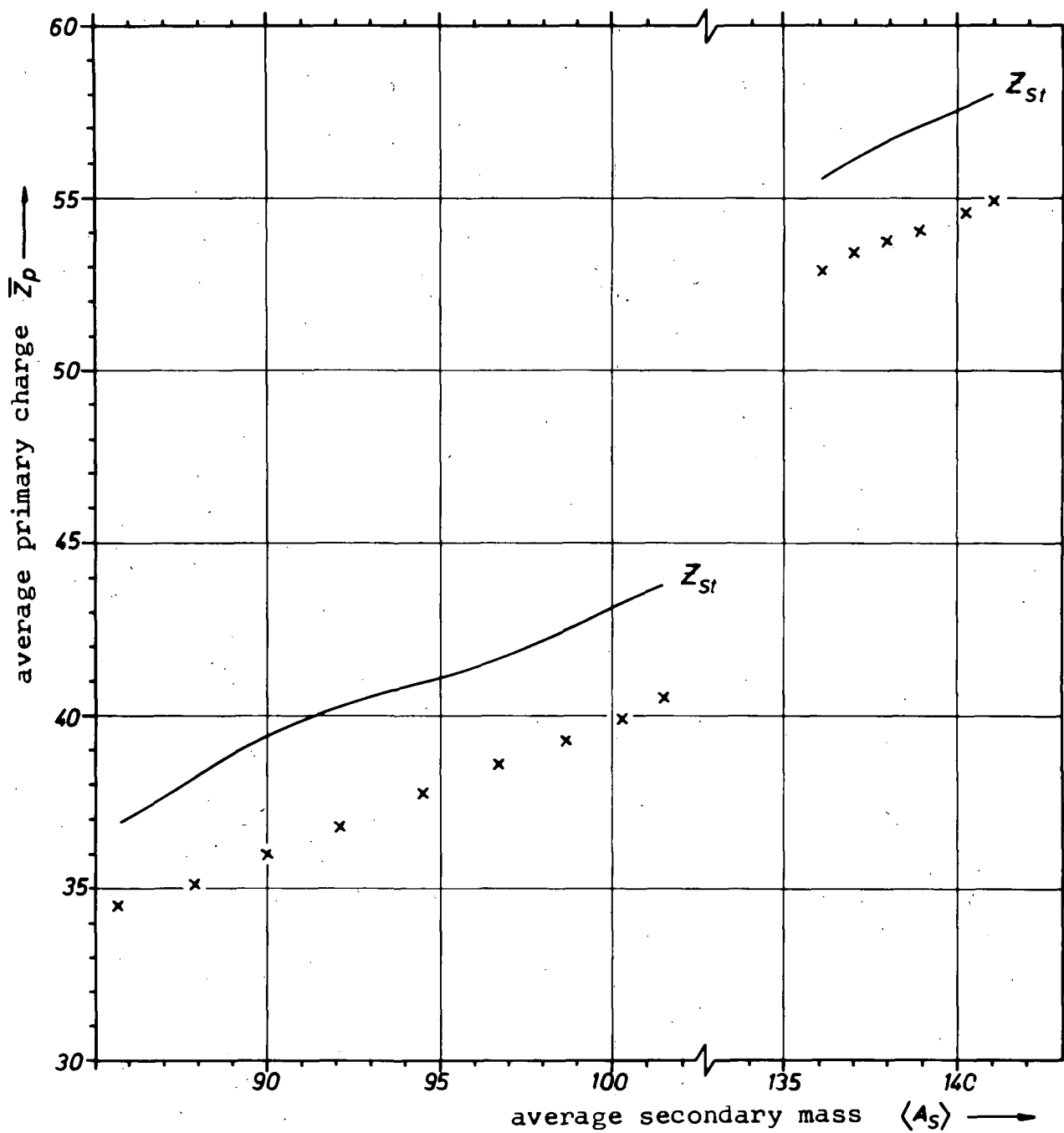


Fig. 1. The measured average primary charge as a function of the mass after prompt neutron emission. Errors correspond to the size of the crosses. The full lines give the values of the average stable charge.

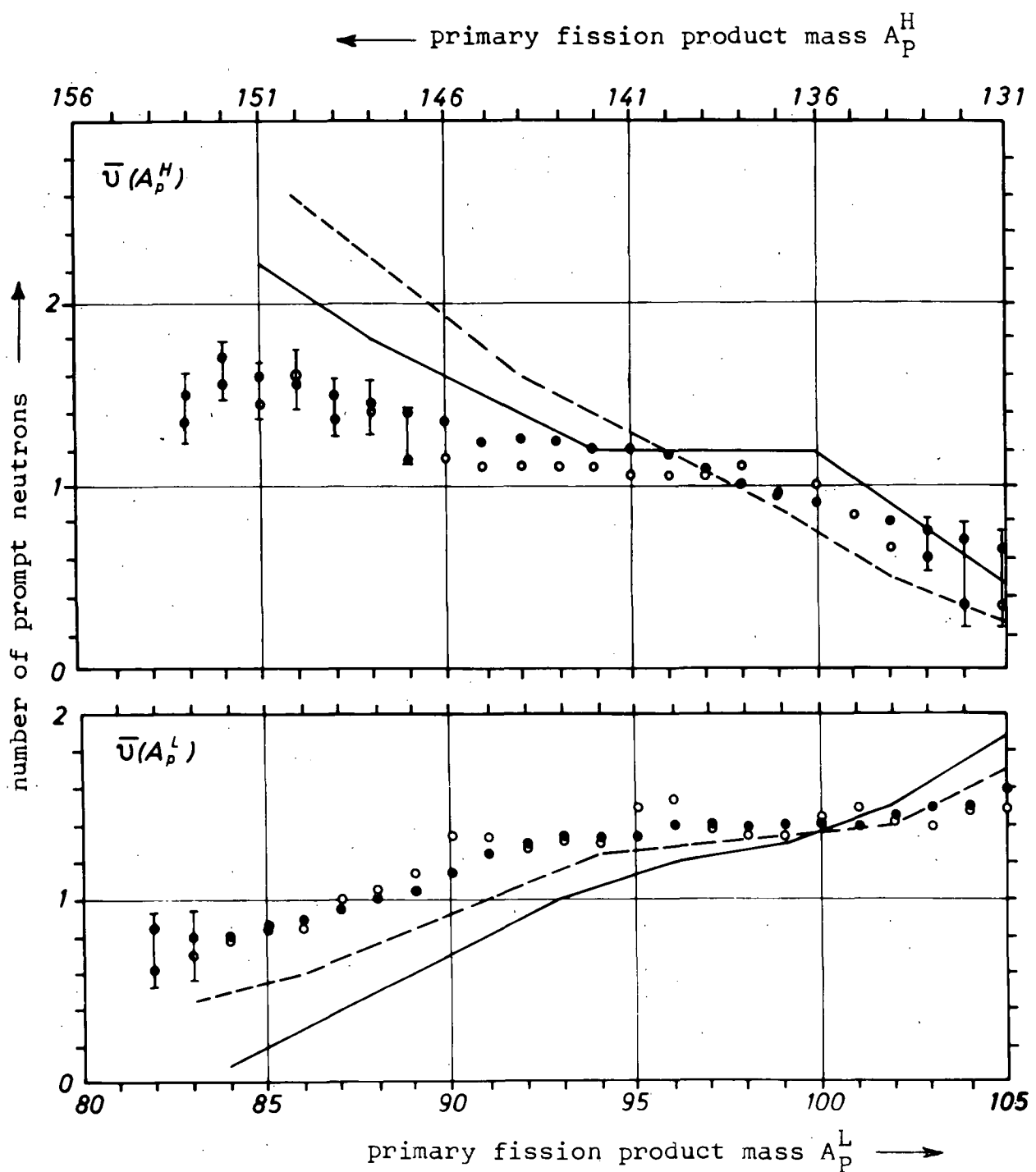


Fig. 2. Average number of prompt neutrons emitted from light and heavy fission fragments. The errors refer to the average value of the data of Milton and Fraser and of Maslin et al. They are given, if they are larger than ± 0.1 M.U.

- | | |
|-------------------------|-----|
| ○ Milton and Fraser (2) | (2) |
| -- Apalin et al. (3) | (3) |
| ● Maslin et al. (4) | (4) |
| — Terrell (5) | (5) |

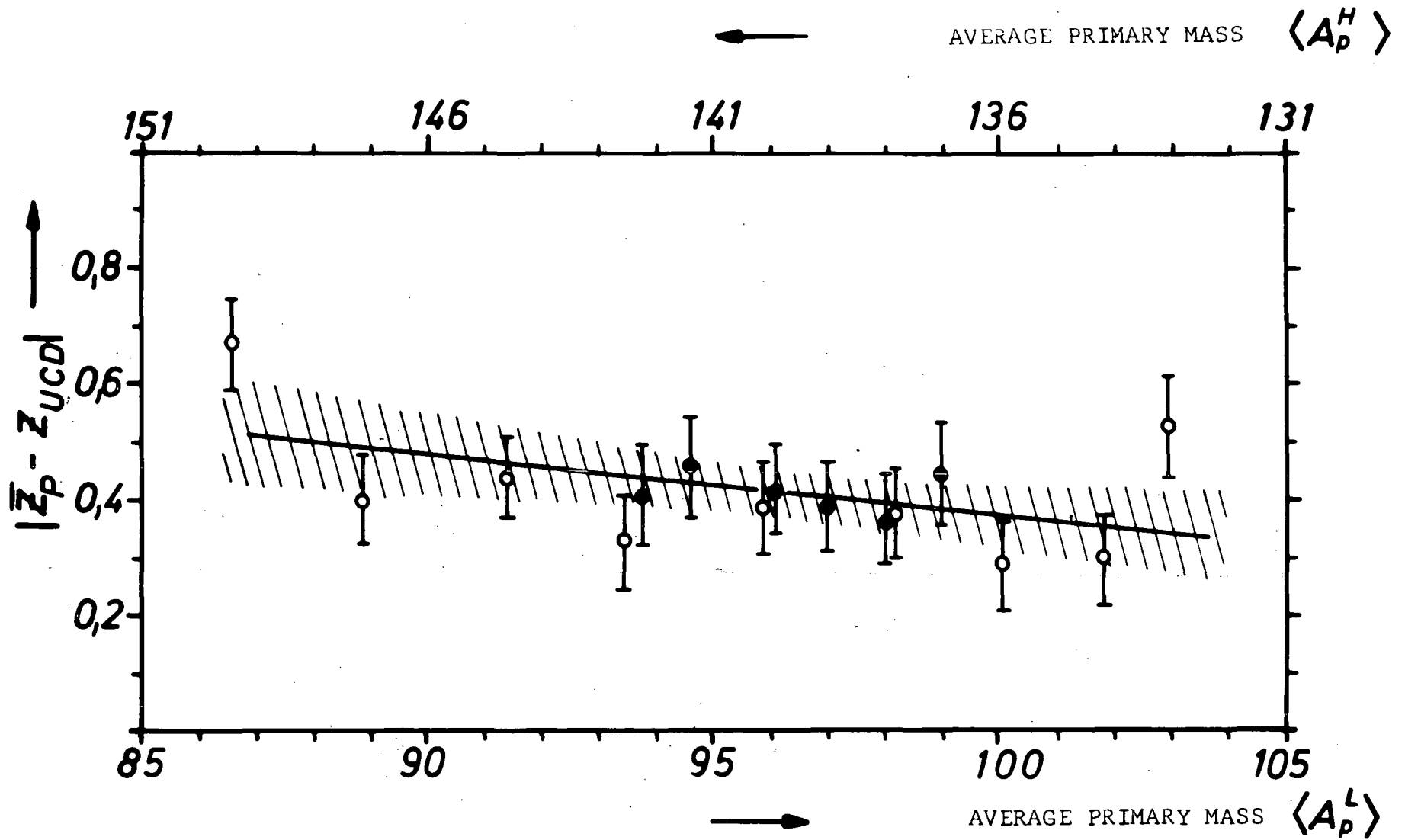


Fig. 3. The measured average primary charges plotted in a Wahl diagram. Open and full circles refer to light and heavy fission products, respectively. The straight line is a weighted least squares fit. A straight line through the measured values will be found with a 90 % probability within the hatched region.

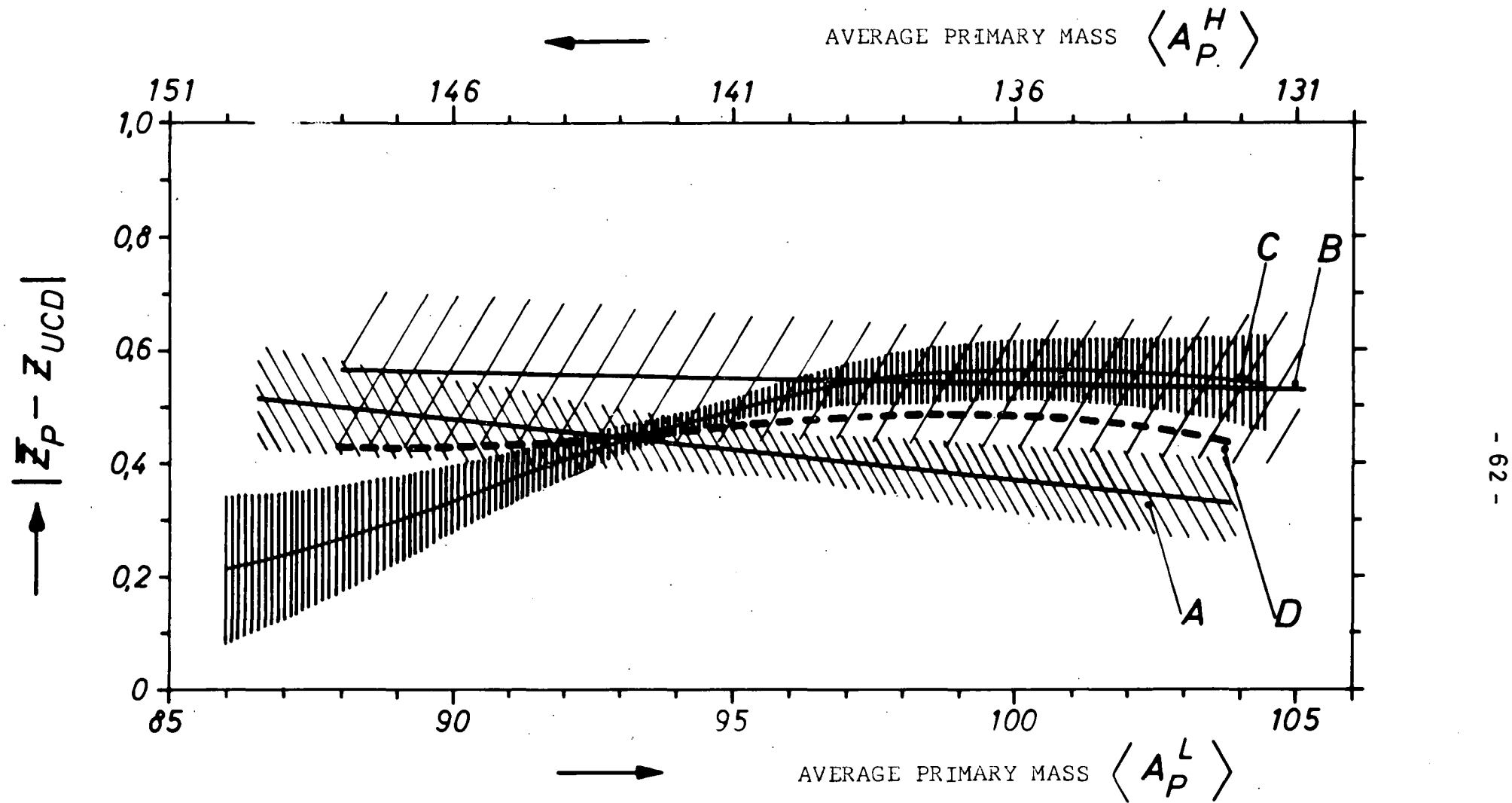


Fig. 4. Comparison of different measurements to determine Z_p : A) this measurement, B) measurement of Reisdorf and Armbruster(1), C) fit to radiochemical data, D) weighted average of all measurements.

VII. INSTITUT FÜR KERNPHYSIK, UNIVERSITY OF FRANKFURT/MAIN (GERMANY)

1. Excitation functions of the nuclear reactions

${}^6\text{Li}(\text{n},\text{p}){}^6\text{He}(0)$ and ${}^6\text{Li}(\text{n},\text{n}'\gamma){}^6\text{Li}(3.56)$

(G. Presser, R. Bass and K. Krüger)

Previously reported work on both reactions (see EANDC progress reports 1965 and 1967) has now been completed.

The (n,p) reaction was investigated from threshold to 9 MeV by neutron activation of a ${}^6\text{LiI}(\text{Eu})$ scintillator. The neutron energy resolution varied between 50 and 200 keV. Relative point to point errors are $\pm 5\%$ and absolute errors $\pm 15\%$. The results are given in fig. 1.

The ($\text{n},\text{n}'\gamma$) reaction was investigated from threshold to 6.5 MeV using a ring scatterer, which consisted of 200 g 96 % enriched metallic ${}^6\text{Li}$. Time of flight techniques were employed to reduce background due to room-scattered neutrons. The neutron energy resolution varied between 50 and 100 keV. Relative point to point errors are 8 - 25 % and absolute errors 12 - 30 %, depending on neutron energy. The results are given in fig. 2.

2. Excitation function of the nuclear reaction ${}^7\text{Li}(\text{n},\text{n}'\gamma){}^7\text{Li}(0.48)$

(G. Presser and R. Bass)

Previously reported work (see Antwerp conference 1965 and EANDC progress report 1965) with a NaI(Tl) γ -detector has been repeated using a 30 cm^3 Ge(Li) detector. The improved pulse height resolution simplified the data reduction and made the background subtraction more reliable. The neutron energy range from 1.0 to 8.8 MeV was covered with 50 keV resolution. Relative point to point errors are 5 - 15 % and absolute errors 10 - 20 % depending on neutron energy. The results are essentially in agreement with the earlier data; numerical values are available from the authors on request.

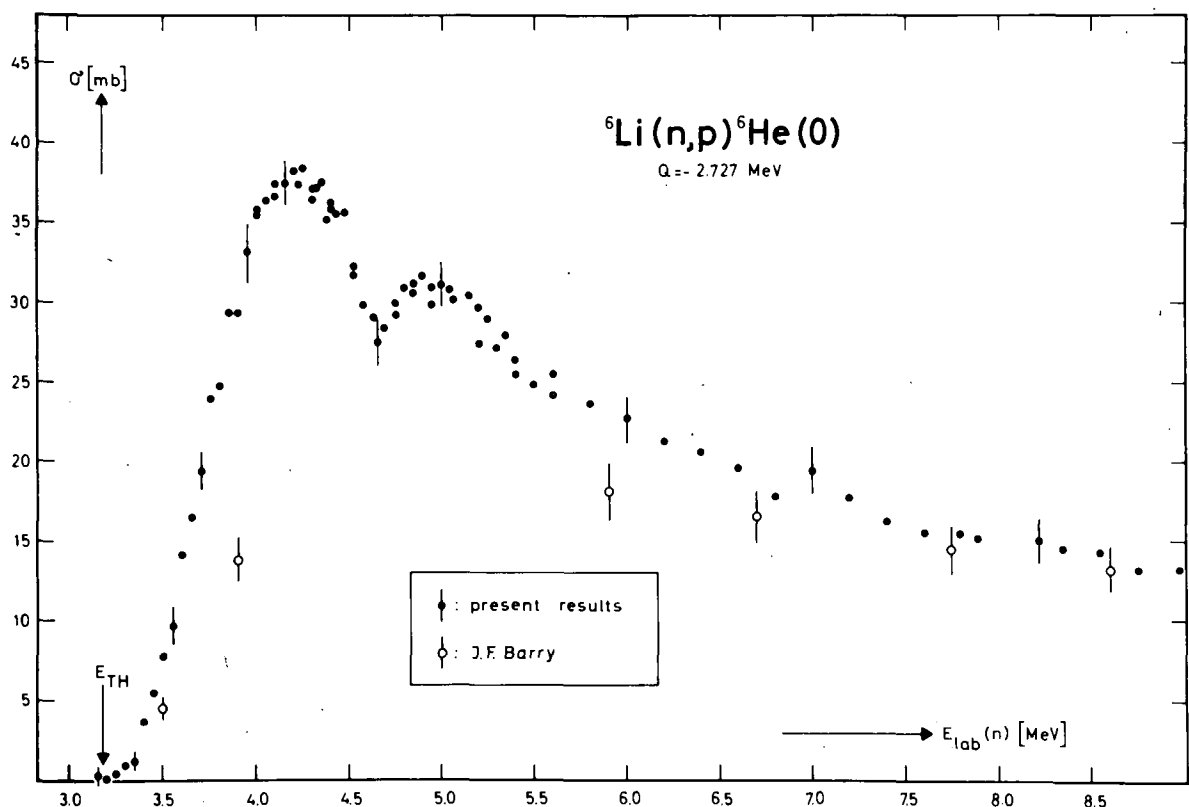


Fig. 1) Excitation function of the reaction ${}^6\text{Li}(\text{n},\text{p}){}^6\text{He}(0)$. The error bars for the present results include relative errors only. Results of J.F. Barry are from Reactor Science and Technology 17 (1963) 273.

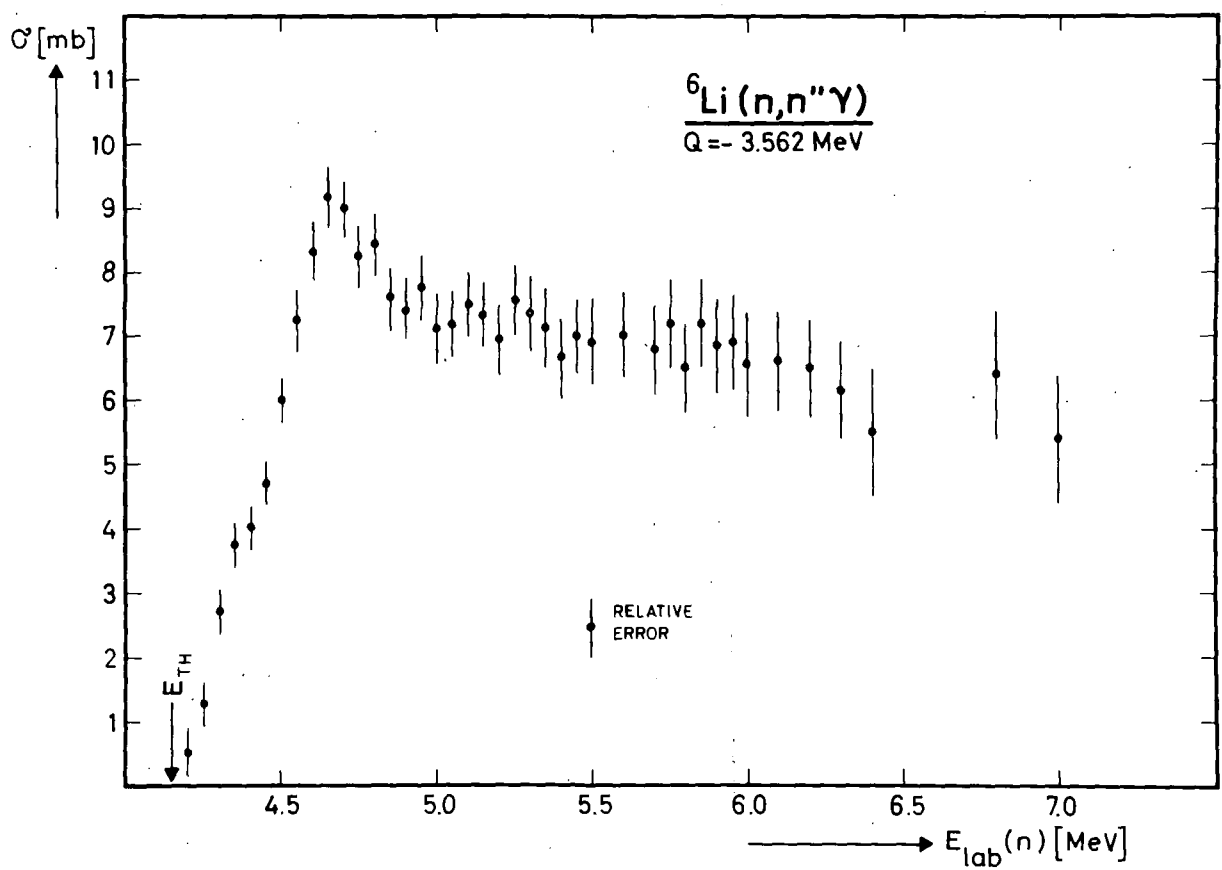


Fig. 2) Excitation function of the reaction ${}^6\text{Li}(n,n'\gamma){}^6\text{Li}(3.56)$.
The error bars include relative errors only.

VIII. PHYSIKALISCHES STAATSINSTITUT, I. INSTITUT FÜR EXPERIMENTAL-PHYSIK, HAMBURG (GERMANY)

1. Angular Distributions for (n,α) Reactions at 14 MeV

U. Seebek, D. Kaack and M. Bormann.

Angular distributions were measured for the groups α_0 and α_{123} from the reaction $^{16}\text{O}(n,\alpha)^{13}\text{C}$ at 14.1 MeV and for the total α -particles from the (n,α) reactions in ^{93}Nb , ^{103}Rh and ^{107}Ag at 14.2 MeV. The α -particles were detected by means of a thin CsI crystal, the pulse-shape discrimination method was used to distinguish α -particles from other particles and γ -radiation. The results are given in Table I.

For the heavier elements the energy spectra and angular distributions of the α -particles were analysed according to the statistical theory. About 60 - 70 % of the total reaction yields have symmetric angular distributions and can be ascribed to evaporation processes. The remaining portions are emitted predominantly at forward angles which makes their origin from direct reactions probable.

Table I: Differential cross sections of (n, α) reactions

$E_n = 14.1 \text{ MeV}$				$E_n = 14.2 \text{ MeV}$						
θ CM	$\frac{d\sigma}{d\Omega} (\text{mb/sr})$	θ CM	$\frac{d\sigma}{d\Omega} (\text{mb/sr})$	θ CM	$\frac{d\sigma}{d\Omega} (\text{mb/sr})$	θ CM	$\frac{d\sigma}{d\Omega} (\text{mb/sr})$	θ CM	$\frac{d\sigma}{d\Omega} (\text{mb/sr})$	
22.9°	1.94 ± 0.09	23.6°	20.9 ± 0.23	37°	1.66 ± 0.29	37°	0.63 ± 0.21	37°	1.21 ± 0.16	
50.1°	0.52 ± 0.05	51.3°	8.8 ± 0.30	57°	1.30 ± 0.12	57°	0.50 ± 0.11	57°	0.60 ± 0.08	
65.5°	1.03 ± 0.07	66.8°	6.4 ± 0.21	81°	0.37 ± 0.07	81°	0.14 ± 0.03	81°	0.26 ± 0.06	
82.3°	0.61 ± 0.08	84.3°	3.9 ± 0.22	99°	0.34 ± 0.07	99°	0.22 ± 0.04	99°	0.29 ± 0.07	
92.6°	0.98 ± 0.11	94.6°	2.5 ± 0.21	123°	0.38 ± 0.09	123°	0.29 ± 0.10	123°	0.32 ± 0.07	
104.6°	1.77 ± 0.11	106.6°	6.0 ± 0.19	143°	0.47 ± 0.19	143°	0.54 ± 0.24	143°	0.54 ± 0.19	
116.1°	1.49 ± 0.20									
136.6°	1.66 ± 0.25									
154.3°	1.23 ± 0.27									
				$\sigma_{tot} = 9.2 \pm 0.7 \text{ mb}$				$\sigma_{tot} = 4.1 \pm 0.7 \text{ mb}$		
								$\sigma_{tot} = 6.7 \pm 0.5 \text{ mb}$		

2. Excitation Functions of (n,p) and (n,2n) Reactions for some Isotopes of K, Mn, Zn, and Cu.

M..Bormann and B. Lammers

The excitation functions of the (n,p) reactions for ^{41}K and ^{64}Zn were measured in the energy region 13 - 18 MeV by means of the activation method. Gamma activities were detected by integral bias gamma counting with a 3"Ø x 2" NaI well-crystal. The neutrons were produced in a water-cooled thin titanium-tritium target via the reaction $^3\text{H}(\text{d},\text{n})^4\text{He}$ with 2 MeV deuterons from a Van de Graaff accelerator. The neutron flux was measured with a 1"Ø x 1" stilbene recoil proton spectrometer. The results are given in Table I. They were compared with statistical theory calculations and good agreement was obtained in most cases.

Table I: Experimental (n,2n) cross - sections in mb

E_n (MeV)	$^{41}\text{K}(n, p)^{41}\text{A}$ $T_{1/2} = 103.5 \pm 2.4 \text{ m}$	$^{55}\text{Mn}(n, 2n)^{54}\text{Mn}$ $T_{1/2} = 313 \pm 7 \text{ d}$	E_n (MeV)	$^{63}\text{Cu}(n, 2n)^{62}\text{Cu}$ $T_{1/2} = 9.65 \pm 0.02 \text{ m}$	$^{65}\text{Cu}(n, 2n)^{\text{Cu}^{64}}$ $T_{1/2} = 762 \pm 10 \text{ m}$
12.99 \pm 0.10	57.4 \pm 6.0	600 \pm 78	13.21 \pm 0.21	399 \pm 27	809 \pm 55
14.10 \pm 0.15	49.2 \pm 4.4	798 \pm 78	14.10 \pm 0.14	552 \pm 37	906 \pm 61
15.03 \pm 0.14	40.5 \pm 4.8	834 \pm 82	15.46 \pm 0.15	705 \pm 48	957 \pm 65
15.57 \pm 0.15	38.4 \pm 4.4	844 \pm 66	16.05 \pm 0.15	737 \pm 50	964 \pm 65
16.16 \pm 0.15	31.5 \pm 3.8	803 \pm 79	16.56 \pm 0.15	760 \pm 52	975 \pm 66
16.66 \pm 0.15	---	820 \pm 80	17.08 \pm 0.14	797 \pm 57	983 \pm 67
17.12 \pm 0.14	27.5 \pm 3.2	881 \pm 86	17.48 \pm 0.14	866 \pm 62	1006 \pm 68
17.84 \pm 0.13	19.8 \pm 2.2	---	18.04 \pm 0.12	895 \pm 72	1052 \pm 59
18.06 \pm 0.13	---	861 \pm 84			
18.19 \pm 0.12	20.9 \pm 2.8				
E_n (MeV)	$^{64}\text{Zn}(n, p)^{64}\text{Cu}$ $T_{1/2} = 756.0 \pm 9.4 \text{ m}$	$^{64}\text{Zn}(n, 2n)^{63}\text{Zn}$ $T_{1/2} = 37.85 \pm 0.06 \text{ m}$	$^{66}\text{Zn}(n, 2n)^{65}\text{Zn}$ $T_{1/2} = 245.7 \pm 1.1 \text{ d}$		
14.10 \pm 0.14	191.7 \pm 12.4	131.1 \pm 8.2	758 \pm 54		
14.82 \pm 0.14	145.4 \pm 9.8	208.1 \pm 10.8	864 \pm 62		
15.46 \pm 0.15	155.4 \pm 10.3	273.8 \pm 17.4	963 \pm 67		
16.05 \pm 0.15	133.3 \pm 8.7	319.5 \pm 20.1	965 \pm 65		
16.51 \pm 0.15	141.4 \pm 9.3	372.1 \pm 23.4	1028 \pm 71		
17.08 \pm 0.14	132.8 \pm 8.9	402.1 \pm 25.4	1081 \pm 75		
17.48 \pm 0.14	120.3 \pm 8.0	408.4 \pm 25.8	1082 \pm 74		
17.84 \pm 0.13	118.1 \pm 7.7	438.3 \pm 27.6	1125 \pm 77		
18.06 \pm 0.13	125.7 \pm 8.0	---	1135 \pm 77		
18.13 \pm 0.11	---	447.7 \pm 40.3	---		
18.19 \pm 0.12	113.9 \pm 7.6	---	---		

**IX. INSTITUT FÜR REINE UND ANGEWANDTE KERNPHYSIK DER
UNIVERSITÄT KIEL (IKK), GEESTHACHT**

1. Fast Chopper

H.H. JUNG, H.G. PRIESMEYER, S. CHAKRABORTY, H. SULITZE

1.1 Resonance Parameters of Cs 133

As part of the total neutron cross section measurements on fission product Caesium, which contains stable Cs 133 and the two radioactive isotopes Cs 135 and Cs 137 to roughly equal parts, total cross section measurements on natural Caesium 133 have been done.

Samples of powdered CsCl of very high purity with four different thicknesses (Tab. I) were run at three different rotor speeds (Tab. II).

18 resonances have been found up to 400 ev. Resonance parameters of 13 of them have been determined by area analysis (Tab. III). For this purpose we used the area analysis program by S. ATTA and J.A. HARVEY (1), which was altered slightly for the use on a CD 3400 computer.

These results will be published in Atomkernenergie at the beginning of 1969. Measurements on fission product Caesium will be started in January 1969.

1.2 Total Cross Section Measurements on Ruthenium

Part of the chopper program is the determination of resonance parameters of Ruthenium isotopes. Runs on natural Ruthenium and on separated isotopes (Ru 100, 101, 102, 104) are planned.

The runs on natural Ruthenium were started in 1968 and will be completed during the next year. Resonance analysis of

these runs is underway. The runs on the separated isotopes are scheduled for 1969.

1.3 A Lithium Glass Detector Bank for Neutron Time-of-Flight Measurements

Under this title a publication has been accepted by Nuclear Instruments and Methods as a letter to the editor. In this article the detector bank of the fast chopper time-of-flight spectrometer has been described.

1.4 Development of a New Liquid Scintillation Counter for Neutron Time-of-Flight Measurements

Based on the work of ROSS et.al. (2), a new liquid scintillation counter for neutron energies up to several hundred ev has been developed.

Solvent and target material is N,N,N,trimethylborazine. 10 percent of IPBP for increasing the solubility of scintillator and phase shifter, and 20 percent of naphthalene for increasing pulse height have been added. BIBUQ, a new product by E. MERCK, Darmstadt, and dimethyl - POPCP served as scintillator and phase shifter resp.

Detectors of about 1 cm geometrical thickness are competitive with lithium glass detectors of about 2 cm thickness when efficiency and signal-to-background ratio is considered (the use of enriched boron for the fabrication of N,N,N,trimethylborazine is supposed). The advantages of the new detector are low cost, the possibility to prepare it easily at the own laboratory without large amount of facilities, and to fit it to all desired geometries.

1.5 Total Neutron Cross Sections of Gross Fission Products

It is intended to do total neutron cross section measurements

on gross fission products. For this purpose, samples of U 235 with tight cannings will be irradiated in a reactor to a certain burnup. After a decay time which is necessary in order to decrease the activity of the samples, transmission measurements on these samples, which contain the whole spectrum of - not too short living - fission products and the remaining U 235, will be done.

Before preparing such measurements, it was necessary to investigate, whether those measurements will be reasonable or not, i.e. whether one can expect to see any individual resonances in the transmission curves - and perhaps - identify them. This is not trivial as there are nearly 200 fission products, and all of them are expected to have a large number of resonances in the energy range of interest (1 to 1000 ev).

Basing on the well known statistical properties of resonance parameters, it is possible to generate by means of Monte Carlo methods total cross sections as function of energy for every fission product. Weighing such cross sections by the nuclide concentrations of the fission products, which can be calculated from the known yields, half lives, and thermal capture cross sections, and summing over all fission products, one gets a total cross section which is not identical with the true cross section, but which shows how it will be in principle.

Basing on the result of such calculations one can decide, whether the measurements of such cross sections will be reasonable or not.

For the generation of the cross sections of the fission products by means of Monte Carlo methods, a FORTRAN routine, called BRWIG was written. The nuclide concentrations were calculated with another FORTRAN routine, called NUCY, which was written by D.R. VONDY (3). NUCY is a zero dimensional, two energy group burnup program, which allows to calculate fission product concentrations as function of neutron flux, ratio of thermal to fast flux, burnup, and time after shut down.

As an example of these calculations, Fig. 1 shows the total cross section curve of a mixture of fission products with the remaining U 235 as function of energy. A thermal flux of $0.5 \cdot 10^{14}$ n/cm²/sec, a fast flux of 1.5×10^{14} n/cm²/sec, 40 percent burnup, and a four weeks period after shut down were assumed in this case. The cross section curve has been corrected for Doppler and resolution effects (20°C sample temperature, and 54 n sec/m resolution for the energy range from 10 to 100 ev, and 27 n sec/m resolution for the energy range from 100 to 1000 ev were assumed).

This curve and other ones show clearly that it is possible to resolve a lot of resonances in the cross section of fission product mixtures up to at least 100 ev with our time-of-flight equipment. Therefore, preparations of such measurements were started.

This theoretical work has been edited as a "Diplomarbeit" (H. SULITZE) and will be published in Atomkernenergie. A description of the computer programs is given in an internal report of the Gesellschaft für Kernenergiewertung in Schiffbau und Schiffahrt mbH., Geesthacht (GKSS).

References:

- (1) ORNL 3205 and Supplement
- (2) Nucl. Instr. Meth. 33 (1965) 194
- (3) ORNL - TM - 361 and Addendum

2. Cristal Spectrometer

K. BRAND and M. SAAD

2.1 The Effect of Chemical Binding on Neutron Cross Sections of Metalhydrides, -deuterides, Uranium Carbide and Uranium Oxide.

The total neutron cross section was measured by a crystalspectrometer at room temperature. The energy range was 0,05 to 0,5 ev and the resolution between 1 and 3 %.

2.1.1 $\text{NbH}_{0,9}$ and $\text{NbD}_{0,86}$

The cross section pro proton shows two well-separated optical niveaus at 0,120 and 0,158 ev. Both are attributed to the 0 - 1 transitions of hydrogen atoms in the metal lattice. This doublet-structure is believed to arise from splitting in the optical band into transverse and longitudinal modes. Another niveau (0 - 2 transition) is observed at 0,315 ev.

The cross section pro deuteron shows the same splitting into two well-separated niveaus at 0,088 and 0,112 ev. The results are published in ATKE 6 (1968), 458.

2.1.2 $\text{TiH}_{1,56}$ was measured with different temperatures up to 470°C .

2.1.3 The cross sections of YH_3 and YD_3 were measured and show no clear niveaus due to the complex structure of these substances.

2.1.4 $\text{UH}_{2,67}$ and $\text{UD}_{2,67}$ (Uranium Hydride and -Deuteride)

The vibration energy was determined to be 0,112 ev for $\text{UH}_{2,67}$ and 0,092 for $\text{UD}_{2,67}$. The second excited state (0,258 ev) of $\text{UH}_{2,67}$ is not the double of the first state.

because of the anharmonic and anisotropic binding. (Results are published in ATKE 6 (1968), 458).

2.1.5 Uranium carbide UC

The vibration energy was determined to be 0,044 ev for (o - 1) transition and 0,086 ev and 0,137 ev for (o - 2) and (o - 3) transition due to second and third excitation of the carbon atom.

2.1.6 Uranium dioxide UO_2

A predicted structure with discrete energy levels is observed. The data show a pronounced structure near 0,035 ev, 0,049 ev and 0,073 ev excitation.

The results will be published in ATKE.

3. Stern Gerlach Experiment with Neutrons

M. NAGIB

The Stern Gerlach experiment has been reconstructed at beam hole 6 at the FRG-1. The adjustment of the apparatus was finished in February. Since March the following measurements have been carried out:

3.1 Measurement of the deviation from magnetic saturation for polycrystalline cobalt metal in the field range $2500 \leq H \leq 25000$ Oe. The metal is of high purity (99,99%) and was heated for about 100 hours at 400°C in vacuum. The experimental result shows proportionality with $1/(H + \frac{4}{3}\pi J_s)^2$, where J_s is the saturation magnetization.

3.2 The deviation from magnetic saturation has been also carried out on plastically deformed nickel after heating for 4 and 8 hours at 750°C . With about 3 dislocations/dislocation group, the results show an agreement with the theory of approach to magnetic saturation in plastically de-

formed face-centered cubic materials (1).

(1) H. KRONMÜLLER, A. SEEGER

J. Phys. Chem. Solids, 18 (1961), 93.

TABLE I

Sample No.

Thickness (Cs 133 - atoms/barns)

6	0.00702
7	0.00186
8 *	0.000421
9 *	0.0000746

* The CsCl-powder of these samples has been diluted by Al_2O_3 in
order to keep the geometrical thickness above 2 mm.

TABLE II

Rotor Speed (rpm)	Covered Energy Range	Resolution (ns/m)	Samples Used
2250	120 to 2.6 ev	175	8, 9
6000	145 to 13 ev	65	6, 7
11900	1300 to 60 ev	33	6

Table III
Resonance Parameters of Cs 133

Reso - nance	Resonance Energy (ev)	$2 g \Gamma_n^o$ (mev)	$\Gamma_n^{(1)}$ (mev)	Γ (mev)	Γ_γ (mev)
1	5.90	2.26	5.5	115	110
2	22.7	1.45	7.5	120	112.5
3	48.0	2.9	20	150	130
4	83.9	0.87	8	120	110 ⁽²⁾
5	95.5	2.5	24	160	135
6	128	12	135	215	80
7	144	0.52	6.2	115	110 ⁽²⁾
8	148	2.3	28	140	110 ⁽²⁾
9	183				
10	193				
11	204	1.5	22	140	110 ⁽²⁾
12	211	0.44	6.4	115	110 ⁽²⁾
13	224	2.1	32	140	110 ⁽²⁾
14	238	32	490	600	110 ⁽²⁾
15	300	6.3	120	230	110 ⁽²⁾
16	364 ⁽³⁾				
17	381 ⁽³⁾				
18	407 ⁽³⁾				

(1) $g = 0.5$ assumed,

(2) assumed values

(3) not yet analysed

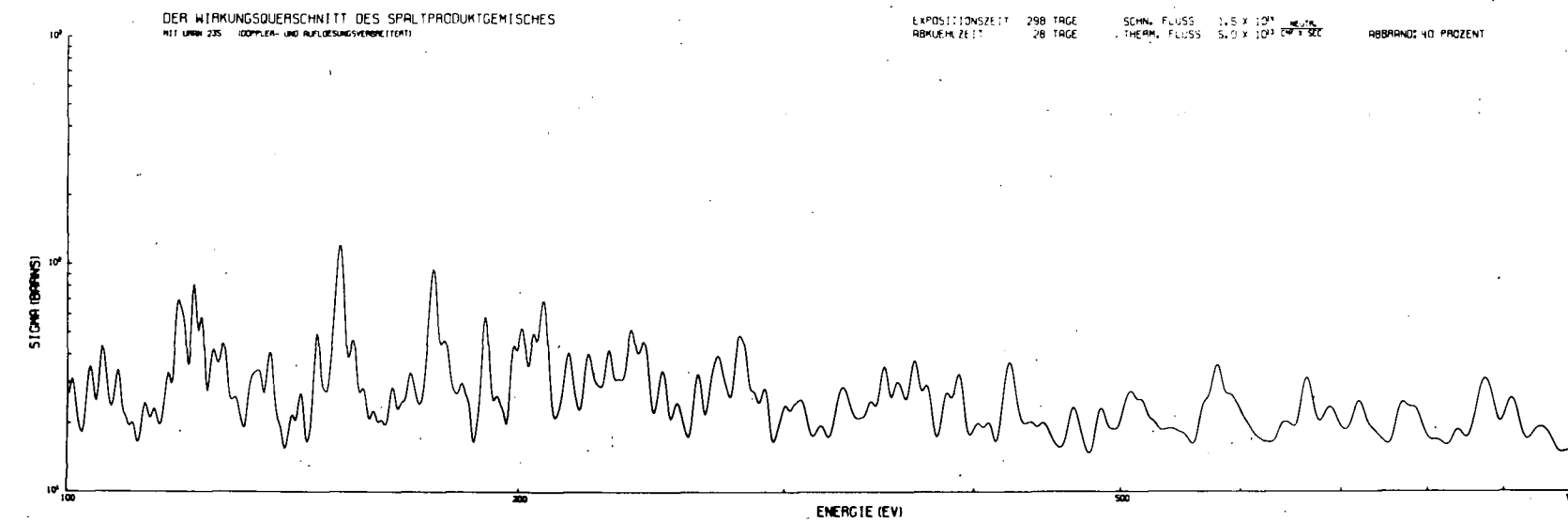
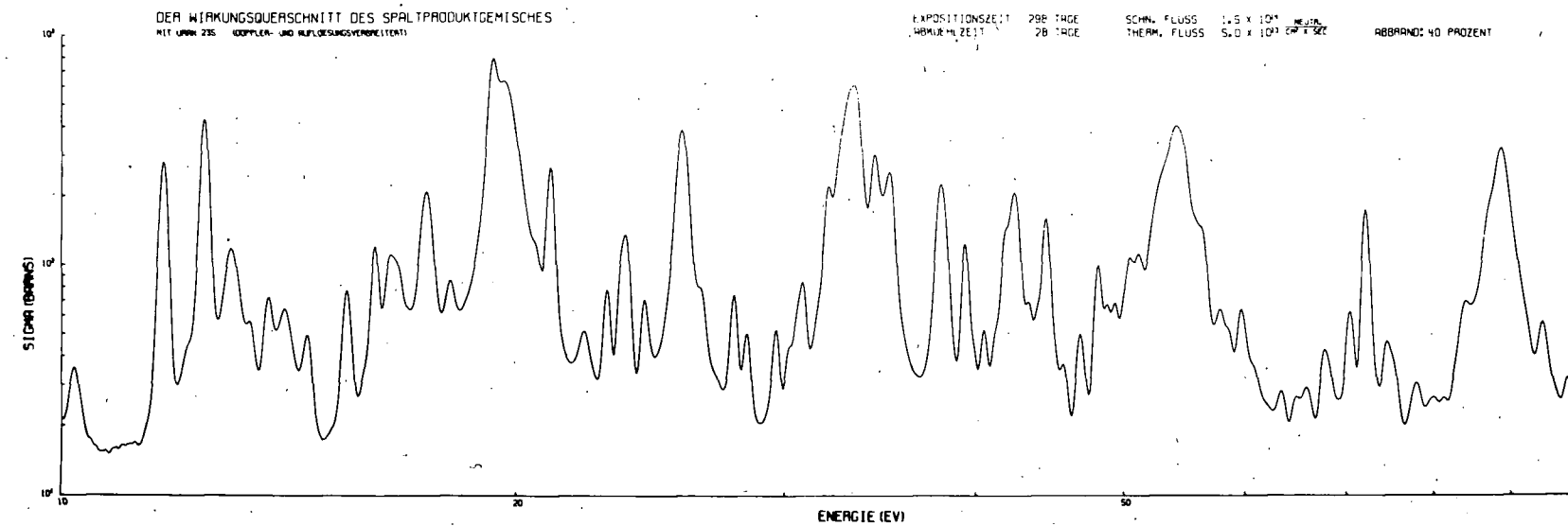


Fig. 1 Total Neutron Cross Section of a Mixture of Fission Products with a ^{235}U Thermal Flux $0.5 \cdot 10^{14}$ n/cm²/sec, Fast Flux $1.5 \cdot 10^{14}$ n/cm²/sec, 40 Percent Burnup. Corrected for Doppler and Resolution Effects.

X. LABORATORIO DI FISICA NUCLEARE APPLICATA, CENTRO DI STUDI NUCLEARI DEL C.N.E.N., CASACCIA (ROMA) (ITALY)

1. Introduction

Last year the Nuclear Physics Group of the "Centro Studi Nucleari della Casaccia" was engaged in the following activities:

- 1) Nuclear resonant scattering experiment.
- 2) Thermal neutron radiative capture experiment.
- 3) Gamma-ray spectroscopy.

Later on the progress we obtained in this year will be briefly described.

2. Nuclear resonant scattering experiment

(M. Giannini, P. Oliva, D. Prosperi, M.C. Ramorino)

Nuclear resonant scattering measurements of neutron capture γ -rays, performed by our group, have been extensively reported in the previous reports and in some papers.

Large Ge(Li) detectors (30 cm^3) with very high resolution (about 10 KeV at 5 MeV) have greatly improved the researches on nuclear resonant scattering, particularly in what concerns γ -inelastic transitions from the resonant level.

The (γ, γ') reaction study gives also a new method to investigate the low energy level scheme.

A first investigation has been performed and a paper is to be published about the resonances Fe-Cd, Cu-Bi, Cu-Sn.

The spectrum scattered from a Cd target has shown 12 inelastic transitions in addition to the elastic transition.

From $\gamma-\gamma$ coincidence and directional correlation measurements, a coherent Cd^{112} level scheme follows. Additional new levels have been deduced.

The spectrum scattered from a Bi target has shown 3 different resonances; $\gamma-\gamma$ directional correlation measurements allowed

us to determine the spin of the most intense resonance. The spectrum scattered from a Sn target has shown 3 inelastic transitions and 2 new resonances in addition to the well known 6908 KeV resonance.

Preliminary measurements are to be performed on Fe-Pr¹⁴¹, Fe-Tl, Cr-Pr¹⁴¹ and Cr-Cu resonances.

3. Thermal neutron radiative capture experiment

(A. Fubini, M. Giannini, D. Prosperi)

The shielding and collimation of the tangential beam-tube of the 1 MeV TRIGA reactor were completed in order to be used for a programme concerning the neutron radiative capture measurements.

The main purpose of our experiments is to obtain more precise information about the nuclear level schemes of the odd-odd nuclei.

A first experiment was performed on the reactor In¹¹⁵(n,γ)In¹¹⁶. The γ-ray spectrum in the 60-6700 KeV energy range was investigated.

Some new M1 transitions to the first excited levels and new other levels were found. Furthermore the energies of some known levels measured with a better precision. The results will be published in "Nuovo Cimento". An experiment on the Cl³⁵(n,γ)Cl³⁶ reaction is in progress.

In the meantime on the same channel a study of the isomeric transitions (half-life from 0,1 to 10 μ sec) is in progress.

Actually the isomeric levels of I¹²⁸ were investigated.

4. Gamma-ray spectroscopy

(M. Giannini)

Some measurements on the γ decay of Eu¹⁵²(T¹¹² 123 γ) in order to give a better picture of the Sm¹⁵² level scheme were performed.

We identified some new γ transitions and performed γ coincidence and γ - γ angular correlation measurements. The results are in print on "Nuovo Cimento".

XI. CENTRO SICILIANO DI FISICA NUCLEARE E DI STRUTTURA DELLA MATERIA, ISTITUTO NAZIONALE FISICA NUCLEARE - SEZIONE SICILIANA, ISTITUTO DI FISICA DELL'UNIVERSITA', CATANIA (ITALY)

1.1. Experimental research work on nuclear structure and reactions

1.2. Nuclear Fission

(S. Lo Nigro, C. Milone)

We have measured the angular distributions of fragments from neutron induced fission of thorium in the range $1.3 < E_n < 1.8$ MeV.

The monoenergetic neutron beams have been obtained from the $^{12}\text{C}(\text{d},\text{n})$ and $^2\text{H}(\text{d},\text{n})$ reactions; the energy spread resulted between 100 and 200 KeV. The fission fragments have been detected by means of nuclear emulsions loaded with thorium nitrate. Each angular distribution of fragments was obtained by analyzing nearly 2000 fission tracks.

At neutron energies $E_n = 1.35; 1.40; 1.45; 1.50; 1.60; 1.65; 1.78$ MeV we have obtained the following values of anisotropy ratios $R(E_n) = N(0^\circ)/N(90^\circ) = 0.91; 0.77; 0.43; 0.27; 0.44; 0.55; 1.08$. The experimental behaviour of $R(E_n)$ may be explained assuming that the fission near the threshold takes place through a $K = \frac{1}{2}$ band; increasing E_n , $K > \frac{1}{2}$ bands open and their contributions reach a maximum concurrent with the maximum of $\sigma_{n,f}$ at $E_n = 1.6$ MeV; at a further rise of E_n , $K = \frac{1}{2}$ bands become dominant again.

The results have been published in Nuclear Physics and communicated at the meeting of the Società Italiana di Fisica [1,2].

1.3. Separation of the reaction mechanism

(G. Corleo, G. Pappalardo, A. Rubbino)

Experimental data on nuclear reactions having the ^{29}Si as intermediate system have been analyzed in order to test the possibili

ty of separation of reaction mechanism. In particular the value of σ_{Fl} deduced by a fluctuation analysis has been compared systematically with the value of σ_{HF} obtained by Hauser and Feshbach calculation of the cross-section.

The results agree within the FRD errors [3].

1.4. Statistical fluctuation analysis of the $^{26}\text{Mg}({}^3\text{He},\alpha)^{25}\text{Mg}$ reaction
(A. Rubbino)

The $^{26}\text{Mg}({}^3\text{He},\alpha)$ reaction has been studied at $E_{3\text{He}} = (4+6 \text{ MeV for}$ the $\alpha_0, \alpha_1, \alpha_2, \alpha_3$ and α_4 groups. The excitation functions were measured in steps of 50 KeV with ${}^3\text{He}$ energy resolution better than 25 KeV and at the angles between 15° and 165° in steps of 7.5° .

The data have been analyzed on the basis of statistical fluctuation theory, obtaining information on some nuclear parameters. Methods of statistical mathematics not so far utilized on the fluctuation analysis have been used in order to evaluate the compound-nucleus contribution in the presence of large direct effects [4].

1.5. Experimental and calculated energy spectra of standard neutron sources

(S. Notarrigo, F. Porto, A. Rubbino, S. Sambataro)

The Am-Be neutron spectrum has been measured with a particular neutron spectrometer. The spectrum has also been calculated taking into account the anisotropy in the angular distributions of neutrons from the ${}^9\text{Be}(\alpha, n)$ reaction.

A very good agreement has been found between the measured and calculated spectra, also as the detailed structures are concerned.

A comparison is also made between experimental data and different calculated spectra for the Pu-Be sources [5].

- 1.6. Fresnel diffraction patterns in the $^{26}\text{Mg}({}^3\text{He},\alpha)^{25}\text{Mg}$ reaction at 5 MeV, analyzed by the methods of complex angular momenta and compared with DWBA

(S. Notarrigo, A. Rubbino, S. Sambataro, D. Zubke)

Differential cross-sections for the $^{25}\text{Mg}({}^3\text{He},\alpha)^{25}\text{Mg}$ reaction have been measured in the energy range 4+6 MeV of the incident beam, in steps of 50 KeV, for 5 α groups leading to the lowest levels of the residual nucleus. The data are compared with DWBA calculations but no good fit has been obtained.

By methods of complex angular momenta a diffraction formula has been derived which fits nicely the experimental data. The diffraction formula has been compared with the DWBA calculations by numerical experiments [6].

- 1.7. $^{29}\text{Si}(d,p)^{30}\text{Si}$ reaction

(G. Calvi, S. Cavallaro, A.S. Figuera, M. Sandoli)

The $^{29}\text{Si}(d,p)^{30}\text{Si}$ reaction has been studied in the 1-2 MeV deuteron energy range in order to obtain some information on the reaction mechanism by measuring the excitation functions and the angular distributions for some proton groups.

From the experimental data it can be suggested that in the investigated energy range the statistical mechanism contributes significantly [7].

- 2.1. Theoretical research work on nuclear structure and reactions

- 2.2. Particle-hole excitations with a complete single-particle basis

II. Scattering amplitudes and resonances

(A. Agodi, F. Catara, M. Di Toro)

An analysis is reported of the continuous spectrum of the particle hole Hamiltonian whose point spectrum was investigated in a previous paper.

The scattering amplitudes have been calculated in the space of all particle-hole states constructed upon the ^{16}O shell model ground state, in the 1^- , 2^- , and 3^- channels with $T = 1$, corresponding to elastic and inelastic scattering of neutrons on ^{15}N , up to 10 MeV incident energy. The opening of the inelastic channels is properly taken into account.

A complete nonredundant basis of p-h states has been used such that the Hartree-Fock scattering is a sort of "orthogonality-scattering". It turns out that this orthogonality scattering appears as a reasonable approximation to the "optical model" scattering as determined with "ad hoc" choice of a single-particle potential.

The resonances have been directly determined from the spectral function of the total Hamiltonian by studying the behaviour of its resolvent, reduced in the subspace of the TD states, at energy values above the continuum threshold E_C , i.e., with a method strictly analogous to that employed to get the point spectrum below E_C .

It is shown that to describe the structure of the nuclear system at a single resonance a single TD state is insufficient and one needs not only (as obvious) the scattering states, but also the other (and possibly all) TD states [8].

2.3. Analitic properties of a class of nonlocal interactions. I (D. Gutkowski, A. Scalia)

The analytic properties of the functions $S(k)$ for a class of non local interactions are studied in the complex k (wavenumber plane).

The interactions considered are given in the momentum representation by

$$\langle \vec{p} | V | \vec{p}' \rangle = -4\pi \frac{\lambda}{M} \sum_{l=0}^L \sum_{i=1}^I \sum_{m=-l}^l g_i(p) g_{il}(p') Y_l^m(\hat{p}) Y_l^{m*}(\hat{p}')$$

where λ is a real number, L and I_l natural numbers.

The $g_{il}(p)$ satisfy the following conditions:

a) they are nonsingular and real for real p ;

b) there exists a unique analytic continuation for every

$g_{il}(p)$ into the complex p plane, apart from isolated singularities, and such a continuation is an even meromorphic function of p ;

c) $\lim_{P \rightarrow \infty} \int_{C_P} dp g_{il}(p) g_{jl}(p) = 0$

where C_P is the half-circle having centre in the origin and radius P , lying in the upper half-plane.

It is shown that a function $D_l(k)$ exists which is meromorphic in the k -plane and such that

$$S_l(k) = \frac{D_l(k)}{D_l(-k)}$$

Characteristic conditions for the existence of bound and virtual states are given. It is shown that poles analogous to the "Ma" ones can exist, and that poles for positive values of k can also exist.

The results are compared with those of the local interactions.

Two specific examples of interactions of the considered class are discussed [9].

2.4. Analitic properties of a class of nonlocal interactions. II (D. Gutkowski, A. Scalia)

A definition is given for the function $S_l(k)$ in the complex l -plane for the class of nonlocal interactions considered in the previous paper I. With the given definition $S_l(k)$ turns to be an analytic function in the complex l -plane, but for a finite number of poles.

Some general properties of the Regge trajectories are discussed and compared with those of the local interactions. Specific examples of Regge trajectories are given [10].

2.5. The role of unitarity in diffractive reactions
(G. Schiffner)

A diffractive reaction is defined by requiring that in its angular distribution the interference term between any pair of partial wave amplitudes of fixed modulus and given angular momentum is maximum. Some sufficient conditions for a binary reaction involving spinless particles to be diffractive are given, using only unitarity and symmetry of the S-matrix. One of these conditions is satisfied if a suitably defined strong absorption holds in the initial and in the final channel and if the partial reaction cross-sections are equal in both channels for each angular momentum. The cases of diffractive reactions involving non vanishing spins and of a reaction between spinless heavy ions are briefly discussed and tests for diffraction are proposed [11].

References

- [1] S. Lo Nigro and C. Milone - Nucl. Phys. A118 (1968) 461.
- [2] S. Lo Nigro and C. Milone - Comm. at the SIF Annual Meeting, Roma 1968, Boll. SIF 62 (1968) 79.
- [3] G. Corleo, G. Pappalardo and A. Rubbino - Boll. SIF 62 (1968) 80.
- [4] A. Rubbino - Nuovo Cimento 54B (1968) 37.
- [5] S. Notarrigo, A. Rubbino, S. Sambataro and D. Zubke - Boll. SIF 62 (1968) 54.
- [6] S. Notarrigo, F. Porto, A. Rubbino and S. Sambataro - Boll. SIF 62 (1968) 82.
- [7] G. Calvi, S. Cavallaro, A.S. Figuera and M. Sandoli - N. Cim. B58 (1968) 363.

- [8] A. Agodi, F. Catara and M. Di Toro - Annals of Physics 49 (1968) 445.
- [9] D. Gutkowski and A. Scalia - Journ. Math. Phys. 9 (1968) 588.
- [10] D. Gutkowski and A. Scalia - Boll. SIF 62 (1968) 6.
- [11] G. Schiffner - Nuclear Physics A113 (1968) 367.

XII. GRUPPO DI ISPRA PER LE MISURE DI SEZIONI D'URTO DEL C.N.E.N.,
ISPRA (VARESE), (ITALY)

1. Spin assignment of neutron resonances

(C. Coceva, F. Corvi, P. Giacobbe, M. Stefanon)

Measurements have been continued at the Linac of CBNM Euratom, Geel (Belgium). An account of these experiments is given in the chapter of CBNM activities.

2. Numerical simulation of the γ -ray cascade

(P. Giacobbe, M. Stefanon, G. Dellacasa)

This work has been published as CNEN report RT/FI(68)20.

3. Gamma-ray spectra from resonance-neutron capture

(C. Coceva, F. Corvi, P. Giacobbe, M. Stefanon)

These measurements were set up at the Linac of CBNM Euratom, Geel (Belgium), within an Euratom-CNEN co-operation programme for nuclear data measurements.

An account of these experiments is given in the chapter of CBNM activities.

XIII. GRUPPO DI RICERCA I.N.F.N. DELLE BASSE ENERGIE DELL'ISTITUTO DI FISICA NUCLEARE DELL'UNIVERSITA', PAVIA (ITALY)

In the course of this year the low-energy group of the Nuclear Physics Institute of the University of Pavia has performed the following experiments:

- a) A total reflecting conical tube with an internal optical surface has been realized in order to collimate a neutron beam to be used in beam-hole fission experiments [1]. The gain in the current density and the thermal spectrum enrichment have been calculated in the used geometrical arrangement. The calculated data have been checked experimentally and the collimator surface reflectivity of about 0.6 has been evaluated. The thermal spectrum of the total neutrons emerging from the conical tube assumes such a behaviour that the average cross section for $1/v$ target is about the double of that relative to the thermal Maxwell distribution with no reflected neutrons.
- b) By using the identification technique described in the previous report, the various light charged particles emitted in the neutron-fission of ^{233}U [2] have been detected. The identified particles are the isotopes of Hydrogen, Helium, Lithium and Beryllium. The yield of ^2H , ^3H , ^3He , ^6He , ^8He , Li and Be relative to the long-range alpha particles emission and the experimental data of the gaussian fits of the energetic distributions of ^3H , ^3He , ^4He , ^6He are reported in Table I.
- c) Because of the instrumentation improvement we were enabled to obtain more accurate data concerning the emission of long-range alpha particles and light nuclei in the fission of ^{239}Pu . We have then repeated the experiment [3] which succeeded in obtaining the whole energetic spectra of ^3H ,

^3He , ^4He , ^6He and the relative yields. The resulting data are summarized in Table I.

References

- [1] M. Cambiaghi, F. Fossati and T. Pinelli - "Nuclear Instruments and Methods" 62 (1968) 233.
- [2] M. Cambiaghi, F. Fossati and T. Pinelli - to be published in "Il Nuovo Cimento".
- [3] M. Cambiaghi, F. Fossati and T. Pinelli - "Bollettino della Società Italiana di Fisica" n. 62 pag. 79 - Communication to the LIV National Congress of S.I.F.

Table I - Yields and energies of light nuclei emitted in the fission of ^{233}U and ^{239}Pu .

	$^4_{\text{He}}$	$^6_{\text{He}}$	$^8_{\text{He}}$	$^3_{\text{He}}$	$^3_{\text{H}}$	$^2_{\text{H}}$	Li	Be	
^{233}U	1	$7.3 \cdot 10^{-3}$	$> 2.3 \cdot 10^{-4}$	$\sim 1.8 \cdot 10^{-2}$	$2.8 \cdot 10^{-2}$	$> 2.4 \cdot 10^{-3}$	$> 2.9 \cdot 10^{-4}$	$> 4 \cdot 10^{-5}$	Particles yield estimated in the total energy interval
^{239}Pu	1	$1.46 \cdot 10^{-2}$	-	$\sim 9.2 \cdot 10^{-3}$	$2.9 \cdot 10^{-2}$	$> 2.8 \cdot 10^{-3}$	-	-	
^{233}U	15.65	14.05	-	14.3	7.0	-	-	-	Most probable energy of the gaussian fits
^{239}Pu	15.8	14.0	-	15.0	8.2	-	-	-	(MeV)

XIV. GRUPPO DI RICERCA INFN - ISTITUTO DI FISICA DELL'UNIVERSITA',
PADOVA (ITALY)

1. Analysis of ($^3\text{He},\alpha$) reactions on ^{25}Mg and ^{26}Mg at 5.50 MeV
(S. Galassini, F. Pellegrini - Nuovo Cimento 53B (1968) 188)

An analysis of the experimental results obtained by ($^3\text{He},\alpha$) reactions on ^{25}Mg and ^{26}Mg nuclei has been performed at an incident energy of 5.50 MeV. The experimental results have been compared with the prediction of the Hauser and Feshbach theory and of a direct interaction pick-up process. The analysis has established that these reactions proceed dominantly through a compound nucleus mechanism.

Good agreement has been found between theory and experiment for a value of the spin cut off parameter $\sigma^2=2$. The inertial momenta thus derived are $J(^{27}\text{Si})=0.34 J_{\text{rig}}$ and $J(^{28}\text{Si})=0.29 J_{\text{rig}}$.

2. About the momentum distribution of nucleon pairs in the ^6Li and ^7Li ground states obtained by nuclear absorption of slow pions
(F. Pellegrini - Nuovo Cimento 54B (1968) 335)

The momentum distribution of nucleon pairs emitted in (π^- , 2n) reactions on ^6Li and ^7Li reflects the total momentum distribution of the original nucleon pairs in target nuclei. Simple shell model predictions are in agreement with the experimental results of Davies, Muirhead and Woulds (Nucl. Phys. 78 (1966) 633).

3. Level structure of ^{45}Ca from the $^{44}\text{Ca}(\text{d},\gamma)^{45}\text{Ca}$ reaction
(F. Brandolini, L. El Nadi, I. Filosofo, F. Pellegrini and C. Signorini - Nuovo Cimento 56B (1969) 137)

Gamma radiation studies from the $^{44}\text{Ca}(\text{d},\gamma)^{45}\text{Ca}$ reaction, observed at a deuteron bombarding energy of 5 MeV, have established that the 1.90 MeV and the 1.43 MeV states of ^{45}Ca have both angular momentum $J = \frac{3}{2}$. The 1.90 MeV level is shown to de-excite with a relative intensity of 12% to the 1.43 MeV state,

of 68% to the 0.176 MeV state and of 20% to the ground state. The 1.43 MeV level is shown to de-excite with a relative intensity of 70% to the 0.176 MeV state and of 30% to the ground state. In addition, for the transition to the 1.90 MeV of ^{45}Ca it has been measured the ($p-\gamma$) angular correlation, in the reaction plane, with the proton counter on the peak of the stripping curve at 25° . The observed gamma angular correlation and the corresponding axis of symmetry are in agreement with the predictions of D.W.B.A. theory. Finally, experimental values of the multipole-mixing parameter δ were deduced and the experimental branching ratios were compared with the predictions of the shell-model theory. Satisfactory agreement between experiment and theory is obtained assuming an effective neutron charge of 0.6e.

Study of the (d,p) reaction on ^{48}Ti and ^{50}Ti nuclei

(K. Grotowski, A. Jasielska, T. Panek, F. Pellegrini and S. Wiktor - Acta Physics Polonica 34 (1968) 939)

Proton spectra from $^{48}\text{Ti}(d,p)^{49}\text{Ti}$ and $^{50}\text{Ti}(d,p)^{51}\text{Ti}$ reactions at incident deuteron energy of 12.9 MeV were measured in wide range of angles. Six proton groups leading to: ground, 1.38, 1.72, 2.50, 3.26 and 3.80 MeV states of ^{49}Ti nucleus, and two proton groups leading to: ground and 1.16 MeV states of ^{51}Ti nucleus were taken for the analysis of angular distributions. The distorted wave, zero range Born approximation method was applied and the ℓ -values as well as spectroscopic factors corresponding to different transitions were obtained. Four different sets of parameters of the deuteron optical potential were used in the D.W.B.A. analysis and their influence on the shape of angular distributions and the magnitude of spectroscopic factors was investigated.

These potentials only, which have the depth of the real potential not lower than about 100 MeV, appeared to be acceptable. In measured angular distributions noticeable effects due to differ-

ent coupling of spin and orbital angular momentum of transferred neutron were observed. The differences in shapes of angular distributions caused by that effect were related to the polarization of protons scattered elastically on Ti nuclei.

5. Elastic and inelastic scattering of fast neutron from C^{12}
(U. Fasoli, D. Toniolo and G. Zago)

A measurement has been performed of 50 angular distributions of elastic and inelastic scattering of neutron from C^{12} in the energy interval 2.5+8.5 MeV. The time of flight technique has been used in conjunction with a PDP8 computer "on line".

The calculations of the angular distribution coefficients and of the phase shifts are in progress.

The polarization induced by the scattering at 2.4 MeV and 50° has been obtained by a double scattering experiment.

6. Gamma rays produced in $(n;n'\gamma)$ reactions
(F. Demanins and G. Nardelli)

Cross-sections for the production of gamma rays by inelastic neutron scattering from Na, Cr, Fe, Ni and Cu have been measured for incident neutron energies from 1 MeV to 4 MeV.

Relative angular distributions for 30 gamma rays produced by the $(n;n'\gamma)$ reaction in Na^{23} , Cr^{50} , Cr^{52} , Cr^{53} , Cr^{54} , Fe^{56} , Ni^{58} , Ni^{60} , Cu^{63} and Cu^{65} were measured over the same energy range and compared with the theoretical predictions of the Satchler formalism using the neutron penetrabilities of Perey-Buck and Bjorklund-Fernbach. The calculated relative angular distributions are in agreement with the experimental values.

For incident neutron energies from 1 MeV to 2.5 MeV the calculated cross sections are larger than the experimental values.

In most cases the calculated cross sections based on the Moldauer theory are in better agreement with the experimental ones than those of the Hauser-Feshbach calculations.

V. SOTTOSEZIONE DI FIRENZE DELL'ISTITUTO NAZIONALE DI FISICA NUCLEARE - ISTITUTO DI FISICA DELL'UNIVERSITA', FIRENZE (ITALY)

The main activity of this group concerns γ ray spectroscopy with the aid of solid state detectors:

1. Level scheme of ^{45}Sc

(P. Blasi, P.R. Maurenzig, R.A. Ricci^(*), N. Taccetti)

The reaction $^{45}\text{Sc}(\text{p},\text{p}'\gamma)$ has been studied making use for the detection of γ -rays of a 5 cm^3 Germanium detector at the 5.5 MeV Van de Graaff accelerator in Legnaro (Padua). From the γ spectra obtained at proton energies variable from 1.5 MeV to 3.9 MeV and from measurements of $\gamma-\gamma$ coincidence carried out by a Germanium detector and a NaI(Tl) detector we obtained the decay scheme of the ^{45}Sc levels up to about 2.0 MeV of excitation energy. Particularly we have pointed out new transitions and measured the relative intensities of the γ 's arising from the decay of the various levels. The data we obtained together with the ones already known allowed us also to make a selection for the position spins of each level. Particularly it has been pointed out a series of spin $3/2^+, 5/2^+, 7/2^+, 9/2^+, 11/2^+$ levels, which may be understood as a band constructed on a void basis in the layer ($2s1d$).

2. Levels of ^{50}V

(P. Blasi, P.R. Maurenzig, N. Taccetti)

The $^{50}\text{Ti}(\text{p},\text{n}\gamma)^{50}\text{V}$ reaction has been studied with the proton beam of the 5.5 MeV Van de Graaff accelerator of the University

(*) Institute of Physics, University of Padua

of Padua, at energies from 3 to 4 MeV. The gamma analysis was performed by means of Germanium detectors. In particular to detect γ rays of low energy ($E < 50$ keV), use has been made of a 5 cm^3 detector prepared by the Solid State Group of the C.N.R. in Florence and assembled in such a way as to allow the gamma to enter from a lateral face of the detector, considerably increasing thus the efficiency for low-energy gamma rays. From gamma spectra, from $\gamma-\gamma$ coincidence measurements between a Germanium detector and a NaI(Tl) detector, and from efficiency measurements, the scheme of the ^{50}V levels has been determined up to 388 keV of excitation energy. The fact that only transitions among the contiguous levels are present has allowed to define the probable spins of such levels that is $6^+, 5^+, 4^+, 3^+, 2^+$ respectively for the fundamental state and for the levels at 226, 320, 355, 388 keV. This decay scheme seems to be in good agreement with the theoretical previsions of a pure $(f_{\frac{7}{2}})^3(f_{\frac{7}{2}})^{-1}$ model. Noteworthy is the fact that in this case, at variance from what generally happens in the $f_{\frac{7}{2}}$ shell, there are no states present (at low energy) which are due to configurations of different type.

3. Half-life measurements in ^{29}P and ^{30}P

(P.G. Bizzeti, A.M. Bizzeti-Sona, A. Cambi, P. Maurenzig, C. Signorini^(*))

The $^{28}\text{Si}(p,\gamma)$ ^{29}P and $^{29}\text{Si}(p,\gamma)$ ^{30}P reactions have been used to determine the half-lives of some levels in ^{29}P and ^{30}P with the attenuated Doppler shift method. The measurements have been made at the Van de Graaff accelerator in Legnaro (Padua),

(*) Institute of Physics, University of Padua

using a 5 cm^3 Germanium detector of 3.5 keV resolution (at $E = 1 \text{ MeV}$). The half-life of the first excited level of ^{29}P results to be $\tau = (1.6 \pm 0.3) \cdot 10^{-13} \text{ s}$; the intensity of the M1 transition towards the fundamental level is then $B(\text{M1}) \sim 0.07 \text{ W.U.}$ comparable to that of the correspondent transition in ^{29}Si . About the measurements in ^{30}P , still in course, we report a preliminary value for the half-life of the 2^- level at 4.14 MeV, $\tau \approx (0.29 \pm 0.12) \cdot 10^{-13} \text{ s}$; the corresponding intensities $B(\text{E1})$ for the transitions to the ground level and to the 1^+ level at 709 keV are respectively $a \approx 2.4 \cdot 10^{-4} \text{ W.U.}$ and $a \approx 0.6 \cdot 10^{-4} \text{ W.U.}$

4. Level scheme of ^{49}V

(P. Blasi, P. Maurenzig, R.A. Ricci^(*), N. Taccetti)

A previous study of the $^{49}\text{Ti}(\text{p},\text{n}\gamma)^{49}\text{V}$ reaction concerning the ^{49}V levels up to 1155 keV has allowed us to identify two levels of positive parity: one at 748 keV of spin $3/2$, the other at 1141 MeV, the former interpretable as a hole state in the (1d2s) layer, the latter (of probable spin $5/2$) of more difficult attribution. To get further information we have carried on the study of the $^{49}\text{Ti}(\text{p},\text{n}\gamma)^{49}\text{V}$ reaction with protons of energy up to 3.6 MeV. From the gamma spectra obtained by Germanium detectors, from gamma-gamma coincidences with Germanium and NaI(Tl) counters and from yield measurements we have reconstructed the scheme of the ^{49}V levels up to a 1664 keV energy. From the intensity ratios of the various γ transitions we get that, among others, there is a 1604 keV level which has positive parity and that the more probable spins for the 1141 keV and 1604 keV levels are $5/2$ and $7/2$ respectively. This seems to indicate that the three levels with positive parity are the first three members of a band made on a hole state of the (1d2s) layer, analogously to what happens in ^{45}Sc and in ^{43}Sc .

(*) Institute of Physics, University of Padua

5. Low-lying levels in ^{143}Pm

(P. Blasi, M. Bocciolini^(*), P. Sona, N. Taccetti)

Gamma transitions between low-lying levels of ^{143}Pm populated in the decay of ^{143}Sm have been investigated by means of lithium drifted germanium detectors. Gamma-rays of 273, 1056, 1173, 1243, 1403, 1516, 1545 keV have been detected; log ft values, levels and spins of ^{143}Pm have been deduced from intensity ratios and coincidence measurements. Evidence for the existence of a 273 keV level which is the $\frac{7}{2+}$ predicted by the pairing plus quadrupole force theory of Kisslinger and Sorensen comes out particularly strong from the analysis of $^{143}\text{Nd}(\text{p},\text{n}\gamma)^{143}\text{P}$ reaction data.

(*) I.N.F.N., Florence subsection

XVI. GRUPPO DI RICERCA DEL CONTRATTO EURATOM-CNEN-INFN - ISTITUTO DI FISICA DELL'UNIVERSITA', BOLOGNA (ITALY)

Preliminary experimental result on the mean lifetime of the 10.94 MeV state of O^{16}

(I. Filosofo^(*), E. Fuschini, C. Maroni, A. Uguzzoni, E. Verondini)

As known, parity-mixing in nuclear states can be experimentally tested by looking for γ -decays of unnatural parity states in O^{16} , which are forbidden by parity selection rule. Specifically, these states have excitation energies of 8.88, 10.94 and 11.06 MeV respectively, as shown in Fig. 1. Among these levels the 10.94 MeV one has been shown [1] to be the most suitable for achieving the best sensitivity in the determination of the parity-mixing coefficient F . In a previous paper [2] an experimental method to measure F in this state was proposed, but the feasibility of such an experiment is strongly dependent on the value of the (not yet measured) mean life of the level.

This note reports a preliminary experimental result about the mean life of the 10.94 MeV level of O^{16} .

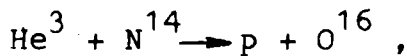
In the experiment, the 3.82 MeV γ -ray spectra from 10.94 MeV level are recorded when the O^{16} ion decays (a) in vacuum, and (b) in a stopping material. It is known [3] that, in order to derive the Doppler shift attenuation from recorded spectra, many corrections must be performed to take into account geometrical effects, finite thickness of the TaN layers, non-linear effects in the ion energy loss, and electronics instabilities. The last effect is particularly important especially when (as in our case) the spectra in situations (a) and (b) are not si-

(*) Institute of Physics, University of Padua

multaneously recorded. However, it is easy to see that electronic fluctuations can be corrected in a very simple way by recording γ -rays from a level of known meanlife (reference level) simultaneously with those of interest, both in cases (a) and (b). In our experiment, the reference level is the 8.88 MeV state whose dominant decay way is via emission of a 2.85 MeV γ -ray.

The meanlife of this state is $\tau_{8.88} = (1.92 \pm 0.29) \times 10^{-13}$ sec [3].

The states of O^{16} are excited by the reaction



induced by the 4 MeV He^3 beam of the Legnaro Van de Graaff, impinging on a TaN target (1000 \AA thick). During the run, two different targets are alternated: in the first one (thick target) the TaN was sputtered (*) on a Ni backing 1 mm thick; in the second one (thin target) the TaN was sputtered on a Ni backing 0.5μ thick. With the thick target the He^3 beam impinges on TaN directly, whereas with the thin target it passes through the backing (in this case the beam energy is obviously increased to compensate the slight energy loss in the backing). Fig. 2 shows the experimental set-up. One can discriminate the O^{16} levels of interest by setting appropriate discriminator bias on the spectrum of the protons detected by the annular solid state detector. Fig. 3 shows a typical proton spectrum. The spectra of the γ -rays in coincidence with the proton group associated with the 8.88 and 10.94 MeV levels are recorded simultaneously in two 512-channel analyzers. Fig. 4 shows a simplified block-diagram of the electronics and Fig. 5 two typical γ -rays coincidence spectra. By assuming the quoted value of $\tau_{8.88}$, our experimental results give

$$\tau_{10.94} = (0.50 \pm 0.25) \times 10^{-13} \text{ sec}.$$

(*) Kindly prepared by Telettra S.p.A., Milan

The quoted standard deviation does not take into account the uncertainty on $\tau_{8.88}$, which, on the other hand, would increase our experimental error of about 5 per cent only. Measurements are in progress both to improve this result and to check the quoted value of $\tau_{8.88}$.

References

- [1] F.C. Michel - Phys. Rev. 133 (1964) B329.
- [2] E. Fuschini et al. - INFN/BE-67/15 (1967).
- [3] R.E. Pixley and W. Benenson - Nucl. Phys. A91 (1967) 177.

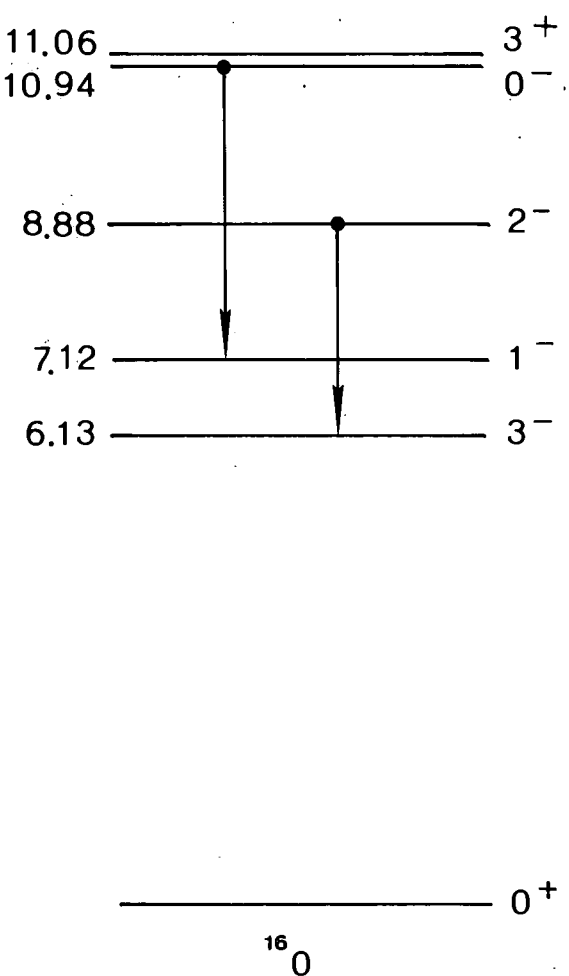


Fig. 1 - Simplified level scheme of O^{16} . Arrows show the γ transitions involved in the Doppler shift attenuation measurement of the present work.

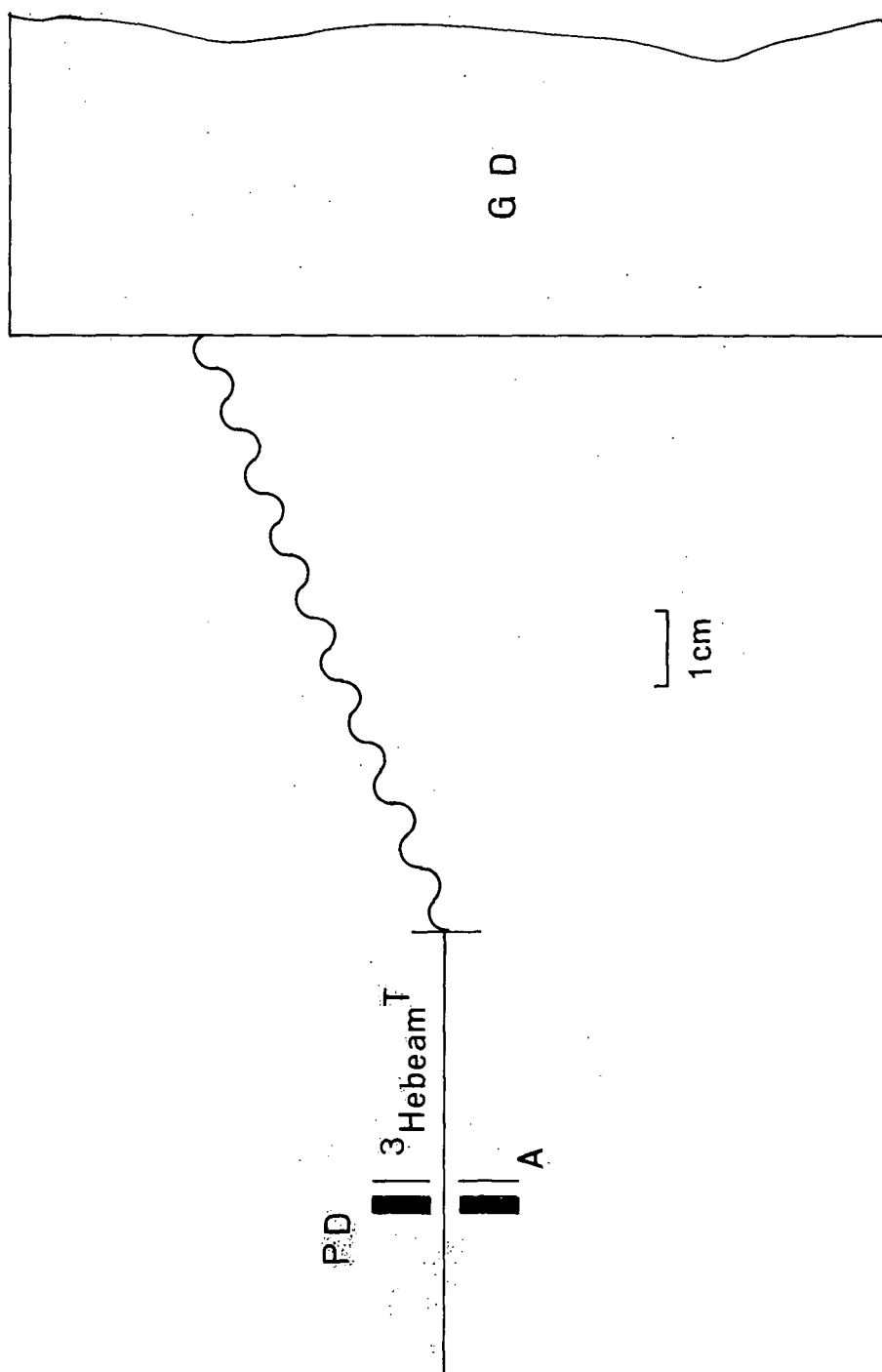


Fig. 2 - Experimental set-up of target and counters.

PD=proton detector (solid state, 800μ thick);
A= 20μ Al absorber to stop He^3 elastically
backscattered; T=TaN target; GD=NaI(tl)5"x5"
 γ -ray detector.

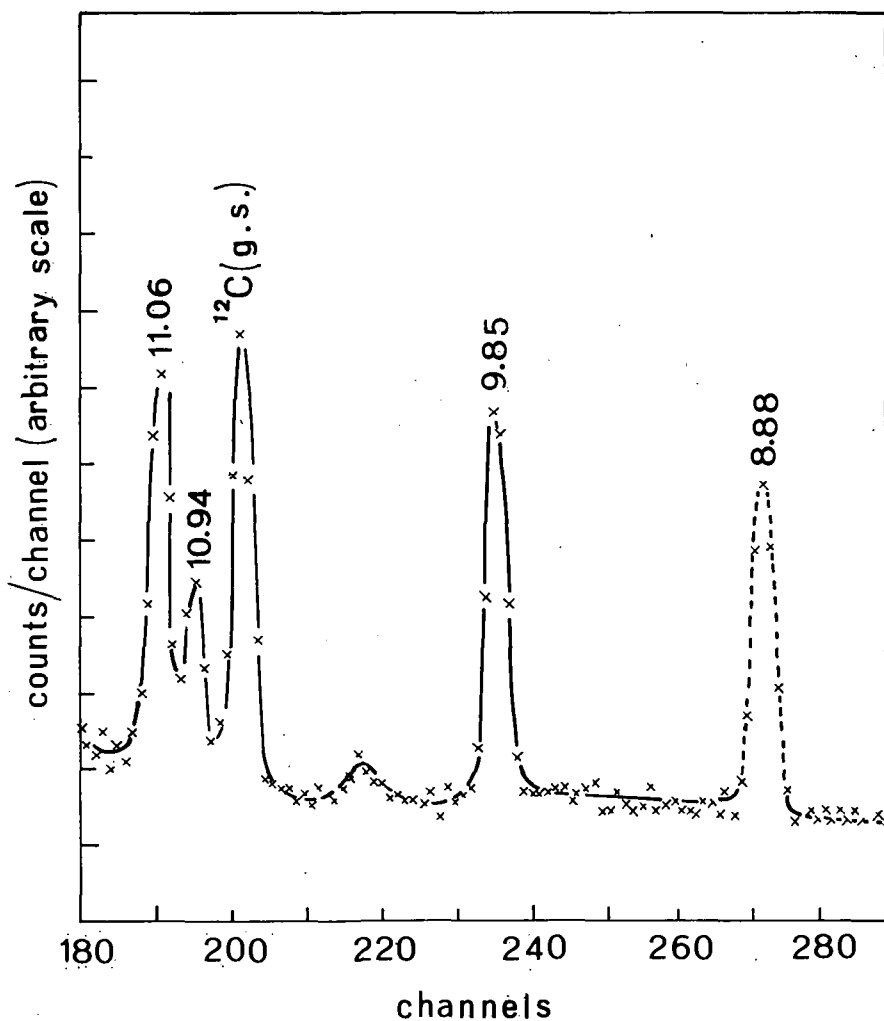


Fig. 3 - Typical proton spectrum from the solid state counter in the energy range of interest.
Excitation energies of the levels associated with proton peaks are quoted.

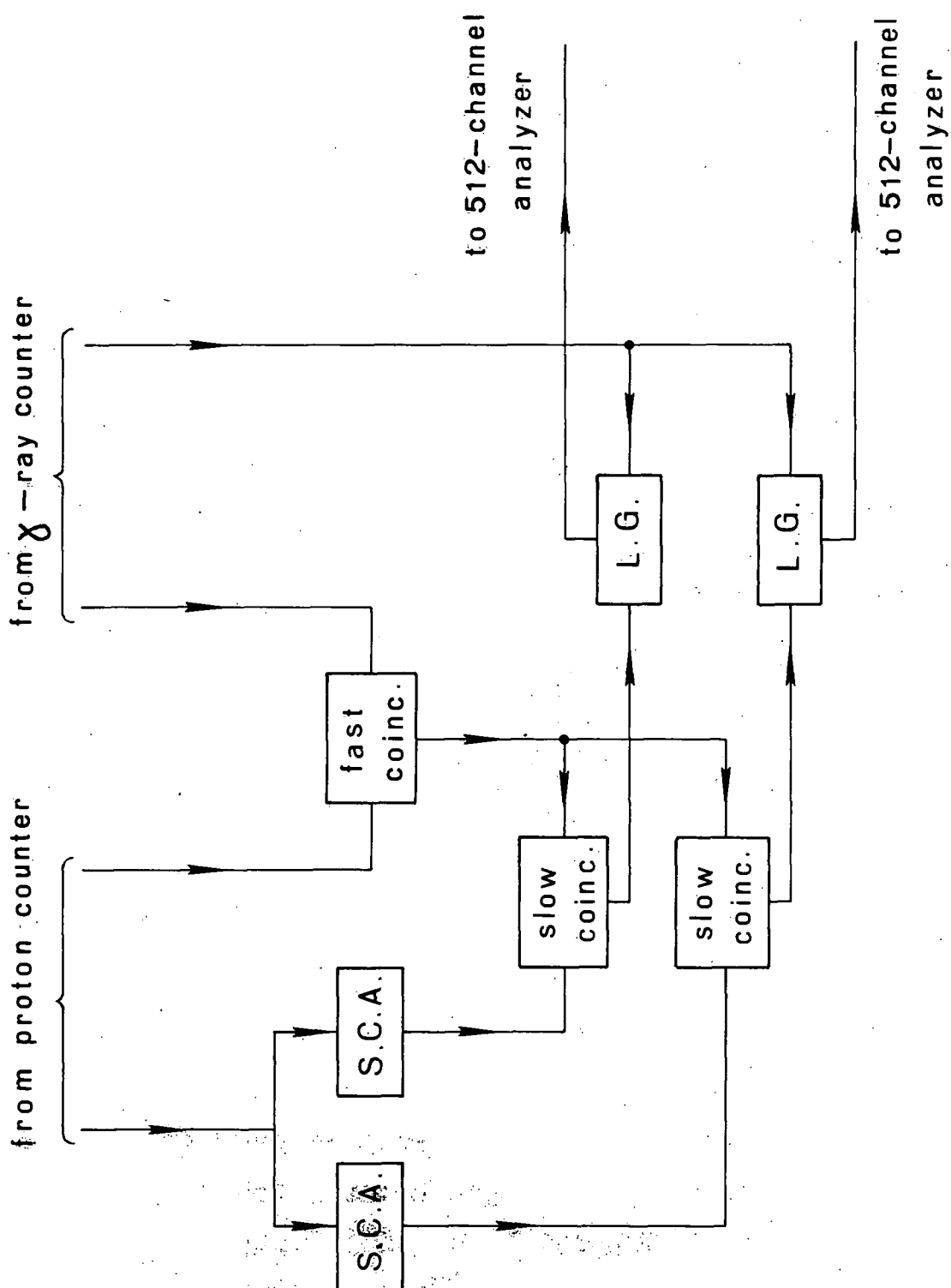


Fig. 4 - Schematic block-diagram of electronics. S.C.A. are single channel analyzers selecting proton peaks from 8.88 and 10.94 MeV O^{16} levels respectively; L.G. are linear gates triggered by slow coincidences.

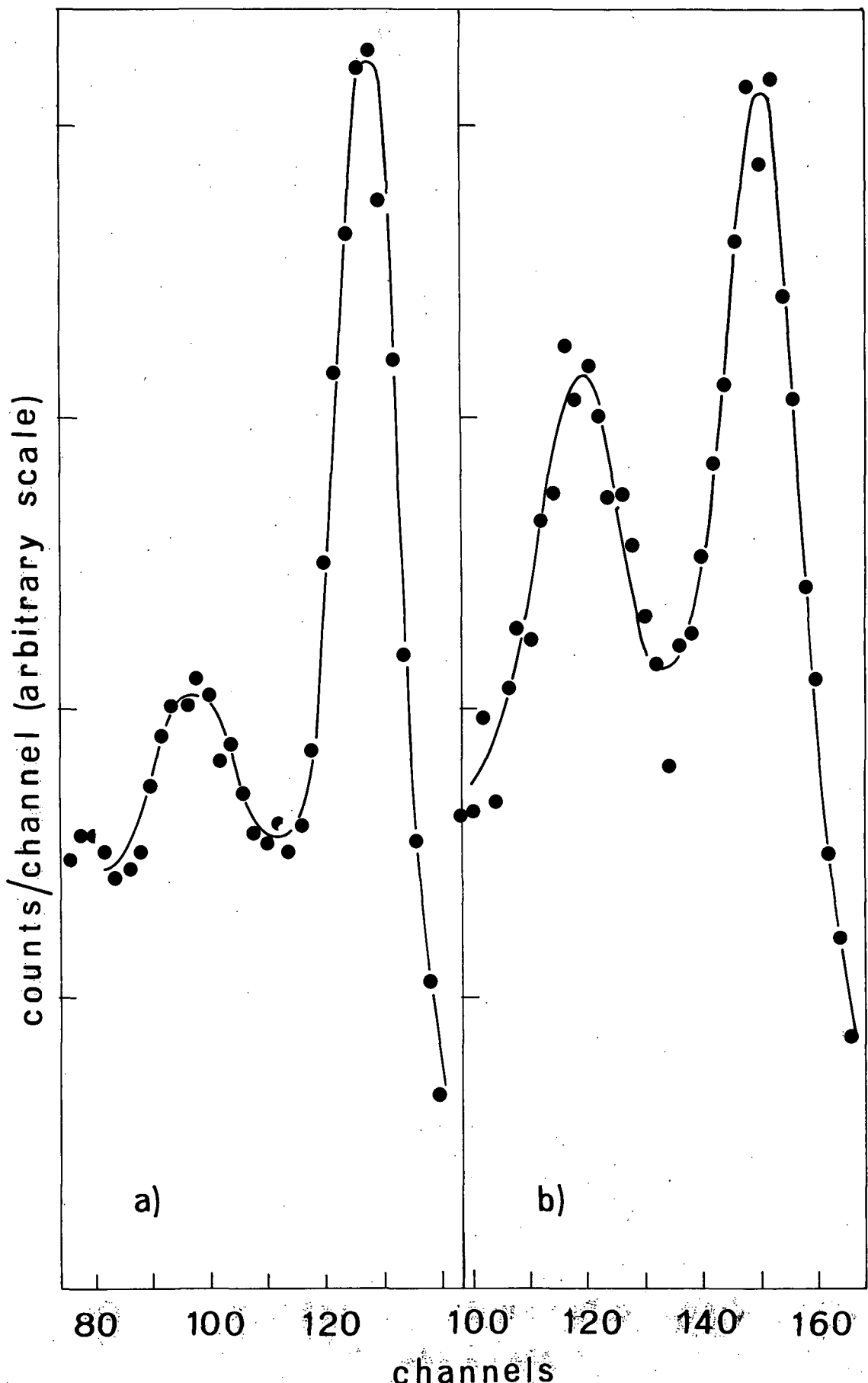


Fig. 5 - (a) Typical coincidence spectrum of the 2.85 MeV γ -rays from 8.88 MeV level of O^{16} .
(b) Typical coincidence spectrum of the 3.82 MeV γ -rays from 10.94 MeV level of O^{16} .

VII LABORATORIO DATI NUCLEARI, CENTRO DI CALCOLO DEL C.N.E.N.,
BOLOGNA (ITALY)

1.1. Theoretical calculations of neutron elastic and inelastic scattering cross sections

1.2. Scattering of 3, 4.3, 6 and 7.5 MeV neutrons from ^{165}Ho (*)
(U. Fasoli (**), P. Sambo (**), T. Toniolo (**), G. Zago (**),
L. Zuffi)

Total cross sections and differential cross sections for both elastic and inelastic neutron scattering have been measured for ^{165}Ho target at the incident energies of 3, 4.3, 6 and 7.5 MeV. The experimental data have been analyzed in terms of a generalized optical model with the coupled-channel method [1].

^{165}Ho has been considered an axially symmetric rigid rotor and the parameter values (Tab. I) of the interaction potential, obtained by fitting the angular distributions (Fig. 3) seem to give a good agreement for $\sigma_T(E)$ and for σ_{Def} [1][2][3][4][5] too (Tab. II).

3. Coupled channel calculation of elastic and inelastic scattering of 17.5 MeV protons by Mg^{25}
(P. Ottaviani, L. Zuffi)

Elastic and inelastic differential cross sections of 17.5 MeV protons scattered by Mg^{25} [6] have been analyzed in terms of coupled channel calculation [7].

The low-lying excited states of Mg^{25} are considered as belonging to two rotational bands practically independent with $K=5/2$

(*) Work performed under the CNEN-University of Padua Contract

(**) INFN Group, Institute of Physics, University of Padua

(ground state band) and $K=1/2$ [6] (Fig. 1).

The nucleus is successfully described by an even-even axially-symmetric inert core plus a nucleon which can be in a set of single particle levels all of which are eigenfunctions of a spheroidal Hamiltonian [8].

Then the direct interaction is described by a non central macroscopic optical potential plus a microscopic particle-odd nucleon interaction which allows the transitions of the last one to different single particle states.

The effective nucleon-nucleon interaction used is a real local central potential of Gaussian shape.

The agreement between theory and experimental data seems to be satisfactory (Fig. 2).

1.4. Elastic and inelastic scattering of neutrons by Sodium at 1.51, 2.47; 4.04 and 6.40 MeV (*)

(V. Benzi, U. Fasoli (**), D. Toniolo (**), G. Zago (**))

The analysis of experimental data has been completed (see EANDC(E)89"U", p. 112). In tables III and IV the various total cross sections are given, whereas Table V gives the coefficients of the Legendre polynomial expansion

$$\sigma(\theta) = \sum_l a_l P_l(\cos \theta)$$

The theoretical analysis was performed in the framework of the generalized adiabatic optical model, assuming a deformation parameter $\beta = 0.45$.

The optical potential was assumed to be of Buck-Perey type, with the following values of the parameters

(*) Work performed under the CNEN-University of Padua Contract

(**) INFN Group, Institute of Physics, University of Padua

V	$= 49.3 - 0.33E \text{ MeV}$	w_D	$= 5.75 \text{ MeV}$
w	$= 0$	v_{SO}	$= 3.0 \text{ MeV}$
a	$= 0.65 \times 10^{-13} \text{ cm}$	b	$= 0.35 \times 10^{-13} \text{ cm}$
R_{ao}	$= 1.25A^{1/3} \cdot 10^{-13} \text{ cm}$	R_{bo}	$= 1.25A^{1/3} \cdot 10^{-13} \text{ cm}$

where E is the neutron energy in the c.m. system and A is the mass number of the target. These parameters are very similar to those obtained by Agee and Rosen from a systematic analysis using a spherical optical model.

A detailed paper will soon appear in Nuclear Physics (1969).

2.1. Photoreaction calculations in the giant resonance energy region for doubly closed shell light nuclei

A detailed analysis of dipole photoreaction cross-sections of ^{12}C , ^{40}Ca and ^{28}Si has been performed in the frame of the one particle-one hole continuum approximation by means of the coupled-channel method [9], [10].

The mixing between proton and neutron channels has been taken into account.

The results have been compared with the experimental data and with those obtained from previous bound state shell-model calculations.

The structure of the giant resonance of ^{16}O has been studied and the ^{16}O photoemission cross-sections calculated with the coupled-channel method have been compared with the results obtained from the eigenchannel reaction theory, assuming the same set of parameter values.

The analysis has confirmed that the fine structure of the ^{16}O giant resonance cannot be explained in the frame of the one particle-one hole approximation and that spurious peaks are obtained from the eigenchannel method [11].

3.1. Collective and direct radiative captures

3.2. Fast nucleon radiative capture

The interference term between direct and collective dipole radiative capture of nucleons by nuclei has been obtained [12]. The cross-section has been written in a Breit-Wigner form as a sum of three terms: direct capture, collective or "resonant" capture and interference term. The nucleon capture cross-section for ^{130}Te , ^{142}Ce and ^{208}Pb have been calculated.

A systematic analysis has been carried out to test the validity of the direct and collective mechanism for the neutron radiative capture by nuclei in a wide range of mass number [13]. It has been found that the two processes can reasonably explain the experimental (n,γ) cross-sections of heavy nuclei ($A > 40$) with magic or near-magic neutron number in the (10+20) MeV neutron energy range, while in the (5+10) MeV energy range a contribution from the compound nucleus mechanism is also necessary. The results have been obtained by using for all the nuclides the same set of optical and bound state parameters consistent with experimental data. A comparison between experimental and calculated cross-sections for the $^{55}\text{Mn}(n,\gamma)$ reaction in the (10+22) MeV energy region is given in Fig. 14.

An attempt has been made to find some regularities which may lead to an empirical expression relating the (n,γ) cross-sections to some fundamental nuclear characteristics [14].

The cross-section for the quadrupole radiative capture of nucleons by nuclei via direct mechanism has been given [15].

The $^{142}\text{Ce}(p,\gamma)$ reaction is investigated in the (10+50) MeV energy range (Fig. 15). It has been shown that for proton energies above 20 MeV the quadrupole contribution to the cross-section may be of the same order of magnitude as the dipole one.

References

- [1] T. Tamura - Rev. Mod. Phys. 37 (1965) 679.
- [2] R. Wagner, P.D. Miller and T. Tamura - Phys. Rev. 29B (1965) 139.
- [3] H. Marshak, A.C.B. Richardson and T. Tamura - Phys. Rev. 150 (1966) 996.
- [4] T.R. Fisher, R.S. Safrata, E.G. Shelley, J. McCarty, S.M. Austin and R.C. Barret - Phys. Rev. 157 (1967) 1149.
- [5] H. Marshak, A. Langford, C.Y. Wong and T. Tamura - Phys. Rev. Lett. 20 (1968) 554.
- [6] G.M. Crawley and G.T. Garvey - Phys. Rev. 167 (1968) 1070.
- [7] T. Tamura - Rev. Mod. Phys. 37 (1965) 679.
- [8] I. Kelson and C.A. Levinson - Phys. Rev. 134 (1964) 269.
G. Ripka - in "Advances in Nuclear Physics" (M. Baranger and E. Vogt eds.) Plenum Press - New York (1968).
- [9] M. Marangoni and A.M. Saruis - Report CEA, Dph-T/Doc/68-54/AMS/f1 (1968).
- [10] M. Marangoni and A.M. Saruis - Report CEA, Dph-T/Doc/68-59/AMS/AN (1968).
- [11] A.M. Saruis and M. Marangoni - Report CEA, Dph-T/Doc/AMS/AN/62-28 (1968).
- [12] G. Longo and F. Saporetti - "Il Nuovo Cimento", 56B (1968) 264.
- [13] G. Longo and F. Saporetti - LIV Congresso S.I.F., Roma, 28 oct.-3 nov. 1968.
- [14] G. Longo and F. Saporetti - CNEN-Report, RT/FI(68)42.
- [15] G. Longo and F. Saporetti - CNEN-Report, RT/FI(68)50; to be published in "Il nuovo Cimento".

Table I - The parameter values of the interaction potential.

β	V (MeV)	W (MeV)	W_D (MeV)	V_{SO} (MeV)	a fermi	b fermi	$R_o = \bar{R}_o$ fermi	β
3	46	0	6	10	0.58	0.40	1.25	0.30
4.3	46	0	6.5	10	0.58	0.40	1.25	0.30
6	46	0	7	10	0.58	0.40	1.25	0.30
7	45.5	0	7.5	10	0.58	0.40	1.25	0.30

Table II - Comparison between experimental and theoretical
 $\sigma_T(E)$ and σ_{Def} of neutron scattered by ^{165}Ho .

E (MeV)	3	4.3	6	7.5
$\sigma_T^{\text{exp}*}$ (barns)	6.25 ± 0.13	5.65 ± 0.12	5.20 ± 0.10	4.90 ± 0.10
σ_T^{th} (barns)	6.26	5.62	5.16	4.97
$\Delta\sigma_{Def}^{\text{exp}**}$	72 ± 20	140 ± 25	70 ± 25	-20 ± 30
$\Delta\sigma_{Def}^{\text{th}}$ (mb)	49.9	127.4	94.1	-21.7

* Present work

** Ref. 5

Table III- Experimental cross-sections (barns) for ^{23}Na at various energies for different levels. Errors are estimated to be $10\pm20\%$ (see text).

Level energy (MeV)	Neutron energy (MeV)			
	1.51	2.47	4.04	6.40
0	2.00	2.79	1.28	
0.44	0.60	0.69	0.39	{ 0.97
2.08		(0.06)	0.21	0.13
2.39			0.11	0.03
$2.64+2.71$			0.21	0.16
2.98			0.14	0.06
3.68			{ not obs.	
3.85				{ 0.18
3.92				
4.43				0.04
4.78				0.07
≥ 5.38				not obs.

Table IV - Comparison between partial, total and theoretical cross-sections (barns)

Neutron Energy (MeV)	Experimental					Theoretical		
	σ_{total}	σ_{el}	σ_{in}	$\sigma_{\text{el}^+ \text{in}}$	$\sigma_{\text{el}^+ n, n'}(0.44)$	σ_{total}	σ_{el}	$\sigma_{\text{el}^+ n, n'}(0.44)$
1.51	2.54 ± 0.05	2.02 ± 0.20	0.60 ± 0.06	2.62 ± 0.26	2.62 ± 0.26	-	-	-
2.47	3.25 ± 0.07	2.79 ± 0.28	0.75 ± 0.08	3.54 ± 0.35	3.48 ± 0.35	-	-	-
4.04	2.23 ± 0.04	1.28 ± 0.13	1.06 ± 0.11	2.34 ± 0.23	1.67 ± 0.17	2.17	1.16	1.47
6.40	1.70 ± 0.04	-	-	1.64 ± 0.17	0.97 ± 0.10	1.82	0.79	1.05

Table V - Legendre polynomial coefficients (c.m.)
(mb/sr)

Energy (MeV)	$a_0 + \Delta a_0$	$a_1 + \Delta a_1$	$a_2 + \Delta a_2$	$a_3 + \Delta a_3$	$a_4 + \Delta a_4$	$a_5 + \Delta a_5$	$a_6 + \Delta a_6$
1.51	161.1 \pm 1.6	92.0 \pm 3.0	52.0 \pm 3.7				
2.47	222.1 \pm 2.3	282.1 \pm 5.0	183.2 \pm 5.4	49.9 \pm 4.7			
4.04	101.5 \pm 1.4	148.4 \pm 3.4	127.1 \pm 4.3	61.8 \pm 3.8	18.8 \pm 3.1		
6.40 a)	73.8 \pm 0.6	79.9 \pm 1.5	113.4 \pm 2.4	107.7 \pm 2.3	91.9 \pm 2.7	43.5 \pm 2.0	24.6 \pm 2.1

a)
(Elastic)+(0.44 MeV inelastic scattering)

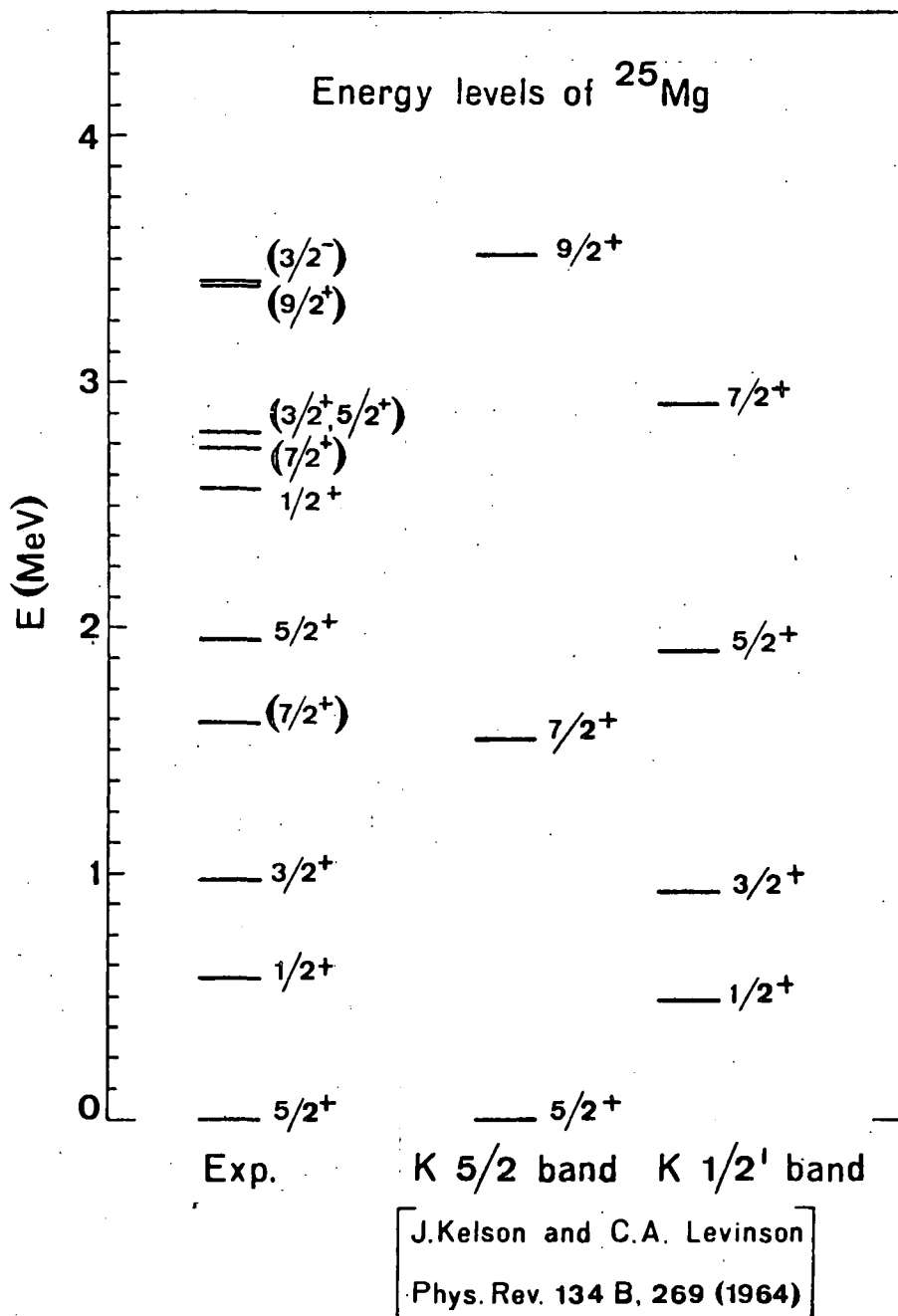


Fig. 1 - ^{25}Mg level scheme.

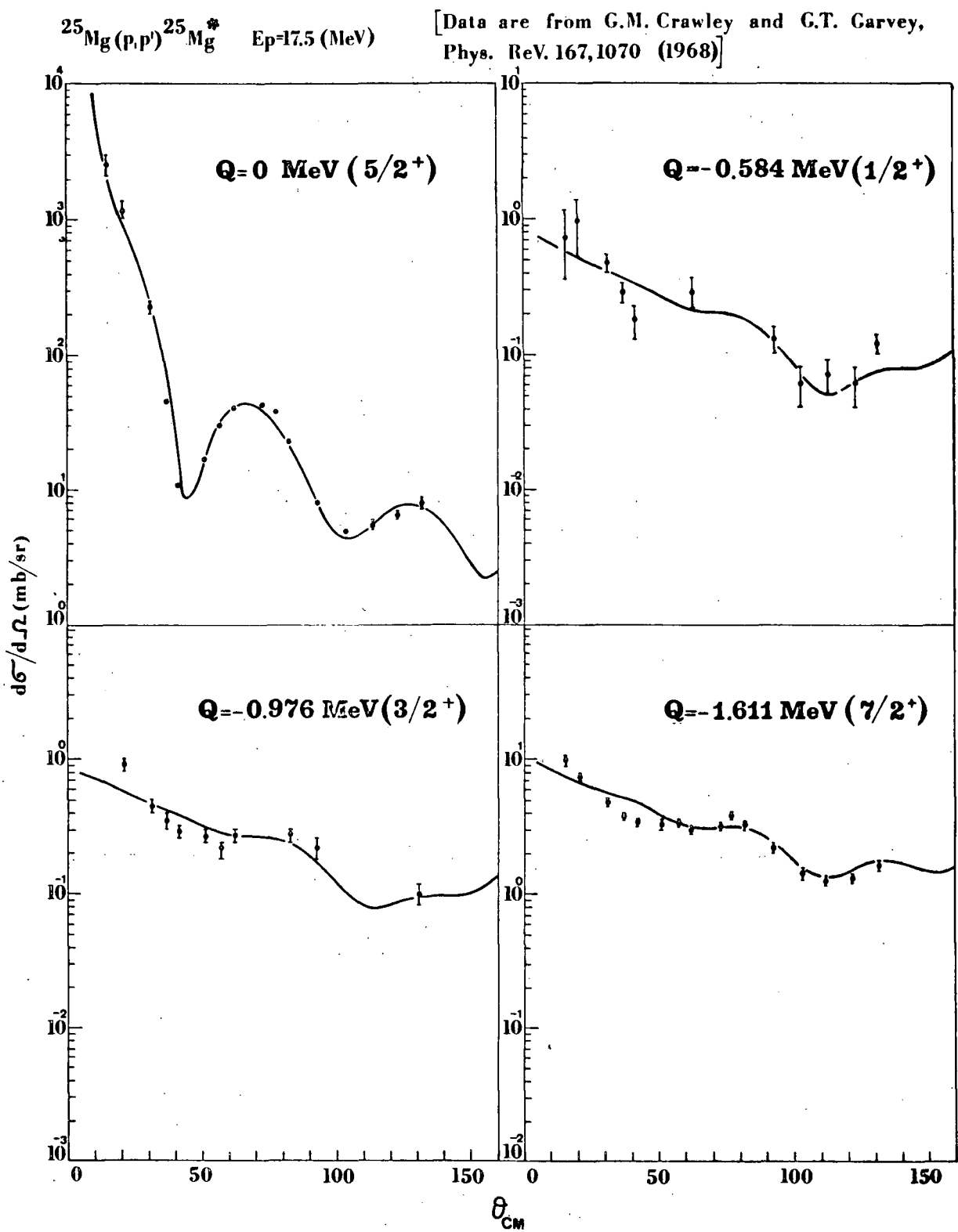


Fig. 2 - Comparison between experimental and theoretical angular distributions of proton scattered by ^{25}Mg .

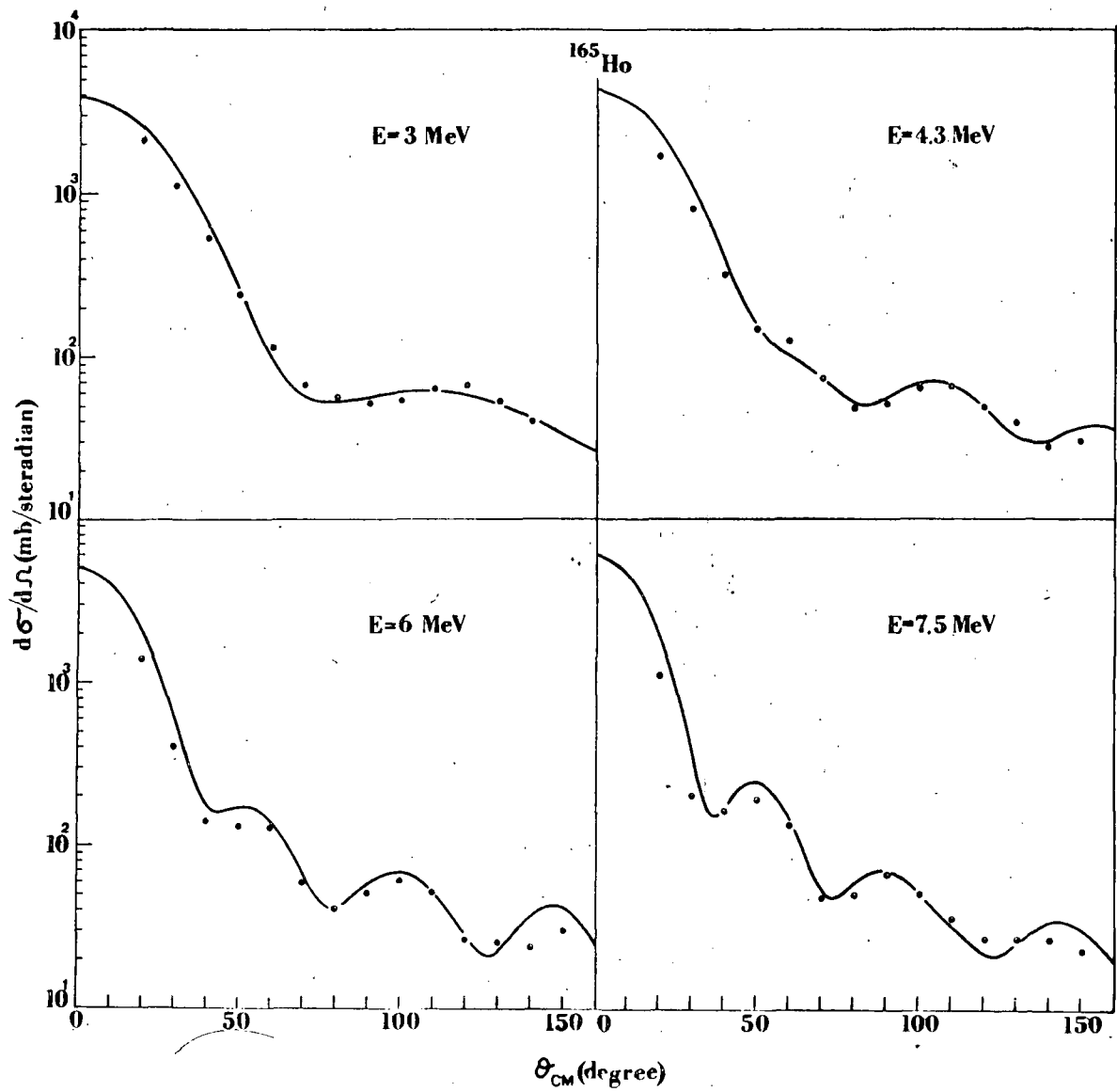


Fig. 3 - Comparison between experimental and theoretical angular distributions of neutron scattered by ^{165}Ho .

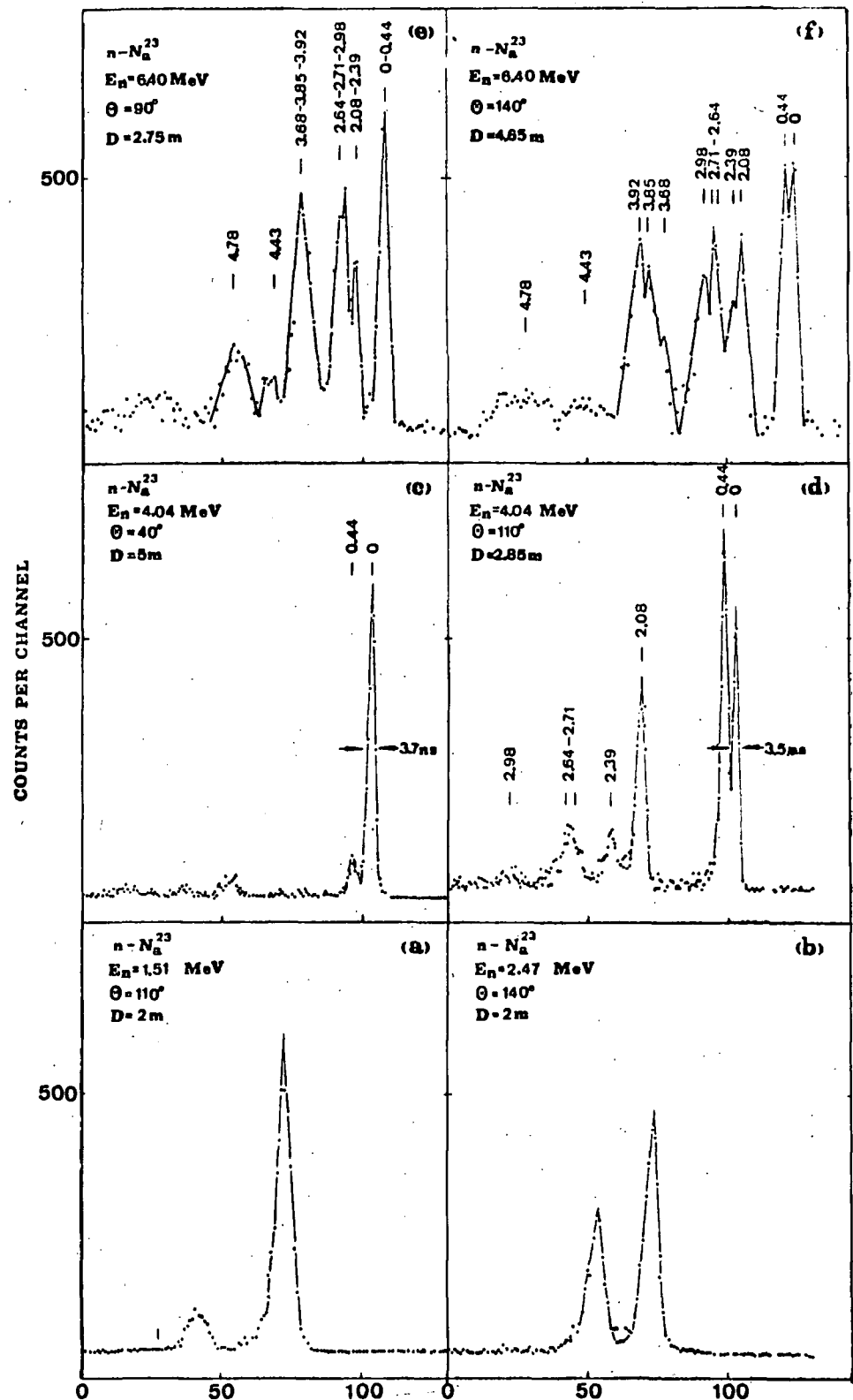


Fig. 4 - Some typical time-of-flight spectra of neutrons with different incident energy E_n scattered by ^{23}Na . The indicated positions of the peaks correspond to the different ^{23}Na levels. D is the adopted time-of-flight base.

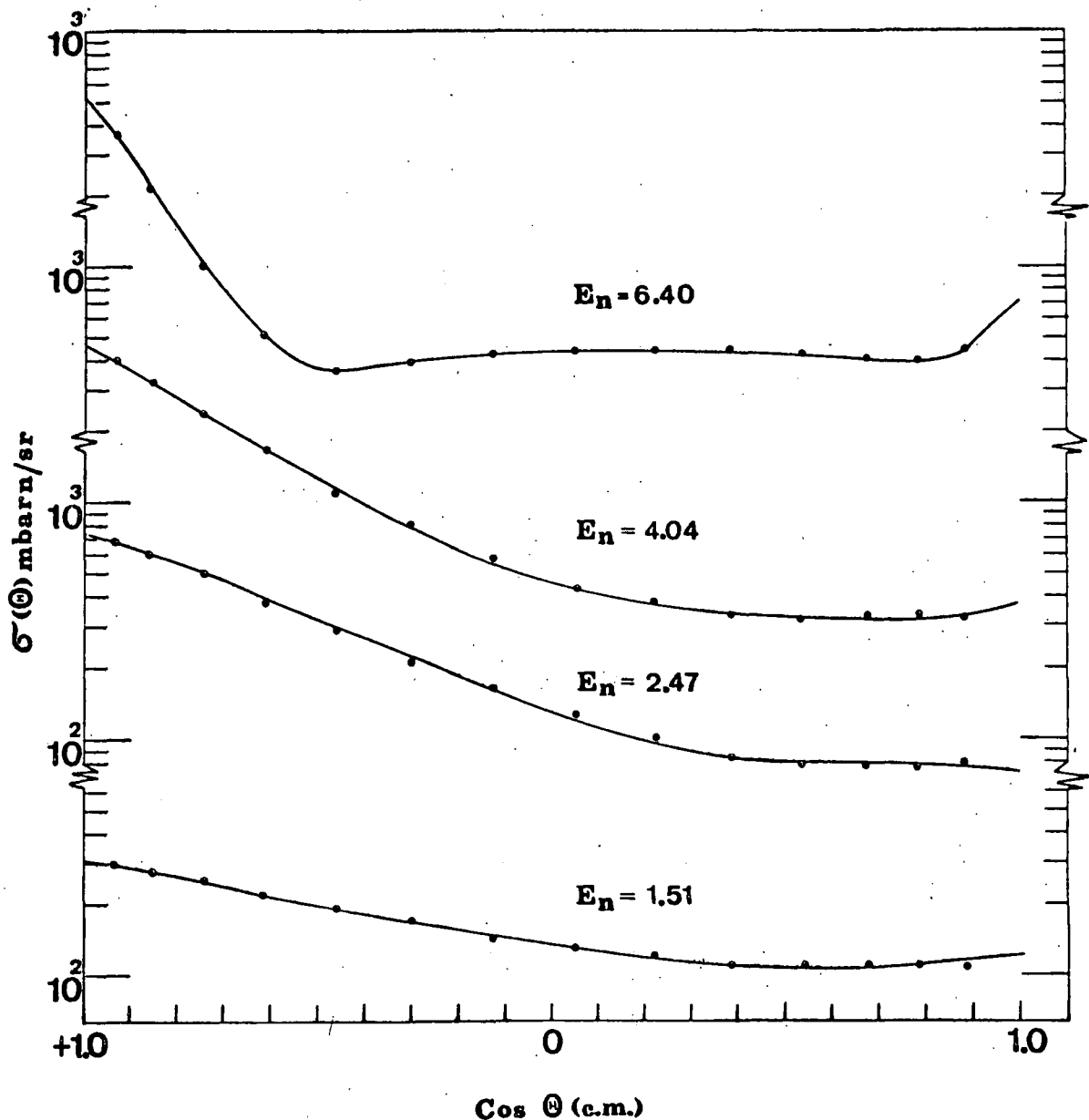


Fig. 5 - Angular distributions of neutrons with incident energies E_n , scattered from ^{23}Na . The three lower curves are relative to the elastic scattering, the fourth curve contains also the contribution of the 0.44 MeV state, not resolved from the ground state. The full line curves are Legendre polynomial fits. The statistical errors are smaller than the diameter of the dots.

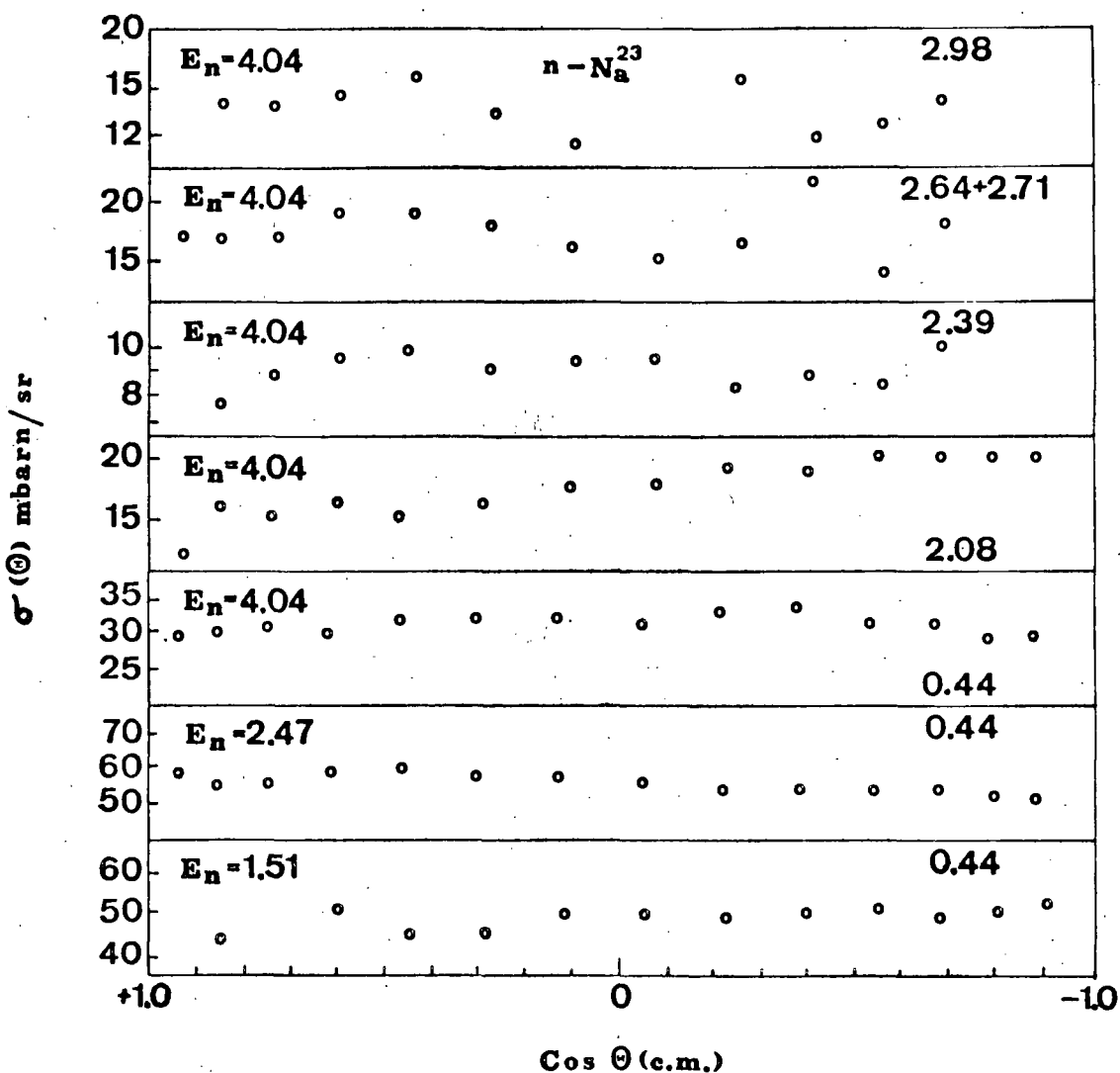


Fig. 6 - Angular distributions of neutrons inelastically scattered by the indicated individual levels (or unresolved groups of levels) of ^{23}Na at 1.51, 2.47 and 4.04 MeV neutron incident energy. The statistical uncertainties are smaller than the diameters of the dots.

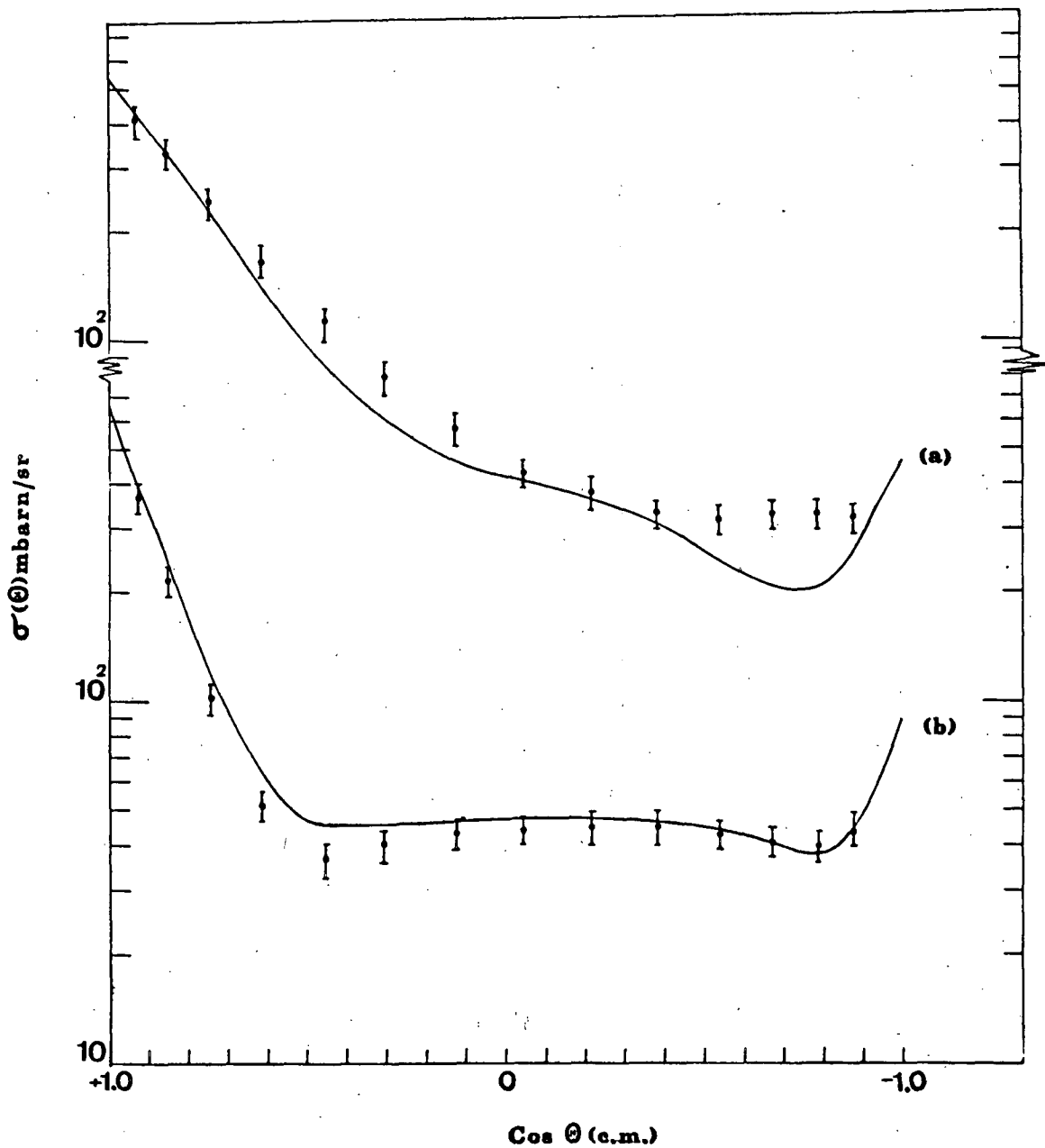


Fig. 7 - Comparison between experimental and theoretical neutron angular distributions of neutrons scattered by ^{23}Na . Curve (a): 4.04 MeV neutron energy; curve (b): 6.40 MeV neutron energy.

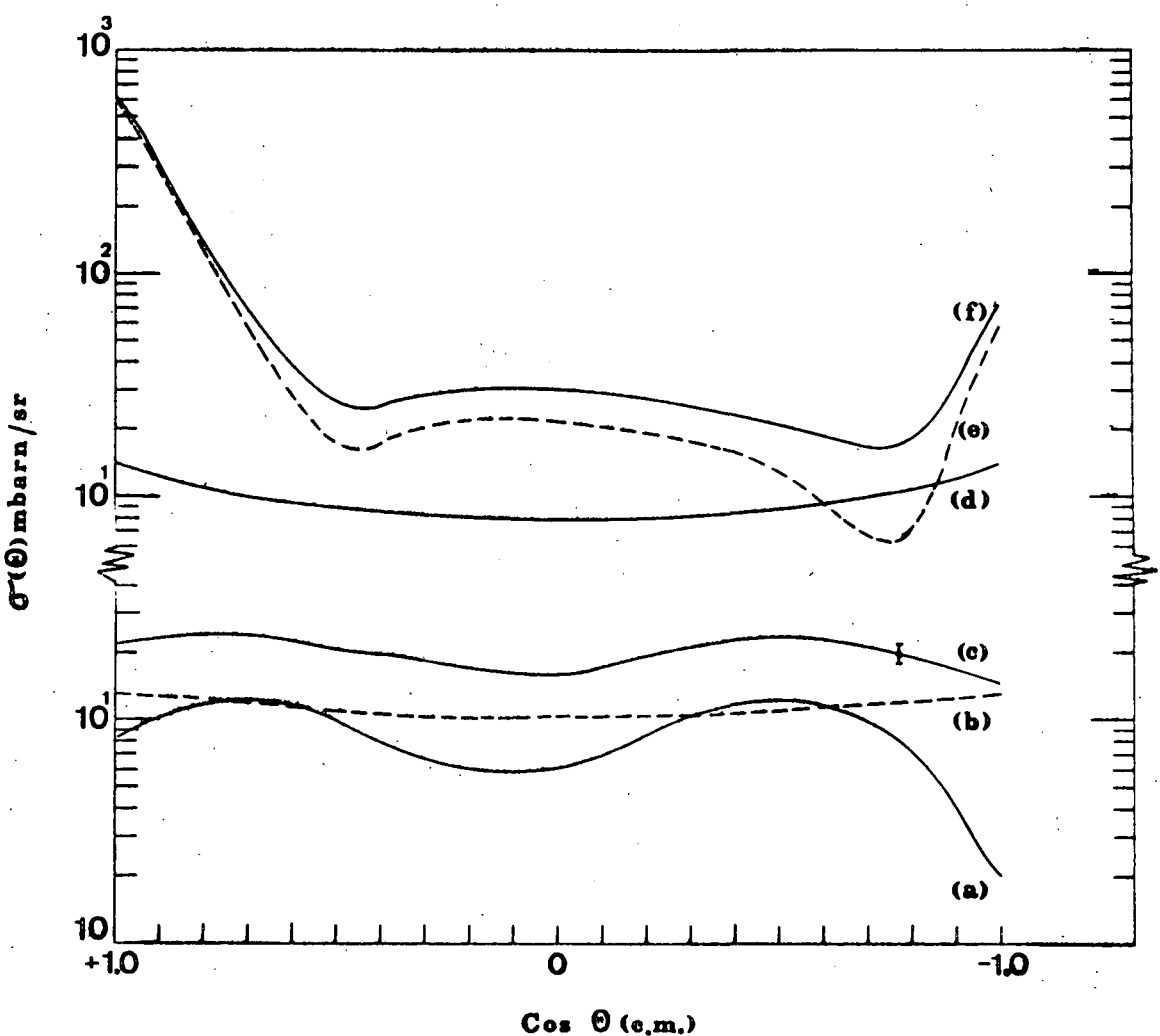


Fig. 8 - The various components of the theoretical curve for neutron scattering at 6.40 MeV. (a): direct inelastic scattering from the 0.44 MeV level; (b): compound inelastic scattering from the 0.44 MeV level; (c): sum of curves (a) and (b); (d): compound elastic scattering; (e): shape elastic scattering; (f): sum of (d) and (e).

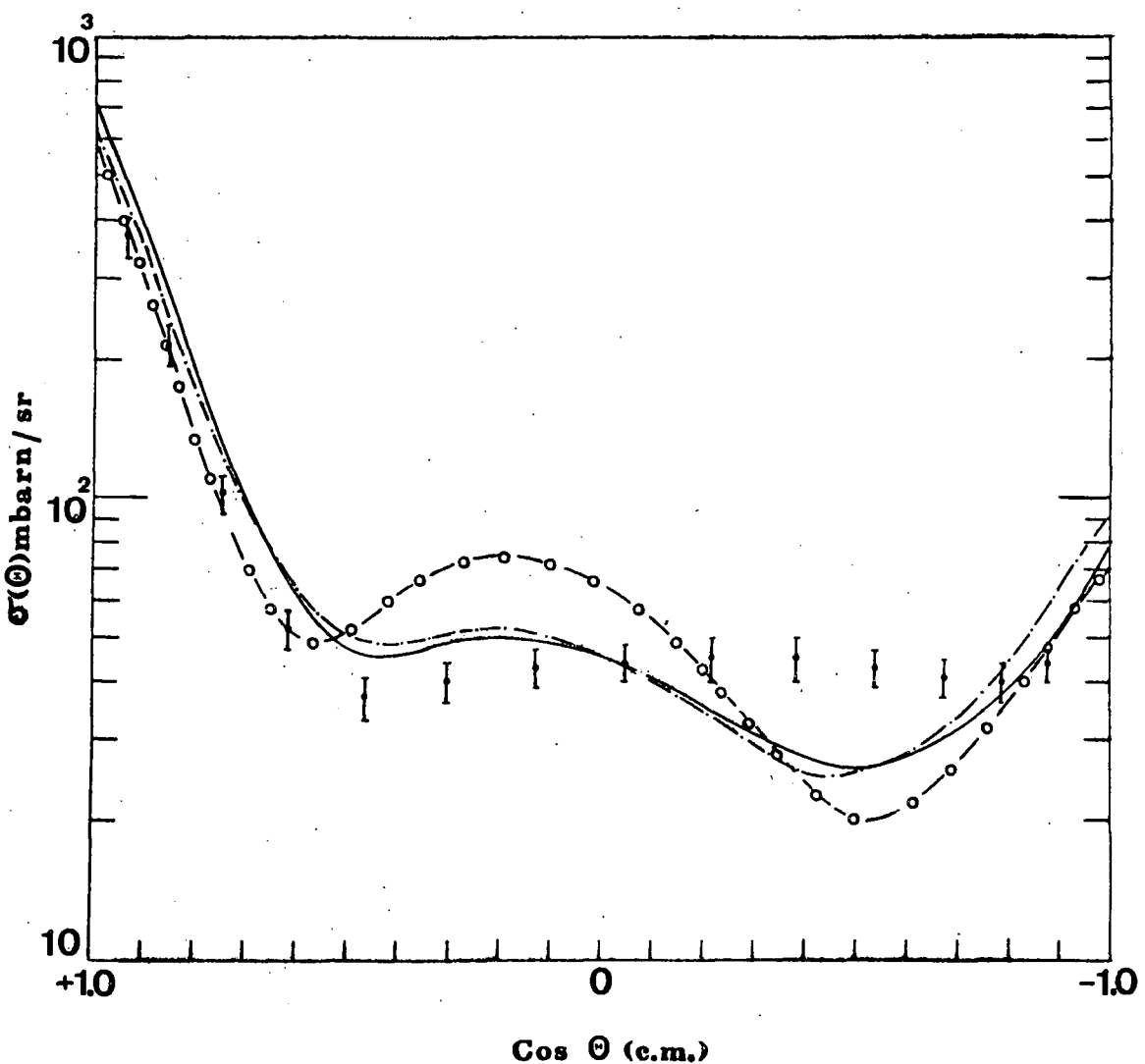


Fig. 9 - Comparison between theory and experiment for the angular elastic and 0.44 MeV inelastic scattering at 6.40 MeV incident neutron energy. The theoretical curves are obtained using different spherical optical potentials.

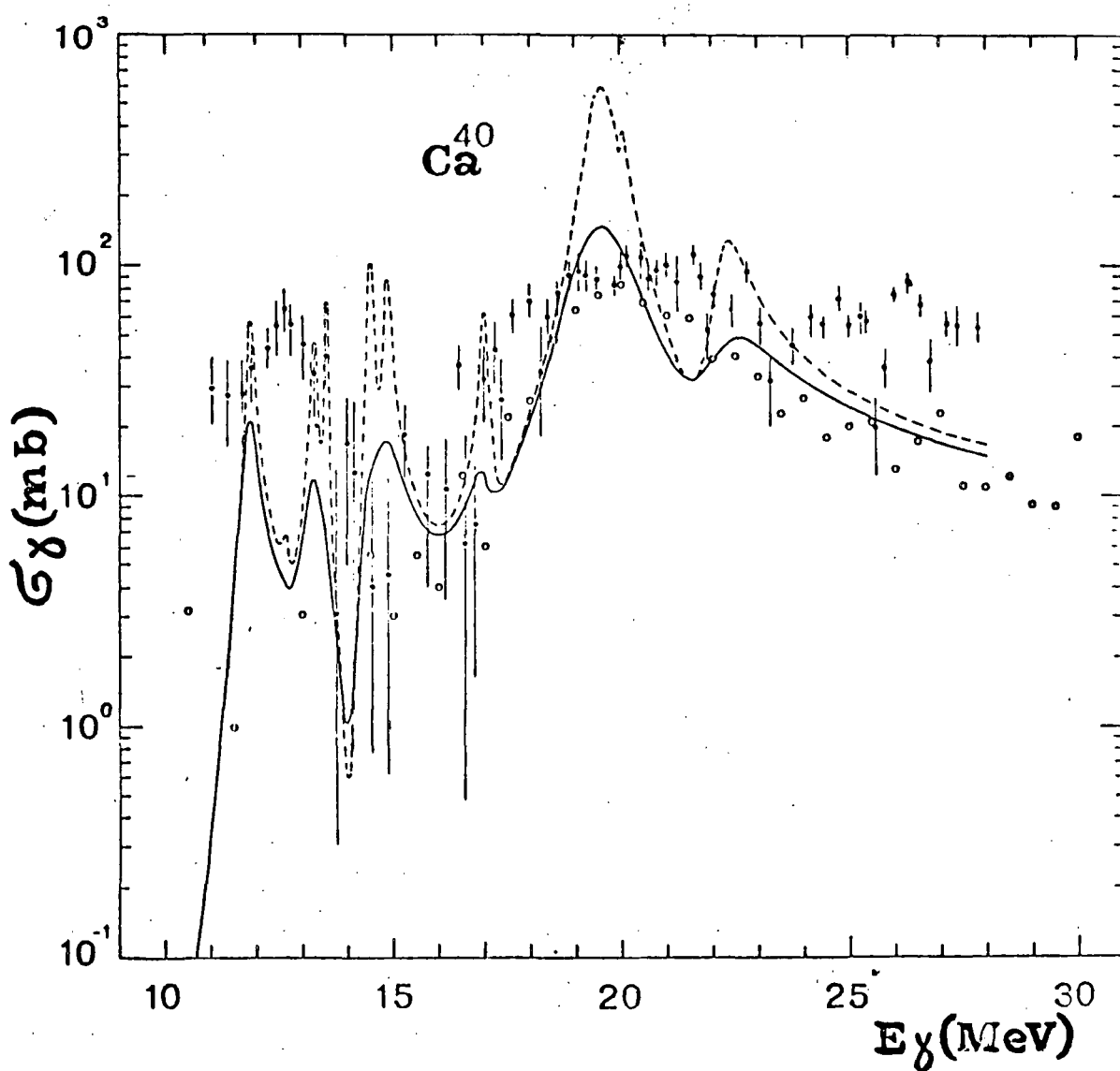


Fig. 10 - Total dipole photoemission cross-section of ^{40}Ca compared with the experimental data. The calculation includes proton and neutron channels. The dashed curve corresponds to an absorptive potential $W = 0$. The full curve corresponds to $W(\text{MeV}) = 0.06E_\gamma (\text{MeV}) - 0.5$.

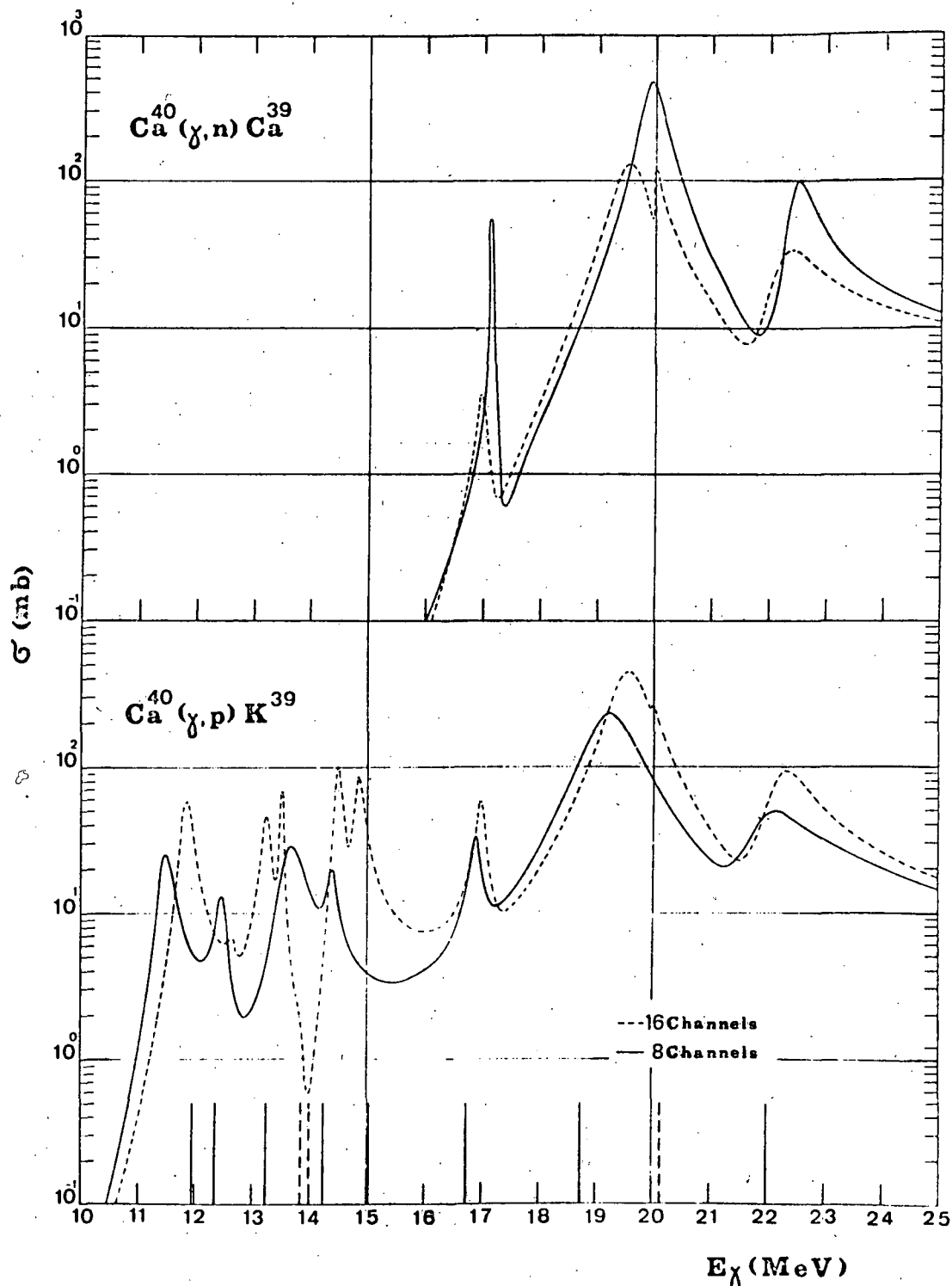


Fig. 11 - Total $^{40}\text{Ca}(\gamma, p)^{39}\text{K}$ and $^{40}\text{Ca}(\gamma, n)^{39}\text{Ca}$ cross-sections calculated with mixing between proton and neutron channels (dashed curves) and without mixing (full curves).

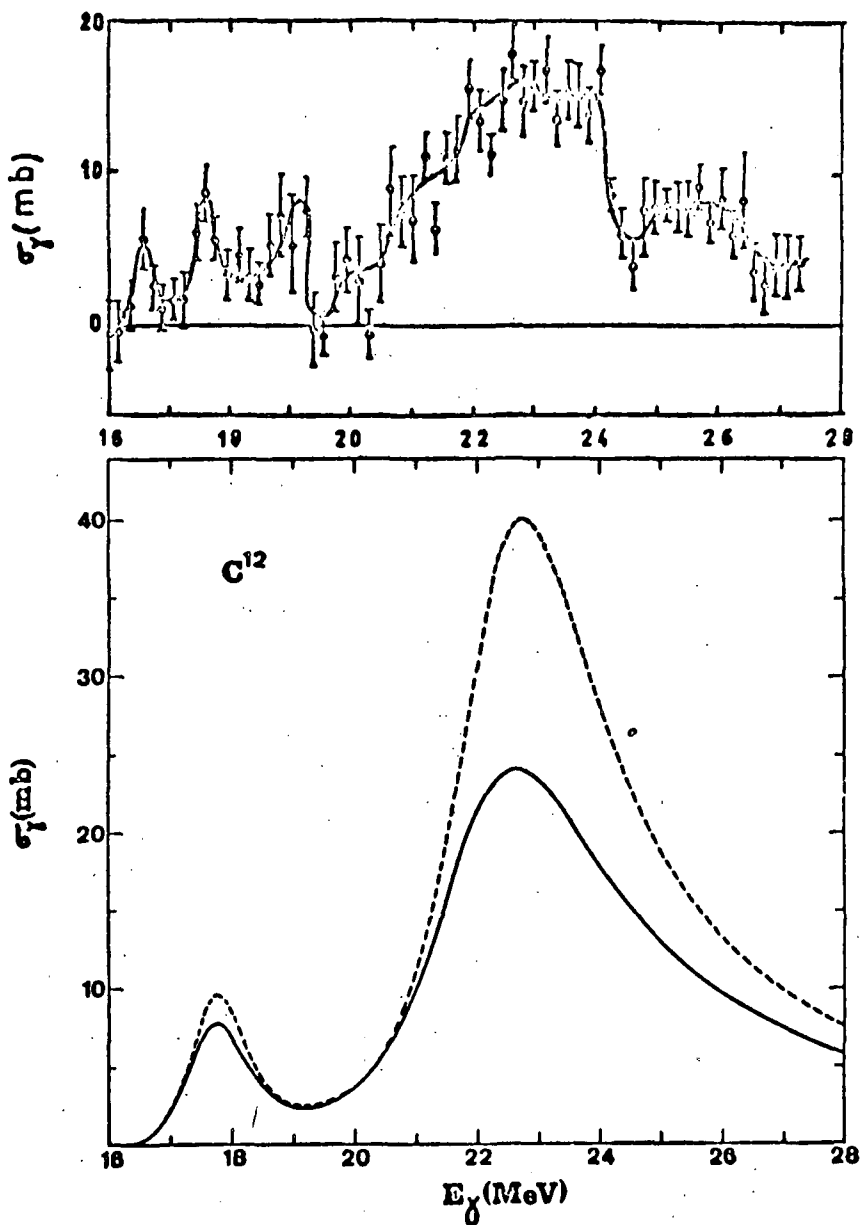


Fig. 12 - Total dipole photoemission cross-section of C^{12} compared with experimental data. The calculation has been performed including both proton and neutron channels. The dashed curve corresponds to an absorptive potential $W=0$. The full curve corresponds to $W(\text{MeV})=0.12 E_\gamma (\text{MeV})-1.9$.

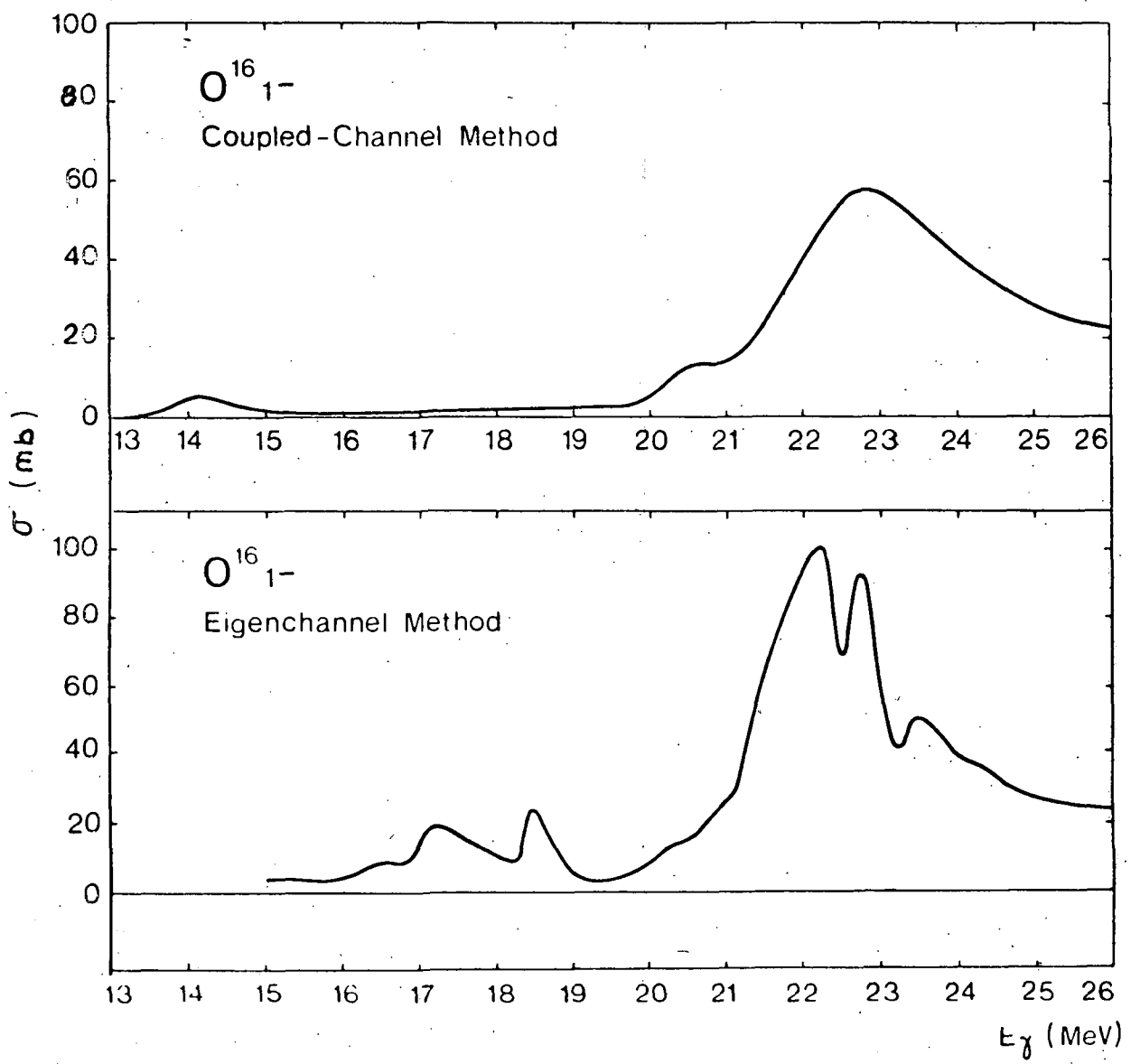


Fig. 13 - Total dipole photoemission cross-section of O^{16} , computed with the coupled-channel method, compared with the results of the eigen-channel method. Equivalent sets of parameter values are assumed in the two calculations.

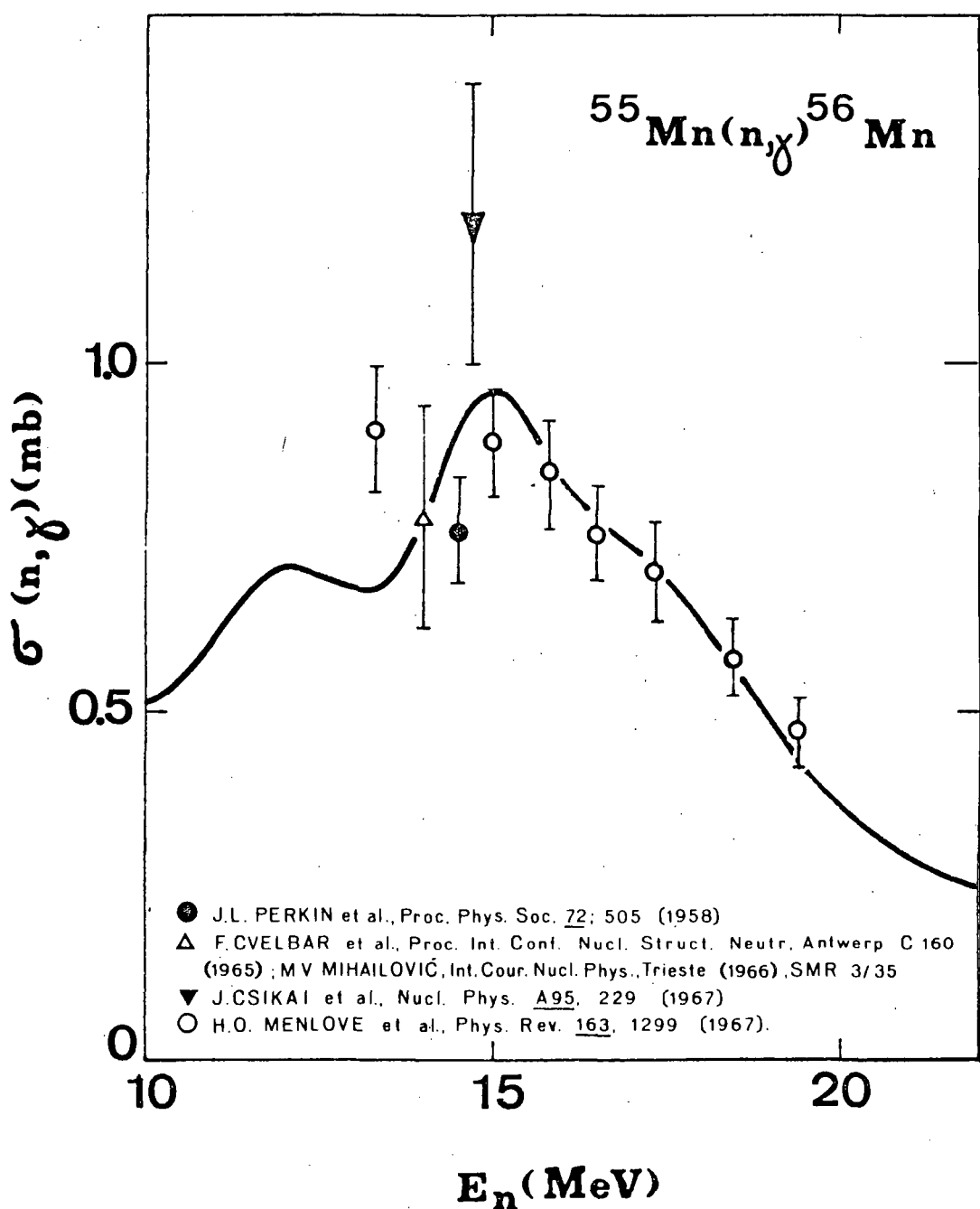


Fig. 14 - Comparison between experimental points and calculated cross sections for the $^{55}\text{Mn}(n,\gamma)$ reaction.

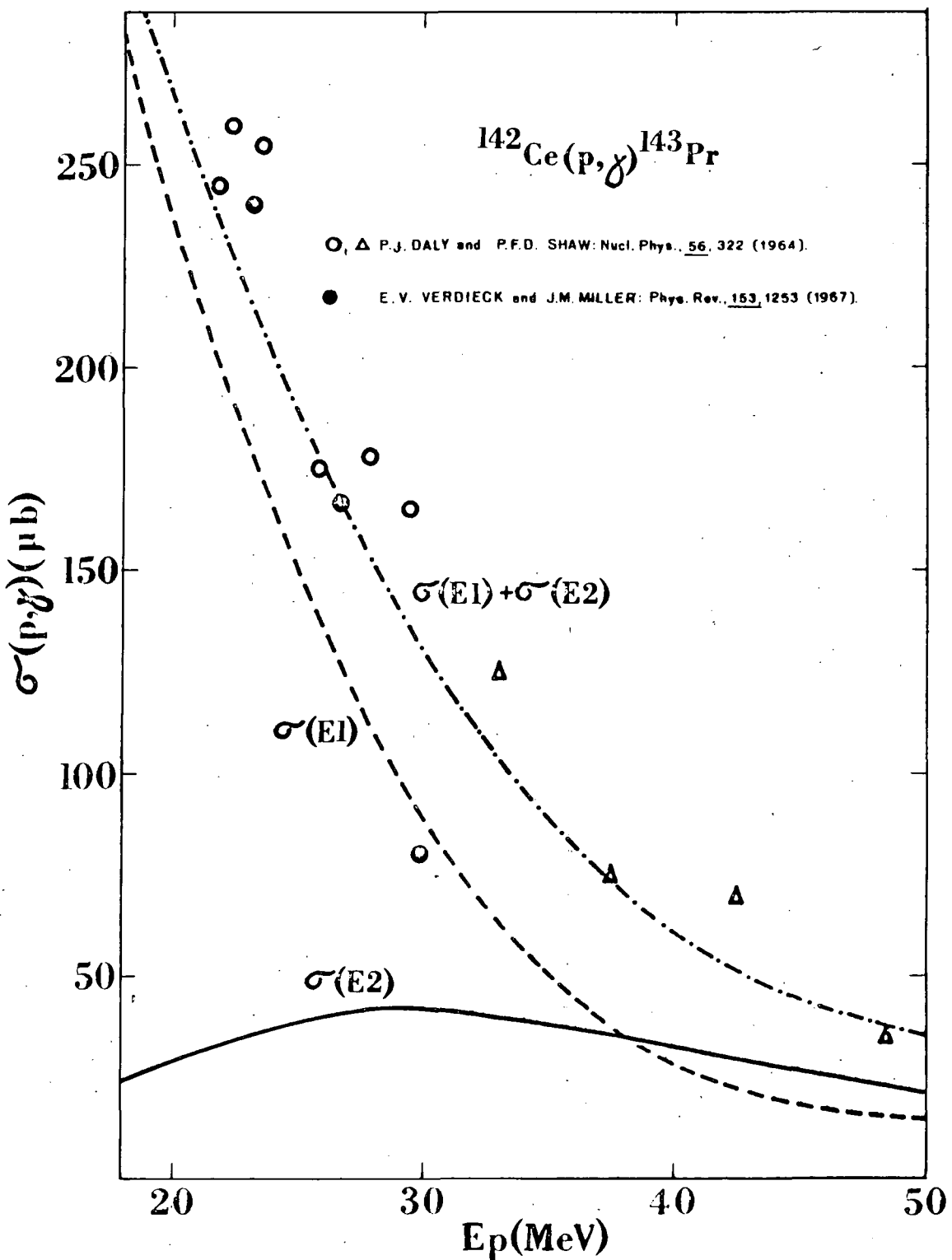


Fig. 15 - Comparison between experimental points and calculated cross sections for the $^{142}\text{Ce}(\text{p},\gamma)$ reaction.

XVIII GRUPPO DI RICERCA DEL CONTRATTO EURATOM-CNEN-INFN, ISTITUTO DI
FISICA DELL'UNIVERSITA', TORINO (ITALY)

Photonuclear studies

Photoneutron in Si and Ni

The structure of the photo absorption cross section observed in the region of the Giant Resonance represents a crucial point for theoretical interpretations of photonuclear reactions, and the photoneutron cross section represents a good test for the theory because the presence of an intermediate structure in the photo absorption cross section reveals itself in photoneutron experiment.

We have measured (γ, Tn) cross section for Si and Ni.

In our experiment samples of natural Si and Ni were irradiated with the bremsstrahlung beam of the Turin 100 MeV Synchrotron. The experimental setup is described in ref. [1,2,3].

The yield curves, measured in steps of 250 KeV, were analyzed with the method proposed by Cook [4] using S_2 smoothing matrices.

The (γ, Tn) cross section for Ni is shown in fig. 1. In the same figure the vertical bars represent the dipole strengths predicted by theory [5]. As one can see, many of the theoretical absorption peaks seem to present in the (γ, Tn) cross section at the proper-energy values, while the relative dipole strengths are not so well reproduced.

The results for Si are plotted in fig. 2.

The experimental data in G.R. region were fitted with a superposition of Lorentz curves thus recognizing the presence of six absorption lines between the threshold and 22 MeV. These are plotted in fig. 3a. The predictions of DTGCM [6] are also given in fig. 3b together with the lines obtained on the basis of a p-h calculation (fig. 3c).

.1. Neutron inelastic scattering from ^{28}Si

Inelastic scattering of 14 MeV neutrons from ^{28}Si has been measured from 30° to 90° up to 7 MeV excitation energy.

Angular distribution for 3^- level excitation at 6.88 MeV has been obtained. At angle greater than 60° excitation of the 3^+ non natural parity level at 6.2 MeV has been revealed.

The values obtained for 3^- level are:

$32^\circ 40'$	4.9 ± 0.4
$42^\circ 58'$	3.6 ± 0.3
$53^\circ 33'$	3.5 ± 0.3
$63^\circ 58'$	4.2 ± 0.3
$74^\circ 20'$	3.3 ± 0.2
$84^\circ 32'$	3.4 ± 0.3
$94^\circ 35'$	6.0 ± 0.1

References

- [1] S. Costa, F. Ferrero, C. Manfredotti, L. Pasqualini, G. Piragino and H. Arenhovel - Nuovo Cimento 48 (1957) 460.
- [2] S. Costa, F. Ferrero, C. Manfredotti, L. Pasqualini, G. Piragino and H. Arenhovel - Nuovo Cimento 51 (1967) 199.
- [3] S. Costa, C. Manfredotti, L. Pasqualini and F. Ferrero - Nuovo Cimento 54A (1968) 344.
- [4] B.C. Cook - Nucl. Instr. Meth. 24 (1963) 256.
- [5] J.B. Seeborn, D. Drechsel, H. Arenhovel and W. Greiner - Phys. Lett. 23 (1966) 576.
- [6] S. Costa, F. Ferrero, L. Ferrero, G. Manfredotti and L. Pasqualini - Nuovo Cimento - to be published.

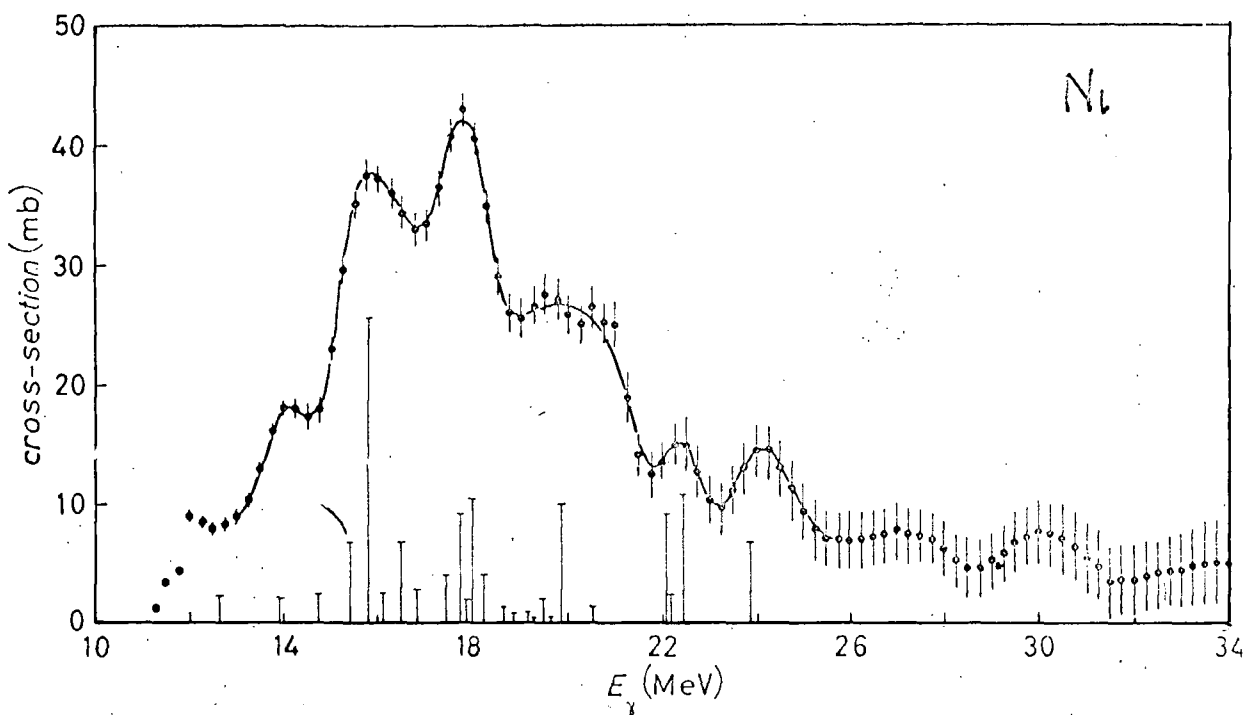


Fig. 1 - (γ, Tn) cross-section for Ni.

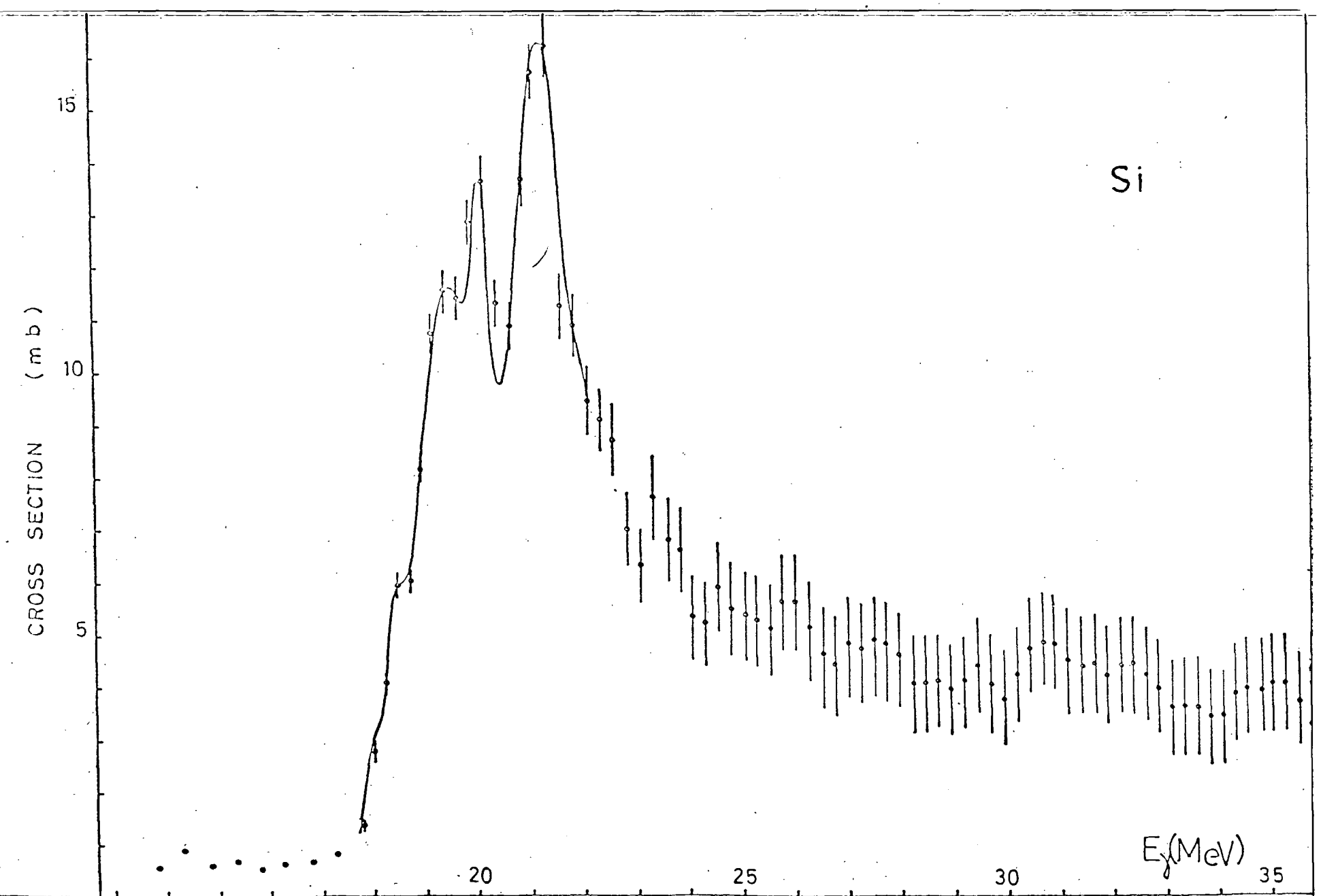


Fig. 2 - (γ ,Th) cross section for Si.

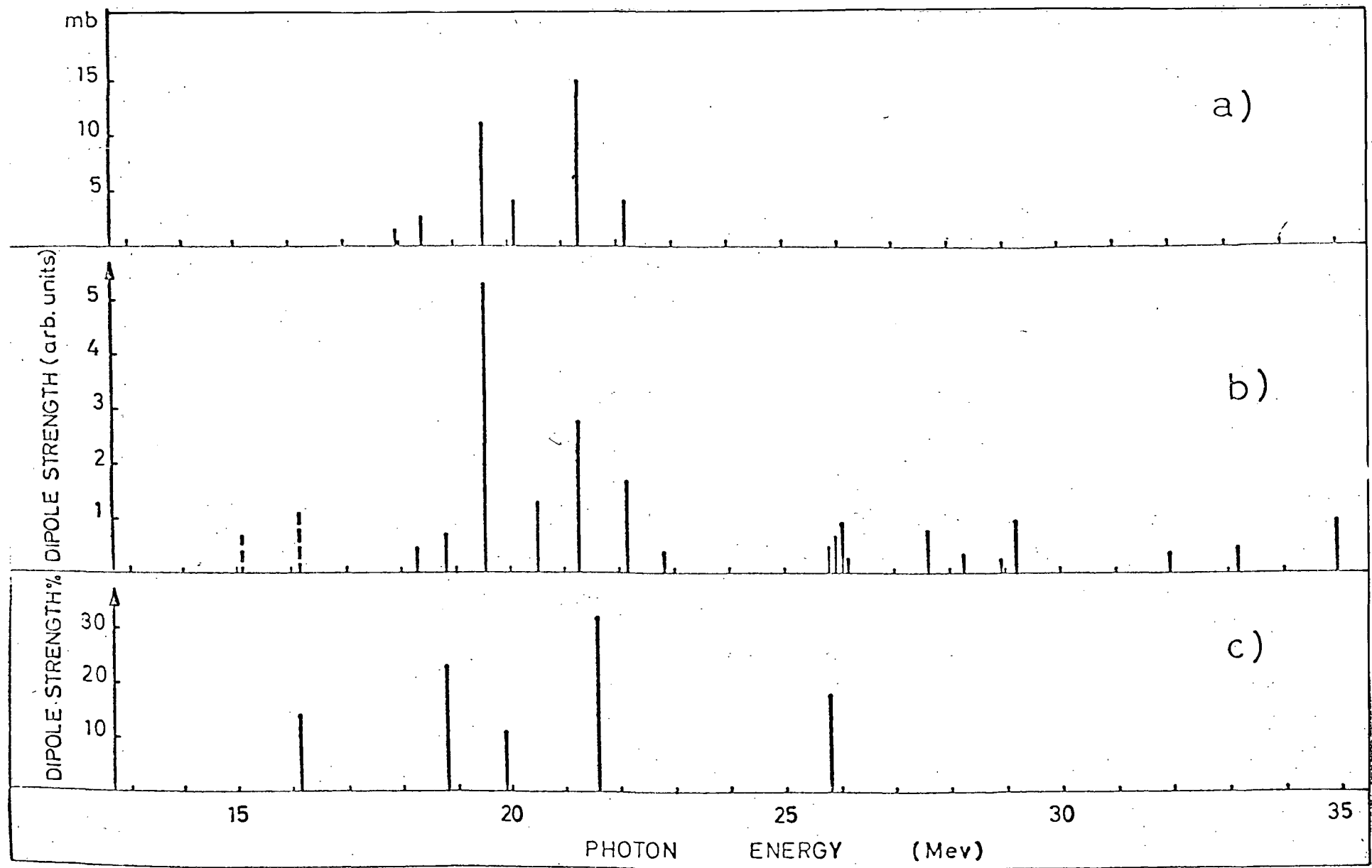


Fig. 3 - Comparison between experimental and theoretical structure of the
(γ , Tn) cross section for ^{28}Si

XIX. SERVICE DES MESURES NEUTRONIQUES FONDAMENTALES - CEA SACLAY (FRANCE) -

R. JOLY

GROUPE DES NEUTRONS THERMIQUES (H. NIFENECKER)

Ce groupe comprend les physiciens suivants : A. Audias, J. Babinet, P. Carlos (jusqu'en octobre 1968), B. Maier (jusqu'en octobre 1968), J. Poitou, M. Ribrag, R. Samama, M. Schneeberger, C. Signarbieux.

Etudes sur la fission -

1. Mode symétrique dans le cas de la fission à basse énergie -

Comme indiqué dans le rapport EANDC (E) - 89, on a repris l'étude de la fission symétrique pour ^{235}U , ^{233}U et ^{239}Pu . Le dépouillement des expériences est en cours.

2. Etude de la distribution corrélée angle-énergie des différentes particules légères dans le cas de la tripartition de ^{235}U induite par neutrons lents - [1]

On a mis en évidence une augmentation de l'énergie des α et des tritons aux petits angles. La distribution angulaire des tritons est moins anisotrope que celle des α .

3. Etude de la variation de la probabilité d'émission de particules de long parcours en fonction de la masse des fragments de fission - (en collaboration avec l'Université de Bordeaux).

La méthode de décontamination des spectres de fission était utilisée pour étudier plus particulièrement les régions symétriques et très asymétriques. Les particules de long parcours étaient détectées par un banc de six détecteurs Si(Au). Le dépouillement est en cours.

4. Mesure de l'émission neutronique prompte des fragments de fission de ^{252}Cf en fonction de leur charge - (en collaboration avec le CEN de Bruyères le Châtel).

On a mesuré simultanément pour un même fragment :

- le nombre de neutrons émis à l'aide d'un détecteur liquide chargé au gadolinium,
- l'énergie des rayons X émis grâce à une jonction Si(Li) ; les rayons X sont caractéristiques de la charge des fragments,
- l'énergie cinétique du fragment à l'aide d'une jonction à barrière de surface.

On a obtenu ainsi la variation du nombre moyen de neutrons en fonction de la charge des fragments. On a pu mettre en évidence une structure fine de cette variation, mais on n'a pas trouvé d'effet dû à la parité de la charge. On a

également obtenu la variation de $d\psi/dE$ en fonction de Z [2] [3]. La figure 1 montre les résultats obtenus pour $\psi(Z)$.

1.1.5. Calcul de l'efficacité des scintillateurs liquides chargés au gadolinium [4]
Un programme de Monte Carlo a été écrit pour simuler des expériences utilisant des scintillateurs liquides chargés au gadolinium dans diverses géométries. Ce calcul permet d'optimiser la géométrie des détecteurs par rapport à l'expérience.

1.2. Spectroscopie nucléaire à l'aide du rayonnement de capture de neutrons thermiques - [5] [6]

Le travail fait en 1968 a surtout consisté à améliorer la précision des mesures d'énergies des raies gamma. Pour ce faire, diverses méthodes de dépouillement ont été mises au point et une étude détaillée des défauts de linéarité des chaînes de détection a été faite.

1.3. Développement des installations expérimentales -

1.3.1. Le groupe disposait en 1967 de deux faisceaux de neutrons thermiques :
- l'un obtenu par diffraction d'un faisceau direct sur un monocristal de plomb. Son intensité est de $2 \cdot 10^6$ n/cm²/s.
- l'autre est un faisceau direct filtré par un monocristal de bismuth et un monocristal de quartz. Son intensité est de $2 \cdot 10^8$ n/cm²/s. Une troisième installation a été réalisée en 1968. Elle est identique à la précédente, mais les monocristaux sont portés à la température de l'azote liquide. Le flux obtenu est de $5 \cdot 10^8$ n/cm²/s.

Enfin, en collaboration avec le Service de Physique du Solide, on a réalisé un tube conducteur de neutrons donnant un flux de $3 \cdot 10^7$ n/cm²/s et d'une longueur de 30m. Un nouveau tube est en voie d'installation sur le même canal. L'utilisation d'une source froide devrait permettre d'obtenir des flux de l'ordre de 2 à $3 \cdot 10^8$ n/cm²/s [7].

1.3.2. L'étude d'une installation produisant un faisceau de rayons gamma monochromatiques d'énergie variable entre 1 et 7 MeV est en cours. Le principe de l'installation est le même que celui de celle réalisée par KNOWLES sur le réacteur NRU de Chalk River.

GROUPE DES NEUTRONS INTERMEDIAIRES - (A. MICHAUDON)

Implantation générale (C. EGGERMANN)

Cette année, les travaux ont porté principalement sur le dispositif de télé-commande des cibles productrices de neutrons. L'installation de ce dispositif est terminée. Après une série d'essais pendant la période d'arrêt annuel de l'accélérateur linéaire, ce dispositif a été mis en service en octobre. Une étude est actuellement en cours pour réaliser un appareillage destiné à la récupération des cibles ayant subi des avaries.

Le nombre et la disposition des bases de vol sont inchangés par rapport à l'année 1967.

Electronique, Calculateur CAE 510, Programme de dépouillement et d'analyse des données (B. CAUVIN, M. SANCHE) [8]

L'équipement électronique a été complété par l'installation d'une 2e chaîne d'enregistrement et d'analyse multiparamétriques à bande magnétique 16 pistes d'une part et d'une chaîne de lecture des bandes magnétiques à 16 pistes associée au calculateur CAE 510 pour être converties en bandes à 7 pistes utilisables directement par les calculateurs d'autre part.

Le calculateur CAE 510 a fonctionné en ligne pendant toute la durée des mesures. Un nouveau programme d'acquisition en ligne a été mis en service. Il permet de coupler le calculateur à 6 expériences simultanées dont une (qui demande un nombre de canaux égal à 16K) accumule directement dans la mémoire centrale du calculateur et les cinq autres dans des blocs-mémoires BM 96 à 4K qui servent ainsi d'extension à la mémoire centrale. Le code logique de certains blocs mémoires BM 96 a d'ailleurs été modifié pour augmenter leur capacité dans le mode d'acquisition en 2×4096 canaux. Le passage de la logique DCB à la logique binaire a permis d'obtenir un continu maximal de 1024 coups par canal pour les deux séries de 4096 canaux. L'acquisition en ligne de l'expérience principale dans la mémoire du calculateur se fait maintenant en mode groupé ce qui permet simultanément l'utilisation d'un des programmes secondaires suivants :

- tracé Calcomp de séries quelconques écrites sur bande magnétique,
- visualisation sur écran cathodique d'une série en cours d'accumulation dans la mémoire centrale.

Ces programmes secondaires permettent aux physiciens de vérifier immédiatement leurs résultats et de procéder à un traitement préliminaire accéléré. Les programmes de dépouillement sur calculateur IBM 360-75 ont été condensés, vérifiés et écrits sur disques magnétiques stockés près des gros calculateurs du C.E.N. Saclay pour permettre leur mise en œuvre prochaine par console IBM 1050 située dans le bâtiment de l'accélérateur linéaire. La compatibilité des modes d'écriture sur bande magnétique par calculateur CAE 510 et 360-75 a été gardée. Ceci nécessiterait l'élaboration de sous-programmes particuliers. Le programme de dépouillement de base (SMNF 022 sur 360-75) a été ainsi écrit de manière modulaire pour que toutes les fonctions d'entrées et de sorties multiples des séries résultats soient présentées sous forme de sous-programmes utilisables facilement par les physiciens.

2.3.

Mesures par temps de vol de neutrons -

Les bases de vol ont été utilisées de la façon suivante :

- Base n°1 : Sections efficaces totales - H. Tellier, J. Dabbs*, H. Derrien
D. Koenig, C. Newstead, M. Sanche
- Base n°2 : Anisotropie des fragments de fission - J. Dabbs*, C. Eggermann
- Base n°3 : Sections efficaces de fission - J. Blons, C. Eggermann
- Base n°4 : Multiplicité des rayons γ de capture - M. Asghar, B. Cauvin,
A. Katsanos, C. Newstead
- Base n°5 : Sections efficaces de diffusion élastique - J. Trochon
- Base n°6 : Spectres des rayons γ de capture - H. Landon**, B. Cauvin,
A. Lottin, D. Paya

2.3.1.

Sections efficaces totales -

La plus grande partie de l'activité a été consacrée à l'étude des isotopes du tellure en provenance du Laboratoire National d'Oak Ridge. Les quantités disponibles pour chaque échantillon enrichi en un isotope déterminé variaient entre 3g (^{123}Te) et 30 grammes. L'enrichissement était de 85% pour le ^{123}Te et supérieur à 95% pour les autres isotopes ($A=122, 124, 125, 126, 128, 130$). Les épaisseurs d'échantillons étaient comprises entre 0,4 et 4,8 grammes par cm^2 . Les distances de vol étaient de 17 mètres pour ^{123}Te et de 53 mètres pour les autres isotopes. La gamme d'énergie étudiée s'étend jusque vers

*) détaché par "Oak Ridge National Laboratory"

**) détaché par "National Bureau of standards"

30keV dans les cas les plus favorables.

Les résultats ont été obtenus par analyse de forme en utilisant la formule de Breit et Wigner à un niveau, élargie par les différents effets expérimentaux (résolution, effet Doppler).

Ces mesures ont permis d'améliorer considérablement les résultats antérieurs obtenus dans d'autres laboratoires.

L'analyse des résultats, telle qu'elle a été conduite jusqu'à présent, permet d'obtenir la fonction densité pour les ondes "S" pour tous les isotopes du tellure (Tableau I). On constate une nette décroissance de " S_0 " en fonction du nombre de masse (Fig. 2) en contradiction avec les calculs effectués avec différents types de modèle optique.

Sur la figure 3, nous avons tracé l'histogramme classique dans lequel la somme cumulative $2g \Gamma_n^0$ est portée pour l'ensemble des résonances de ^{126}Te situées en-dessous de l'énergie E(eV) en fonction de E. La fonction densité S_0 pour l'isotope ^{126}Te est déduite directement de la pente de cet histogramme.

De plus, quelques mesures ont été faites sur les éléments suivants :

- tellure naturel : échantillon épais refroidi à la température de l'azote liquide ; base de vol de longueur $L = 100$ mètres ;
- Thulium, échantillons épais refroidis à la température de l'azote liquide ; base de vol de longueur $L = 50$ mètres.

3.2. Anisotropie des fragments de fission [9]

Cette étude a consisté dans la mesure de l'anisotropie des fragments de fission lorsque cette dernière est induite par des neutrons de résonances non polarisés (c'est-à-dire tels qu'ils sont issus de la cible de l'accélérateur linéaire) dans des noyaux de ^{235}U alignés.

L'appareillage mis au point par J. Dabbs à Oak Ridge a été transporté à Sac-lay pour faire cette mesure dont le but était de déterminer la valeur moyenne du nombre quantique K dans les résonances. La mesure a duré environ 220heures avec une base de vol de 5 mètres pour une gamme d'énergie s'étendant de 0,3eV à 175eV. La température moyenne du cristal $\text{UO}_2\text{Rb}(\text{NO}_3)_3$ était de 0,61K.

Pour une cinquantaine de résonances situées en-dessous de 50eV, la valeur effective de K semble distribuée autour d'une valeur intermédiaire ($1 \leq K \leq 2$).

Au plus, quelques résonances ont une valeur de K voisine de 0, contrairement à ce qui peut être déduit d'une théorie simple des voies de sortie. Une petite

résonance située à 4,85eV semble avoir nettement la valeur $K \neq J$.

Les résultats sont en cours d'interprétation.

2.3.3.

Sections efficaces de fission -

L'effort principal a été porté sur la mesure de la section efficace de fission de ^{239}Pu avec un détecteur d'un type nouveau mis au point en 1967. C'est un scintillateur gazeux fonctionnant à la température de l'azote liquide et contenant 1 gramme de ^{239}Pu [10] [11]. Les mesures préliminaires de 1967 ont été améliorées en 1968 avec une résolution nominale de 1ns/m (longueur de la base de vol 50m). Le nombre de coups au sommet de la résonance à 75eV est de 6500 par canal de 100ns. La qualité de cette mesure est nettement supérieure à celle de mesures similaires effectuées dans d'autres laboratoires. L'analyse a permis d'obtenir les résultats suivants : [12] [13]

- 1 - les paramètres des résonances, analysées par le formalisme à un niveau jusqu'à une énergie de 440eV ;
- 2 - le spin pour une quinzaine de résonances supplémentaires ;
- 3 - le coefficient d'autocorrélation qui est nettement différent de zéro, ce qui confirme l'existence d'une structure intermédiaire, interprétée comme étant probablement due à la fission en-dessous du seuil dans la voie 1^+ (Fig.).
On a, par ailleurs, calculé la section efficace moyenne de fission jusqu'à 25keV.

2.3.4.

Multiplicité des rayons γ de capture -

La méthode qui consiste à déterminer le spin des résonances par l'étude de la multiplicité des rayons γ de capture dans ces résonances a été étendue à plusieurs autres noyaux. Pour la première fois, elle a été appliquée à un noyau fissile, le ^{235}U [14]. Afin de réduire la contribution des rayons γ de fission, les seuils de discrimination ont été réglés à des valeurs relativement élevées : 4,5MeV pour la voie "simple" et 1,1MeV pour la voie "coïncidence". De plus, une plaque de plomb d'épaisseur 1cm a été interposée entre l'écharillon de ^{235}U et les cristaux de NaI. Dans ces conditions, les rapports R ainsi obtenus sont nettement séparés en deux groupes pouvant correspondre aux valeurs de spin $J\pi = 3^-$ et $J\pi = 4^-$ (Fig.5). Les résultats sont en bon accord avec les spins des deux résonances à 8,8eV et 12,4eV déterminés par une méthode de diffusion élastique au C.E.N. de Mol.

Les mesures relatives à d'autres noyaux (holmium, iodé et antimoine) sont en cours de dépouillement.

3.5. Sections efficaces de diffusion élastique -

Le détecteur utilisé pour ces mesures est composé de 8 cellules de scintillateur liquide NE 321 A (diamètre 47mm, épaisseur 1,5mm) couplées optiquement à des photomultiplicateurs EMI 9514 A et 9536. Les impulsions dues aux rayons γ sont éliminées par discrimination de forme. [15]

Ce détecteur est installé à 32,75m de la cible de l'accélérateur linéaire. Il est entouré d'une épaisse protection en paraffine borée afin de diminuer le bruit de fond.

La principale application de ces mesures est la détermination du spin des résonances, lorsqu'il n'est pas trop élevé.

Les noyaux suivants ont été étudiés ou sont en cours d'étude :

- ^{125}Te : échantillon, enrichi en ^{125}Te , d'épaisseur $0.387 \cdot 10^{-3}$ atm/barn et $0.758 \cdot 10^{-3}$ atm/barn ; gamme d'énergie : de 200 à 4000eV ; le spin d'une trentaine de résonances a pu être attribué.

- ^{123}Te : échantillon enrichi en ^{123}Te , d'épaisseur $0.967 \cdot 10^{-3}$ atm/barn ; gamme d'énergie : de 200 à 1000eV ; le dépouillement est en cours.

- ^{239}Pu : mesure préliminaire avec un échantillon de ^{239}Pu , d'épaisseur $n = 4 \cdot 10^{-4}$ atm/barn. La contribution des neutrons de fission est évaluée en utilisant des cellules de scintillateur liquide NE 213 qui ne contiennent pas de ^{10}B .

- Les résultats obtenus en 1967 sur le gadolinium ont été dépouillés et un certain nombre de spins ont pu être obtenus : 5 pour ^{155}Gd et 19 pour ^{157}Gd . Ils sont en excellent accord avec ceux qui ont été déduits de la mesure de la multiplicité des rayons γ .

3.6. Spectre des rayons γ de capture radiative -

Un effort important a été fait pour améliorer les conditions de travail, particulièrement sur les points suivants :

- rétablissement des caractéristiques du détecteur Ge-Li et de l'électronique après la surcharge provoquée par l'éclair γ émis à chaque cycle par l'accélérateur linéaire. Dans les conditions usuelles de fonctionnement ($L=12\text{m}$, 1000 impulsions de 100ns par seconde), cet éclair γ provoque une dissipation d'énergie de quelques centaines de MeV dans le détecteur à chaque impulsion.

Cette surcharge a été pratiquement éliminée en interposant entre la cible en uranium et l'échantillon, contre la cible, un écran très épais de plomb. Il masque ainsi la partie de la cible qui émet des rayons γ de freinage, mais

laisse intacte la plus grande partie du ralentisseur qui émet les neutrons de résonances. Dans ces conditions, la contribution de l'éclair γ dans le détecteur a été réduite à quelques MeV, ce qui permet d'utiliser une électronique classique à bonne résolution. Le gain de la chaîne électronique est rétabli à sa valeur nominale environ $5\mu s$ après l'émission de l'éclair γ . A une distance de vol de 12 mètres, ce temps correspond à celui de neutrons de 30keV. Cette énergie est bien supérieure à celle des résonances dont on étudie le spectre des rayons γ de capture.

- bruit de fond : l'installation de nouvelles collimations et de protections en bismuth a permis de réduire le bruit de fond et donc d'observer des transitions de plus faible intensité.

Les noyaux suivants ont été étudiés :

- Fer : résonances à 1.15keV et à 29,2keV de ^{56}Fe (diode coaxiale Ge-Li de 30cm^3) [16]

Dans la première résonance, une raie non primaire de 900keV a été observée qui n'était pas connue auparavant. Elle a permis d'identifier la cascade de 6340keV \rightarrow 900keV aboutissant à l'état $3/2^-$ de 366keV dans ^{57}Fe .

Dans la deuxième résonance, bien que la résolution soit satisfaisante, le bruit de fond est trop important pour que l'analyse du spectre soit possible.

- Antimoine : (détecteur : diode plane Ge-Li de 8cm^3 de résolution environ 3keV à 1MeV).

L'analyse des spectres de rayons γ dans les résonances situées en-dessous de 120eV est en cours. La figure 6 montre le spectre brut tel qu'il a été observé dans la résonance à 6,24eV de ^{121}Sb .

2.4.

Analyse des sections efficaces des noyaux fissiles à l'aide d'un formalisme à plusieurs niveaux - (H. DERRIEN)

Cette étude a été faite, en partie, au Laboratoire National d'Oak Ridge avec la collaboration de Gérard de Saussure ; les noyaux étudiés sont le ^{235}U et le ^{239}Pu . Pour le ^{235}U , une courbe théorique a été calculée dans le domaine d'énergie allant de 0.1 à 100eV et s'adaptant aux sections efficaces totale (mesures faites à Saclay), de capture et de fission (mesures faites auprès de l'accélérateur linéaire de RPI). Le formalisme utilisé est celui de D.B. Adler et F.T. Adler. Pour le ^{239}Pu , l'étude a été faite sur la section efficace totale entre 5 et 160eV sur les courbes expérimentales de Saclay, par l'utilisation du même formalisme. On obtient un très bon accord entre la courbe théo-

rique et les résultats expérimentaux ; mais l'interprétation physique des paramètres est très difficile, étant donné la complexité de la transformation permettant de passer des paramètres du formalisme d'Adler aux paramètres de la matrice R (transformation orthogonale diagonalisant la matrice des niveaux A). Cette étude peut être néanmoins très utile aux pilologues.

L'étude des sections efficaces totale et de fission du ^{239}Pu (obtenues à Sac-lay sur des échantillons refroidis à la température de l'azote liquide) se poursuit actuellement en utilisant d'autres formalismes multiniveaux dérivés de la théorie de la matrice R : formalisme de Vogt et formalisme de Reich-Moore. Pour ce dernier formalisme, le programme utilisé emploie la méthode des moindres carrés, les dérivées de la fonction théorique, par rapport aux paramètres des résonances, étant calculées par une méthode numérique.

Pour ce dernier formalisme, les premiers résultats sont très encourageants ; en particulier, on confirme l'existence d'une seule voie de sortie fission pour l'état de spin 1^+ du noyau composé, et deux voies de sortie pour l'état de spin 0^+ .

GROUPE DES NEUTRONS RAPIDES - (J.L. LEROY)

Les travaux décrits ci-dessous ont été effectués autour du Van de Graaff de 5 MeV de Cadarache, par D. ABRAMSON, A. ARNAUD, J.C. BLUET, P. FARDEAU, G. FILIPPI, E. FORT, J. GENTIL, D. HEBERT, J.L. HUET, C. LERIGOLEUR, J.L. LEROY, I. SZABO.

Commande de l'accélérateur et des expériences associées au moyen d'un calculateur électronique -

L'essentiel de ce projet était réalisé au début de 1968, et le fonctionnement automatique a été largement utilisé. Il a permis d'augmenter le temps d'utilisation des installations d'un facteur 2 environ. Cette année, quelques commandes supplémentaires ont été réalisées. En outre, on s'est efforcé d'améliorer la programmation du système pour la rendre plus souple grâce à une utilisation plus importante du FORTRAN. Chaque fonction élémentaire de commande, de réglage ou d'acquisition peut être faite au moyen d'un sous-programme écrit en langage Symbol et appelable en FORTRAN.

Le programme FORTRAN de gestion de l'expérience se compose donc principalement d'instructions d'appel de ces sous-programmes, séparées par des instructions logiques, permettant d'effectuer le choix entre différentes options prévues initialement. Il comporte également une partie de calcul, qui permet la réduction des données brutes.

Eventuellement, le programme élabore les nouvelles valeurs des réglages de l'expérience, en fonction des résultats déjà acquis. Au cas où le programme est trop encombrant, on peut le séparer en plusieurs tronçons qui sont chargés et exécutés successivement par le moniteur d'enchaînement de travaux, écrit par Mademoiselle BEAUVAL, du DCE/SACLAY.

L'état actuel du système a été décrit récemment [17]

3.2.1. Etude de la réponse du compteur étalon - (Fig. 7)

Cet appareil a déjà été décrit ailleurs [18] [19]

L'étude expérimentale de la réponse a été poursuivie.

La valeur absolue de l'efficacité a été mesurée entre 100 et 500keV, par comparaison avec un scintillateur de verre au ^6Li étalonné par la méthode de la particule associée, et en comparant le système avec une cuve de sulfate de manganèse ; le schéma de cette dernière expérience est représenté par la figure 8 .

Entre 2 et 4MeV, la forme de la courbe de réponse a été mesurée en utilisant les propriétés de symétrie de la réaction (d,d). A 2,6MeV, la valeur absolue de l'efficacité a été obtenue grâce à un comptage dans un angle solide défini des protons de la réaction D(d,p)T et au rapport des sections efficaces des réactions D(d,n) ^3He et D(d,p)T. Un bref compte-rendu de ces diverses expériences a été publié [19].

Ces mesures ont été poursuivies dans le but d'améliorer la précision. Au stade actuel, la courbe de réponse est donnée par la table suivante, à $\pm 4\%$ près

Energie (MeV)	0.100	0.250	0.500	2.000	2.500	3.000	3.500	4.000	4.300
Efficacité	0.139	0.135	0.134	0.133	0.126	0.123	0.113	0.106	0.102

3.2.2. Etude de la section efficace de la réaction $^6\text{Li}(n,\alpha)\text{T}$ entre 100 et 400 keV -

A partir des mesures d'efficacité du scintillateur de verre au ^6Li , faites par la méthode de la particule associée, on peut trouver la section efficace de cette réaction, à condition de connaître le nombre d'atomes de lithium dans le scintillateur et de faire la correction de diffusion multiple.

Cette dernière correction a été recalculée en tenant compte de la rétrodiffusion par le verre du photomultiplicateur et de la dégradation d'énergie des neutrons [20] .

Pour vérifier ce calcul, on a mesuré le rapport des comptages de deux scintillateurs de formes différentes en fonction de l'énergie entre 100 et 350keV

après correction au moyen des facteurs calculés, on obtient une valeur constante à $\pm 2\%$ près. Ce rapport est égal à 1,4% près à celui des épaisseurs des scintillateurs.

Le nombre d'atomes de ${}^6\text{Li}$ dans un scintillateur au lithium naturel (NE 901), avait été déterminé par une mesure d'absorption totale de neutrons thermiques [21] ; la valeur trouvée était en bon accord avec les indications données par le constructeur.

Ce scintillateur était ensuite comparé au scintillateur NE 905, enrichi au ${}^6\text{Li}$, qui sert dans la mesure de particule associée, dans le but de déterminer le nombre d'atomes de celui-ci.

Nous avons découvert récemment que cette comparaison faite avec des neutrons de 250 keV, était entachée d'une erreur d'environ 20%, car le scintillateur appauvri compte des neutrons par un autre processus que la réaction ${}^6\text{Li}(\text{n},\alpha)\text{T}$. Cet effet est négligeable pour les scintillateurs enrichis. L'expérience était faite au faisceau pulsé, de façon à éliminer les γ émis par la cible et les neutrons diffusés. Dans ces conditions, les valeurs de section efficace données en [21] sont trop fortes d'environ 20 - 25%.

Si l'on admet provisoirement les nombres d'atomes donnés par le constructeur et en appliquant la correction de diffusion multiple [20], on trouve, pour la section efficace de la réaction ${}^6\text{Li}(\text{n},\alpha)\text{T}$, les valeurs données par la figure 9 .

On peut voir, pour les énergies supérieures à 250 keV que nos résultats se rapprochent beaucoup plus de ceux de SCHWARTZ que de ceux de GABBARD et BAME.

3. Mesure de la section efficace de fission entre 120 et 370 keV - [22]

Cette mesure a été faite en 1967, mais n'avait pas été publiée, car la calibration du détecteur de neutrons ne nous paraissait pas suffisamment assurée. La figure 10 donne les résultats de cette mesure qui se rapprochent plus des résultats de WHITE que de ceux de ALLEN et FERGUSSON.

4. Mesure des distributions angulaires de la diffusion élastique sur ${}^6\text{Li}$ - [23]

Le dispositif de mesure a déjà été décrit [24].

Les résultats sont donnés par la figure 11. Ils sont en bon accord avec les résultats obtenus à Geel par COPPOLA et KNITTER.

4. GROUPE "EVALUATION" - (P. RIBON, J.P. L'HERITEAU)

A la demande des physiciens des réacteurs, des activités concernant l'évaluation des données neutroniques ont débuté au sein du SMNF à la fin de 1967. Durant cette première année, un effort important a été consacré à la mise au point de programmes concernant le traitement de l'information, principalement des données neutroniques provenant du CCDN ; cette tâche n'est pas encore terminée.

4.1. Les travaux d'évaluation proprement dits ont concerné deux problèmes :

4.1.1. Valeurs de $\bar{\alpha}$ du ^{239}Pu au-delà de 1keV -

Cette étude comprend un examen critique des expériences et évaluations antérieures, et deux essais d'évaluations :

a) dans le premier, nous avons calculé $\bar{\alpha} = \langle \sigma_c \rangle / \langle \sigma_f \rangle$ d'après les valeurs expérimentales de $\langle \sigma_t \rangle$ et $\langle \sigma_f \rangle$, en évaluant $\langle \sigma_d \rangle$ et $\langle \sigma_{in} \rangle$. Ces valeurs étaient moyennées sur un intervalle de l'ordre du keV. Cette méthode est assez peu précise car, outre l'erreur provenant de l'évaluation de $\langle \sigma_d \rangle$ (le facteur correctif F_{nn} peut être faussé par d'éventuelles structures intermédiaires), $\bar{\alpha}$ dépend beaucoup de $\langle \sigma_f \rangle$: une erreur de 10% sur celle-ci donne une erreur de 20% sur $\bar{\alpha}$. Or les valeurs de $\langle \sigma_f \rangle$ sont très dispersées : la zone hachurée de la figure 12 correspond à $\bar{\alpha}$ déduit de deux évaluations de $\langle \sigma_f \rangle$. Cette évaluation nous a néanmoins conduit à conclure en la présence d'un maximum de $\bar{\alpha}$, très large, aux alentours de 2keV. Les résultats préliminaires de ORNL (EANDC (US) 109 A) portés sur la figure 1 sont en bon accord avec cette évaluation et montrent, eux aussi, l'existence de ce pic très large vers 2keV. Il faut remarquer, à ce propos, que la valeur $\alpha = (\sigma_t - \sigma_f - \sigma_d) / \sigma_f$ sera très sensible à des structures intermédiaires de fission.

b) le second essai fut effectué par J.Y. BARRE au CEN Cadarache : les jeux multigroupes servant aux calculs des réacteurs rapides sont ajustés d'après quelques expériences critiques (méthode "BARRAKA"). Pour obtenir un bon accord, il est nécessaire de modifier considérablement certaines des valeurs initiales : ce fut le cas de $\bar{\alpha}$ pour ^{239}Pu qui dut être augmenté de près de 50% en-dessous de 10keV (courbe en tirets de la figure 12).

Cette méthode permet encore moins que la précédente de prévoir les structures fines, mais elle donne une indication intéressante sur la valeur moyenne qui est, en l'occurrence, en bon accord avec les derniers résultats expérimer.

2. Paramètres des résonances des noyaux fissiles

Quelques études furent effectuées afin de comparer les valeurs données par différents auteurs. Elles montrent d'assez grandes discordances ; nous les illustreront par les Γ_f et les sections efficaces de fission de ^{235}U .

a) La figure 13 représente la distribution des largeurs de fission pour 4 jeux de paramètres : Saclay (A. MICHAUDON et al. 1964), Karlsruhe (Evaluation de SCHMIDT, 1966), Westinghouse (D.W. DRAWBAUGH et A. GIBSON, 1966) et Geel (M. CAO et al, 1967). Les zones d'énergies ne sont pas les mêmes dans tous les cas, mais il s'agit toujours d'une analyse à un seul niveau. Les distributions sont incompatibles entre elles : les valeurs moyennes de Γ_f déterminées d'après elles sont données ci-dessous.

Saclay	Dubna	Karlsruhe	Westinghouse	Geel
45 meV	50meV	65meV	150meV	50meV

Les résultats de Dubna (Van Shi Di et al, 1965) sont très voisins de ceux de Geel.

Ces distributions peuvent être décrites par des lois en X^2 à 2 ou 3 degrés de liberté.

b) La section efficace de fission moyenne peut être évaluée d'après les valeurs expérimentales ou d'après les paramètres de résonances ; les deux résultats devraient évidemment être en accord. Le tableau II représente les valeurs de l'intégrale de σ_f dans des zones d'énergies contigües évaluées soit d'après la somme directe des sections efficaces données par différents auteurs (colonne 2), soit d'après la somme des aires des résonances (colonnes 3 à 7).

Il apparaît que $\langle\sigma_0 \Gamma_f\rangle$ est très sous-évalué, sauf pour celui résultant de l'analyse de DRAWBAUGHT et GIBSON ; ceci est à rapprocher du fait que ces auteurs donnent de très grandes valeurs de Γ_f .

Il faut bien noter que les expérimentateurs sont souvent conscients de l'existence de niveaux non analysés ; mais le désaccord atteint le facteur 2 dans des zones où presque toutes les résonances sont résolues : seule l'existence de grandes valeurs de Γ_f semble pouvoir l'expliquer.

c) Afin d'essayer de résoudre ces problèmes, nous entreprenons une étude complète des sections efficaces de ^{235}U à toutes énergies ($E_n < 15\text{MeV}$).

4.2.

Une étude plus générale a été entreprise sur les formalismes permettant la description des sections efficaces dans le domaine des résonances (formules multiniveaux). De nombreuses méthodes sont actuellement utilisées à peu près toutes basées sur la théorie de la matrice R ; certaines impliquent des inversions de matrices, une autre permet d'obtenir une bonne description des courbes expérimentales mais sans pouvoir obtenir les paramètres de la matrice R.

Nous essayons une méthode approchée permettant une très bonne description des sections efficaces. Il est bien connu que celles-ci peuvent s'exprimer en fonction des éléments d'une matrice A sur l'espace des niveaux obtenue par l'inversion d'une matrice A^{-1} d'éléments :

$$A_{\lambda\lambda'}^{-1} = (1 - \delta_{\lambda\lambda'}) \frac{i}{2} G_{\lambda\lambda'} - \delta_{\lambda\lambda'} (E - \mathcal{E}_\lambda)$$

avec : $\mathcal{E}_\lambda = E_\lambda - i \frac{\Gamma_\lambda}{2}$

$$G_{\lambda\lambda'} = \sum_\alpha [R_{\lambda\alpha}]^{1/2} [R_{\lambda'\alpha}]^{1/2}$$

La matrice A^{-1} peut se décomposer en une matrice diagonale, D^{-1} facilement inversible, et d'une matrice complémentaire N^{-1} dont les éléments diagonaux sont nuls. Or, ces éléments non diagonaux ($\sim G_{\lambda\lambda'}$) sont petits devant les éléments diagonaux ($E - \mathcal{E}_\lambda$) et l'on peut écrire :

$$A = D + DN^{-1}D + DN^{-1}DN^{-1}D + DN^{-1}DN^{-1}DN^{-1}D + \dots$$

Le premier ordre correspond à la formule de Breitt et Wigner à un niveau. Le second terme peut s'écrire, à un coefficient près :

$$\frac{1 - \delta_{\lambda\lambda'}}{(E - \mathcal{E}_\lambda)(E - \mathcal{E}_{\lambda'})} = \frac{1}{(\mathcal{E}_\lambda - \mathcal{E}_{\lambda'})(E - \mathcal{E}_\lambda)} + \frac{1}{(\mathcal{E}_{\lambda'} - \mathcal{E}_\lambda)(E - \mathcal{E}_{\lambda'})}$$

avec $\lambda \neq \lambda'$, et peut donc se ramener à une somme de termes de Breitt et Wigner à un niveau. Les termes d'ordre 3 et 4 peuvent, de même, se ramener à des sommes de pôles simples et doubles ; finalement, au 4e ordre, la matrice de collision U peut s'exprimer simplement comme une somme de la forme :

$$U \sim \frac{CPS_\lambda}{(E - \mathcal{E}_\lambda)} + \frac{CPD_\lambda}{(E - \mathcal{E}_\lambda)^2}$$

les coefficients CPS et CPD étant indépendants de l'énergie E (dans la mesure où les paramètres servant au calcul de $G_{\lambda\lambda'}$, en particulier Γ_n , sont indépendants de E).

La précision du calcul dépend évidemment des rapports Γ_α/D . Elle peut être très bonne même si $\Gamma_\alpha/D \sim 0,5$ si l'on inclut les pôles doubles (développement au 4e ordre). Pour illustrer cela, nous donnons un exemple : il correspond aux premières résonances de ^{235}U étudiées il y a quelques années. La

comparaison a été faite par rapport aux résultats donnés par le programme MUFLÉ . L'accord est très bon pour la section efficace totale (Fig.14) : alors que l'erreur (ϵ_1) atteint 20-30% en précision 1 (formule de Breitt et Wigner à 1 niveau), elle n'atteint que 3% en précision 2 (ϵ_2) et 1 à 2% en précision 4 (ϵ_4). Cette erreur serait encore plus faible si l'on tenait compte de l'effet Doppler qui tend à moyennner les sections efficaces.

La prise en compte de l'effet Doppler introduit des fonctions du type

$$\frac{\Gamma}{2\Delta\sqrt{\pi}} \int_{-\infty}^{+\infty} \frac{1}{E' - \varepsilon_\lambda} \exp - \frac{(E-E')^2}{\Delta^2} dE' = D * \frac{\Gamma}{2} \frac{1}{E - \varepsilon_\lambda} = \mathcal{Q} - i\Psi$$

et $D * \frac{1}{(E - \varepsilon_\lambda)^2}$

Ces fonctions peuvent assez facilement être calculées ; cette méthode d'approximation du formalisme multiniveaux permettrait sans doute dans la plupart des cas une analyse de forme par une méthode des moindres carrés des résultats expérimentaux.

GROUPE DES REACTIONS PHOTONUCLEAIRES (R. BERGERE)

Ce groupe a continué d'utiliser en 1968 le système de production de "gammas monochromatiques" par annihilation en vol des positons produits à la sortie de l'accélérateur linéaire de 45 MeV et sélectionnés ensuite en énergie (entre 5 et 35 MeV) par une optique magnétique à 3 aimants. L'adjonction d'une quatrième section à l'accélérateur linéaire en 1969 doit permettre de doubler le flux de positons de 20 MeV et d'étendre de 35 à 55 MeV environ la plage de production des "gammas monochromatiques". L'installation d'une deuxième optique magnétique, symétrique de la première, permettra de monter simultanément deux expériences photonucléaires. La première optique continuera à être spécialisée dans l'étude des réactions (γ, xn) à l'aide du scintillateur liquide de 500 litres, chargé à 0,5% de gadolinium et d'efficacité égale à 60% environ pour la détection des photoneutrons [25] .

Avec l'installation existante, les résultats obtenus concernaient les réactions suivantes :

1/- (γ, n) ($\gamma, 2n$) ($\gamma, 3n$) ($\gamma, 4n$) sur ^{181}Ta avec évaluation à $22 \pm 2\%$ des neutrons d'effet direct produit par réactions (γ, n) en compétition avec la réaction ($\gamma, 2n$). On a également pu montrer par disparition du processus ($\gamma, 2n$) devant ($\gamma, 3n$), puis du processus ($\gamma, 3n$) devant ($\gamma, 4n$) dès que cela était énergétiquement possible, que les photoneutrons de multiplicité ≥ 2 étaient des neutrons

d'évaporation. [26] (Fig.15).

2/ - $(\gamma, n)(\gamma, 2n)(\gamma, 3n)$ sur ^{165}Ho , ^{159}Tb et ^{139}La [27] avec mise en évidence d'une contribution pour Ho et Tb non représentée par les raies de Lorentz décrivant l'absorption dipolaire dans la résonance géante (Fig. 16).

Cette contribution pourrait être l'absorption quadrupolaire E_2 prévue dans le modèle collectif hydrodynamique par Legensa et Greener (Nucl. Phys. A 92 (1967) 673). Le dédoublement observé de la résonance géante pour Ho, Tb et Ta a permis de retrouver le moment quadrupolaire de ces noyaux déformés.

Les réactions $(\gamma, n)(\gamma, 2n)(\gamma, 3n)$ ont également été étudiées sur les noyaux suivants : iodé, cérium, samarium, erbium et lutécium. Les résultats correspondants sont en cours de publication. De même, les résultats expérimentaux concernant les réactions $(\gamma, n) \rightarrow (\gamma, 4n)$ dans le ^{208}Pb viennent d'être acquis.

Enfin, sur le noyau $^{39}\text{Y}^{89}$ on essaye actuellement d'étudier simultanément :

1 - la résonance géante $\sigma(\gamma, n) + \sigma(\gamma, 2n) + \sigma(\gamma, 3n)$

2 - le rapport de branchement vers le niveau isomérique à 394 keV ($\tau = 0,332\text{ms}$) dans $^{39}\text{Y}^{88}$ consécutif à une réaction (γ, n) . L'application du formalisme de Huizenga et Vandenbosch (Phys. Rev. 120 (1960) 1305) à nos résultats expérimentaux devrait permettre d'accéder au moment d'inertie du noyau $^{39}\text{Y}^{88}$.

3 - Le dédoublement isobarique (absorption d'un photon dans la résonance dipolaire géante avec $\Delta T = 0$ ou $\Delta T = 1$) prévue par S. Falieross et al. (Phys. Letters 19 (1965) 398).

BIBLIOGRAPHIE -

1. M. SCHNEEBERGER - Thèse (1968)
2. H. NIFENECKER, M. RIBRAG, J. FREHAUT, J. GAURIAU - (à paraître)
3. H. NIFENECKER, A. AUDIAS, C. SIGNARBIEUX, J. FREHAUT, M. SOLEILHAC - Rapport C.E.A. (à paraître)
4. J. POITOU, H. NIFENECKER, C. SIGNARBIEUX - Rapport C.E.A. (à paraître)
5. G. PERRIN, J. GIRARD, R. SAMAMA, B.P. MAIER, P.J. CARLOS - Rapport C.E.A. (à paraître)
6. J. GIRARD, R. SAMAMA, P.J. CARLOS, B.P. MAIER, G. PERRIN - J. de Phys. (à paraître)
7. J. FAGOT - Thèse (1968)

8. B. CAUVIN, M. HUET, M. SANCHE - J. de Phys. (à paraître)
9. J.W. DABBS, C. EGGERMANN, B. CAUVIN, A. MICHAUDON, M. SANCHE
A.P.S. Meeting - Miami Beach (Flo) - 1968
10. J. BLONS, M. DUMAZERT, C. EGGERMANN, J. FERMANDJIAN,
Y. PRANAL - J. de Phys. (à paraître)
11. J. BLONS, M. DUMAZERT, C. EGGERMANN - Nucl. Instr. and Meth.
(à paraître)
12. D. PAYA, J. BLONS, A. FUBINI, A. MICHAUDON - Conférence sur la
Structure Nucléaire (Dubna - Juillet 1968)
13. J. BLONS, C. EGGERMANN, A. MICHAUDON - C.R. Acad. Sciences
267(1968)901
14. M. ASGHAR, A. MICHAUDON, D. PAYA - Phys. Letters 26B (1968) 664
15. J. TROCHON, M. ASGHAR, B. LUCAS, P. RIBON - Nucl. Inst. and
Meth. (à paraître)
16. H. LANDON, B. CAUVIN, A. MICHAUDON - A.P.S. Meeting - Miami
Beach (Flo) 1968.
17. J.C. BLUET, J.L. LEROY, P. FARDEAU - J. de Phys. (à paraître)
18. E.A.N.D.C. (E) 89 (1968) 191.
19. J.L. LEROY, J.L. HUET, I. SZABO, C. LERIGOLEUR, D. ABRAMSON
J. de Phys. (à paraître)
20. E. FORT - Rapport SMNF (à paraître)
21. E. FORT, J.L. LEROY - Conférence AIEA "Nuclear Data for Reactors"
(Paris, 1966)
22. I. SZABO, P. QUENTIN - Rapport SMNF (à paraître)
23. D. ABRAMSON, C. LERIGOLEUR - Rapport SMNF (à paraître)
24. C. LERIGOLEUR, D. ABRAMSON - J. de Phys. (à paraître)
25. H. BEIL, R. BERGERE, A. VEYSSIERE - Nucl. Instr. and Meth. (à paraître)
26. A. VEYSSIERE, H. BEIL, R. BERGERE - C.R. Acad. Sc. 267-B (1968) 234
27. R. BERGERE, H. BEIL, A. VEYSSIERE - Nucl. Phys. A 121 (1968) 463.

TABLEAU I

Fonction densité S_0 pour les isotopes au tellure

A	Limite E (keV)	Nombre de résonances	$S_0 \times 10^4$
122	10.8	42	0.80 ± 0.18
123	0.66	26	0.98 ± 0.27
124	28	84	0.68 ± 0.10
125	7.8	114	0.50 ± 0.07
126	17.7	65	0.26 ± 0.05
128	21.8	38	0.27 ± 0.06
130	30.1	22	0.14 ± 0.04

TABLEAU II

Section efficace de fission du ^{235}U

Zone d'énergie	$\sum_{E_1} \sigma_F \delta E$	Evaluation d'après				
		$\frac{\pi}{2} \sum_{E_1} \sigma_0 F$	Saclay	Dubna	Karlsruhe	Westinghouse
5 - 7,4	$61,5 \pm 3$	38,0	42,4	50,3	57,5	
7,4 - 10	212 ± 15	197	202	203	234	206
10 - 15	213 ± 10	104	173	159	219	116
15 - 20,5	292 ± 20	240	269	259	311	274
20,5 - 37	423 ± 20	196	328	343	477	226
37 - 41	480 ± 25	337	396	284	466	405
41 - 60	860 ± 50			786	958	323
60 - 73	290 ± 20			256		86
73 - 100	640 ± 40			538		(180)
100 - 113	215 ± 25			169		(115)

Figure 1

AVERAGE NUMBER OF NEUTRONS

AS A FUNCTION OF THE FRAGMENTS CHARGE

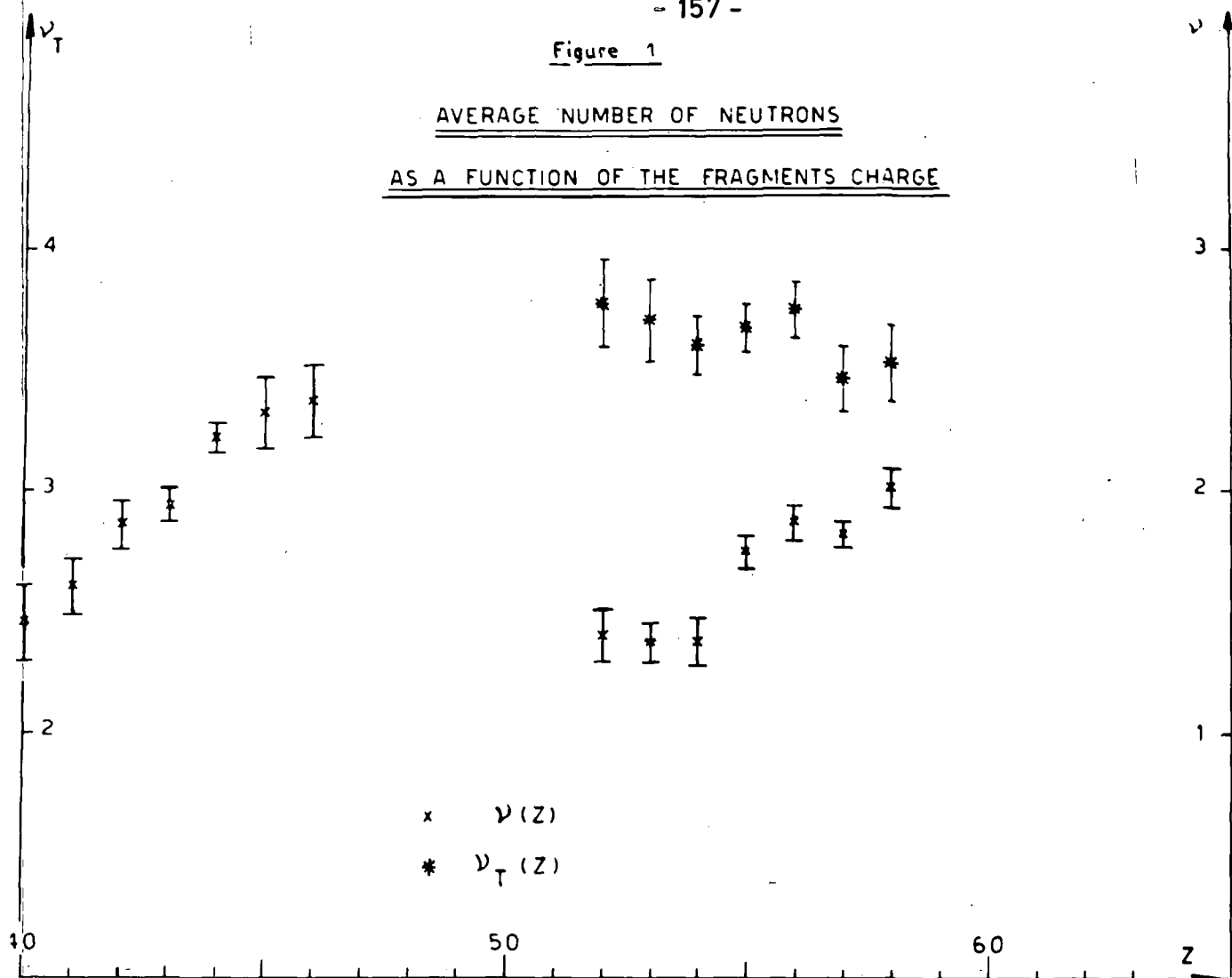
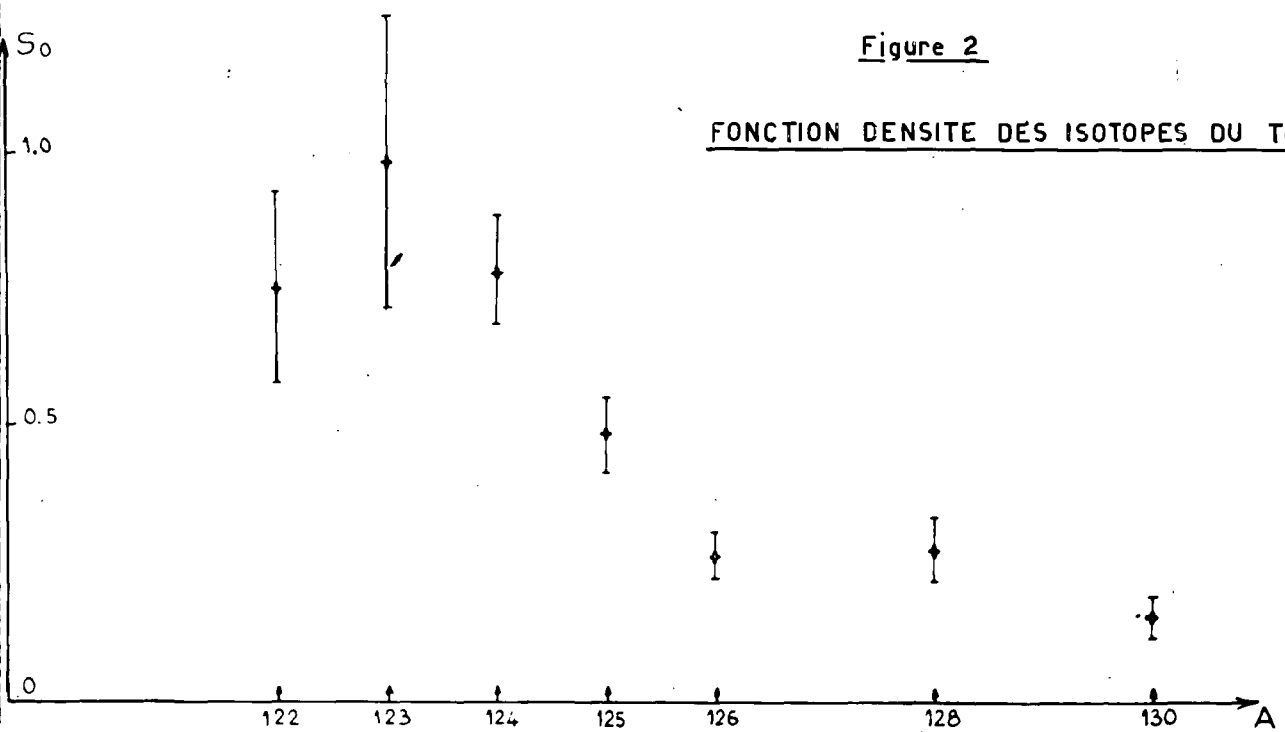


Figure 2

FONCTION DENSITE DES ISOTOPES DU Te



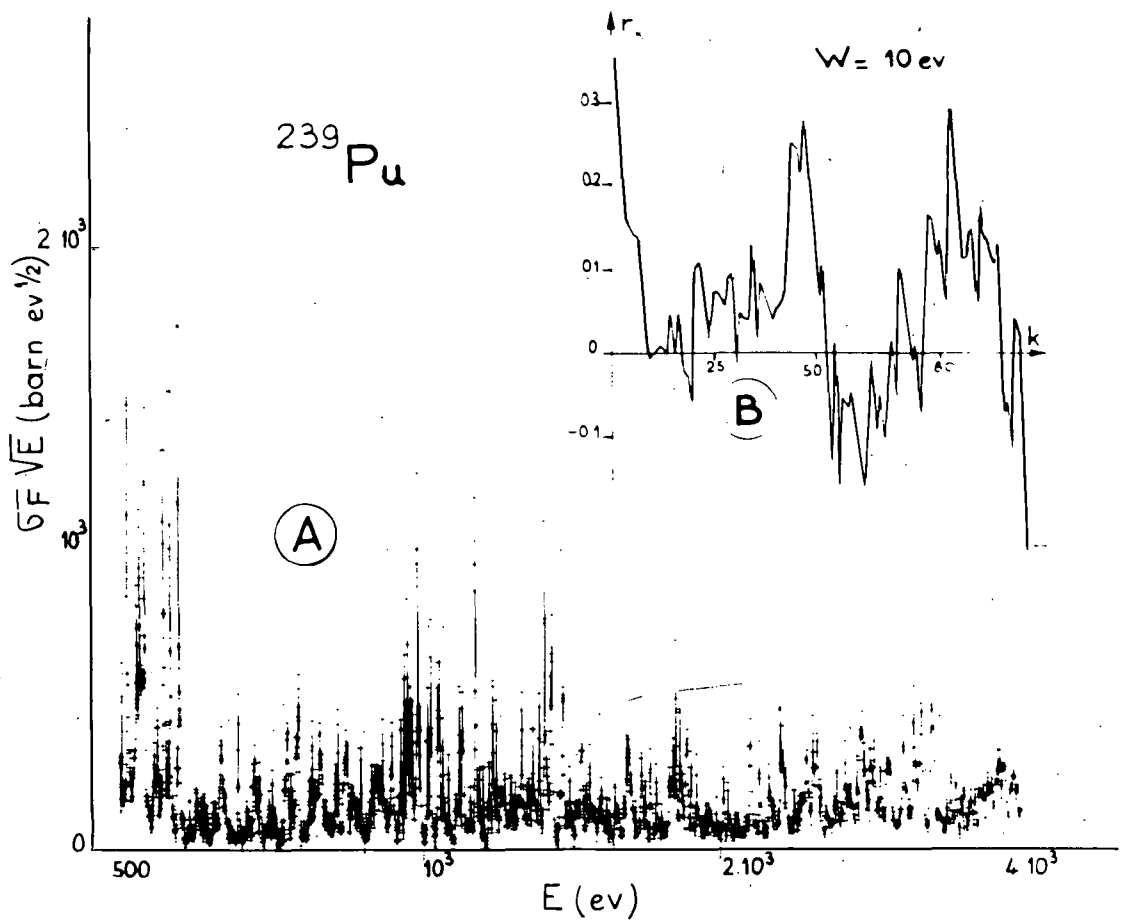
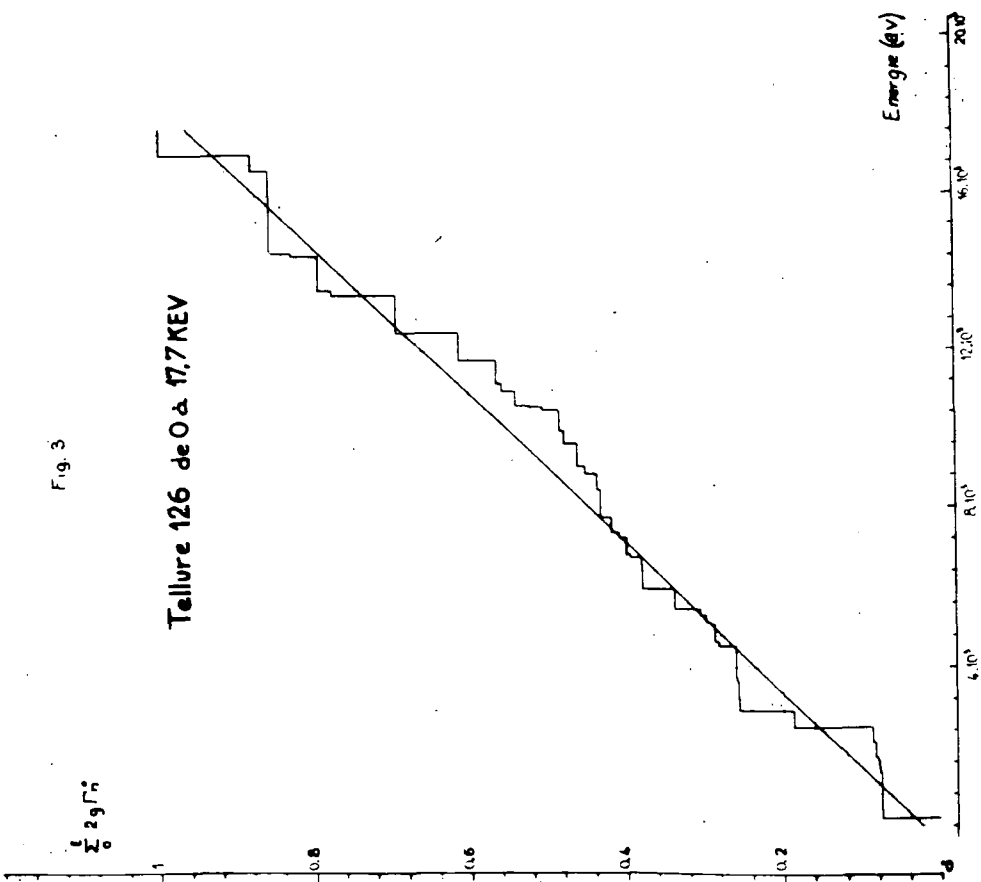


Fig. 3

Tellure 126 de 0 à 17.7 KEV



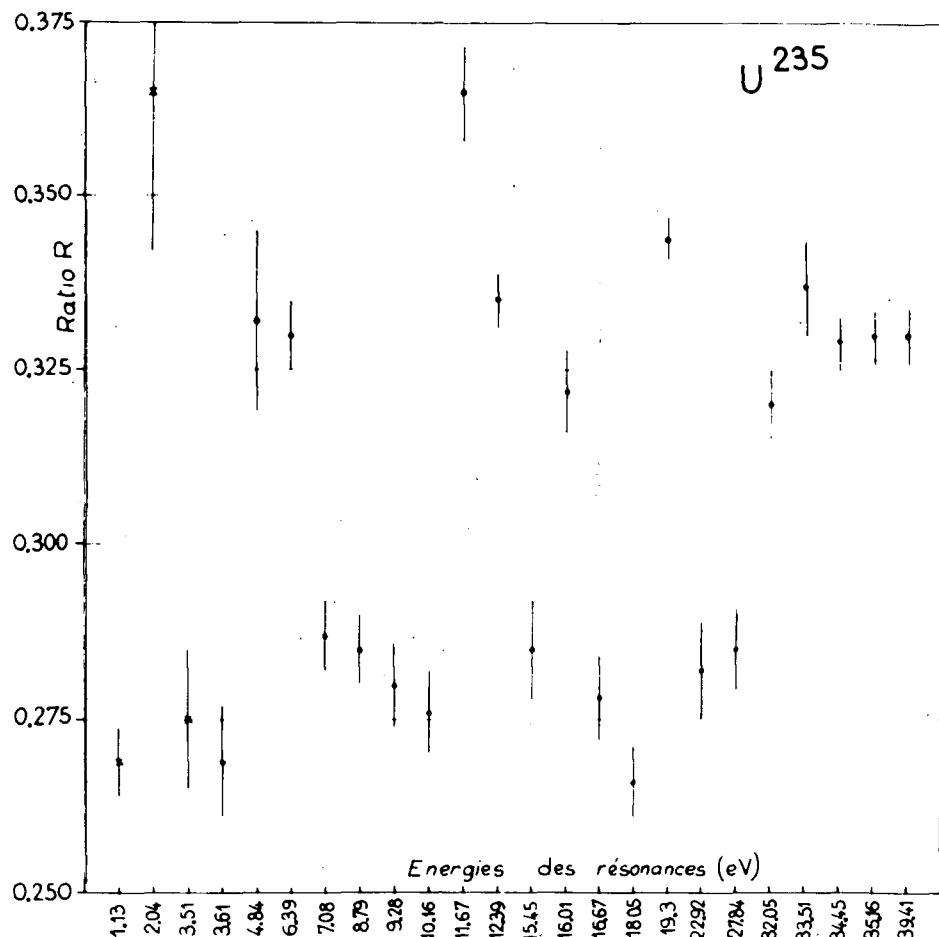


Fig. 5

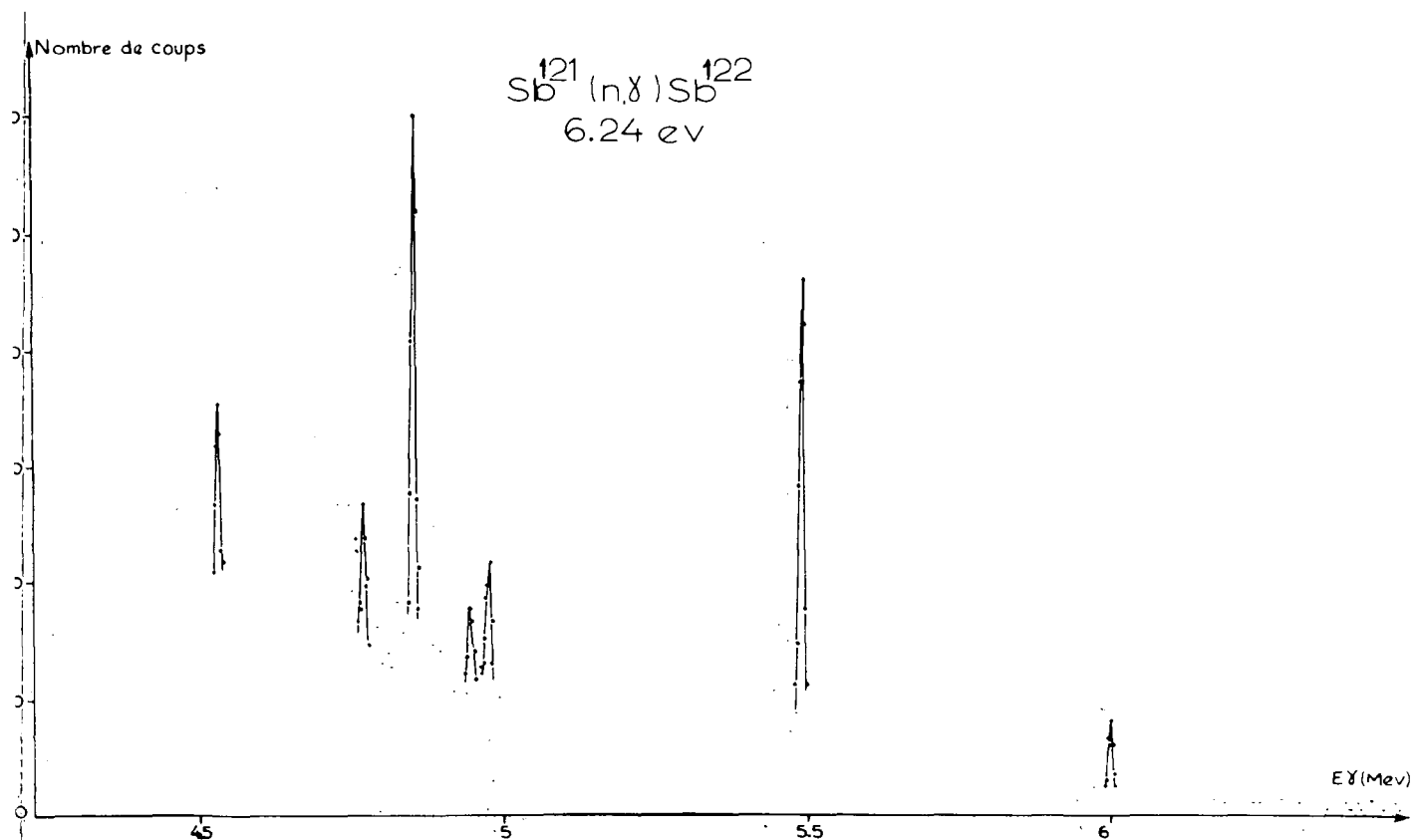


Fig. 6

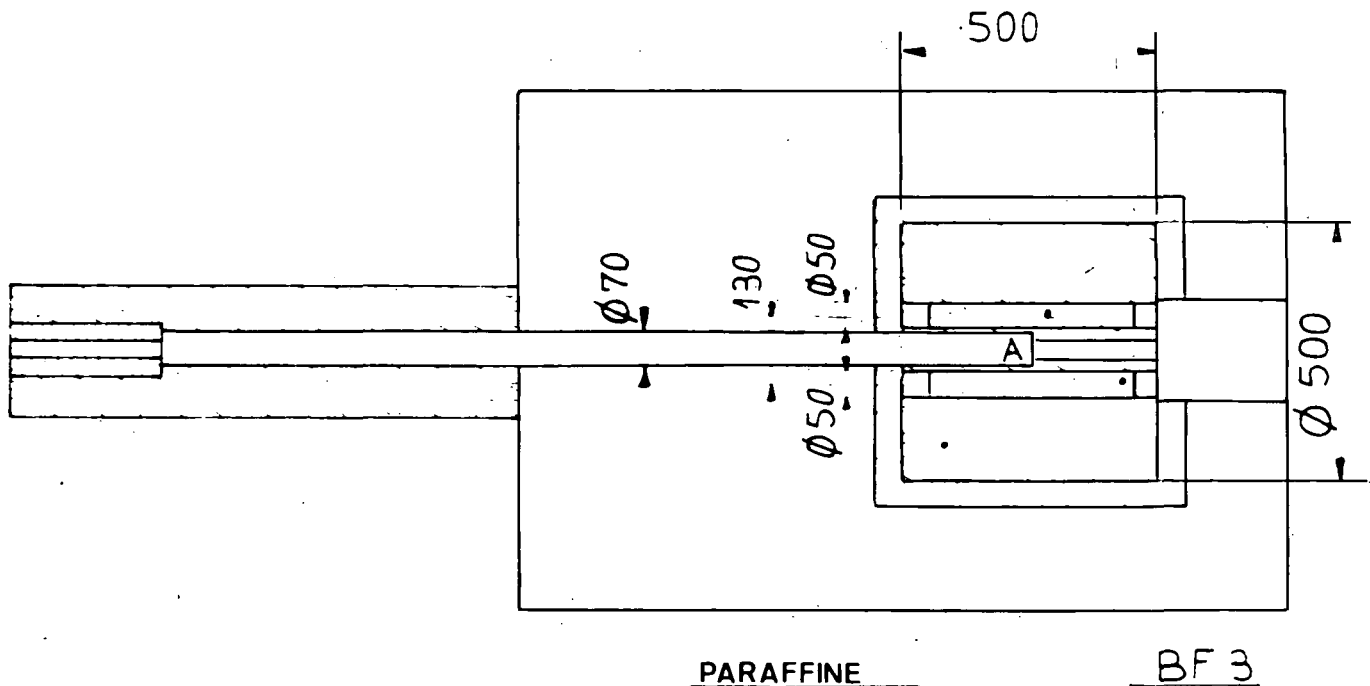


Fig 7

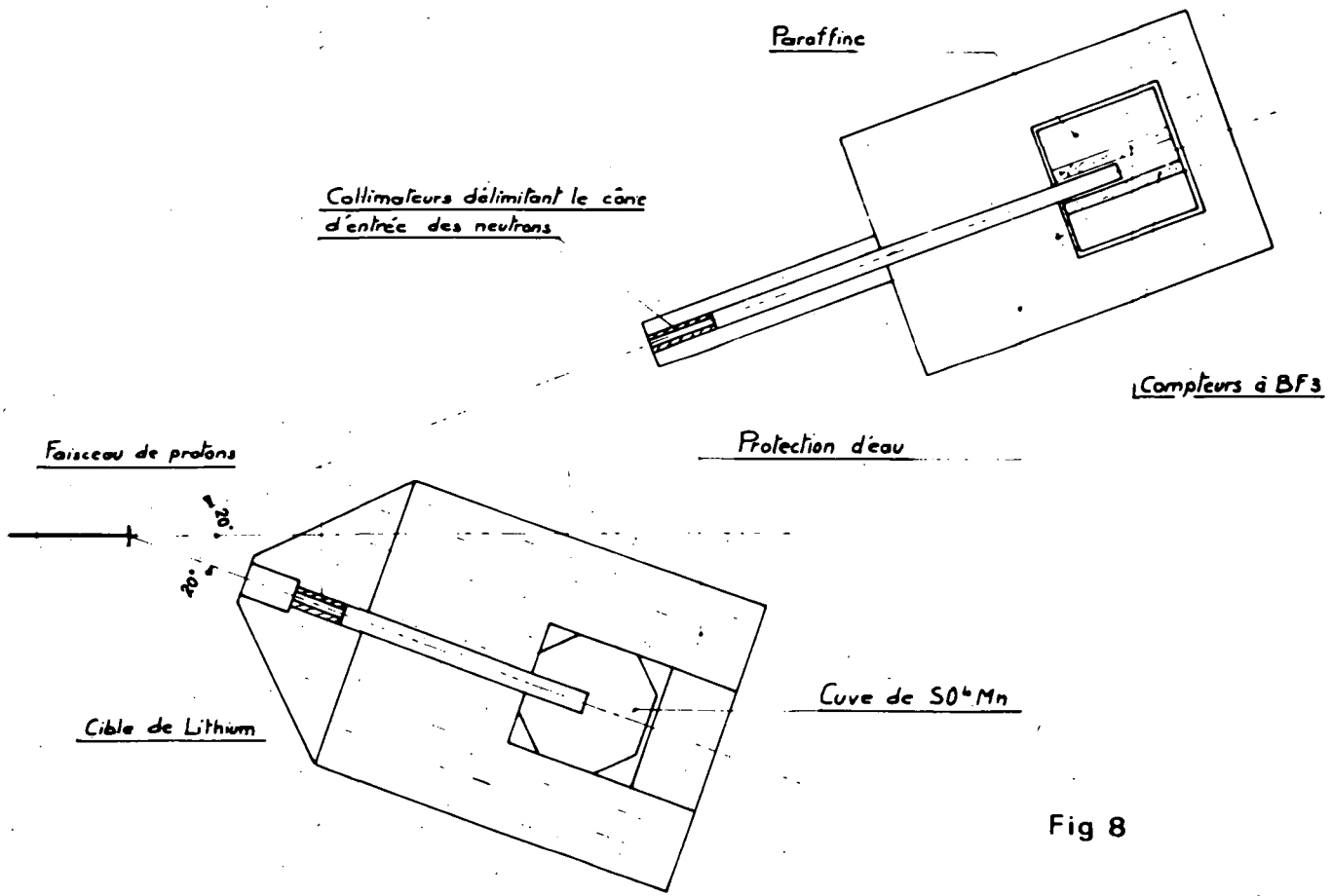
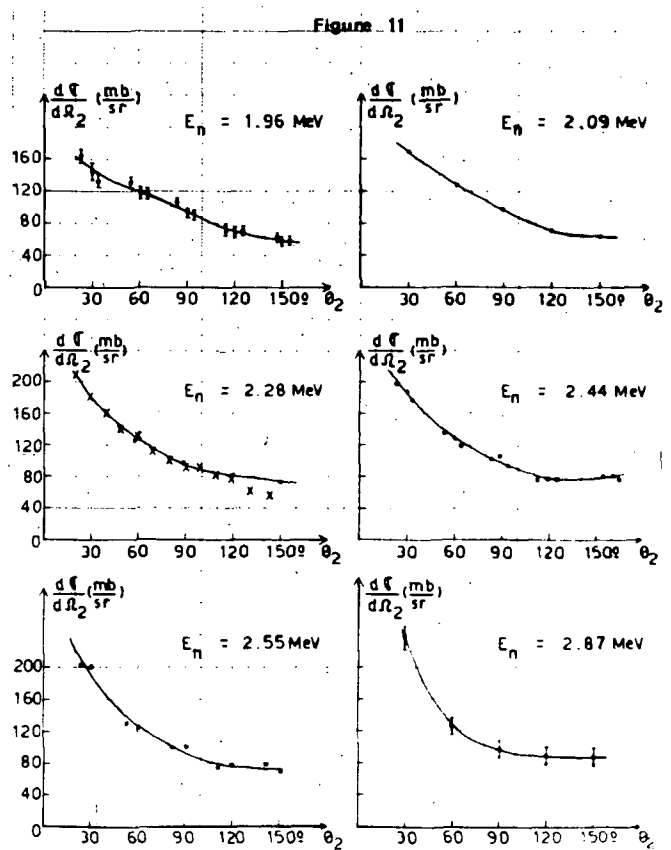
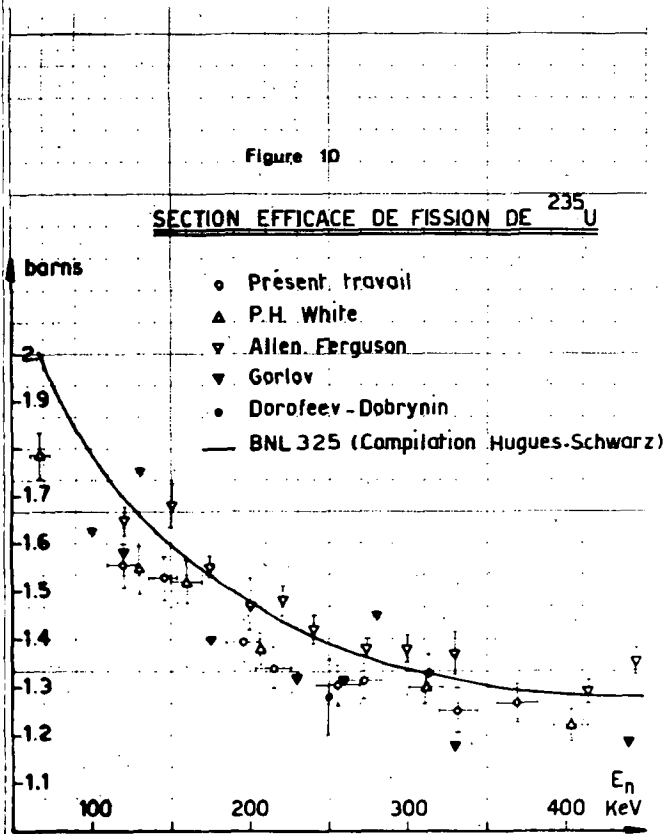
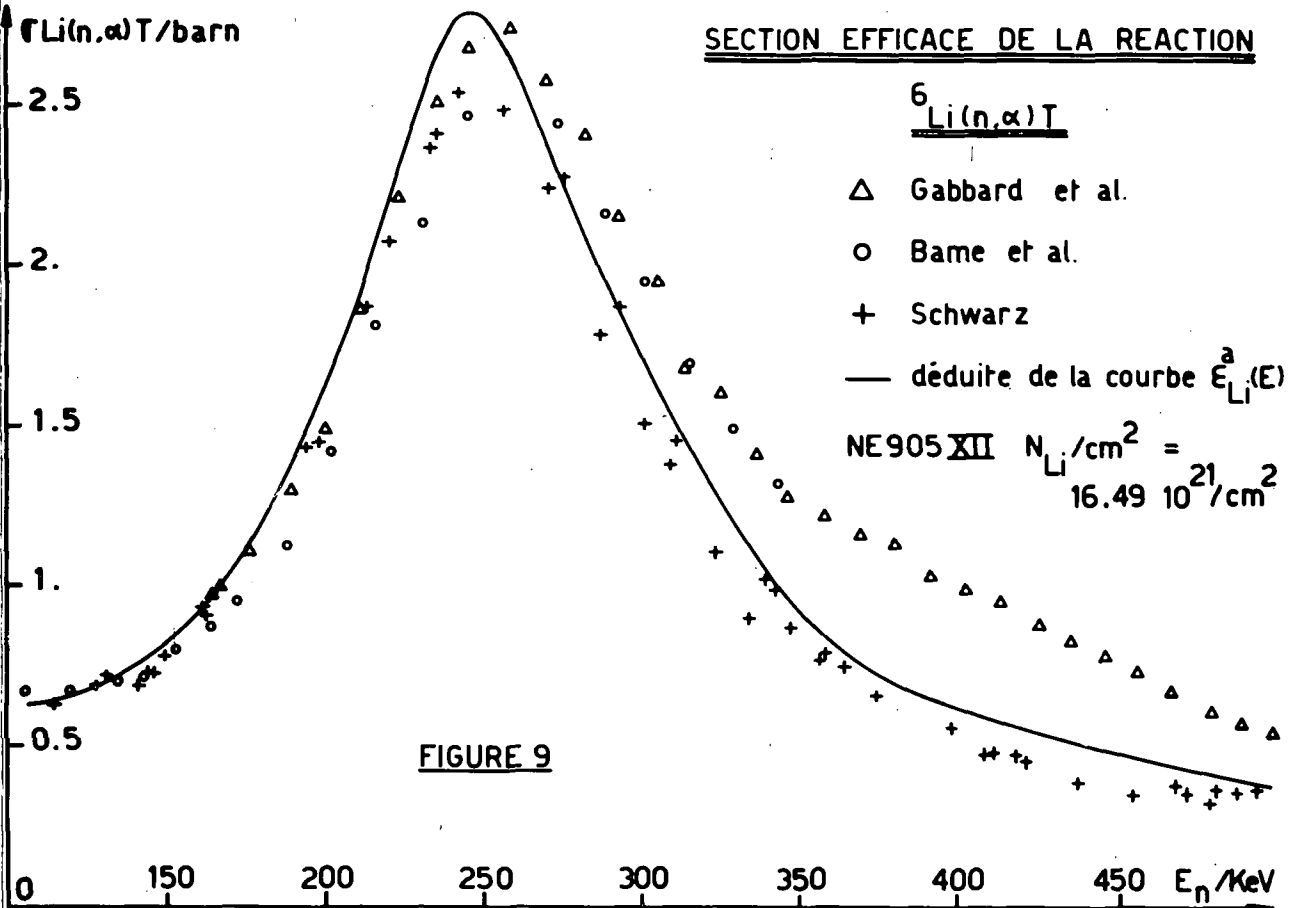


Fig 8



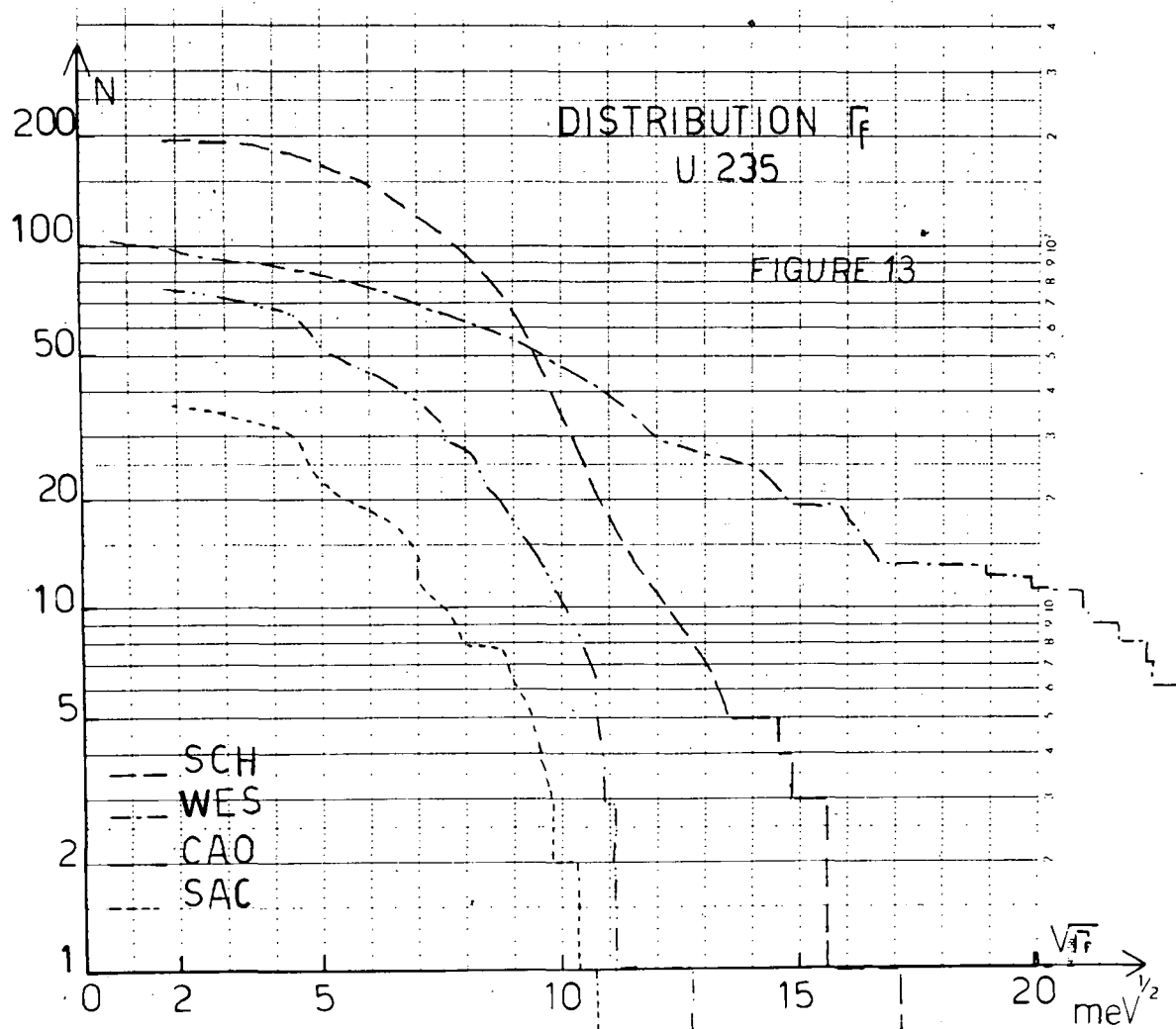
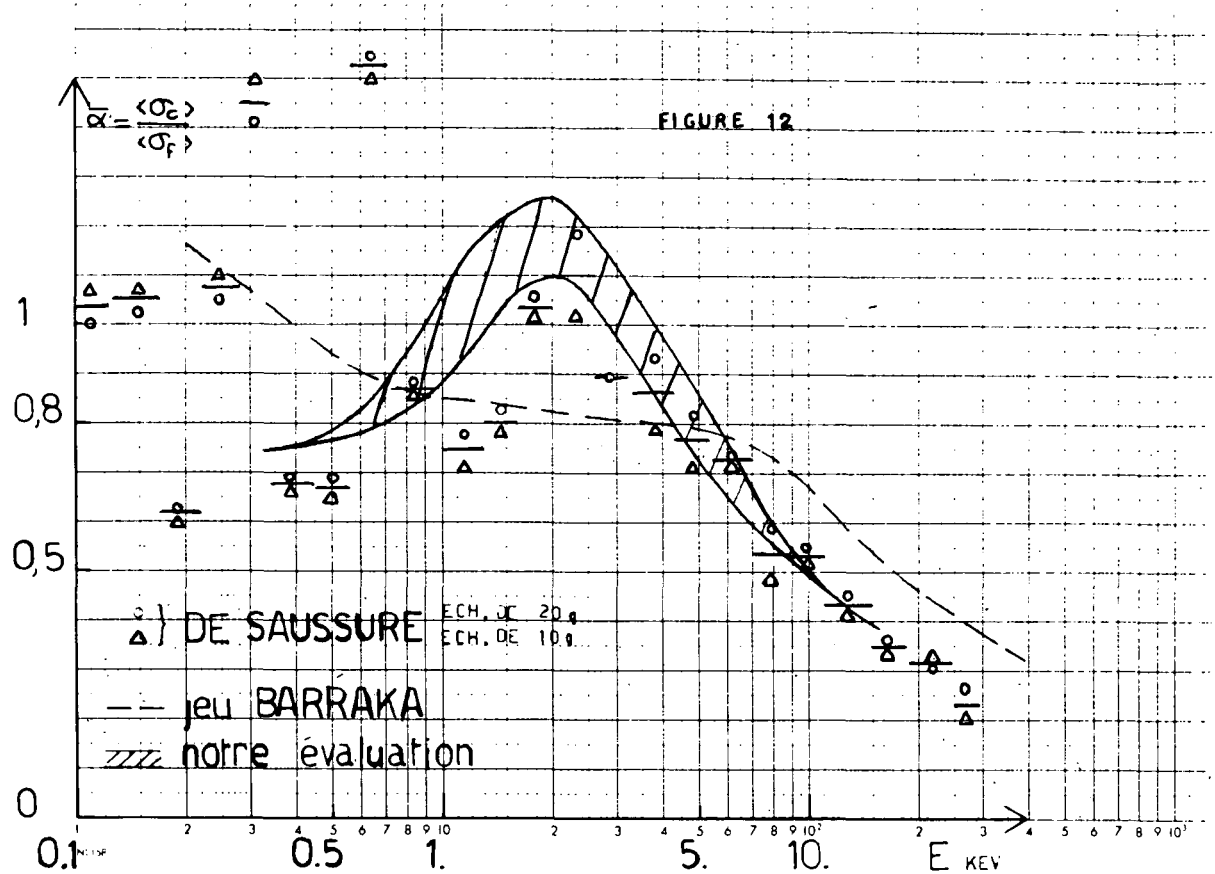
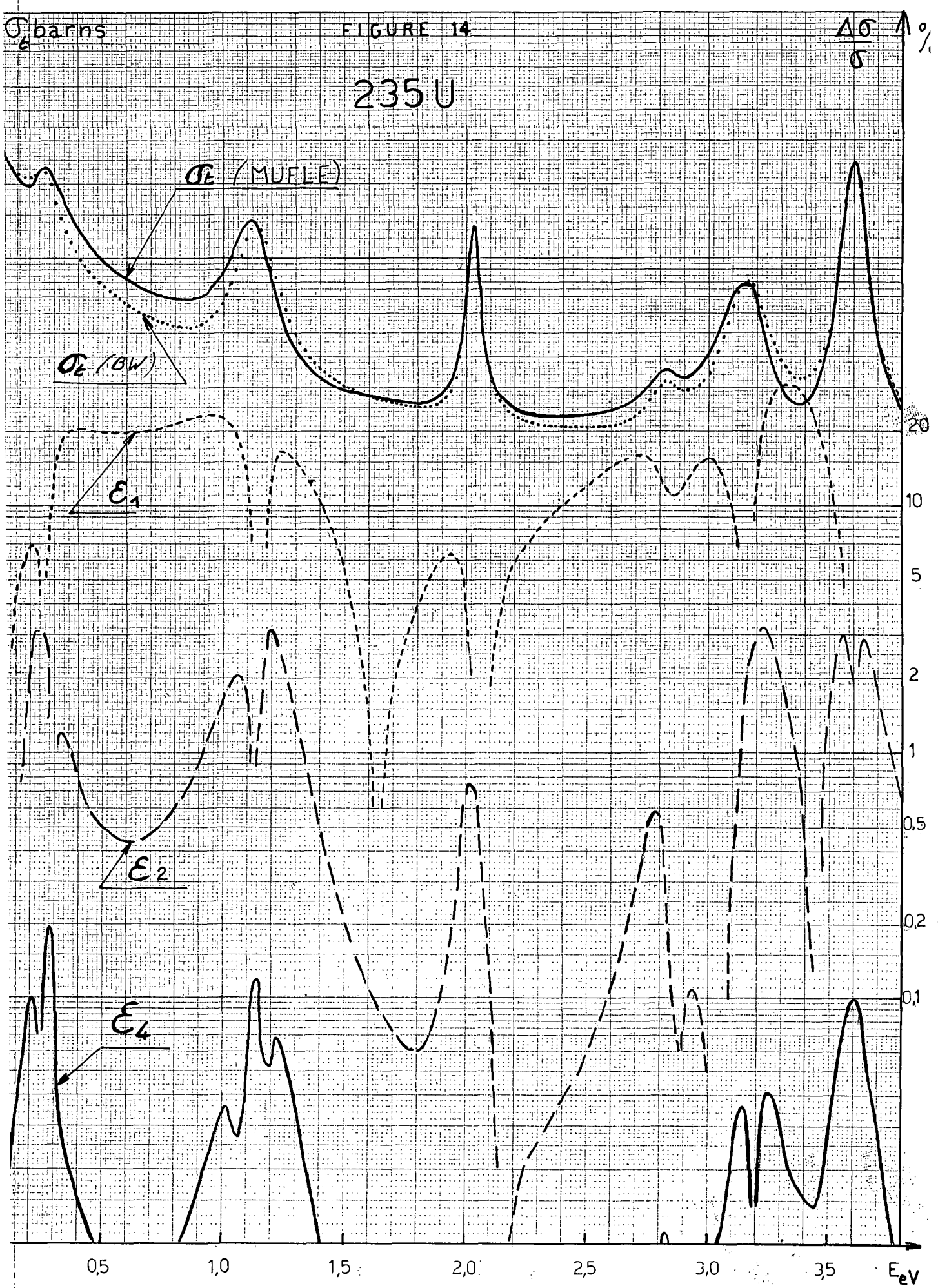


FIGURE 14



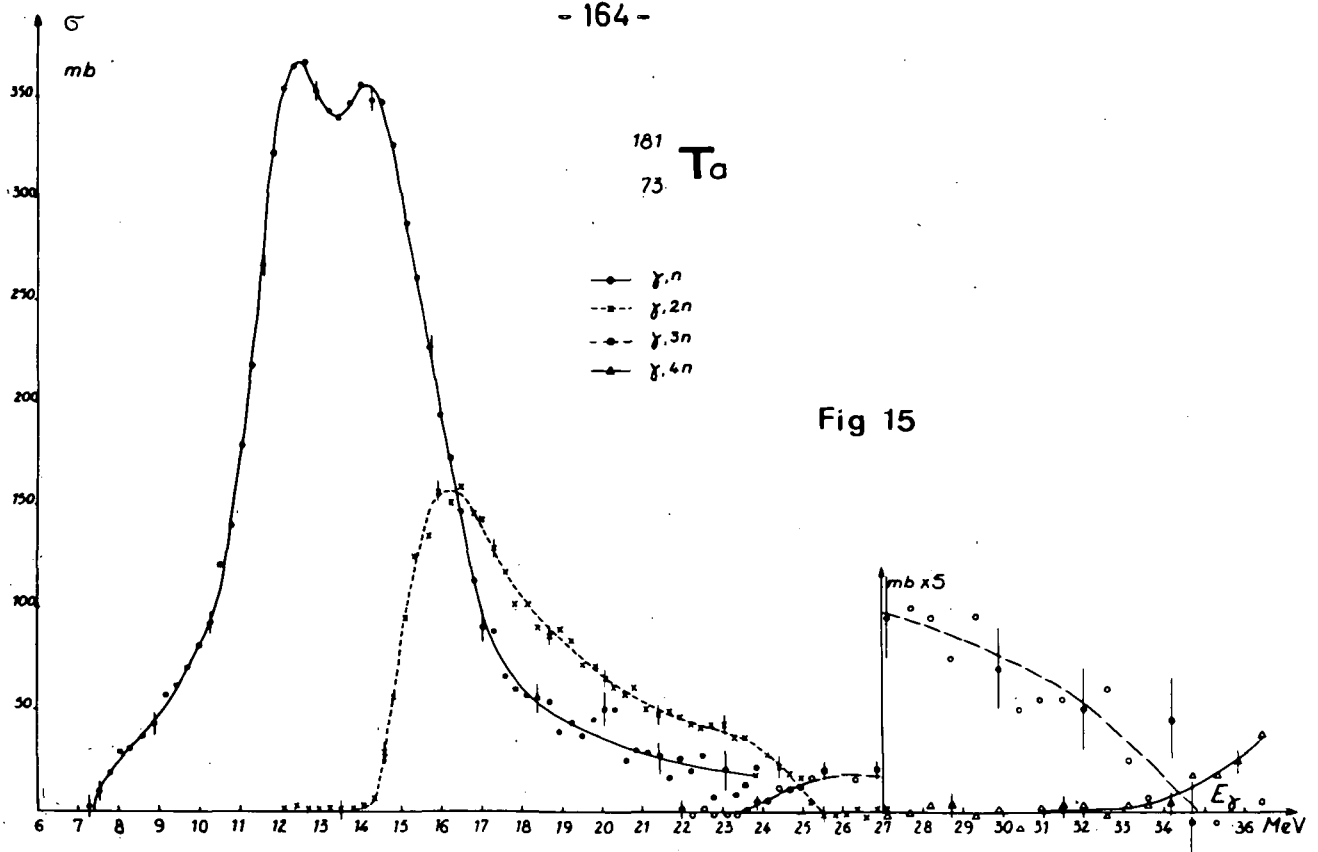


Fig 15

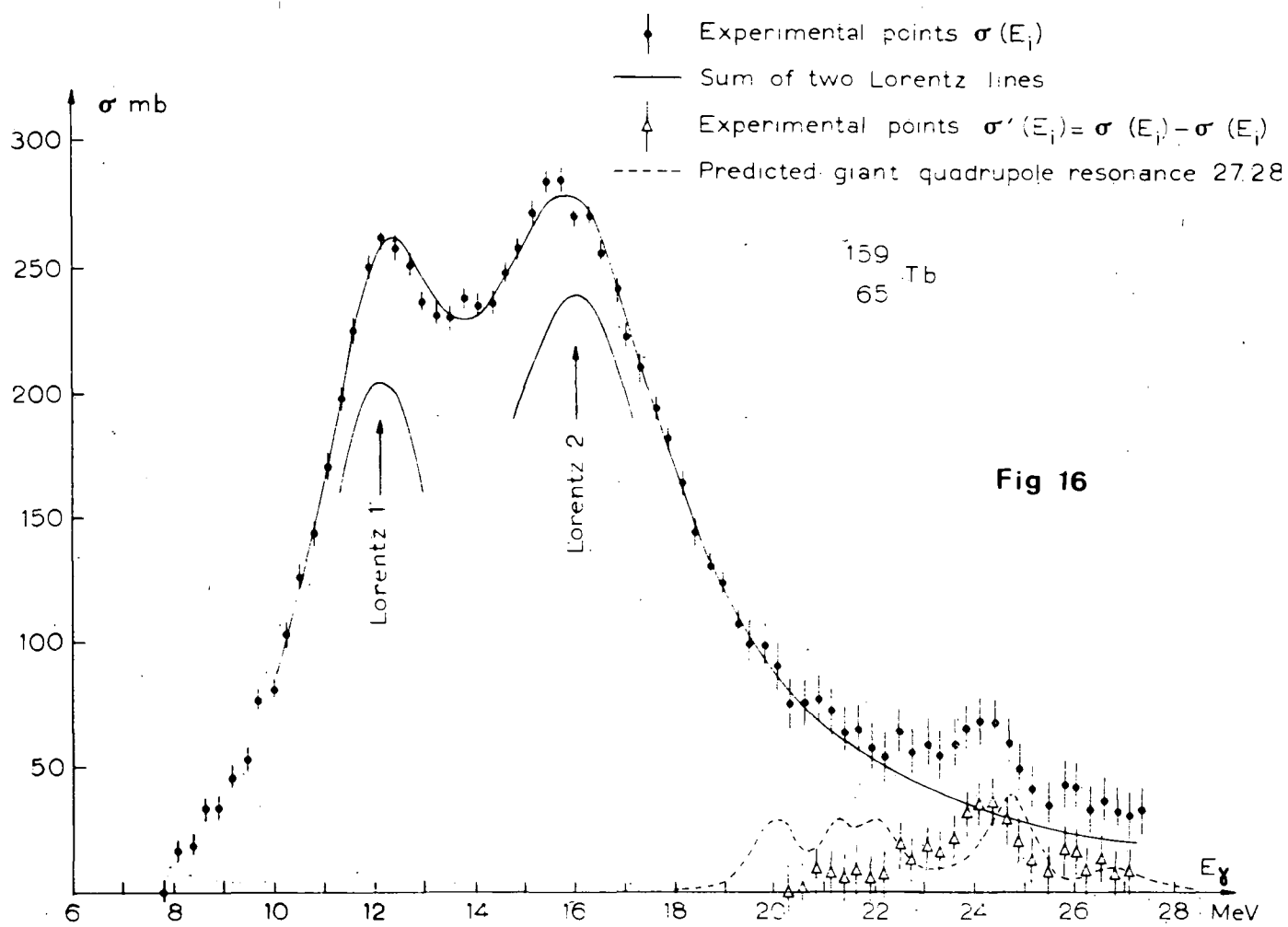


Fig 16

XX. SERVICE DE PHYSIQUE EXPERIMENTALE -

CENTRE D'ETUDES DE BRUYERES-le-CHATEL - C.E.A. (FRANCE)

P. LEUBA - D. DIDIER

1. APPAREILLAGE -

1.1. Accélérateur Van de Graaff Tandem 12 MeV - (A. DANDINE, J.C. CIRET)

1.1.1. Diminution de la largeur de la bouffée par hachage après accélération -

Un équipement destiné à réduire la largeur de la bouffée par hachage après accélération est en cours de réalisation.

La largeur à mi-hauteur de la bouffée de protons doit être ramenée de 4 nanosecondes environ à 1 nanoseconde au prix d'une diminution de l'intensité. La mise en service est prévue pour le printemps 1969.

1.1.2. Installation d'un "Stripper" à feuilles de Carbone -

Le nouveau "Stripper" sera mis en place en mars 1969. Au cours d'essais préliminaires, le courant d'ions s'est trouvé augmenté dans un rapport 1,5 à 2.

Le montage réservera la possibilité de fonctionnement avec la fuite d'oxygène, sans ouverture de l'accélérateur.

1.1.3. Système de hachage à la nanoseconde d'un faisceau Van de Graaff 2 MeV -

(A. ADAM, J.C. BROGNON, J. CABE, M. CANCE) -

L'étude des diffusions élastique et inélastique des neutrons sur les noyaux ainsi que l'étude des réactions (p, n) et (d, n) à Q positif ou faiblement négatif, nous ont conduits à mettre au point un système de hachage du faisceau permettant de délivrer à une fréquence de 10MHz des bouffées d'une largeur de 1 à 3ns suivant la tension appliquée sur les plaques de déflection. Ce système permet de défléchir des protons, deutérons et Hélium 3 et d'étudier toutes les réactions (x, n) par mesure du temps de vol.

2. Acquisition et traitement des données - (P. FERNIER, J. LABBE, JR LAGET, G. MARIN) -

Au cours de l'année 1968, le système de traitement CAE 510 a été exploité d'une manière intensive tant pour exécuter des calculs relatifs aux expériences que pour réaliser des acquisitions de données en ligne et leur exploitation.

2.1. Réseau d'ordinateurs CII 10.020 et 10.070 -

L'installation existante étant surchargée, on a décidé son remplacement par un système de traitement d'information en ligne comprenant plusieurs ordinateurs hiérarchisés. Cette solution sépare les deux fonctions acquisition et exploitation ; elle a été dictée par la multiplicité des demandes (4 accéléra-

teurs) et la distribution des centres de mesure entre deux bâtiments assez éloignés l'un de l'autre. L'acquisition est confiée à deux ordinateurs CII 10.020 ayant une configuration simplifiée et situés dans chacun de ces bâtiments. Ces ordinateurs primaires seront reliés à un secondaire CII 10.020 également, centralisant les calculs et capable d'assurer une partie de l'exploitation. Enfin, une liaison entre l'ordinateur d'exploitation (secondaire) et un ordinateur plus puissant (tertiaire) CII 10.070, nous permettra de mettre au point et de faire exécuter à distance des calculs plus importants. L'installation de l'ensemble de ce système de traitement devrait être terminée au début de l'année 1970.

1.2.2. Calculs scientifiques -

Il a été nécessaire, pour répondre aux besoins des physiciens de mettre au point une série de programmes de calcul dans les chapitres suivants :

a) simulation.

- correction de diffusion multiple et d'atténuation dans un diffuseur,
 - réponse d'un scintillateur organique aux neutrons entre 2MeV et 14MeV.
- b) analyse automatique de spectres pour le calcul de sections efficaces.
- c) ajustement paramétrique (linéaire et non linéaire) de fonctions théoriques sur des données expérimentales nécessitant entre autre la mise en œuvre de la méthode de DAVIDON.

2. ETUDE DE LA REACTION $p + ^{11}B \rightarrow 3\alpha$ PAR LA METHODE DES COÏNCIDENCES.

(M. CADEAU, J.P. LAUGIER, G. MOUILHAYRAT, F. PERRAULT, F. SAVIOZ).

Notre étude a porté sur le mécanisme de production du système 3α dans la réaction : $p + ^{11}B \rightarrow ^{12}C \rightarrow \alpha + ^8Be$ et $^{8}Be \rightarrow \alpha + \alpha$

Nous avons pu mettre en évidence trois effets de natures différentes :

- l'effet des niveaux du noyau intermédiaire ^{8}Be = réaction séquentielle,
- l'effet des niveaux du noyau composé ^{12}C = effet de spin,
- un effet d'interférences.

Nous avons développé un formalisme qui nous a permis de rendre compte quantitativement de tous les spectres observés expérimentalement.

2.1. Effet des niveaux du noyau intermédiaire ^{8}Be : pour des énergies incidentes protons inférieures à 8MeV, nous avons montré que la réaction étudiée est essentiellement séquentielle avec passage par le niveau fondamental et le premier niveau excité du noyau intermédiaire de ^{8}Be .

Effet des niveaux de ^{12}C : nous avons mis en évidence l'existence d'un effet de spin (spin et parité) dans une région très étroite du plan des énergies (E_1, E_2) (E_1 et E_2 énergies des particules détectées dans le système du centre de masse). Cet effet de spin se traduit par une absence d'événements dans la zone du plan des énergies correspondant à deux particules émises à 180° l'une de l'autre dans le système du centre de masse ; dans ce cas, la particule non détectée a une énergie nulle. La conservation du moment angulaire ne permet d'observer dans cette région que des particules α provenant de la désintégration d'un niveau de ^{12}C de spin pair et de parité positive.

Nous avons observé cet effet pour des résonances à $1,4\text{MeV}$ [1] et $7,18\text{MeV}$ d'énergie incidente des protons [2] ; ces deux énergies correspondent à des résonances, dans le ^{12}C , d'énergie d'excitation de $17,23\text{MeV}$ et $22,54\text{MeV}$. Ces deux résonances ont un spin 1^- . Par contre, nous n'avons pas observé un tel effet pour une énergie de protons de $4,9\text{MeV}$ ($20,44\text{ MeV}$ dans le ^{12}C) ce qui nous permet de dire que cette résonance a un spin pair et une parité positive. [3]

Effet d'interférences : pour deux énergies incidentes de protons de $1,4\text{MeV}$ et $4,9\text{MeV}$ correspondant à des énergies d'excitation dans le ^{12}C de $17,23\text{MeV}$ (niveau 1^-) et de $20,44\text{MeV}$ (spin et parité inconnus) nous avons mis en évidence des phénomènes d'interférences. Ces phénomènes d'interférences apparaissent lorsqu'on se trouve dans une région du plan des énergies E_1, E_2 où les deux contributions du premier état excité du ^8Be se croisent (cas de $1,4\text{MeV}$) ou sont assez rapprochés (cas de $4,9\text{MeV}$).

Ces interférences sont maximales quand les deux contributions sont exactement superposées, elles diminuent et s'annulent pratiquement quand les deux centres des contributions sont séparés de $\Gamma/2$ (Γ largeur du premier niveau excité de ^8Be). Ces interférences se traduisent par une variation apparente de la largeur du premier niveau excité de ^8Be . Nous n'avons pas observé de variations sur l'énergie d'excitation de ce niveau.

Nous avons pu donner une expression théorique du spectre, rendant compte d'une façon satisfaisante des variations observées. Pour cela nous avons considéré le déphasage entre les ondes associées aux particules détectées,

qui produit les interférences, comme un paramètre arbitraire.

Dans les régions où ils se produisent, ces effets d'interférences sont dus à l'indétermination sur l'ordre d'émission des particules détectées et à l'in-discernabilité de ces mêmes particules (trois particules α).

Du point de vue expérimental, les méthodes d'enregistrement utilisées présentent les caractéristiques suivantes : [4]

- utilisation de cibles de bore autoporté,
- refroidissement des détecteurs semi-conducteurs employés,
- enregistrement de 3 paramètres pour définir chaque évènement ; les énergies des deux particules détectées et le temps qui sépare les instants de détection de ces deux particules,
- utilisation d'un calculateur en ligne.

3. ETUDE DES INTERACTIONS DEUTERON - LITHIUM - (G. BRUNO, J. DECHARGE)

L. FAUGERE, M. LEBARS, G. SURGET)

3.1. Réaction $^6\text{Li}(\text{d},\alpha)^4\text{He}$ -

Nous avons repris la mesure de la section efficace en valeur absolue pour la réaction $^6\text{Li}(\text{d},\alpha)\alpha$, entre 2 et 12MeV à l'aide du Van de Graaff Tandem. Les résultats étaient bien connus entre 2MeV et 5MeV, mais plus fragmentaires au-delà de cette énergie. Les distributions angulaires ont été mesurées de 30° à 170° , avec un pas de 10° . Pour cela, nous détectons les produits de la réaction simultanément sur 8 diodes semiconductrices, espacées de 20° . Une deuxième mesure réalisée après avoir décalé l'ensemble des détecteurs de 10° nous permet d'obtenir rapidement 15 points de distribution angulaire. Les mesures ont été faites avec un pas d'énergie de 0,25MeV. Les résultats obtenus sont en accord avec les mesures antérieures dans la gamme 2MeV - 5MeV.

3.2. Mesures à basse énergie à l'aide de l'accélérateur Van de Graaff 400keV -

- Réactions $^6\text{Li}(\text{d},\alpha)^4\text{He}$: $^6\text{Li}(\text{d},\text{p}_0)^7\text{Li}$; $^6\text{Li}(\text{d},\text{p}_1)^7\text{Li}$ *

Nous avons mesuré en valeur absolue, la section efficace de ces réactions pour des énergies de deutérons comprises entre 80keV et 300keV. Les principales difficultés rencontrées ont été la contamination des cibles par des dépôts de traces d'hydrocarbures et le problème de l'épaisseur des cibles pour des deutérons incidents d'énergie faible. Le premier point a été résolu par l'utilisation de pompes turbomoléculaires et un piégeage efficace des vapeurs lourdes à proximité immédiate des cibles. Pour le deuxième point, nous avons

évalué les taux de réaction en cible très mince grâce à une méthode décrite par FIEDLER et KUNZE (Nuclear Physics A 96 (1967) 513-520). Nos mesures ont été faites à un angle de 135° . Pour avoir la section efficace intégrée, nous avons supposé que les distributions angulaires étaient isotropes. Nos résultats sont compatibles avec ceux de PHILIPPS et SAMYER (LA 1578), et montrent que la loi de GAMOW est applicable à ces réactions dans le domaine d'énergie étudié.

- Réaction $^6\text{Li}(\text{d},\text{n})^7\text{Be}$.

Nous avons entrepris de mesurer la section efficace de la réaction $^6\text{Li}(\text{d},\text{n})^7\text{Be}$ entre 80keV et 300keV, en comptant le nombre de noyaux ^7Be formés. Le ^7Be décroît vers le ^7Li avec une période de 54 jours, en passant dans 12% des cas par $^7\text{Li}^{*(0,478)}$. La détection du γ de désexcitation de $^7\text{Li}^*$ par un détecteur au Ge(Li) nous permettra de remonter au nombre de noyaux ^7Be formés. La section efficace en valeur absolue sera déterminée par comparaison avec la section efficace de la réaction : $^6\text{Li}(\text{d},\text{p}_1)^7\text{Li}^{*(0,478)}$. Les résultats sont encore fragmentaires, la méthode nécessitant un temps très long d'irradiation et de comptage après irradiation.

Réaction à trois corps - $^7\text{Li}(\text{d},\alpha_1)^5\text{He} \quad . \quad ^5\text{He} \rightarrow \alpha_2 + \text{n}$.

Nous avons continué notre étude de cette réaction séquentielle en mesurant des distributions angulaires de la première étape de la réaction, entre 0,6MeV et 2MeV. Les résultats sont en cours d'exploitation à l'aide du formalisme de la matrice R. Nous pensons qu'ils nous permettront de préciser les spins et parités des niveaux à 17,28 et 17,48MeV d'excitation du noyau intermédiaire ^9Be .

D'autre part, les spectres biparamétriques en coïncidence (α_1, α_2) ont été complétés, et des calculs sont en cours, qui doivent nous permettre de retrouver les formes de spectres observés.

SPECTROMETRE A TEMPS DE VOL POUR L'ETUDE DES REACTIONS (n,D) et (n, ^6Li)

(M. CADEAU, J.P. LAUGIER, G. MOUILHAYRAT, F. PERRAULT, F. SAVIOZ)

Pour mesurer des sections efficaces différentielles de l'ordre de quelques millibarns par stéradian, nous avons été amenés à mettre au point un spectromètre ayant à la fois un très faible bruit et un faible seuil.

La figure 1 correspond au schéma de principe du spectromètre à temps de vol. Les neutrons de 14MeV utilisés sont produits par la réaction $\text{T}(\text{d},\text{n})^4\text{He}$; les deutérons de 150keV étant fournis par un accélérateur Samès 600keV. L'ins-

tant d'émission du neutron est déterminé par la méthode de la particule associée.

Le diffuseur, placé dans le cône d'émission des neutrons est situé au centre d'un goniomètre qui permet de faire des distributions angulaires. La base de vol maximale de l'ensemble est de 2,40m.

Les neutrons sont détectés par un scintillateur organique.

Les caractéristiques principales recherchées pour ce spectromètre nous ont obligés à résoudre les problèmes suivants :

- protection du scintillateur,
- association au détecteur de deux photomultiplicateurs mis en coïncidence pour éliminer leur bruit de fond propre,
- discrimination neutron-gamma possédant une bonne résolution avec un seuil faible et stable.

Une chaîne d'analyse multiparamétrique permet de corrélérer le temps de vol avec l'un des paramètres suivants :

- signal de discrimination neutron-gamma,
- énergie du proton de recul dans le scintillateur qui sert de détecteur,
- énergie du proton de recul dans le diffuseur si celui-ci est un scintillateur (ceci nous permet d'isoler la diffusion sur l'hydrogène, élément de référence, et de mesurer l'efficacité et la courbe de réponse des détecteurs employés).

La résolution en temps obtenue à 14MeV avec un scintillateur de deux pouces est de 1,2ns.

Nous avons utilisé ce spectromètre pour l'étude des réactions $n+D$ et $n+^6Li$. Pour la première de ces réactions, l'échantillon d'eau lourde servant d'abord comme diffuseur, a été remplacé par un scintillateur deutéré, ce qui a permis d'enregistrer les coïncidences neutron-proton.

L'exploitation des résultats de la réaction $D(n,2n)p$ est en cours.

Nous avons abordé deux types d'interprétation du problème à trois nucléons :

- l'un à partir des équations FADDEEV,
- l'autre à partir du formalisme phénoménologique mis au point pour les réactions conduisant à trois particules chargées dans la voie de sortie (Rapport CEA R.3670).

SECTIONS EFFICACES TOTALES NEUTRONIQUES -

(A. ADAM, J. CABE, M. CANCE, M. LABAT, M. LAURAT, M. LONGUEVE).

Mesure de la section efficace totale neutronique du silicium entre 1,150MeV et 5MeV -

Ces mesures font suite à celles déjà effectuées sur le silicium entre 400keV et 1200keV qui nous avaient permis de mettre en évidence trois résonances pour lesquelles on avait pu déterminer les largeurs Γ_n et le moment angulaire total J [5] [6]. Ces derniers résultats ont été obtenus à l'aide d'un accélérateur Tandem 12MeV à source pulsée. Les neutrons produits par la réaction $T(p,n)^3\text{He}$ avaient une dispersion en énergie de l'ordre de 5keV. Un dispositif de sélection par temps de vol réduisait le niveau du bruit de fond.

Les résultats obtenus (Fig.2) montrent l'existence de résonances isolées.

L'exploitation des résultats est en cours pour déterminer les paramètres de ces différentes résonances à l'aide d'une formule de BREIT et WIGNER à plusieurs niveaux.

Recherche d'une structure intermédiaire dans la section totale neutronique du soufre entre 1,150MeV et 4,75MeV -

Ces mesures de sections efficaces totales neutroniques concernent la recherche d'une structure intermédiaire dans le corps de A moyen [7]. Nous avons utilisé un Van de Graaff Tandem 12MeV à source pulsée et la réaction $T(p,n)^3\text{He}$ comme source de neutrons dont la dispersion en énergie était de l'ordre de 5keV. Les résultats obtenus montrent l'existence d'un grand nombre de fines résonances très rapprochées (Fig.3). Celle qui est située à 1,760MeV bien séparée correspond à un niveau auquel nous avons attribué le spin 5/2. L'exploitation des résultats est en cours pour déterminer les paramètres de ces différentes résonances.

Les moyennes effectuées sur des intervalles d'énergie ΔE compris entre 20 et 500keV font apparaître un maximum à une énergie d'environ 2,850MeV qui se conserve en position et amplitude pour des moyennes comprises entre 300 et 500keV. La largeur à mi-hauteur de ce maximum est de l'ordre de 300keV pour une amplitude de 1 barn (Fig.4).

5.3. Mesure de la section efficace totale neutronique du titane entre 1,150MeV et 4MeV -

Ces mesures font suite à celles déjà effectuées sur le titane entre 150keV et 1200keV [6]. Ces derniers résultats entre 1,150MeV et 4MeV environ ont été obtenus à l'aide d'un accélérateur Tandem 12MeV à source pulsée. Les neutrons produits par la réaction $T(p,n)^3He$ avaient une dispersion en énergie de l'ordre de 5keV. La méthode du temps de vol a été utilisée pour sélectionner les neutrons et éliminer le bruit de fond. Les résultats corrigés des diffusions aux petits angles sont donnés avec une précision de l'ordre de 4% sur la figure 5. L'échantillon utilisé était du titane naturel contenant 8% de ^{46}Ti ; 7% de ^{47}Ti ; 74% de ^{48}Ti ; 6% de ^{49}Ti et 5% de ^{50}Ti de 3cm de diamètre et 4cm de long. La courbe de la figure 1 présente de nombreux pics qui sont des résonances partiellement résolues correspondant à des niveaux se recouvrant plus ou moins. Une exploitation de ces résultats par la théorie du modèle statistique est actuellement en cours.

6. DIFFUSION ELASTIQUE DES NEUTRONS DE 400keV A 1200keV SUR LE TITANE NATUREL - (A. ADAM, J. CABE, M. CANCE, M. LAURAT, M. LONGUEVE).

Ce travail fait suite à des mesures de sections efficaces totales sur le titane entre 150keV et 1200keV (fig.6) [6] et s'inscrit dans le cadre de la recherche d'une structure intermédiaire dans cette gamme d'énergie [7] [5].

Nous avons mesuré deux courbes d'excitation à 54° et 90° annulant respectivement P_2 et les termes impairs des polynômes de Legendre ainsi que trois distributions angulaires aux énergies respectives de 605keV, 705keV et 815keV. Ces énergies correspondent aux minimum et maximum d'une résonance de largeur 100keV environ. La figure 7 présente les trois distributions angulaires après correction faite par une méthode de Monte Carlo des diffusions multiples et de l'absorption dans l'échantillon de 3cm de diamètre et 5cm de haut. Ces mesures ont été réalisées en utilisant des cibles épaisses de façon à recouvrir plusieurs résonances. La figure 8 compare les résultats expérimentaux à un développement en série de polynômes de Legendre. Nous poursuivons ce travail par une nouvelle série de mesures de distributions angulaires à 900keV, 1MeV et 1,100MeV pour étudier la contribution des différentes résonances sur le maximum centré aux environs de 720keV. La précision sur les points expérimentaux que nous présentons est d'environ 7%.

FISSION - (J. FREHAUT, J. GAURIAU, G. MOSINSKI, M. SOLEILHAC).

Durant l'année 1968, nous avons perfectionné l'électronique associée à la mesure de \bar{V} . Le stockage de l'information se fait maintenant sur bande magnétique incrémentale. Cette technique permet d'améliorer la précision des mesures et doit nous permettre également de réaliser simultanément des mesures de \bar{V}_p et de σ_f relatives sur les matériaux fissiles étudiés.

Avec ce dispositif, nous avons amélioré les mesures de \bar{V}_p entre 1,5 et 15MeV sur ^{235}U , ^{238}U et ^{239}Pu publiées dans E.A.N.D.C. (E) 89 U.

Au cours de l'année 1969, nous envisageons de mesurer les sections efficaces de fission de ^{238}U et ^{239}Pu relatives à celle de ^{235}U .

L'utilisation de la réaction ($p, ^7\text{Li}$) doit nous permettre d'étendre notre domaine d'énergie de neutrons jusqu'à environ 500keV.

Des mesures sont en cours afin d'effectuer des mesures ($n, 2n$) et ($n, 3n$) sur matériau fissile en utilisant la technique du gros scintillateur liquide.

En collaboration avec l'équipe de M. NIFENECKER (SMNF) de Saclay, nous avons réalisé pour la fission spontanée du ^{252}Cf la mesure du nombre moyen de neutrons de fission émis par l'un des deux fragments en fonction de la charge de ce fragment.

ETUDE DU RAYONNEMENT GAMMA PRODUIT PAR DIFFUSION INELASTIQUE DE NUCLEONS - (G. HAOUAT, J. LACHKAR, Y. PATIN, J. SIGAUD).

La désexcitation électromagnétique des niveaux peuplés par diffusion inélastique des neutrons ou des protons sur divers noyaux est étudiée expérimentalement. Les photons sont détectés au moyen d'un spectromètre gamma multi-mode [8] qui peut, grâce à un traitement approprié des informations, fonctionner simultanément :

- en spectromètre photoélectrique et anti-Compton dans la gamme 0,3 - 8MeV,
- en spectromètre de paires au-dessus de 1,022MeV,
- en spectromètre à absorption totale dans la gamme 60-300keV.

La résolution en énergie est de l'ordre de 5,5keV pour des photons de 1MeV et le rapport d'atténuation Compton est de 8 à la même énergie du rayonnement.

L'optimisation de la résolution en temps des détecteurs Ge(Li) coaxiaux et de gros volume [8] a permis la discrimination par chronométrie des neutrons diffusés et des gammas de désexcitation. La résolution en temps est de l'ordre de 5ns pour des photons d'énergie supérieure à 800keV.

Diverses expériences ont été réalisées pour une énergie de neutrons de

$8,72 \pm 0,6$ MeV sur les corps suivants : ^7Li , ^{10}B , ^{12}C , Sb naturel, W naturel, ^{197}Au , ^{209}Bi , ^{238}U . Elles complètent des mesures déjà faites avec des neutrons incidents de 2,5 et 14 MeV [9].

Dans le cas des isotopes pairs-pairs du tungstène (^{182}W , ^{184}W , ^{186}W) il apparaît expérimentalement que les premiers niveaux d'excitation de la bande rotationnelle fondamentale $K = 0$ et le premier niveau de la bande γ vibrationnelle $K = 2$ sont particulièrement favorisés.

Dans le but d'étendre cette étude au cas des noyaux fissiles, la corrélation des neutrons avec les rayonnements gamma émis a été enregistrée. Il est ainsi possible de distinguer les photons émis après diffusion inélastique des photons de fission. Les résultats d'une première étude entreprise sur ^{238}U semblent confirmer les observations faites sur des isotopes pairs-pairs du tungstène.

Enfin, la comparaison des spectres gamma produits par réactions $(n, n'\gamma)$ et $(p, p'\gamma)$ sur ^{197}Au a été faite pour tenter de mettre en évidence les divers mécanismes de réactions mis en jeu. L'exploitation de ces expériences est en cours.

BIBLIOGRAPHIE -

- 1 J.P. LAUGIER, M. CADEAU, G. MOUILHAYRAT, L. MARQUEZ
J. Physique 29 (1968) 829
- 2 L. MARQUEZ, J.P. LAUGIER, R. BALLINI, C. LEMEILLE, N. SAUNIER,
J. REY - *Nucl. Phys.* 97 (1967) 321
- 3 J.P. LAUGIÈR - Thèse Orsay 1968 - Rapport CEA R 3670.
- 4 J.P. LAUGIER, M. CADEAU, P. FERNIER, J.P. LAGET, G. MOUILHAYRAT,
P. NICOLAS - *Nucl. Instr.* (à paraître)
- 5 J. CABE - Thèse Paris 1968 - Rapport CEA R 3279
- 6 G. BARDOLLE, J. CABE, M. LAURAT, M. LONGUEVE - EANDC (E) 89
- 7 J. CABE, M. LAURAT, P. YVON, G. BARDOLLE - *Nucl. Phys.* A 102
(1967) 92.
- 8 G. HAOUT, J. LACHKAR, J. SIGAUD - *J. de Phys.* (à paraître)
- 9 G. HAOUT, J. LACHKAR, J. SIGAUD - EANDC (E) 89

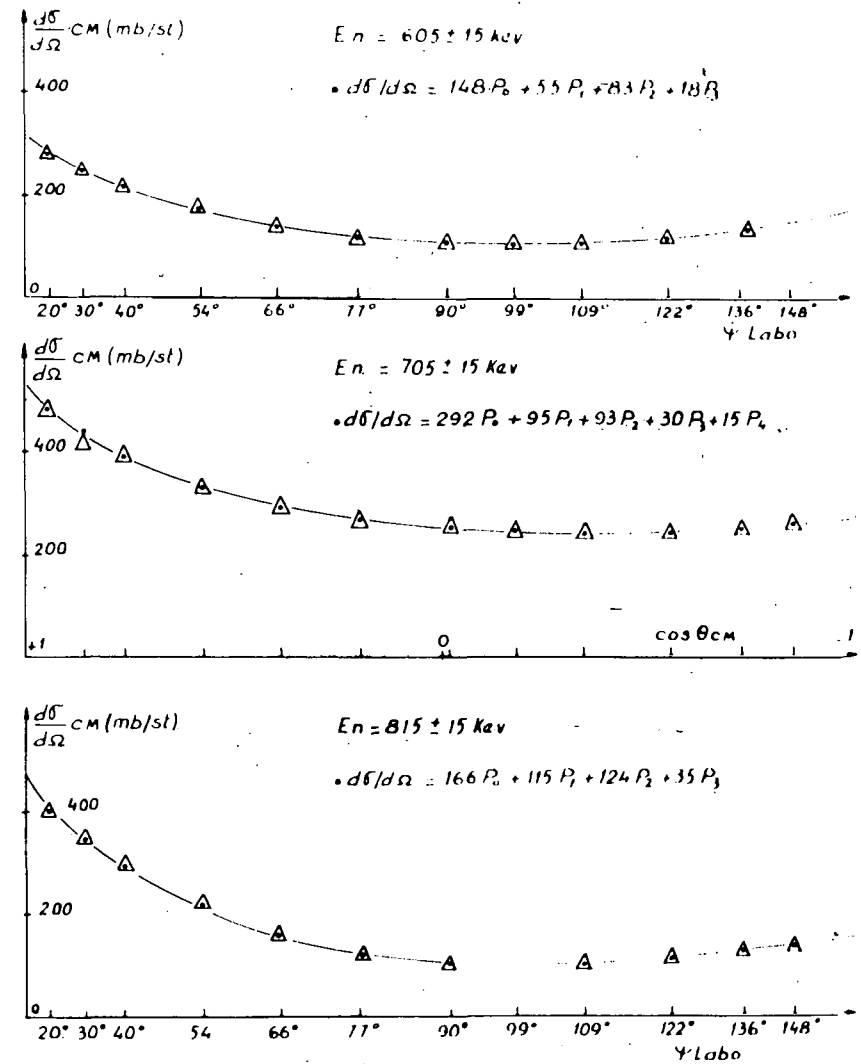
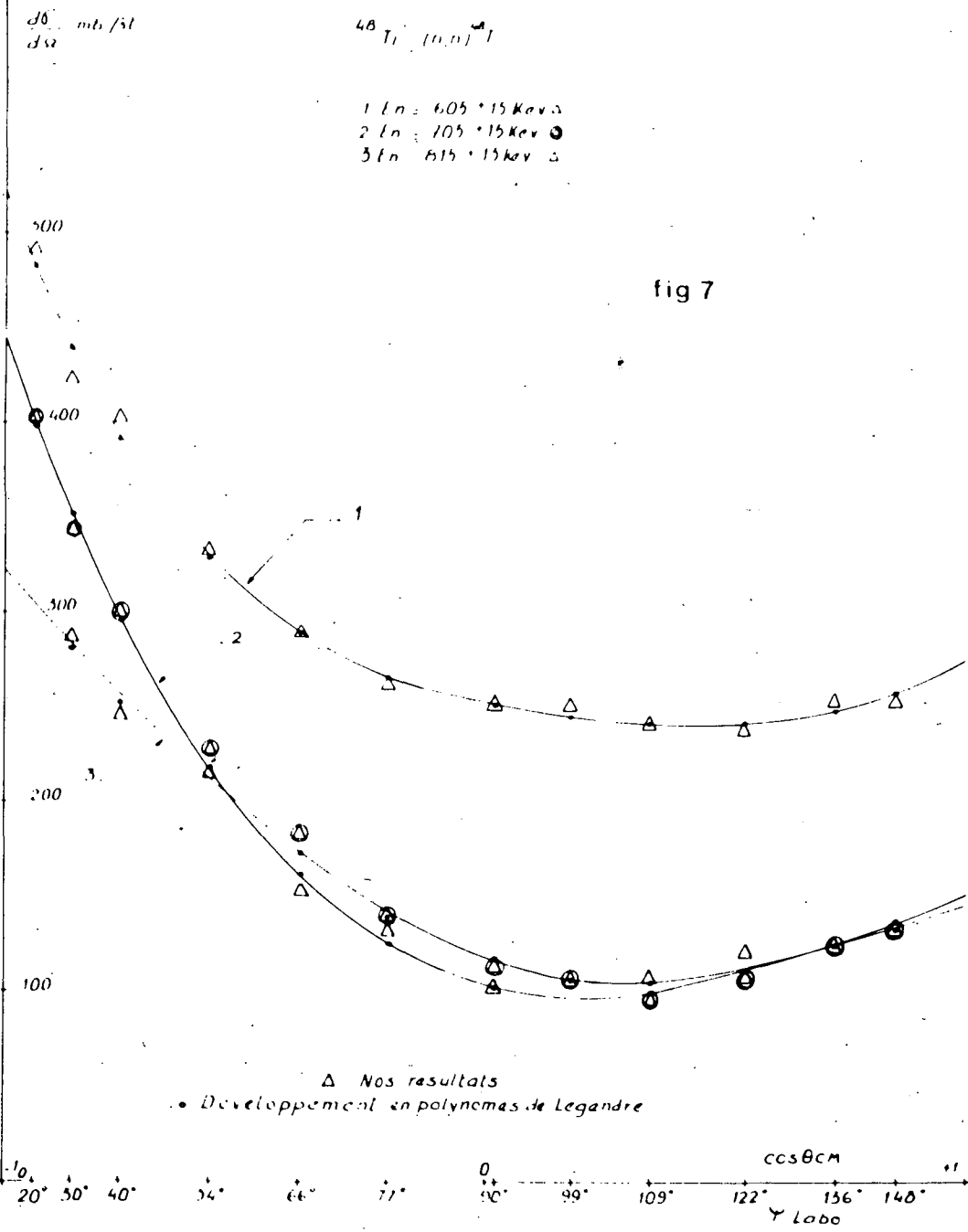
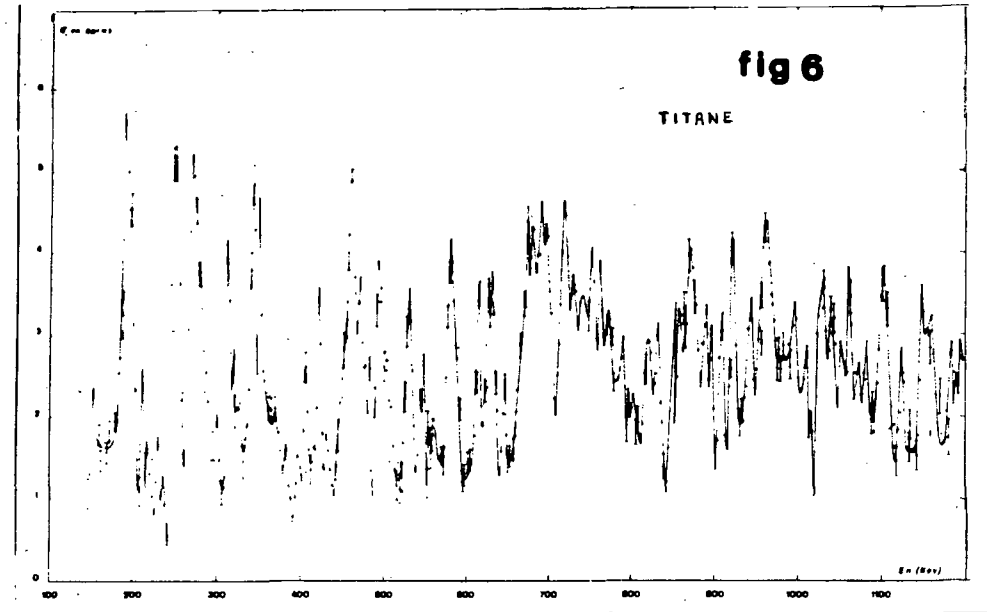


fig 8

fig 6

TITANE



TITANE

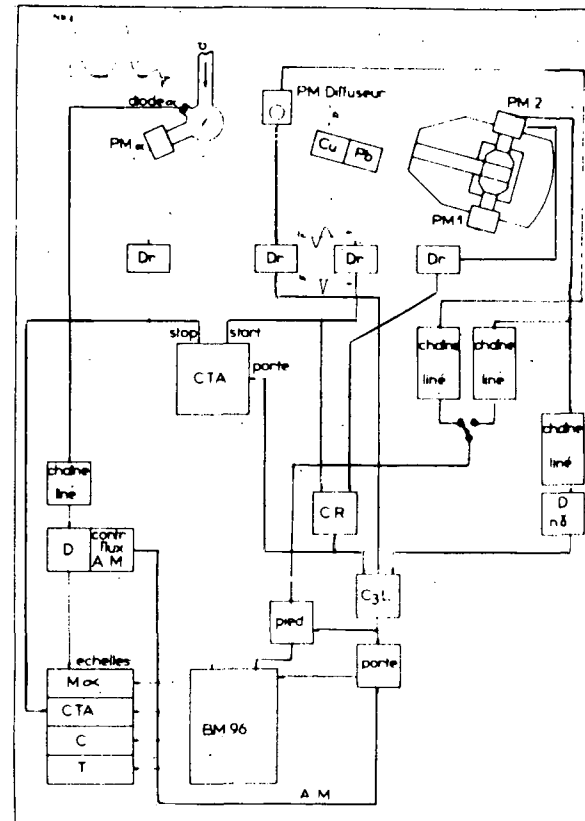
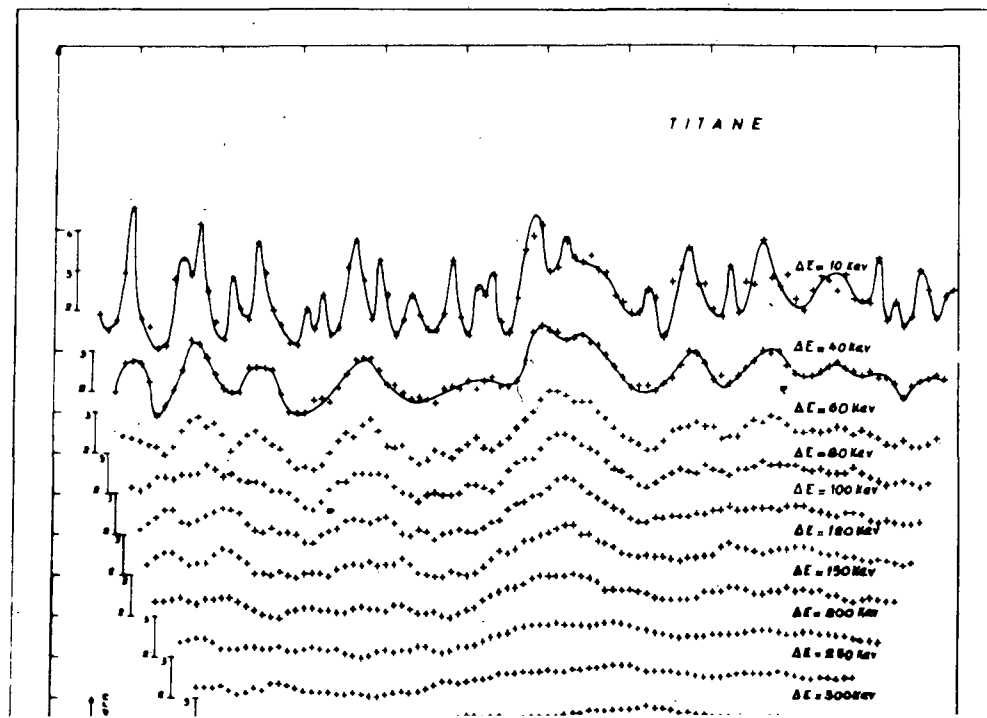
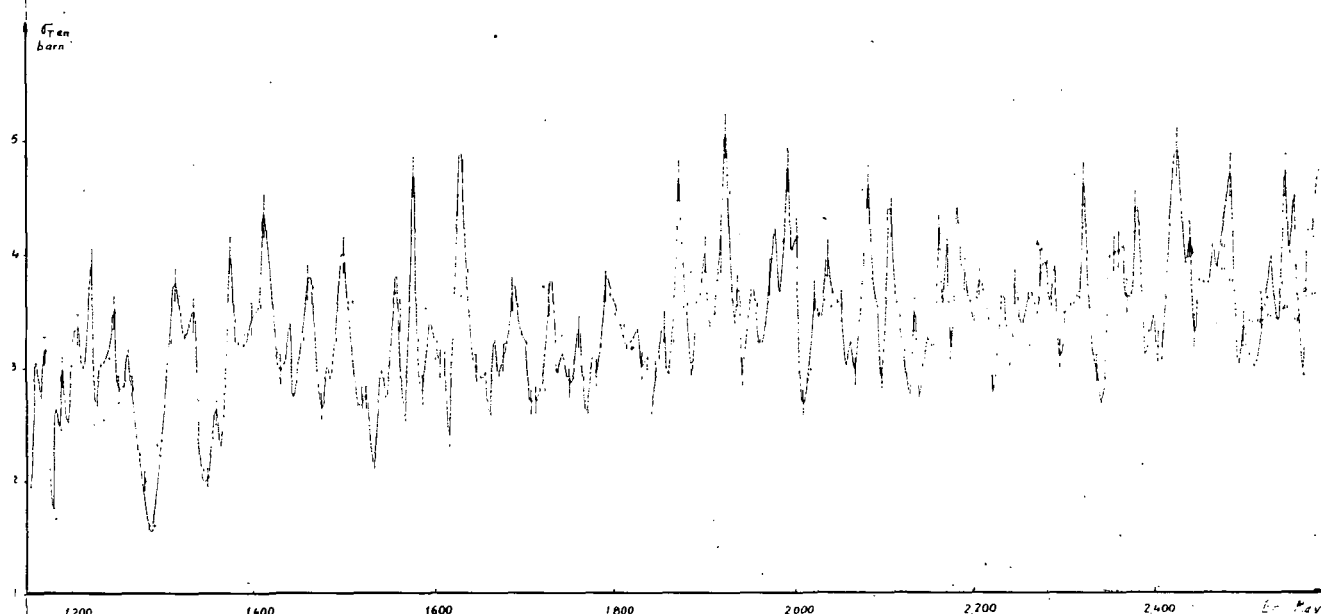
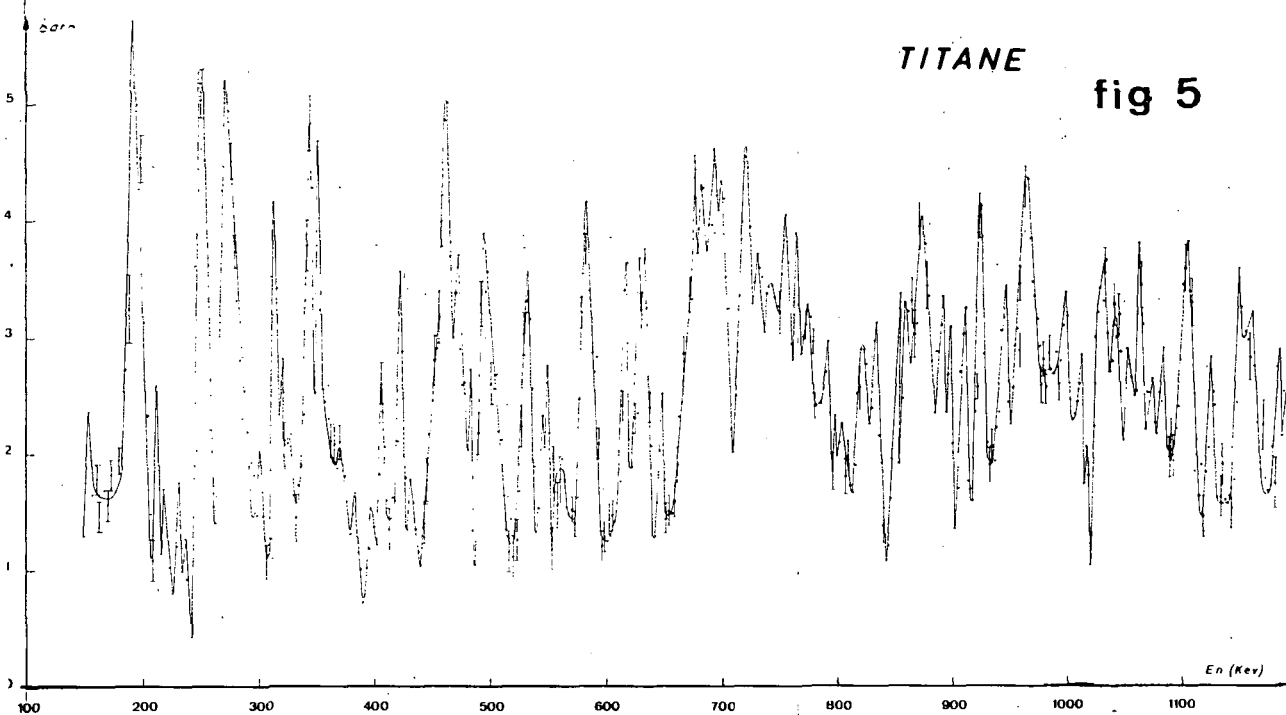


Fig.1 : Schéma de principe du spectromètre à temps de Vol.

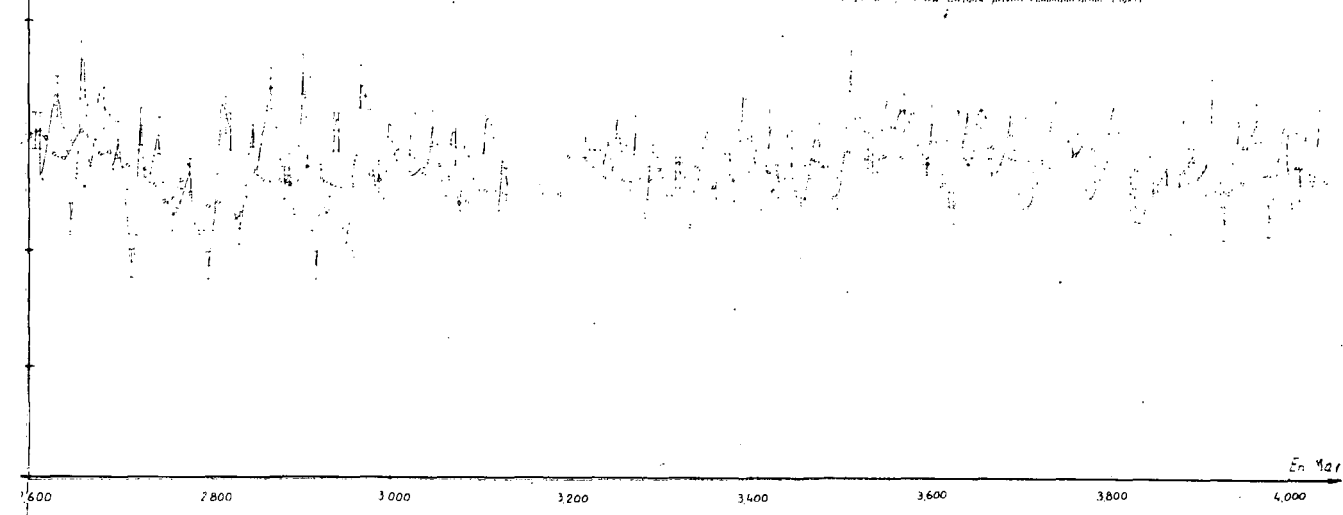
TITANE

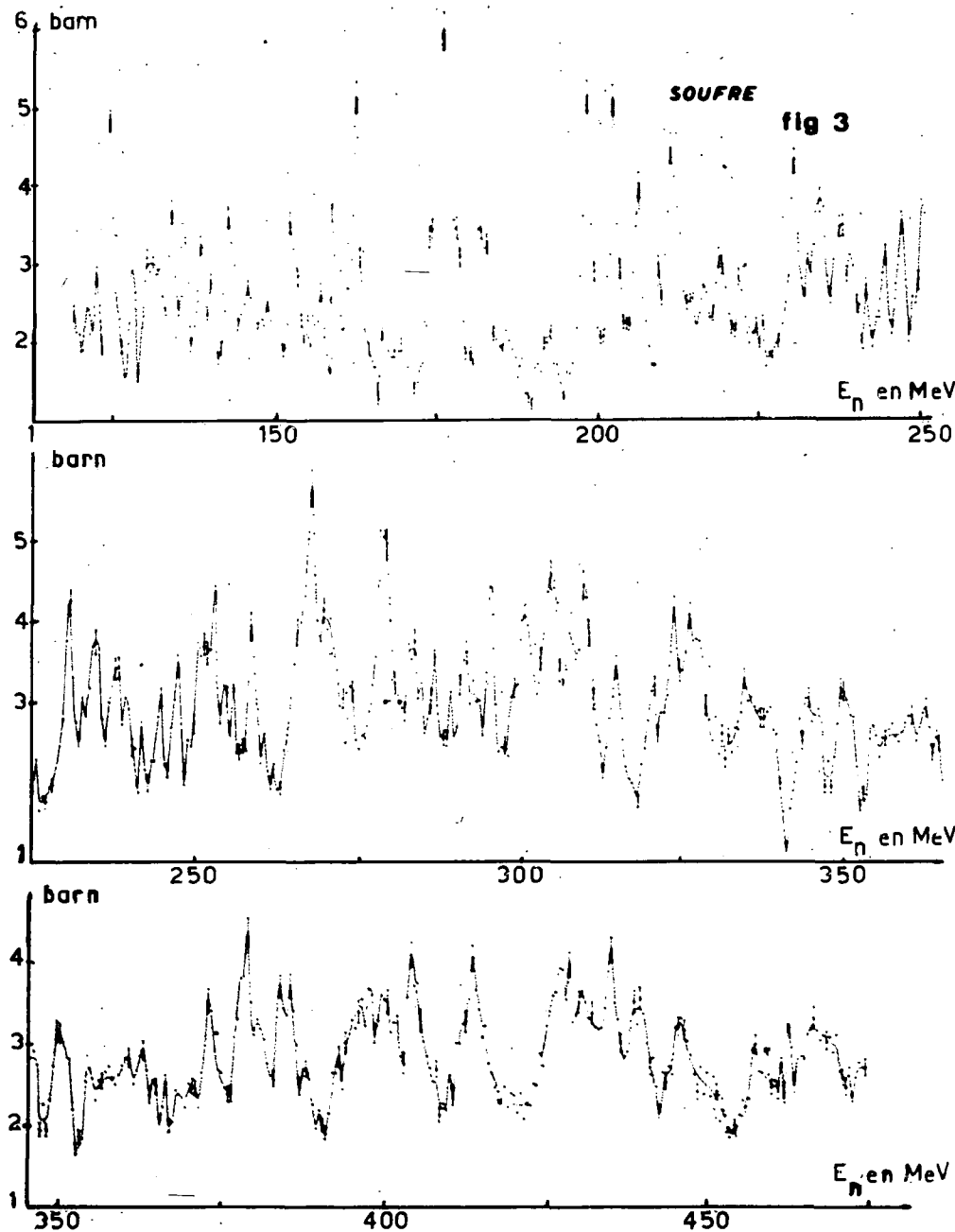
fig 5



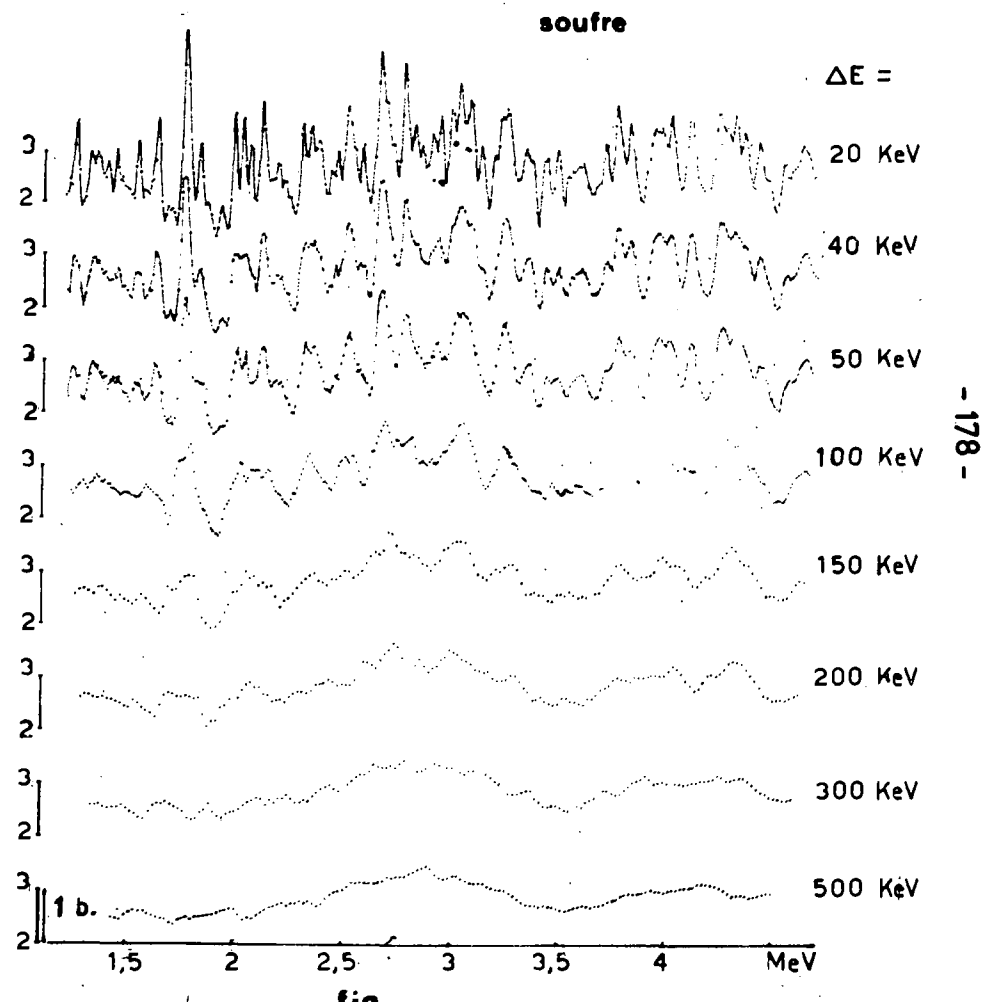
TITANE

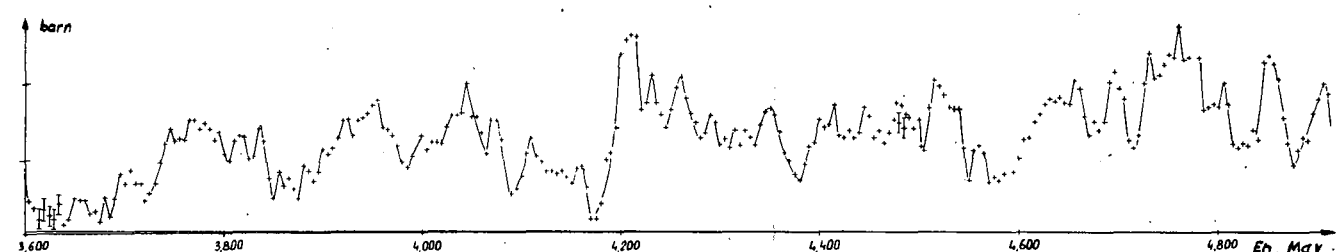
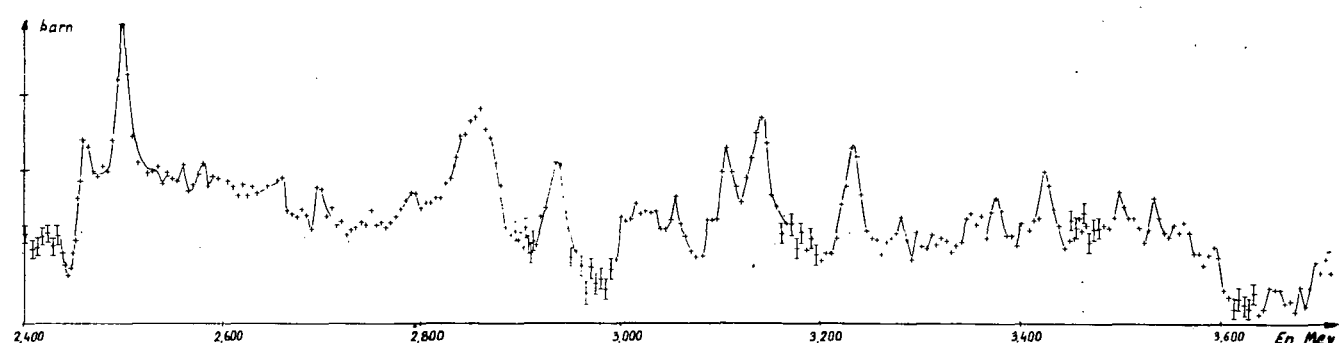
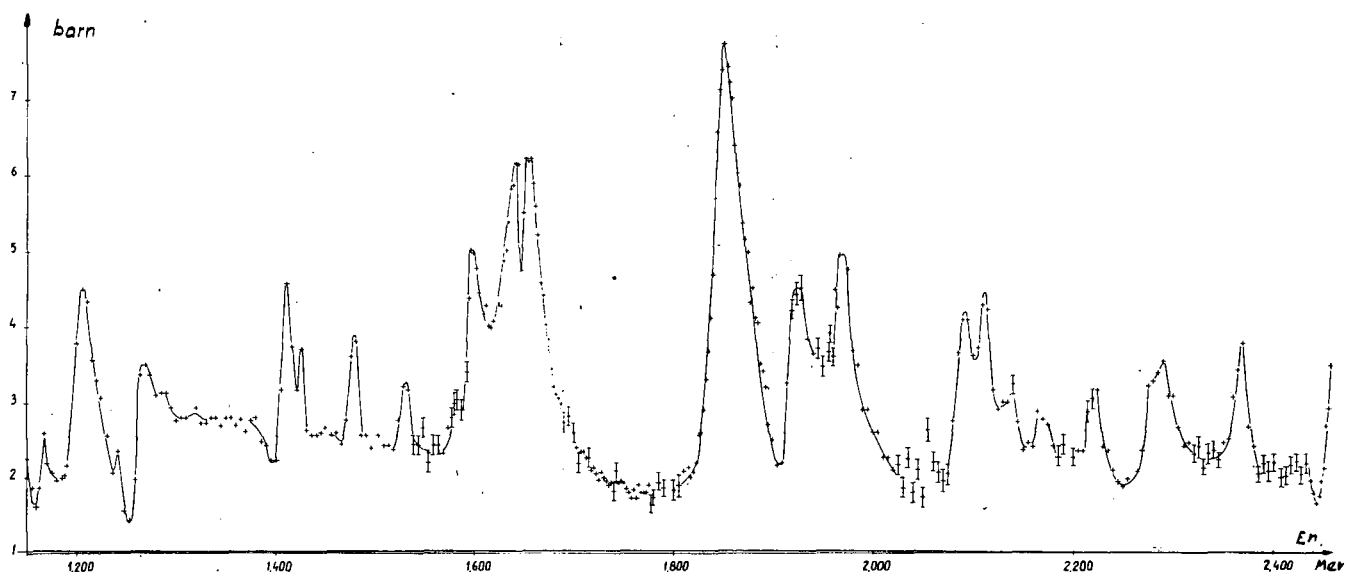
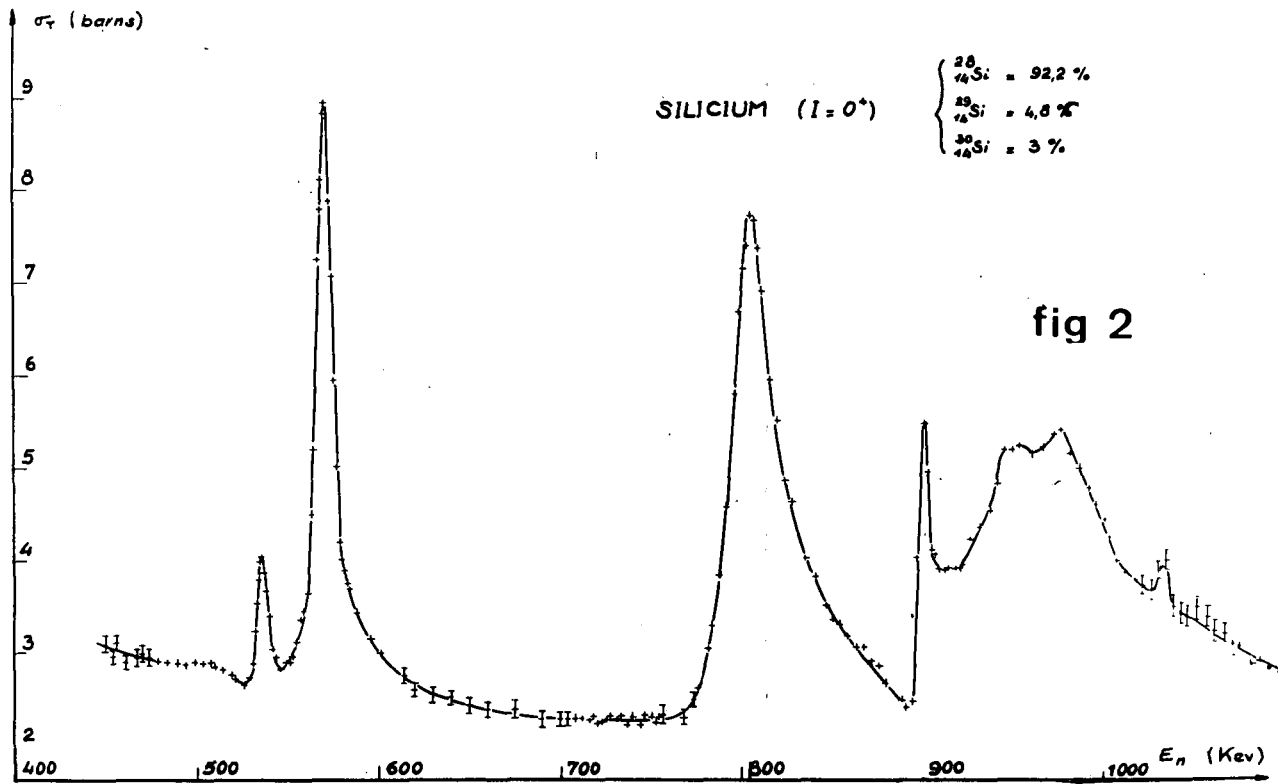
• High resolution
• Reference: R.D. Evans et al.
• Data taken from the literature, private communication, EDBA





SOUFRE fig 3





XXI . SECTION MESURES NUCLEAIRES - CENTRE D'ETUDES DE LIMEIL - C.E.A. FRANC

A. PERRIN.

1. SPECTROMETRE GAMMA UTILISANT UN DETECTEUR Ge(Li) ET FONCTIONNANT SIMULTANEMENT EN SPECTROMETRE DE PAIRES ET EN ANTI-COMPTON [1]

Ce spectromètre est conçu plus spécialement pour l'analyse des spectres de renvoi des gammas produits par des neutrons monocinétiques.

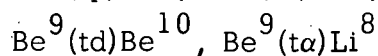
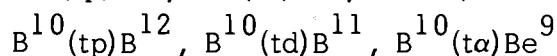
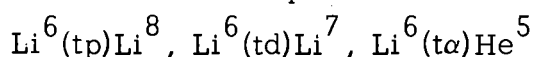
En spectrométrie anti-Compton avec une source de ^{60}Co la réduction du fond Compton est de 75 à 80%, sans atténuation du pic photoélectrique.

En spectromètre de paires, avec une source de RaD Be ($E_{\gamma} = 4,43\text{MeV}$), la réduction du fond Compton sous le pic de double échappement est supérieure à 10, avec une efficacité du mode de fonctionnement variant de 30% à 50% suivant la largeur de fenêtre choisie sur la voie somme du scintillateur NaI(Tl) (Fenêtre entre 900keV et 1,1MeV = 30% - Fenêtre entre 350keV et 1,1MeV=50%)

2. ETUDE DES REACTIONS PRODUITES PAR IONS TRITIUM SUR LES NOYAUX LÉGERS.

Nous avons modifié les installations d'un accélérateur d'ions "Philips" 1MeV afin d'accélérer des ions tritium. La gamme d'énergie couverte est 300keV-1MeV avec un courant de tritons de 60nanoampères sur la cible.

Nous allons entreprendre la série de mesures suivantes :



mesure des distributions angulaires, courbes d'excitation, sections efficaces en valeur absolue.

3. SPECTRES DE RENVOI DES GAMMAS PRODUITS PAR DES NEUTRONS DE 5MeV, 6,6MeV ET 8,7MeV SUR LES CORPS SUIVANTS : CARBONE, ALUMINIUM, FER ET BISMUTH [2]

Nous avons mesuré les spectres de renvoi des gammas produits par des neutrons de 5MeV, 6,6MeV et 8,7MeV sur les corps suivants :carbone, aluminium, fer et bismuth.

La détection est faite à 90° par rapport à la direction des neutrons incidents, au moyen d'un détecteur NaI(Tl) $4'' \times 4''$.

Nous donnons les valeurs en mb/sr des sections efficaces différentielles à 90° des raies gammas les plus importantes. (tableau I)

Nous comparons nos résultats avec les valeurs données par d'autres auteurs.

SPECTRES DE RENVOI DES GAMMAS PRODUITS PAR DES NEUTRONS DE 14,1 MeV
SUR LES CORPS SUIVANTS : CARBONE, AZOTE, OXYGENE, ALUMINIUM, FER
ET PLOMB. [3]

Nous mesurons les spectres de renvoi des gammas produits par des neutrons de 14,1 MeV sur les corps suivants : carbone, azote, oxygène, aluminium, fer et plomb.

La détection est faite à 90° par rapport à la direction des neutrons incidents, au moyen d'un détecteur Ge(Li).

Nous donnons les valeurs en mb/sr des sections efficaces différentielles à 90° des raies gammas les plus importantes. (tableau II)

Nous comparons nos résultats avec les valeurs données par divers auteurs.

BIBLIOGRAPHIE .

- 1 G. GRENIER, C. POUSSIER - Rapport CEA R. 3562,
- 2 A. BERTIN, F. BERTRAND, G. CLAYEUX - Rapport CEA, à paraître.
- 3 G. CLAYEUX, G. GRENIER - Rapport CEA, à paraître.

TABLEAU I
Sections efficaces différentielles

Corps	E_{γ} (MeV)	Réaction probable	Transition	$d\sigma / d\Omega$ en mb/sr à 90°		
				$E_n = 5$ MeV	$E_n = 6,6$ MeV	$E_n = 8,7$ MeV
Carbone	4,43	$^{12}\text{C} (n, n') ^{12}\text{C}^*$	$4,43 \rightarrow 0$		$17,5 \pm 4,5$	$15,8 \pm 4,1$
Aluminium	0,842	$^{27}\text{Al}(n, n') ^{27}\text{Al}^*$	$0,84 \rightarrow 0$	$7,1 \pm 1,6$	$6,2 \pm 1,4$	$4,2 \pm 0,9$
	1,013	$^{27}\text{Al}(n, n') ^{27}\text{Al}^*$	$1,013 \rightarrow 0$	$16,3 \pm 3,6$	$17,5 \pm 3,8$	$13,6 \pm 3,0$
	1,72	$^{27}\text{Al}(n, n') ^{27}\text{Al}^*$	$2,731 \rightarrow 1,013$	$10,5 \pm 2,3$	$13,2 \pm 2,9$	$8,9 \pm 2,0$
	2,21	$^{27}\text{Al}(n, n') ^{27}\text{Al}^*$	$2,21 \rightarrow 0$	$19,7 \pm 5,1$	$18,1 \pm 4,7$	$17,7 \pm 4,6$
	2,976	$^{27}\text{Al}(n, n') ^{27}\text{Al}^*$	$2,976 \rightarrow 0$			
	3,00	$^{27}\text{Al}(n, n') ^{27}\text{Al}^*$	$3,0 \rightarrow 0$	$13,3 \pm 3,5$	$11,9 \pm 3,1$	$10,4 \pm 2,7$
Fer ^{56}Fe 91,5 %	0,850	$^{56}\text{Fe}(n, n') ^{56}\text{Fe}^*$	$0,847 \rightarrow 0$	$75,1 \pm 16$	$123,9 \pm 27,2$	$56,6 \pm 12,4$
	1,03	$^{56}\text{Fe}(n, n') ^{56}\text{Fe}^*$	$3,12 \rightarrow 2,085$	$1,0 \pm 0,2$	$1,7 \pm 0,4$	$3,4 \pm 0,7$
	1,24	$^{56}\text{Fe}(n, n') ^{56}\text{Fe}^*$	$2,085 \rightarrow 0,847$	$19,8 \pm 4,4$	$39,8 \pm 8,7$	$36,3 \pm 8$
	1,81	$^{56}\text{Fe}(n, n') ^{56}\text{Fe}^*$	$2,658 \rightarrow 0,847$	$20 \pm 4,4$	$30,8 \pm 6,8$	$10,3 \pm 2,2$
	2,09		$2,939 \rightarrow 0,847$			
	et 2,11	$^{56}\text{Fe}(n, n') ^{56}\text{Fe}^*$	$2,957 \rightarrow 0,847$	$10,4 \pm 2,7$	$9,7 \pm 2,5$	$6,1 \pm 1,6$
	2,6	$^{56}\text{Fe}(n, n') ^{56}\text{Fe}^*$	$3,45 \rightarrow 0,847$	$14,2 \pm 3,7$	$13,2 \pm 3,4$	$9,7 \pm 2,5$
Bismuth	0,9	$^{209}\text{Bi}(n, n') ^{209}\text{Bi}^*$	$0,894 \rightarrow 0$	$30,6 \pm 6,7$	$19,6 \pm 4,3$	$12,3 \pm 2,7$
	1,605	$^{209}\text{Bi}(n, n') ^{209}\text{Bi}^*$	$1,605 \rightarrow 0$	$90,1 \pm 19,8$	$86,3 \pm 18,9$	$60,3 \pm 13,2$

TABLEAU II
SECTIONS EFFICACES DIFFÉRENTIELLES

$E_n = 14,1 \text{ MeV}$, Détecteur : Ge (Li)

Corps	E_γ (MeV)	Réaction probable	Transition	$d\sigma/d\Omega$ en mb/sr à 90°	ENGESSER et THOMPSON ¹⁾ $E_n = 14,7 \text{ MeV}$	MORGAN ²⁾ $E_n = 14,8 \text{ MeV}$	GOLDBERG ³⁾ $E_n = 15 \text{ MeV}$
Carbone	4,43	$C^{12}(n, n')C^{12*}$	$4,43 \rightarrow 0$	$9,6 \pm 1,6$	$13,1 \pm 1,3$		12,8
Azote	1,63	$N^{14}(n, n')N^{14*}$	$3,945 \rightarrow 2,312$	$1,2 \pm 0,2$	$2,2 \pm 0,7$	1,6	
	2,31	$N^{14}(n, n')N^{14*}$	$2,31 \rightarrow 0$	$2,5 \pm 0,5$	$4,7 \pm 0,9$	3,3	
	3,68	$N^{14}(n, d)C^{13*}$	$3,68 \rightarrow 0$	$1,1 \pm 0,3$	$2,7 \pm 0,9$	1,8	
	3,85	$N^{14}(n, d)C^{13*}$	$3,85 \rightarrow 0$	$1,5 \pm 0,3$		1,8	
	4,46	$N^{14}(n, \alpha)B^{11*}$	$4,46 \rightarrow 0$	$6,2 \pm 2,2$	$5,0 \pm 1$	3,0	
	5,10	$N^{14}(n, n')N^{14*}$	$5,10 \rightarrow 0$	$3,5 \pm 0,7$	$4,3 \pm 1,4$	2,2	
	5,83	$N^{14}(n, n')N^{14*}$	$5,83 \rightarrow 0$	$0,7 \pm 0,2$		1,2	
	6,81	$N^{14}(n, \alpha)B^{11*}$	$6,81 \rightarrow 0$	$1,7 \pm 0,4$		2,2	
Oxygène	2,74	$O^{16}(n, n')O^{16*}$	$8,87 \rightarrow 6,13$	$2,2 \pm 0,5$	$3,8 \pm 0,4$	2,4	
	3,09	$O^{16}(n, \alpha)C^{13*}$	$3,09 \rightarrow 0$	$1,5 \pm 0,4$	$1,6 \pm 0,3$	1,7	
	3,68	$O^{16}(n, \alpha)C^{13*}$	$3,68 \rightarrow 0$	$3,0 \pm 0,6$	$5,5 \pm 1,1$	4,3	
	3,85	$O^{16}(n, \alpha)C^{13*}$	$3,85 \rightarrow 0$	$2,4 \pm 0,5$	$2,6 \pm 0,5$	2,8	
	4,43	$O^{16}(n, n' \alpha)C^{12*}$	$4,43 \rightarrow 0$	$1,9 \pm 0,4$	$1,5 \pm 0,5$	1,6	
	6,13	$O^{16}(n, n')O^{16*}$	$6,13 \rightarrow 0$	$11,2 \pm 2,0$	$12,2 \pm 1,2$	7,7	
	6,92	$O^{16}(n, n')O^{16*}$	$6,92 \rightarrow 0$	$2,4 \pm 0,5$	$3,8 \pm 0,9$	2,2	
	7,12	$O^{16}(n, n')O^{16*}$	$7,12 \rightarrow 0$	$3,7 \pm 0,7$	5 ± 1	1,8	
Aluminium	0,840	$Al^{27}(n, n')Al^{27*}$	$0,84 \rightarrow 0$	$2,8 \pm 0,2$	$7,0 \pm 1,4$		$3,8 \pm 1,5$
	1,01	$Al^{27}(n, n')Al^{27*}$	$1,01 \rightarrow 0$	$3,2 \pm 0,3$	$10,5 \pm 1,1$		$9,0 \pm 4$
	1,81	$Al^{27}(n, d)Mg^{26*}$	$1,81 \rightarrow 0$	$10,1 \pm 0,8$	$13,7 \pm 2,7$		20 ± 9
	2,21	$Al^{27}(n, n')Al^{27*}$	$2,21 \rightarrow 0$	$8,3 \pm 1,5$	$10,8 \pm 1,1$		12 ± 4
	3,0	$Al^{27}(n, n')Al^{27*}$	$3,0 \rightarrow 0$	$7,8 \pm 1,4$	$7,9 \pm 1,6$		
Fer	0,85	$Fe^{56}(n, n')Fe^{56*}$	$0,847 \rightarrow 0$	$37,6 \pm 2,2$	$56,7 \pm 5,8$		49 ± 13
	0,93	$Fe^{56}(n, 2n)Fe^{55*}$	$0,93 \rightarrow 0$	$4,3 \pm 0,3$	$11,7 \pm 3,9$		
	1,24	$Fe^{56}(n, n')Fe^{56*}$	$2,085 \rightarrow 0,847$	$22,0 \pm 1,4$	$23,9 \pm 2,3$		28 ± 7
	1,30	$Fe^{56}(n, 2n)Fe^{55*}$	$1,32 \rightarrow 0$	$8,4 \pm 0,6$	$7,4 \pm 2,5$		
	1,41	$Fe^{56}(n, 2n)Fe^{55*}$	$1,41 \rightarrow 0$	$2,0 \pm 0,2$			
	1,81	$Fe^{56}(n, n')Fe^{56*}$	$2,658 \rightarrow 0,847$	$3,8 \pm 0,4$	$5,4 \pm 0,6$		
	2,60	$Fe^{56}(n, n')Fe^{56*}$	$3,45 \rightarrow 0,847$	$2,4 \pm 0,5$	$3,7 \pm 0,8$		
Plomb	0,569	$Pb^{207}(n, n')Pb^{207*}$	$0,569 \rightarrow 0$	$38,0 \pm 3,2$			
	0,803	$Pb^{206}(n, n')Pb^{206*}$	$0,803 \rightarrow 0$	$38,7 \pm 3,1$	$45,5 \pm 9$		
	0,897	$\{Pb^{207}(n, n')Pb^{207*}$	$0,897 \rightarrow 0$				
		$\{Pb^{206}(n, n')Pb^{206*}$	$1,68 \rightarrow 0,80$	$22,2 \pm 1,8$	$26,3 \pm 9$		
	0,980	$Pb^{206}(n, n')Pb^{206*}$	$1,78 \rightarrow 0,803$	$12,6 \pm 1,4$			
			$2,71 \rightarrow 1,63$				$Pb^{207}(n, n')Pb^{207}$
							$1,9 \cdot 0,89 \frac{d\sigma}{d\Omega} = 17,3 \pm 5,8$
	1,08	$Pb^{207}(n, n')Pb^{207*}$	$1,63 \rightarrow 0,57$	$33,8 \pm 3,1$			
	1,43	$Pb^{207}(n, n')Pb^{207*}$	$2,339 \rightarrow 0,897$	$11,5 \pm 1,5$			
	1,769	$Pb^{207}(n, n')Pb^{207*}$	$2,339 \rightarrow 0,57$	$28,3 \pm 3,0$	$12,9 \pm 2,6$		
	2,01	$Pb^{208}(n, n')Pb^{208*}$	$2,61 \rightarrow 0$	$19,1 \pm 3,8$	$20,3 \pm 2,1$		

XXII. LABORATOIRE DE PHYSIQUE NUCLEAIRE - C.E.A. GRENOBLE (FRANCE)

Pr. BOUCHEZ.

1. MISE EN EVIDENCE DE L'INTERACTION NEUTRON-NEUTRON ET NEUTRON-PROTON DANS LA REACTION D(n,nnp) A 14,5 MeV PAR SPECTROMETRE A DOUBLE TEMPS DE VOL -

Après la mise en évidence de l'interaction neutron-neutron par la détection des deux neutrons au même angle (30° Lab.), une seconde expérience multi-paramétrique avec détection des neutrons à des angles différents (30° , -80° Lab.) a permis la mise en évidence de l'interaction neutron-proton (2500 événements) avec le même appareillage [1] et les mêmes conditions de traitement. Les phénomènes parasites de double-diffusion sont évalués par une méthode de Monte-Carlo [2] et les résultats triés sont comparés à des modèles basés sur la théorie des diagrammes de Feynmann [3].

2. $^7\text{Li}(n,n'\gamma)$ A 14 MeV - (Fig.1)

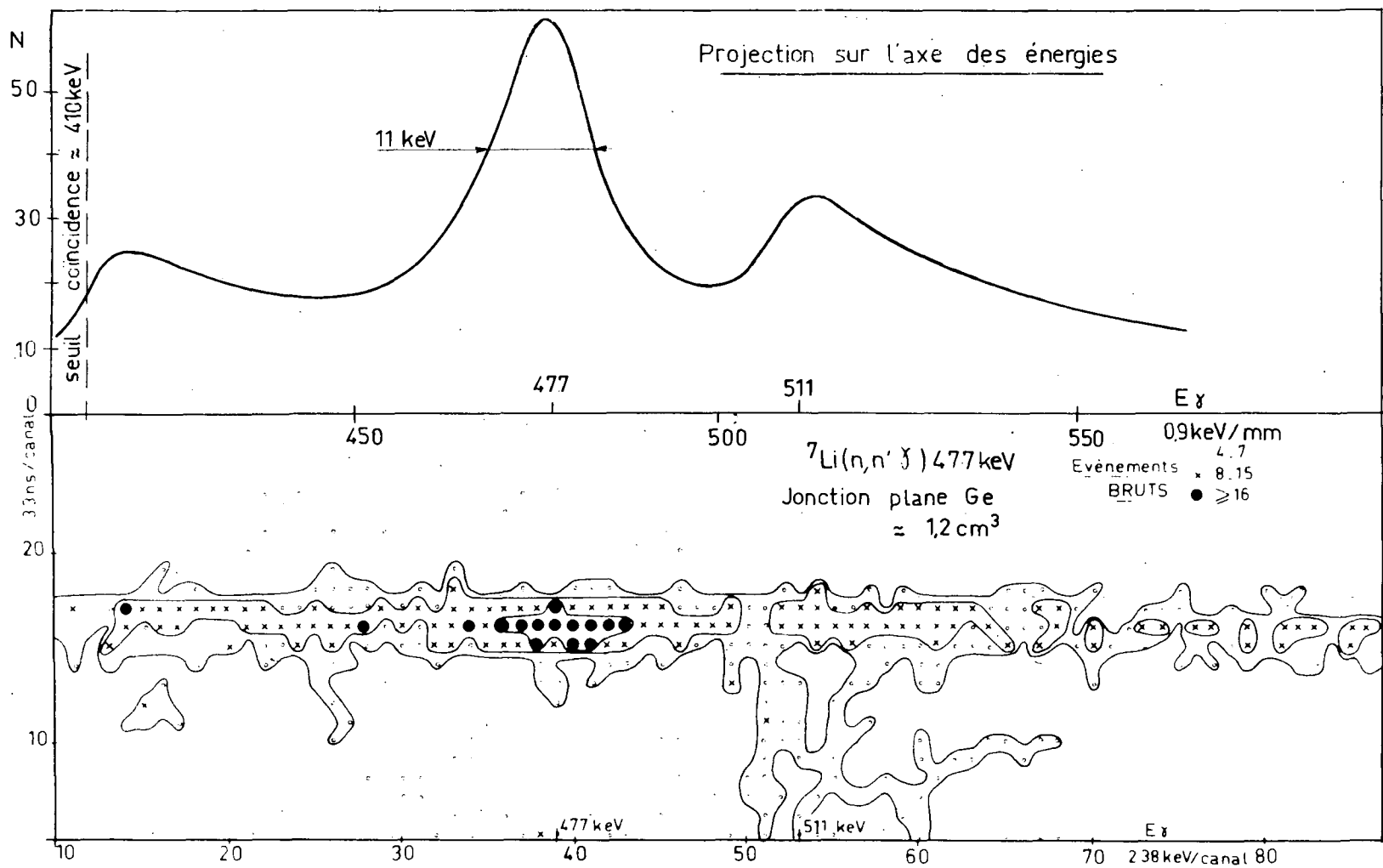
On a observé le rayonnement photonique à 477 keV de désexcitation du ^7Li au moyen d'un détecteur au germanium de $1,2\text{cm}^3$. Le nombre de coïncidences n,γ obtenues permet d'évaluer la section efficace de la réaction $^7\text{Li}(n,n'\gamma)^7\text{Li}^*$ 477 keV : $\sigma = (76 \pm 10) \text{ mb}$ en accord avec la mesure 80 mb (± 10 mb) faite par Benveniste [4].

Le dispositif expérimental utilise une analyse biparamétrique avec des résolutions en temps et en énergie respectives de 4ns et 6 keV [5]. Nous pensons utiliser ce dispositif pour l'étude des neutrons de capture à 14 MeV sur ^{181}Ta et ^{209}Bi .

REFERENCES

- [1] C. PERRIN* et al - J. de Phys. (à paraître)
- [2] C. DUCHARME - Thèse Docteur d'Université, Grenoble (1968) n°990
Rapport C.E.A. (à paraître)
- [3] S. DESREUMAUX - Thèse 3e cycle (à paraître)
C. PERRIN* - Thèse Doctorat ès Sciences Physiques (à paraître)
J.C. GONDRAND[†] - Thèse Doctorat ès Sciences Physiques (à paraître)
- [4] J. BENVENISTE et al. - Nuclear Physics, 38 1962 300
- [5] C. SONREL - Thèse Docteur-Ingénieur (à paraître)

* Institut des Sciences Nucléaires - Université de Grenoble (France).



Spectre biparamétrique (énergie/temps-de-vol) obtenu dans l'expérience ${}^7\text{Li}(n,\gamma)n'$ à 14,5 MeV ; le neutron incident est détecté par la particule associée, le γ de 477 keV par un détecteur de Ge ($\approx 1,2 \text{ cm}^3$) à structure plane.

XXIII. SERVICE D'ETUDES DE PROTECTION DE PILES -

C.E.A. FONTENAY-AUX-ROSES (FRANCE) - R. VIDAL

1. SECTIONS EFFICACES EFFECTIVES DE ^{233}U DANS LES RESEAUX A EAU LOURDE

Des expériences en vue de la mesure des sections efficaces effectives de fission et de capture et du η de ^{233}U ont été effectuées dans le réacteur MINERVE avec des échantillons d'utanium métallique contenant de faibles quantités de ^{233}U .

Ces mesures effectuées dans un réseau à eau lourde sont en cours d'interprétation.

2. MESURES DU RAPPORT CAPTURE SUR FISSION DU $^{239}\text{Pu}(\alpha)$ DANS UN SPECTRE VOISIN DE CEUX DES REACTEURS A NEUTRONS RAPIDES -

Les expériences en vue de la mesure du α_9 ont été effectuées dans l'assemblage ERMINÉ placé au centre de MINERVE. Deux méthodes ont été utilisées : l'une basée sur les mesures des rapports des coefficients de danger du ^{239}Pu et du bore et des taux de fission et de capture du ^{239}Pu et du bore. L'autre utilise la méthode de la chambre locale pour mesurer le taux de fission du ^{239}Pu comparée à une source de ^{252}Cf .

Une première série d'expériences a été réalisée ; tous les résultats sont en cours d'interprétation et permettront de définir la valeur de α_9 dans le spectre d'ERMINÉ avec une précision voisine de 15%.

Une autre méthode pour atteindre α_9 a été développée. Elle consiste à irradiier au centre du réacteur OSIRIS dans une capsule dont l'épaisseur est de 10mm de bore 10, des échantillons de ^{235}U , de ^{238}U et de ^{239}Pu . On mesure la variation de la composition isotopique des échantillons et on déduit le rapport des taux de fission par une mesure avec des chambres à fission dans le réacteur ISIS qui est la maquette exacte d'OSIRIS. La combinaison de ces deux séries de résultats permet d'atteindre α_9 , α_5 et α_8 pour le spectre d'irradiation avec une précision voisine de 7% pour 5 mois d'irradiation.

La capsule sera déchargée très prochainement afin d'obtenir les premiers résultats et une nouvelle sera irradiée pour une durée d'environ 1 an, ce qui permettra d'améliorer la précision des résultats. (note CEA n° N.989)

3. MESURE DE L'ENERGIE DEGAGEE PAR LES MATERIAUX FISSILES IRRADIES -

Une mesure calorimétrique de la puissance résiduelle dégagée par les éléments combustibles irradiés dans un spectre thermique est en préparation.

IV. CENTRE DE PHYSIQUE NUCLEAIRE DE L'UNIVERSITE DE LOUVAIN (Belgium)

1. Study of monoenergetic neutron sources

G. DECONNINCK, J. ROYEN

The reaction $V^{51}(p,n)Cr^{51}$ has been studied between 2.2 and 4 MeV. The aim of this work is to measure the angular distributions of the neutrons in order to determine the possibility of using this reaction as a source of monoenergetic neutrons. It is shown that for some applications this source is better than the conventional ones because of the slow variation of intensity and energy with angle and also because of the ease with which the targets can be made and utilized.

A detailed paper on this work will be published.

XXV. CENTRE D'ETUDE DE L'ENERGIE NUCLEAIRE (C.E.N.-S.C.K.) Mol, Belgium

1. Neutron Spectrometry

1.1. Crystal Spectrometer

F. POORTMANS

Total and activation cross section measurements have been performed on Eu between 0.020 eV and 0.6 eV in collaboration with the reactor physics department. Partial results have been communicated at the second conference on neutron cross sections and Technology (Washington, March 1968). Accurate values for the total cross section at 0.0253 eV and the isomeric ratios of the three lowest resonances have been obtained. It is seen that the relative population of the 9.3 hr isomeric level of ^{152}Eu is quite different for these three resonances although they have the same spin. The resonance parameters of the bound level have been deduced. Further work is in progress in order to check the Westcott $g(T)$ function. A contract with IAEA has been signed for measurements of the scattering cross sections of ^{235}U and ^{239}Pu below 1 eV. These experiments are in preparation.

1.2. Neutron Resonance Scattering

F. POORTMANS, H. CEULEMANS, E. MIGNECO ⁺, J. THEOBALD ⁺

This research is conducted in cooperation with C.B.N.M., Euratom, Geel under the terms of contract EUR/c/4146/67 f. As the experiments are performed at the C.B.N.M. Linac these activities are reported in the C.B.N.M. part of this Report.

+ C.B.N.M., Euratom, Geel

1.3. Neutron Resonance Total Cross Sections

H. CAMARDA ^{*}, H. CEULEMANS, G. HACKEN ^{*}, W.W. HAVENS, Jr. ^{*},

H. LIOU ^{*}, J. RAINWATER ^{*}, M. SLAGOWITZ ^{*} and S. WYNCHANK ^{*}

A series of experiments performed at the Nevis Synchrocyclotron of Columbia University, U.S., allowed the collection of data for 26 separated isotopes and 14 natural elements including $W^{182,184,186}$, Cu^{63} , $Eu^{151,153}$, Hf^{177} , $Sr^{86,87,88}$, $Er^{166,167,168,170}$, $Gd^{154,158}$, Lu^{175} , $Sm^{152,154}$, $Yb^{17,172,173}$, $Nd^{142,144,146}$, In^{115} , U^{235} , Ta , W , La , Lu , Fe , In , Yb , Pr , Cu , Nd , Er , Na , Ar . Resonance spectra were obtained from a few eV up to as high as 100 keV in some cases. The high-energy resolution of these data is ≤ 0.2 ns/m. More information on these experiments may be found elsewhere (†).

1.4. Radiative Capture Cross Section (Low keV Region)

F. RAHN ^{**}, C. HO ^{**}, J. FELVINCC ^{**}, E. MELKONIAN ^{**},

W.W. HAVENS Jr., ^{*}, H. CEULEMANS and J. RAINWATER ^{*}

Preliminary testing of the modified Moxon-Rae type detectors and data acquisition equipment was conducted at the 40 m and 100 m flight paths of the Neutron Velocity Selector at the Nevis Synchrocyclotron. The materials used during the tests were Au, Mn, In, Cu and Zr. The peak-to-background ratio obtained at the 78 eV level in Au^{198} was 15 to 1. Further information on these experiments has been given elsewhere (1) .

* Physics Department, Columbia University, New York, N.Y.

** Department of Nuclear Engineering, Columbia University, New York, N.Y.

(1) Pegram Nuclear Physics Laboratories Progress Report, June 68 tot

1.5. Cross Section Calculations from Nuclear Theory and Systematics

L. DE CORTE and H. CEULEMANS

An effort, up to now of limited scope and applications, has been initiated in order to complement experimental data in areas where the latter are difficult to obtain such as capture cross sections for neutron-rich nuclides formed during nuclear fission, or inelastic scattering cross sections. For these calculations the computer programme NEARREX (2) will be used.

1.6.. Publications and Communications

Cross Section Measurements for the Reactions ^{151}Eu (n,γ) ^{152}Eu between 0.01 eV and 0.5 eV.

F. Poortmans, A. Fabry and I. Girlea, Neutron Cross Sections and Technology, Vol. 1, p. 883, Washington, March 1968

Recent Improvements of the Nevis Synchrocyclotron Neutron Velocity Spectrometer

M. Slagowitz et al., Bull. Am. Phys. Soc., Vol. 13, n° 4, paper JG11
Neutron Resonance Spectroscopy I: W^{182,184,186} and Cu^{63,65}

H. Camarda et al., Bull. Am. Phys. Soc., Vol. 13, n° 4, paper KG11

Neutron Resonance Spectroscopy II:

G. Backen et al., Bull. Am. Phys. Soc., Vol. 13, n° 4, paper KG12

(2) NEARREX, a computer code for nuclear reaction calculations, ANL-6978,
P.A. Moldauer, C.A. Engelbrecht, G.J. Duffy.

2. Fission Physics and Chemistry

2.1. Fission cross-section measurements with fission track detectors.

M. NEVE de MEVERGNIES and P. del MARMOL

A thermal neutron fission cross-section of 39 ± 4 pb was measured for ^{232}Th in the thermal column of the BR1 reactor at Mol by means of a Makrofol detector. This value is in rough agreement with the 60 ± 20 pb measurement of Korneev, Skobkin and Flerov (Sov. Ph. JETP, 10 (1960) 29).

2.2. Identification of short-lived isotopes in fission

P. del MARMOL

A branching ratio of $64 \pm 8\%$ was measured for the decay of $14.1 \text{ s}^{83}\text{As}$ tot $70 \text{ s}^{83m}\text{Se}$ and results concerning yields and half-lives of ^{83}As and ^{84}As were published.

A fast radiochemical method ($\sim 5\text{s}$) for the separation of short-lived selenium isotopes in fission has been completed.

2.3. Delayed neutron precursors

P. del MARMOL

A compilation and evaluation of experimental data for individual delayed neutron precursors up to september 1968 has been completed for the Journal "Nuclear Data". The following properties are covered: half-life, neutron emission probability, charge and mass assignment, methods of production, β -decay properties leading to neutron emitting states, neutron spectra as well as the measured or estimated Q_β energy of the parent and neutron separation energy of the daughter nucleus.

2.4. Publications

M. Nève de Mévergnies and P. del Marmol, Neutron cross sections and technology, Proceedings of a Conference, Vol. I, p. 611, National Bureau of Standards, Washington, 1968.

P. del Marmol, J. Inorg. Nucl. Chem., 30, (1968) 2873

P. del Marmol, p. 75 and p. 242, "Delayed Fission Neutrons", Edit. I.A.E.A., Vienna (1968).

3. Inelastic Scattering of Slow Neutrons

S. HAUTECLER

The physical content of the Krebs model, which was originally formulated in order to explain the lattice dynamics of bcc and fcc metals, has been applied to hcp metals. The metal is considered as a set of spherical ions, of uniform charge distribution, embedded in an electron sea. The elements of the dynamical matrix have been deduced by assuming central spring interactions extending up to the sixth neighbours, and a screened Coulomb interaction between all ions. Six relations between the eight parameters introduced in the model and the five elastic constants have been obtained by the method of long waves. It was found that the lattice equilibrium condition obtained by equating the two expressions for C_{44} requires that the long-range interaction cancels out. It was concluded that the Krebs force-model does not describe a crystal in equilibrium. A possible way to fulfill the lattice equilibrium condition would be to introduce a tangential interaction for one of the neighbouring layers.

Important modifications have been made on the BR2 time-of-flight spectrometer. At the present time, the spectrometer is equipped

with 8 evacuated flight paths, maximum section $40 \times 20 \text{ cm}^2$, 4 m long. Each bank of detectors consists of 7 BF₃ counters, 2" in diameter. The flight paths can be moved in a shielded room, the scattering angles ranging from 0° tot 120°. In addition, there is in the incident monochromatic beam a calibration flight path supporting 2 BF₃'s, 1" in diameter, of low sensitivity ($\sim 5\%$). Measurements of phonon scattering were started on a ZnO single crystal. Although the volume of the sample was less than 2 cm³, the ratio of the phonon peak to the background was acceptable.

Publications

S. Hautecler and M. Nève de Mévergnies, Neutron Inelastic Scattering, Vol. I, 91, Edit. IAEA, Vienna, 1968.

4. Thermal Neutron Data (Standards)

A.J. DERUYTTER *, P. PELFER **, W. BECKER ***

This research is performed under the terms of contract EUR/c/4146/67 f, between CBNM (Euratom) and SCK-CEN (Mol), using neutron beams from the BR2 and BR1 reactors.

4.1. 2200 m/s fission cross-section of ^{235}U

The neutron induced counting-rates of high quality foils of elemental natural boron and evaporated $^{235}\text{U F}_4$ layers have been compared in identical geometry and neutron beam with a solid-state detector.

Neutron energy selection is made with a slow chopper and simultaneous pulse-height and time-of-flight spectra are recorded. (Energy range: 2 meV to 0.1 eV)

* CBNM, Euratom, Geel

** Research Fellow, CBNM, Euratom, Geel

+ Research in association with Kernforschungsanlage Jülich (W. Wegener)

Because of the interest in σ_f -values at very low neutron-energies a measurement at low rotor revolution speed of about 40 revolutions per second was also performed. The first run was made at a rotor speed of 92 r.p.s. The rotor transmission probability for neutrons with very low energy is much higher for the lower rotor speed and for this reason σ_f -values could be deduced down to 2 meV. The absolute precision of the amount of ^{235}U on the layers and consequently of the σ_f -values is however limited by the accuracy of the ^{234}U α -half life. Work on the α -half-lives of the uranium isotope continues at CBNM, Geel.

Preliminary results on the first high revolution-speed group of data were presented at the "Neutron Cross-Sections and Technology Conference" at Washington, March 1968. An extensive report on all data is being prepared.

4.2. 2200 m/s fission cross-section of ^{239}Pu

The experimental procedure is identical to the one discussed for ^{235}U . The isotopic composition of the samples is 99.979% ^{239}Pu ; 0.002% ^{240}Pu and 0.001% ^{241}Pu . The precision on the amount of Pu is determined by the precision of the α -half life of ^{239}Pu (24.360 ± 50) yrs of about 0.2%. The agreement between the published values for the α -half lives of ^{239}Pu is very good, but one is no longer very confident in this value because of the CBNM experience with absolute chemical definitions. Good separation between α -particles (and pile-up pulses) and fission fragments of ^{239}Pu is obtained. The comparison with the standard boron layers is started.

4.3. Comparison of the spontaneous fission of ^{240}Pu and thermal neutron induced fission of ^{239}Pu

This program was interrupted because of lack of personnel but is now restarted with the help of a student of the "Rijksuniversiteit Gent". The bidimensional analyzing system, as well as the computer programs to calculate energy and mass-distributions from the raw data were already tested with ^{235}U + thermal neutrons. Final measurements await the arrival of the ($^{239}\text{Pu} + ^{240}\text{Pu}$)-source, expected beginning of 1969.

5. Integral cross sections measurements and nuclear data related to reactors.

5.1. Evaluation of nuclear data for activation detectors.

A. FABRY, P.P. DAMLE, H. VANDENBROECK, D. LANGELA

A code error has been found in the compilation of resonance integrals reported in Blg 421 [1], which fortunately only affects the data relative to ^{151}Eu and ^{176}Lu .

A revised version of this report will shortly be issued in collaboration with the staff of the Laboratorio Fisica e Calcolo Reattori, CNEN, Casaccia, Italy, including a review of the most recent publications as well as the new experimental results obtained at Casaccia and at Mol.

5.2. Integral determination of 2200 m/sec activation cross sections.

A. FABRY, R. JACQUEMIN

Thermal cross sections have been measured by the activation technique for the reactions $^{98}\text{Mo}(\text{n},\gamma)^{99}\text{Mo}$ and $^{175}\text{Lu}(\text{n},\gamma)^{176m}\text{Lu}$ relatively to $^{197}\text{Au}(\text{n},\gamma)^{198}\text{Au}$. The irradiations have been performed in a rotating graphite plug inserted into the BR1 horizontal thermal column, at a location where the epithermal flux is negligible (Au cadmium ratio : $\sim 10^5$) and the thermal neutrons are distributed according to a

maxwellian law of known temperature ($20^\circ C$). The small corrections for the thermal flux depression [2] have been carefully checked by changing the thickness of the samples, which were alloys with aluminium of various compositions for Au and Lu (prepared and assessed at CBNM, Euratom, Geel).

The resulting cross sections are :

$$\begin{aligned} {}^{98}\text{Mo} (n,\gamma) {}^{99}\text{Mo} & : \quad \sigma_o = (0.120 \pm 0.005) b \\ {}^{175}\text{Lu} (n,\gamma) {}^{176m}\text{Lu} & : \quad \sigma_o = (16.4 \pm 0.9) b \\ (\text{for } \sigma_o (\text{Au}) = 98.7 \text{ b})[1] \end{aligned}$$

The Westcott g [3] factors have been computed from known resonance parameters [1] [4] and found to lie close to unity; although strictly equal to 1 for ${}^{175}\text{Lu}$ within error margin, some doubt still remains upon that correction due to the existence of an important contribution of unknown bound levels (the thermal absorption cross section of ${}^{175}\text{Lu}$ is computed to be 13,8 b [1] from resolved resonance parameters while the measured value is 23 ± 3 b [5] and is consistent with the well known absorption data for both ${}^{176}\text{Lu}$ [1] and elemental Lu [6]). The previously unknown isomeric yield ratio $\frac{\sigma_o^m}{\sigma_o^m + \sigma_o^g}$ for ${}^{175}\text{Lu}$ is approximately 70% and could increase with neutron energy, especially at the resonances at 5,24 and 14,1 eV.

5.3. Integral cross section measurements in the ${}^{235}\text{U}$ thermal fission neutron spectrum

A. FABRY, M. DE COSTER

A paper has been presented at the Second Conference on "Neutron cross sections and technology" Washington, March 4-7 (1968) [7]; the abstract follows :

" As a first step in a long term applied research programme under consideration in relation with the development of a fast breeder prototype, capture cross sections averaged over the uranium-235 thermal fission neutron spectrum have been measured by the activation technique for a few nuclides; they most often were found to disagree with earlier similar studies.

"The important features of the present method are briefly discussed. Included is a criticism of the uncertainties in the uranium-235 thermal fission spectrum itself, mainly based on recent integral studies and on new measurements of the ^{238}U (n,f) and ^{235}U (n,f) average cross sections using fission track detectors.

"The resulting average capture cross sections are compared with evaluated differential data."

As an illustration of the observed difficulties related to the fission spectrum and/or fission cross sections, it should be noted that if the U-235 (n,f) and U-238 (n,f) differential energy cross-sections as recommended by Hart [8] (a reasonable compromise between the conflicting most recent evaluations [9] [10]) are weighted with the fission spectrum shape as tentatively modified by Grundl [11], values of 1246 ± 25 mb and 336 ± 10 mb are respectively found rather than 1250 ± 25 mb and 301 ± 9 mb when using the conventional fission spectrum representation [12]; our experimental integral values are 1335 ± 130 mb and 353 ± 30 mb, the absolute errors tending to cancel out in the comparisons if the ratios between these cross-sections are taken. The U-235 (n,f) average fission spectrum cross-section is seen to be rather insensitive to the exact fission spectrum shape; least-squares interpretation of critical masses for a lot of fundamental spherical fast

assemblies in terms of corrective factors for differential energy cross-sections has led to a curve [13] systematically higher than all the most recent evaluations, resulting in an average fission spectrum cross-section of 1325 mb, very close to our experimental figure.

Since the completion of this work, the use of fission track detectors has been considerably refined and accuracies of the order of $\pm 2\%$ can now be achieved; new measurements are currently in progress for the case of the ^{235}U thermal fission neutron spectrum and are under preparation for the ^{239}Pu -case.

5.4. Use of intermediate standard neutron spectra for the improvement of nuclear data for fast reactors.

A. FABRY, J.C. SCHEPERS, P. VANDEPLAS

The facility for generation of a flexible family of primary intermediate standard neutron spectra [14] is still under design. This is a one-dimensional (spherical) source system, whose central spectra are derived from the ^{235}U thermal fission neutron spectrum by partial moderation and absorption in such a way that the accuracy of their description should ultimately reflect the accuracy of the $^1\text{H}(\text{n},\text{n})$ and $^{10}\text{B}(\text{n},\alpha)$ differential energy cross sections and of the fission spectrum essentially. These spectra, whose mean energy depends upon the amount of moderation introduced, i.e. simply upon the thickness of an inner polythene shell, will be used for precise integral cross section measurements.

In order to support the development of experimental methods needed for the extensive study of the primary facility, another much more simple arrangement [15] is presently under completion in the mock up cavity [14] of 50 cm diameter hollowed out in the horizontal graphite thermal column of the BR1 reactor : this is a 5 cm thick and 24,5 cm outer diameter natural uranium metal shell, with an inner spherical screen of 15 mm thick vibro compacted boron carbide cladded into 1 mm aluminium. The central spectrum in this facility simulates reasonably well the central spectrum of large dilute fast breeders and for energies above 100 keV depends mainly upon the nuclear data of natural uranium. Such a system could be duplicated rather easily in other laboratories and is tentatively proposed as a secondary standard useful for the intercomparison of experimental techniques. The spherical shell transmission method [16] associated to differential neutron spectrometers [14] will be applied in both the primary and secondary standard systems, i.e. with completely different input spectra. The first nuclide to be studied in this way is ^{238}U . The depleted spherical shells are being manufactured. Transport calculations in the detailed conditions planned for these experiments have shown [15] that they will offer powerful semi-integral checks of the downscattering ($E \geq 100$ keV) and the shielded capture ($10 \text{ keV} \leq E \leq 100 \text{ eV}$) cross-sections for this nuclide. Special emphasis is paid upon the development of an interpretation scheme for these integral and semi-integral experiments which will include reasonable physical grounds like statistical theories and the optical model of nuclear reactions.

References for § 5.

- [1] P.P. DAMLE, A. FABRY, H. VANDENBROECK - Report Blg 421 (1967)
- [2] D.F. SHOOK, D. BOGART, D.L. ALGER, R.A. MULLER - Nucl. Sci. Eng. 26, 453-461 (1966)
- [3] C.H. WESTCOTT - Report AECL 1101 (1960)
- [4] J.R. STEHN et al. - AEC report BNL-325 suppl. 2 (1966)
- [5] J.H. BASTON et al. - J. Nucl. Eng. A/B 13, 35 (1960)
- [6] IAEA Conference on "Nuclear Data for Reactors", Paris (1966).
paper CN-23/20 (BRUNNER, WIDDER)
paper CN-23/129 (ZIMMERMAN et al.)
- [7] A. FABRY, M. DE COSTER - Second conference on "Neutron cross-sections and technology" Washington DC, 4-7 March (1968)
NBS special publication n° 299 vol. II p. 1263 -1269
- [8] W. HART - Report AHSB (S) R124 (1967)
- [9] J.J. SCHMIDT - Report KFK 750 (1968)
- [10] W.G. DAVEY - Nucl. Sci. Eng. 32, 35-45 (1968)
- [11] J.A. GRUNDL - Nucl. Sci. Eng. 31, 191-206 (1968)
- [12] B.E. WATT - Phys. Rev. 87, 1037 (1952)
- [13] G. RAKAVY, Y. REISS, D. SAMOUCHA, Y. YEIVIN - Fast reactor physics, Vol. I, p. 255 (1968), IAEA.
- [14] A. FABRY, P. VANDEPLAS - Fast reactor physics, IAEA, Vol. I p. 389-411 (1968)
- [15] A. FABRY, J.C. SCHEPERS, P. VANDEPLAS - "Status of the work about the generation of intermediate standard neutron spectra at Mol". Prepared for submission at EACRP meeting, London, February 1968.
- [16] H.A. BETHE et al. - J. Nucl. Eng. 3, 207 (1956); 3, 273 (1956); 4, 3 (1957); 4, 147 (1957).

VI. REACTOR CENTRUM NEDERLAND PETTEN

1. RCN activities

1.1. Circular polarization of gamma radiation after capture of polarized thermal neutrons (K.Abrahams)

A beam of thermal neutrons, extracted from the High Flux Reactor at Petten is polarized by reflection on a system of 74 cobalt mirrors each of dimension $100 \times 5 \times 2$ mm. The mirrors are arranged in a focussing Soller slit system and magnetized by an electromagnet. The beam is focussed at the target 3.5 meter from the exit of the Soller slit¹⁾. The focus spot is 2 cm broad and a few cm high and the flux F at the target is $3 \cdot 10^7 \text{ cm}^{-2} \text{ s}^{-1}$; the polarization is 85%.

After capture of the polarized neutrons circularly polarized gamma radiation will be sent out. If θ is the angle between neutron polarization and γ ray, the circular polarization is given by:

$$P_\gamma = P_n R \cos \theta.$$

R is related to the spins of the intermediate states, the mixing of spins in the capturing state and to the multipole mixture in the γ transitions. These parameters we would like to determine.

The polarization of the γ radiation is measured by transmission through magnetized iron. The transmitted γ radiation is detected by a 17 cm^3 and a 30 cm^3 Ge(Li)-detector facing each other. The pulses of each detector are routed to one of four quadrants of a 4096 channel analyser. The procedure of the measurements is as follows: The neutron polarization is inverted in 10 sec. periods by a magnetic guide field system²⁾, the multichannel analyser is put in addition mode for positive neutron polarization and in subtraction mode for negative neutron polarization. The effects are of the order of 1% and the measuring time is a few weeks per sample. In fig.1 the experimental arrangement is sketched.

Measurements on K, S, Ti, Ca, Co, Cd, and Pb have been performed³⁾, using our previous mirror system, which lead to a smaller flux and polarization as that quoted above. Several spin assignments could be made.

Publications

- 1) K.Abrahams, W.Ratynski, F.Stecher-Rasmussen and E.Warming, Nuclear Instruments and Methods 45 (1966) 293.
- 2) K.Abrahams, O.Steinsvoll, P.J.M.Bongaarts and P.W.de Lange, Rev.Sci. Instr. 33 (1962) 524.
- 3) K.Abrahams and W.Ratynski, Nucl.Phys. A124 (1969) 34.

1.2. Proposal for integral measurements of cross sections of fission product isotopes (M. Busstraan)

A fast-thermal critical facility (STEK) is being erected at the RCN site at Petten for integral measurements of cross sections of fission product isotopes. The measurements will be performed by a reactor oscillator passing through the centre of the fast core. The spectrum of this fast core will be variable ranging from harder than that of a Na cooled breeder to softer than that of a steam cooled fast breeder. The measurements will be performed in at least five different spectra. It is expected that STEK will come into operation in May 1969.

2. F.O.M. activities

2.1. Thermal-neutron capture γ -ray spectroscopy (P. Spilling¹⁾, H. Gruppelhaar, A.M.F. Op den Kamp and A.M.J. Spits)

1) Present address: Technische Hogeschool, Eindhoven, Nederland. Measurements on thermal-neutron capture γ rays started in Petten in 1964 with angular correlation studies of the nuclei phosphorus, sulfur and chlorine^{1,2,3)}. The spectrometer consisted of two large NaI crystals. Since that time the mechanical part of the apparatus has not been changed. In fig. 2 a vertical cross section through the radial beam hole, used for the experiments is shown. The beam is collimated by a two meters long collimator, consisting of lead and aluminium. The fast neutrons are scattered out of the beam by means of quartz and bismuth single crystals. This neutron filter is cooled to liquid nitrogen temperature, which gives an increase in the thermal-neutron flux of a factor 3.8. After further collimation a clean beam of thermal neutrons is obtained. At the place of the target the thermal-neutron flux is about 10^7 neutrons per cm^2 and per sec. One of the two NaI crystals, together with the heavy lead shielding is visible in fig. 2. This detector can rotate in a vertical plane perpendicular to the beam.

Since the last two years a high-resolution Ge(Li) detector is used, chiefly for the recording of "single" spectra. Special attention is given to the energy calibration. Mostly the uncertainties in the energies are less than 1 keV. With such a careful determination of the γ -ray energies decay schemes can be constructed with a high degree of consistency. Furthermore, excitation energies and the Q value can be determined with high precision. Other results of the analysis are branching ratios.

Up to now rather complete decay schemes have been constructed for the following final nuclei: ^{32}P , $^{25,26}\text{Mg}$, $^{41,43,45}\text{Ca}$, ^{20}F and ^{13}C (refs. 4-9).

As an example in fig. 3 the spectrum of the $^{44}\text{Ca}(\text{n},\gamma)^{45}\text{Ca}$ reaction is shown. The thermal-neutron cross section for this reaction is 1.1 b. The available amount of ^{44}Ca (enrichment 97%) was only 200 mg.

The combination of a high neutron flux, a relatively low γ -background and a high-resolution Ge(Li) detector gives the possibility of measuring capture γ -ray spectra of small amounts of enriched isotopes.

With the combination of a 12.7×12.7 cm NaI crystal and a 23 cm^3 Ge(Li) detector some $\gamma\gamma$ -coincidence and $\gamma\gamma$ -angular correlation measurements were performed on ^{43}Ca and ^{45}Ca , using a 16-window digital discriminator¹⁰⁾. These investigations are a part of the program of the Dutch Foundation for Fundamental Research on Matter ("Stichting voor Fundamenteel Onderzoek der Materie", F.O.M.).

Laboratory:

Reactor Centrum Nederland, Petten and Physical Laboratory State University, Utrecht.

Publications:

- 1) Investigation of the reactions $^{31}\text{P}(\text{n},\gamma)^{32}\text{P}$ and $^{32}\text{S}(\text{n},\gamma)^{33}\text{S}$, G. van Middelkoop and P. Spilling, Nucl. Phys. 72 (1965) 1.
- 2) Gamma-gamma angular correlation measurements in the $^{35}\text{Cl}(\text{n},\gamma)^{36}\text{Cl}$ reaction, G. van Middelkoop and P. Spilling, Nucl. Phys. 77 (1966) 267.
- 3) Investigation of the $^{32}\text{S}(\text{n},\gamma)^{33}\text{S}$ reaction, G. van Middelkoop and H. Gruppelaar, Nucl. Phys. 80 (1966) 321.
- 4) Gamma rays from the $^{31}\text{P}(\text{n},\gamma)^{32}\text{P}$ reaction, G. van Middelkoop, Nucl. Phys. A97 (1967) 209.
- 5) Thermal-neutron capture gamma rays from natural magnesium and enriched ^{25}Mg , P. Spilling, H. Gruppelaar and A.M.F. Op den Kamp, Nucl. Phys. A102 (1967) 209.
- 6) Thermal-neutron capture gamma rays from natural calcium, H. Gruppelaar and P. Spilling, Nucl. Phys. A102 (1967) 226.
- 7) The reactions $^{12}\text{C}(\text{n},\gamma)^{13}\text{C}$ and $^{19}\text{F}(\text{n},\gamma)^{20}\text{F}$, P. Spilling, H. Gruppelaar, H.F. de Vries and A.M.J. Spits, Nucl. Phys. A113 (1968) 395.
- 8) Investigation of the $^{44}\text{Ca}(\text{n},\gamma)^{45}\text{Ca}$ reaction, H. Gruppelaar, P. Spilling and A.M.J. Spits, Nucl. Phys. A114 (1968) 463.
- 9) Investigation of the $^{42}\text{Ca}(\text{n},\gamma)^{43}\text{Ca}$ reaction, H. Gruppelaar, A.M.F. Op den Kamp and A.M.J. Spits, to be published in Nucl. Phys.
- 10) A 16-window digital discriminator for the Laben 4096-channel analyser, P. Spilling, H. Gruppelaar and P.C. van den Berg, Contr. to the Symposium on Nuclear Electronics, Versailles, Sept. 10-13, (1968).

2.2. Nuclear orientation experiments with neutrons (H.Postma, E.R. Reddingius, J.Mellema and R.Kuiken)

Measurements concerning angular distributions of gamma rays emitted from aligned ^{59}Co and ^{149}Sm nuclei after capture of neutrons of 0.047 eV were continued. A single crystal of copper was used to deflect a useful beam by Bragg reflection at (111) planes from a primary beam of the Dutch high flux reactor.

With the usual power of 30 MW a flux of $2 \times 10^6 \text{ n/cm}^2 \text{ s.}$ was obtained. The above-mentioned nuclei were aligned in single crystals of $\text{Ce}_2(87\% \text{ Zn}, 13\% \text{ Co})_3(\text{NO}_3)_2 \cdot 24 \text{ D}_2\text{O}$ and $(96\% \text{ Ce}, 4\% \text{ Sm})_2\text{Mg}_3 \cdot 24 \text{ D}_2\text{O}$. These samples could be cooled to temperatures of about 0.01 to 0.03 K with aid of adiabatic demagnetizations starting at initial conditions of 1 K and 14 kOe. A fully automated equipment for doing adiabatic demagnetizations repetitively was used. For ^{149}Sm nearly complete alignment could be obtained. Spin assignments could be made for a rather large number of levels of ^{60}Co and ^{150}Sm .

In cooperation with the UKAERE experiments concerning the angular distribution of fission fragments of ^{235}U aligned in single crystals of rubidium uranyl nitrate cooled to temperatures as low as 60-100 mK with a $^3\text{He}-^4\text{He}$ dilution refrigerator were started. First some preliminary experiments were done at the high flux reactor in Petten. They were later followed by experiments in one of the fast neutron beams of the 45 MeV linear electron accelerator at Harwell. The preliminary conclusion is that for most of the resonances in ^{235}U the value of the K quantum number is small. This is in agreement with a similar experiment done by J.W.T.Dabbs.

Publication

H.Postma, Kernoriëntatie-experimenten met laag-energetische neutronen, Ned.T.Natuurk. 43 (1968) 264.

1. REACTOR.
2. INPILE COLLIMATOR.
3. MIRROR SYSTEM.
4. GUIDE FIELD.
5. FIELD FLIPPER.
6. PERMANENT GUIDE FIELD.
7. TARGET.
8. ANALYSING MAGNET.
9. Ge(Li) DETECTOR.
10. BEAM CATCHER
11. BEAM SHUTTER.

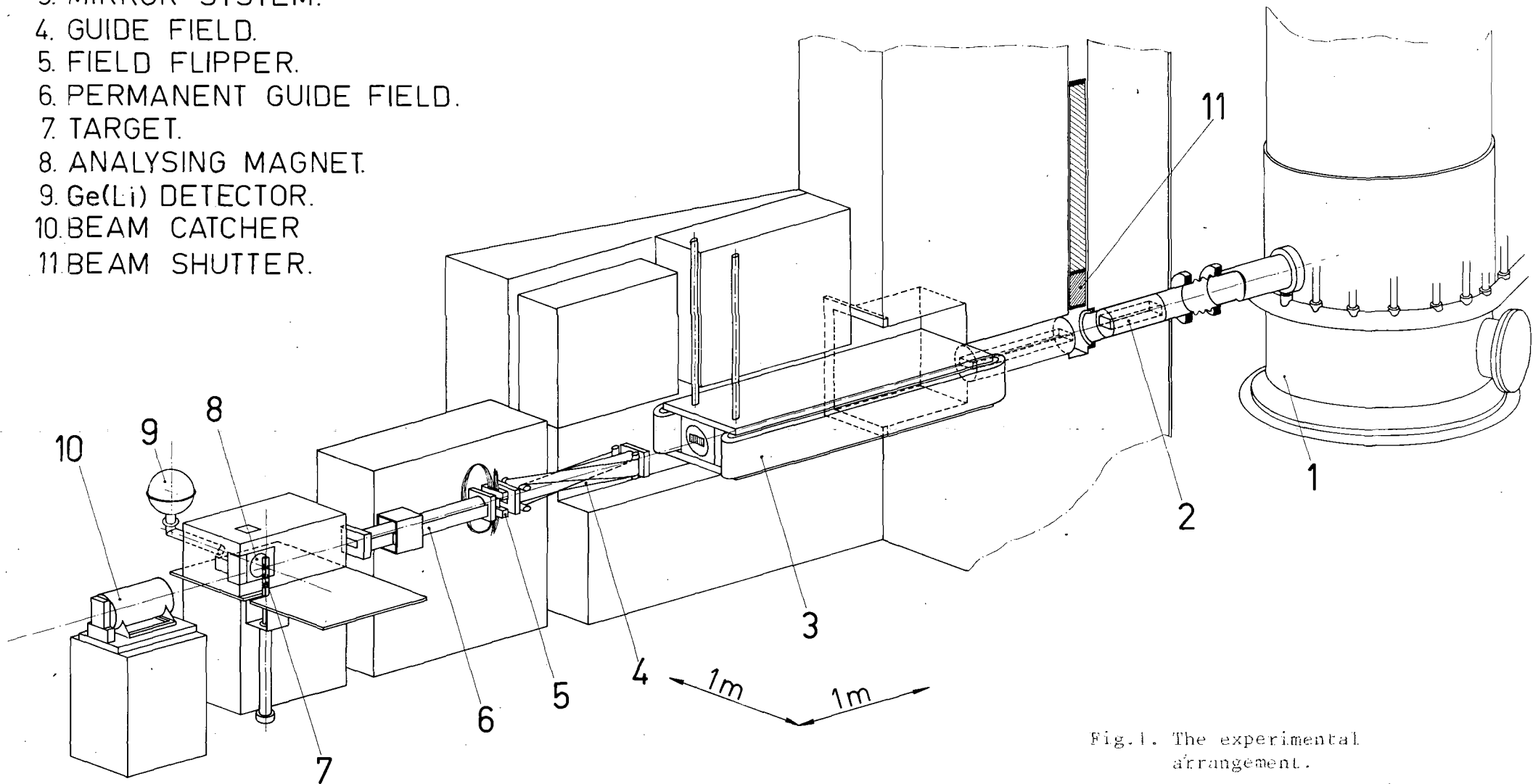
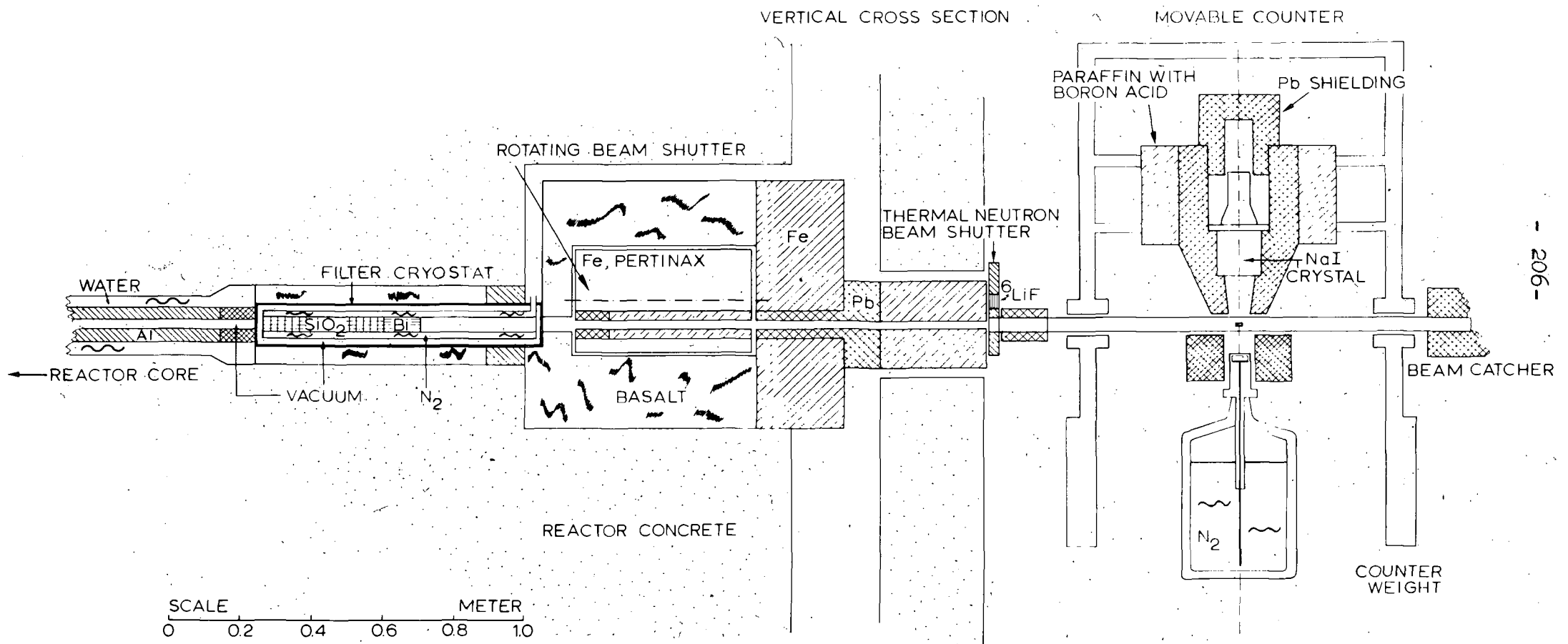


Fig. 1. The experimental arrangement.
(See fig. 1 of ref. 3).



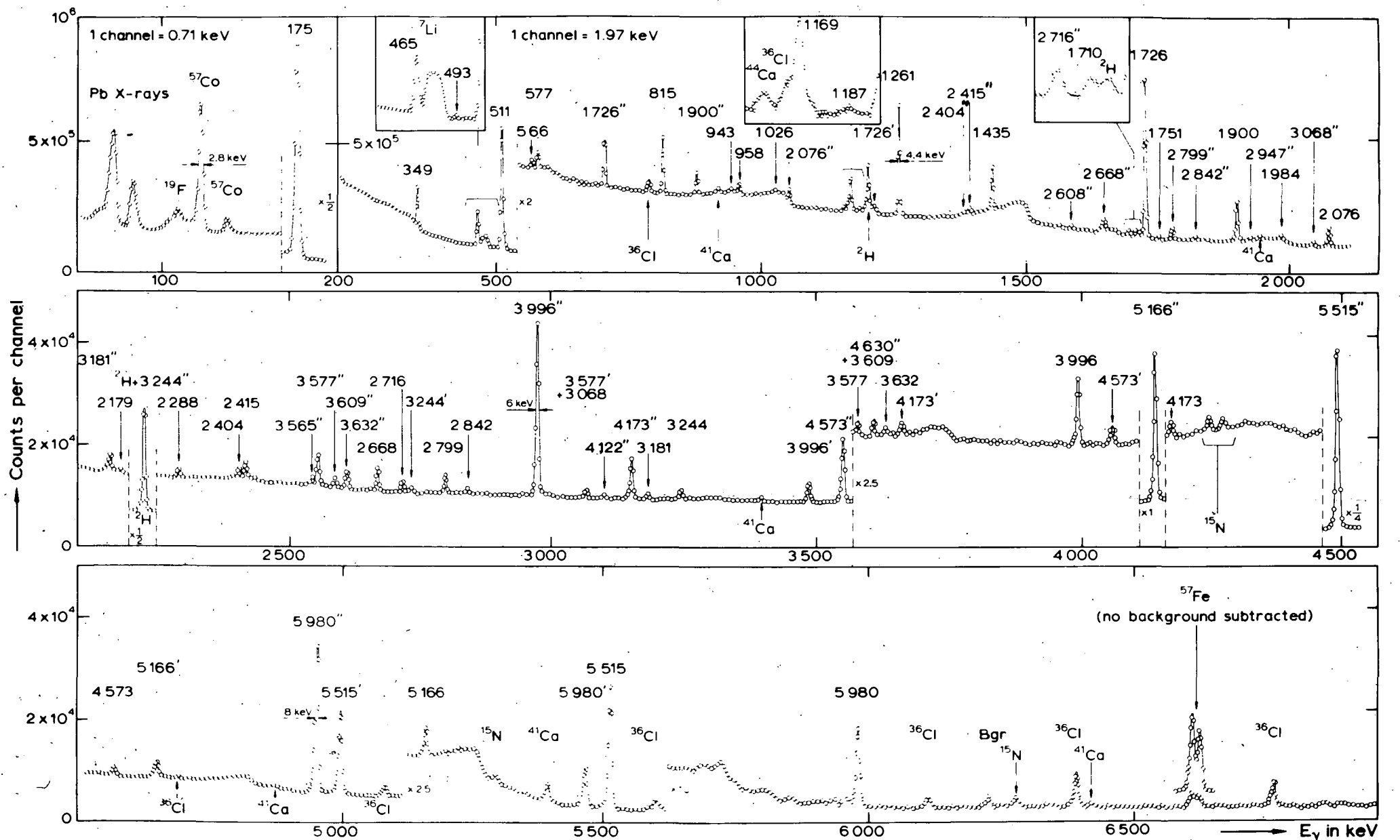


Fig.3

XXVII. CENTRAL BUREAU FOR NUCLEAR MEASUREMENTS
EURATOM, Geel, Belgium

1. Measurements at the Linear Accelerator

1.1. Total Cross Sections

1.1.1. Total Cross Section of ^{240}Pu

K.H. Böckhoff, W. Kolar

The results have been published (1) and an extract including supplementary theoretical interpretations has appeared in the proceedings of the 1968 Washington "Conference on Neutron Cross Sections and Technology" (1a).

1.1.2. Total Cross Section of ^{233}U

K.H. Böckhoff, G. Carraro, W. Kolar

This cross section has been measured from 0.7 eV up to 800 eV. In the energy range from 0.7 eV - 150 eV a 1 cm ^{10}B -loaded liquid scintillator (with pulse shape discrimination) has been employed, while in the energy range from 65 eV - 800 eV a $\frac{1}{2}$ inch thick Li 6 glass detector has been used. These two detectors have at low energies a higher efficiency than the $^{10}\text{B-NaI(Tl)}$ detector. For neutron energies below 10 eV, where resolution effects are negligible our results and those of Pattenden and Harvey (ORNL-TM-556) agree within the error limits, except for the peak value of the resonances at 1.55 eV and 1.78 eV. In this case samples were too thick, to give meaningful results. In the higher energy range good resolution enabled the resolving of many resonances. As an example fig. 1 shows the measured total cross section between 44 and 96 eV. The evaluation of the resonance parameters using the multilevel shape fit program of Adler and Adler is in progress.

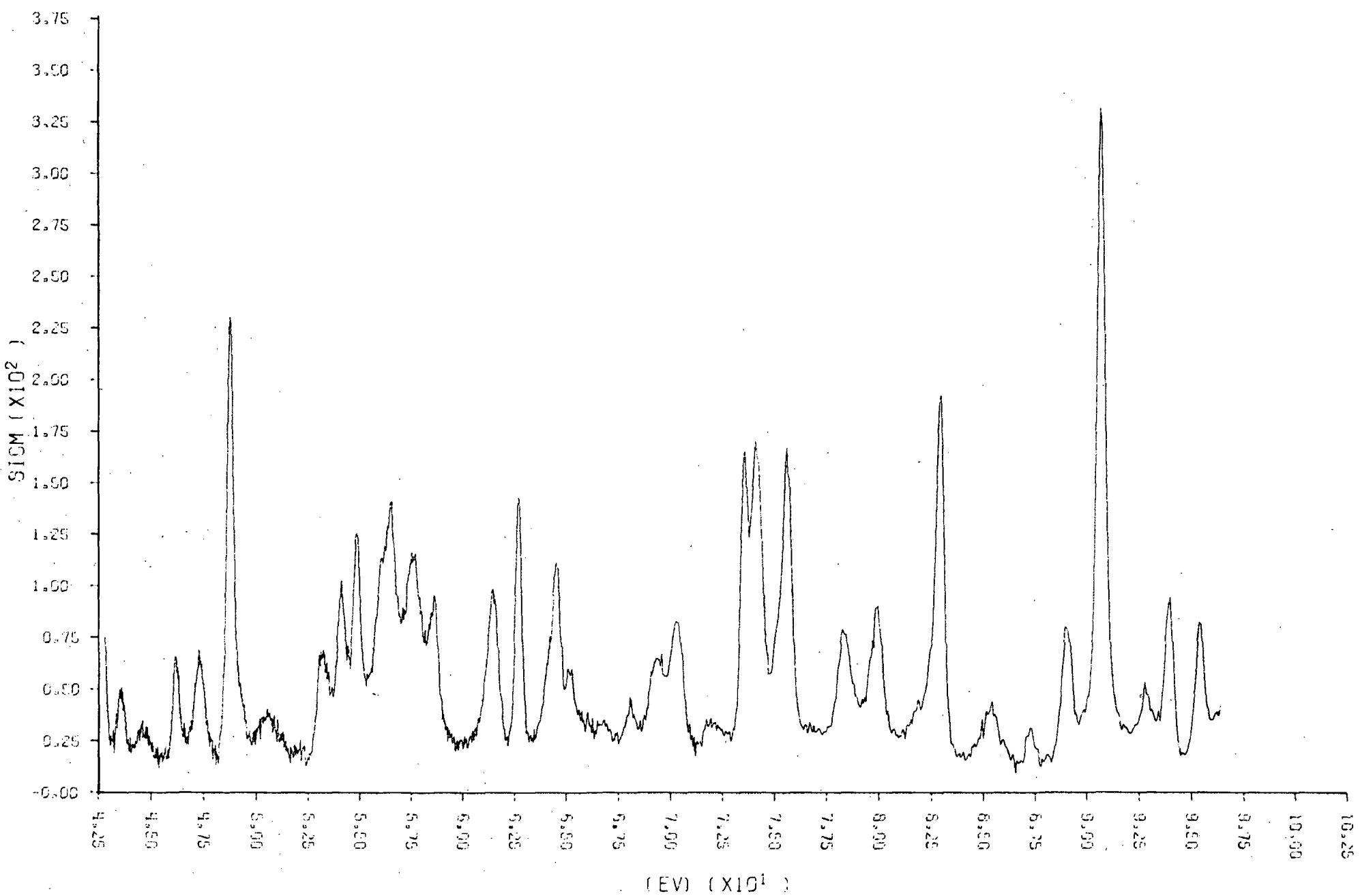


Fig.1: Total cross section of ^{233}U between 43 and 96 eV

1.1.3. Total Cross Section of ^{238}U

G. Carraro, W. Kolar

The total cross section has been measured between 65 eV and 800 eV. The sample thickness was 4.36 g/cm^2 , which should make it possible to determine also the resonance parameters of the small resonances with a better accuracy. (Discrepancies in the BNL values up to 100 %). Data reduction and analysis using the area program of Atta and Harvey are in progress. It is planned to extend the measurements and the analysis up to about 10 keV neutron energy.

1.1.4. Resonance Parameters of the 132 eV resonance of Co

G. Carraro, W. Kolar

The Atta-Harvey program could not be employed successfully up to now for the analysis of this resonance. A too high number of input data caused convergence difficulties.

1.2. Fission Data

E. Migneco, J. Theobald

1.2.1. Subthreshold Fission Cross Sections

The experiment on ^{240}Pu , which has lead to the discovery of intermediate states in the exit channels of the fission process has been published (3). A measurement on ^{241}Am is prepared.

1.2.2. Fission Cross Section of ^{235}U

A correlation analysis* was applied to CBNM cross section data of ^{235}U . It yielded a quasi periodical autocorrelation effect, which has been interpreted on the base of the existence of intermediate states in the $(\text{InK}) \rightarrow (4^- 1)$ channel (5).

* P.A. Egelstaff, J. Nucl. Energy 7 (1958) 35.

1.2.3. Fission Cross Section of ^{233}U

The fission cross section of ^{233}U has been measured with the neutron detector from 0.7 eV to 1.5 keV and with a spark chamber fission fragment detector (5) from subthermal energies up to 50 eV. The neutron detector measurements have a nominal resolution of about 3, 5 and 20 ns/m. The resolution of the spark chamber measurements is about 10 and 200 ns/m. The data have been reduced and are prepared for resonance parameter analysis. For this purpose the multilevel program "Codilli" of Adler has been modified for our IBM 1800 computer.

1.3. Scattering Data

E. Migneco, J. Theobald

1.3.1. Scattering Cross Section of ^{240}Pu

The scattering data of ^{240}Pu have been analysed after performing calculations, which correct for self-screening and multiple scattering. These corrections have been checked at Harwell with a Monte Carlo program. The results of this measurement were presented at the Second Conference on Neutron Cross Sections and Technology in Washington, D.C., March 1968.

1.3.2. Scattering Cross Section of Nd

The scattering cross section of Nd has been measured with the same detector, already used for the ^{240}Pu measurement. The scattering yield has been normalized with the scattering cross section of lead. A sample changer has been used to minimise the effect of possible threshold drifts of the pulse shape discriminator. The analysis of the results was performed together with the capture data obtained by Weigmann.

Fig. 2 shows a spectrum of the reduced scattering yield.

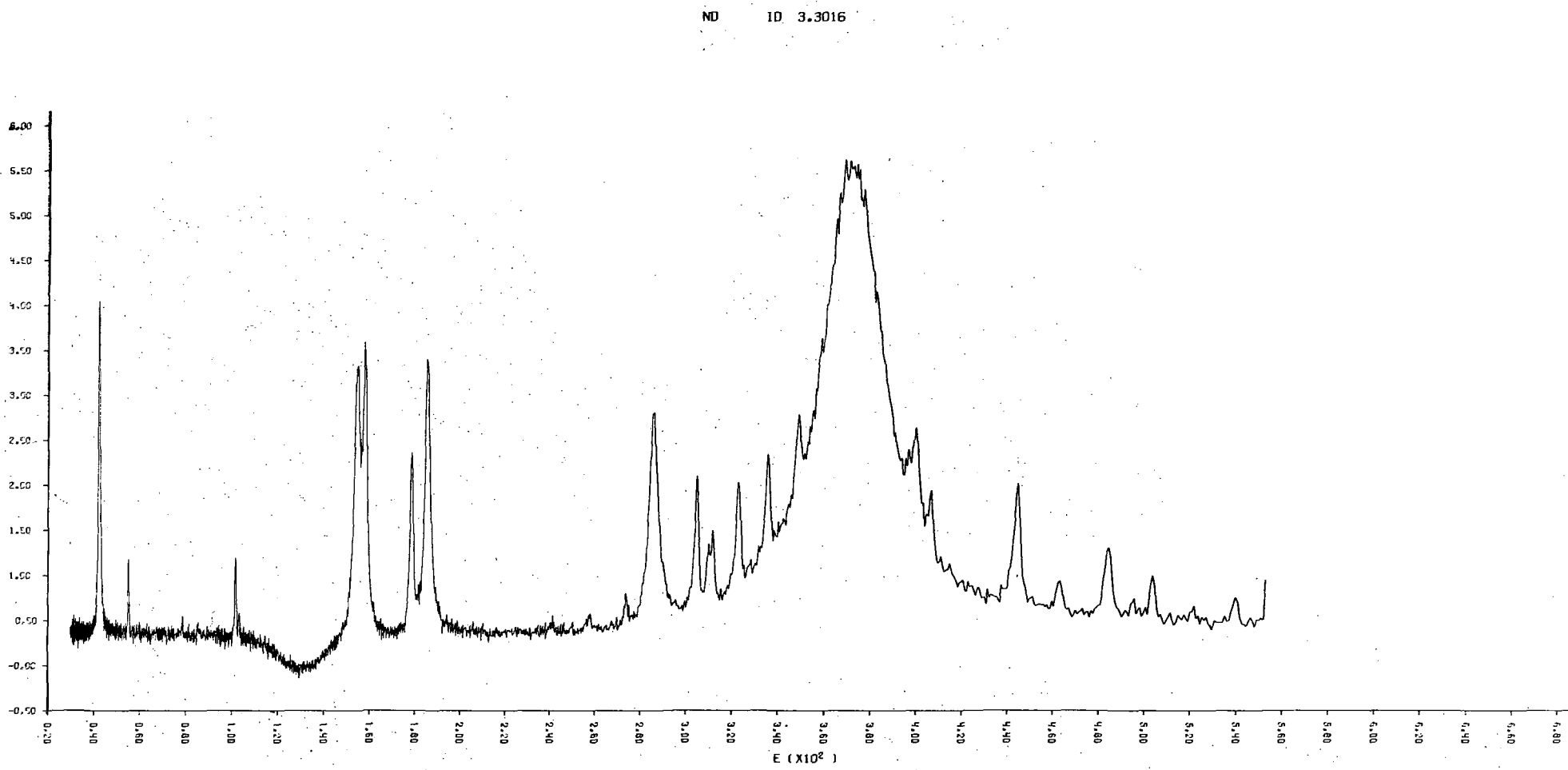


Fig. 2: Reduced scattering yield of Nd between 20 and 550 eV

For measurements on separated isotopes the shielding of the detector and sample changer system is going to be improved.

3.3. Scattering Cross Section of Fissile Isotopes

F. Poortmans,⁺ H. Ceulemans⁺, J. Theobald, E. Migneco

For scattering measurements on fissile isotopes a ^{10}B loaded liquid scintillator detector has been surrounded by a large scintillator tank which acts as an anti-fission detector. Final tests of the detector system are under way.

Furthermore a detector system intended for scattering measurements below 100 eV on fissile isotopes, especially on ^{235}U was tested, in the framework of a CEN-CBNM association contract.

The detector system consists of nine ^3He proportional counters (10 atmospheres pressure, 2.5 cm diameter and 15 cm active length) and is mounted inside a 30 meter flight path station. Special care has been taken to reduce the background level, in order to make it possible to do scattering experiments on resonances for which Γ_n/Γ is of the order of a few percent. The detector system has the following characteristics:

1. time of flight resolution: below 50 eV, the resolution $\Delta E/E$ is of the order of 0.8 %. The detectors have a relatively small jitter time ($\pm 0.5 \mu\text{sec}$), so below 50 eV the resolution broadening is mostly due to the uncertainty in the flight path ($\pm 10 \text{ cm}$)
2. overall efficiency: approximately $18 \cdot 10^{-2} \cdot E^{-1/2}$ (E in eV)

⁺ SCK-CEN, Mol

3. the detector is not sensitive to gamma rays
4. the relative efficiency for fission neutrons is $2 \cdot 10^{-3} \sqrt{E}$ (E in eV) per fission
5. the overall neutron background is $2 \cdot 10^{-3}$ times the count rate obtained if all the incident neutrons are scattered by the target.

As can be seen from these data, the fission neutron background is still the most important factor. For a resonance at 50 eV for which $\Gamma_f/\Gamma_n = 70$ the fission neutron background is the same as the resonant scattering contribution. However this background can be measured quite accurately, so that it seems possible to start scattering measurements on ^{235}U with this detector system.

A short run on ^{181}Ta has yielded values for the neutron widths which are in very good agreement with published results. Measurements on ^{235}U will be started in the beginning of 1969.

1.4. Neutron Capture Measurements

H. Weigmann, J. Winter

1.4.1. Capture Cross Sections

Measurements of capture cross sections have been continued on samples of natural Cu, natural Nd, and ^{238}U . The results of the measurements on Cu are contained in a paper (7). An area analysis of the data yields information on resonance parameters: For large resonances ($\Gamma_n \gg \Gamma_\gamma$) with known isotopic assignments values of Γ_γ or, if the spin of the resonance is unknown, $2g\Gamma_\gamma$ are obtained. In some cases, it was possible to assign the spin of the resonance from the measured $2g\Gamma_\gamma$ assuming a fairly constant radiation width. For a number of small resonances ($\Gamma_n \ll \Gamma_\gamma$) with unknown isotopic assignment, values of $4ag\Gamma_n$ (a =isotopic

abundance) have been determined. The distribution of these values, including those of the stronger resonances known from literature, shows an excess of small widths which is attributed to p-wave levels. From this, the p-wave neutron strength function for natural Cu is estimated to be

$$S_1 = (0.30 - 0.14) 10^{-4}$$
$$+ 0.18$$

Two runs on a natural Nd sample have been made with nominal resolution varying from 1.8 nsec/m to 22 nsec/m. An example of a time-of-flight spectrum is shown in fig. 3. The shape of the neutron spectrum has been measured with both, BF_3 -counters and a ^{10}B -slab viewed by a NaI-crystal. Absolute normalization has been done by the "black resonance" method, using the resonances in Ag at 5.2, 16.3 and 51.4 eV. Resonance analysis has been performed together with an analysis of the scattering data on Nd obtained by Migneco and Theobald. The results are discussed below.

Measurements on ^{238}U have been performed in the energy range from 5 eV to 30 keV with samples of thickness $1.02 \cdot 10^{-3}$, $3.06 \cdot 10^{-3}$, and $1.01 \cdot 10^{-2}$ atoms/barn.

Nominal resolutions were the same as in the case of Nd. Again, the neutron spectrum was measured with BF_3 -counters and with a ^{10}B -slab viewed by a NaI-crystal. For normalization with the "black resonance" method, both, resonances in Ag as well as the resonances at 6.67 eV and at 81.1 eV in ^{238}U are used. Analysis of the data is in progress.

1.4.2. Capture γ -ray Spectra

1.4.2.1. Measuring system

The electronic system is described in a paper presented at the "International Symposium on Nuclear

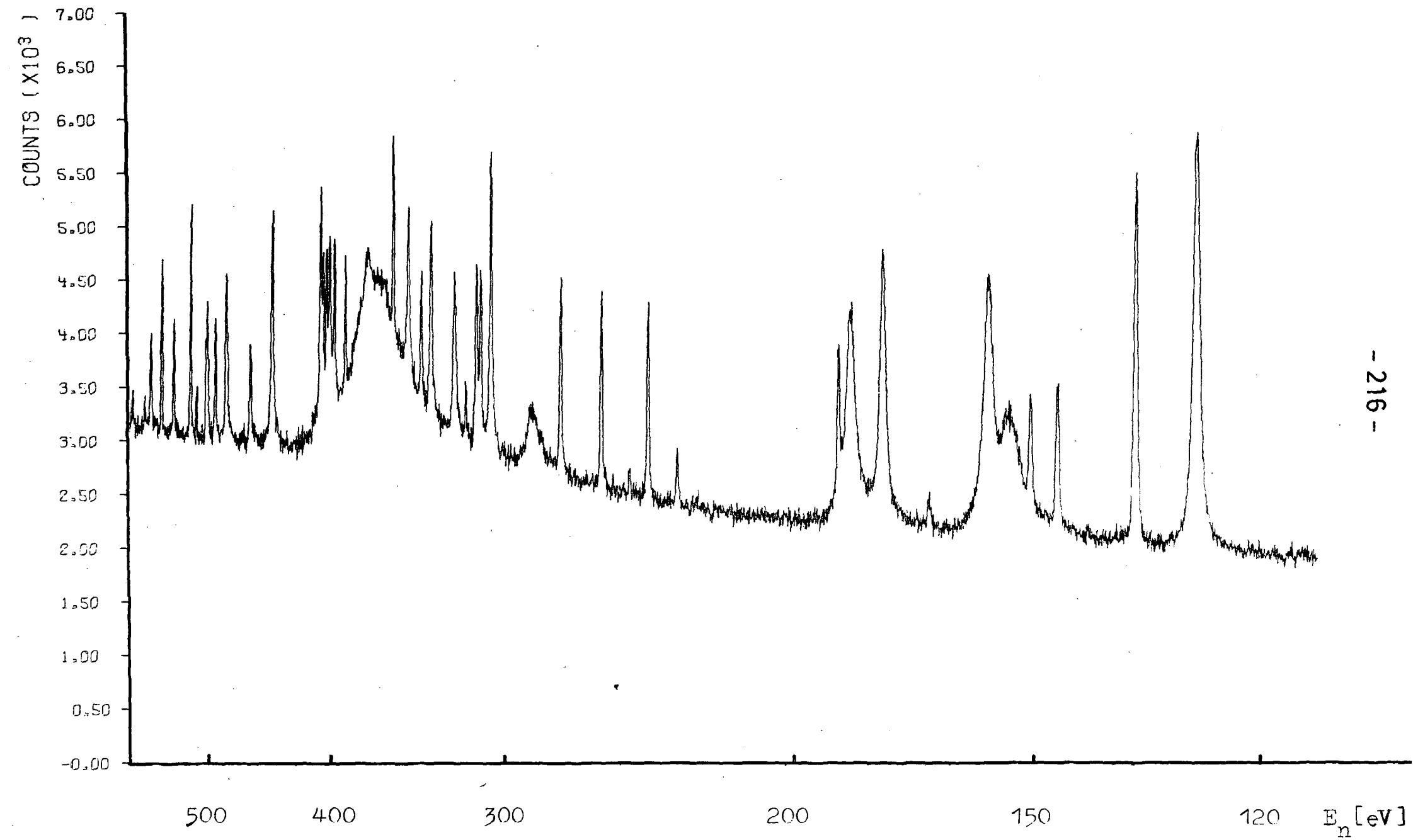


Fig.3: Time-of-flight spectrum from neutron capture in Nd between 120 and 600 eV

"Electronics", Versailles, September 1968 (8) the abstract of which follows:

A two-parameter system used for the measurement of γ -spectra or neutron capture resonances is described. The bursts of neutrons delivered by the CBNM linear accelerator are bombarding a sample and the resulting γ -spectra are measured by means of a Ge(Li)-detector. The signals of the detector are analysed corresponding of their times of occurrence and their amplitudes, thus yielding simultaneous information on neutron energy and γ -spectra. Time analysis is performed by means of a time coder with 256 channels while amplitudes are analysed by an analog-to-digital converter with 4096 channels. Special characteristics of the electronic system are:

- a) rapid recovery after the γ -flash of the linear accelerator. A general solution usable for all electronic overload problems is given. Its theoretical limits and the chosen realisation are discussed.
- b) Simplification of data handling. The usefulness of a digital window comparator is shortly demonstrated.

Finally the results obtained are summarized together with some proposals for further developments.

4.2.2. Measurements on ^{235}U

The knowledge of the spins of resonances of ^{235}U is necessary for a more accurate resonance analysis and for a better understanding of the fission process itself.

Measurements of the capture γ -ray spectra for the neutron energy range from 5eV to 40eV have therefore been performed on a metallic sample of ^{235}U (200 mg/cm^2 ; 93% ^{235}U). With spin and parity being

$7/2^-$ for ^{235}U the capture state must be 3^- or 4^- . For 18 resonances spin assignments have been made (table III) based on the relative intensity of the 642.3 keV γ -ray (transition from the 2^- level at 687.6 keV to the 2^+ level at 45.28 keV in ^{236}U). This transition was chosen because it is one of the strongest lines in the spectrum and a calculation by means of W.P. Pönitz' γ -ray cascade model (W.P. Pönitz, Z. Physik 197 (1966) 262) showed that its intensity should be about 25% higher in resonances with 3^- . (γ -transitions following capture below 250 keV could not be observed due to the natural activity of the sample whereas the intensities of the primary γ -rays in the case of ^{235}U are very weak and additionally subject to fluctuations thus giving only in one case a definite assignment).

The agreement with other measurements, i.e. Asghar et al. (M. Asghar, A. Michaudon and D. Paya, Phys. Lett. 26B (1968) 664), Cowan et al.

(G.A. Cowan, B.P. Bayhurst and R.J. Prestwood, Phys. Rev. 130 (1963) 238) and Mehta (G.K. Mehta, Diss. Columbia University 1963, INDSWG(US)-5) is generally good. A paper is in preparation.

Table III: Spins of ^{235}U Resonances

E_n (eV)	Spin J	E_n (eV)	Spin J
6.39	4	22.94	3
7.08	3	23.42	4
		27.82	4
9.29	3	30.86	3
12.39	4	32.07	4
15.40	3	33.53	4
16.08	3	34.39	(3)
16.69	3	35.20	4
19.31	4	39.41	4
21.08	3		

1.5. Standard Cross Sections

1.5.1. Normalization of relative ^{235}U fission Cross-Section in the resonance region

A.J. Deruytter, C. Wagemans *

Often the cross-section curves are normalized with respect to a resonance integral determined from crystal spectrometer or chopper measurements around a reactor, that are then normalized to a 2200 m/s-value.

In the present experiment measurements were performed with the Geel Linac to energies below thermal energy, enabling a direct normalization of the cross-section curve to the 2200 m/s σ_f -value. With this absolute cross-section-curve an absolute resonance integral can be calculated for further normalizations. As almost all relative σ_f -measurements come down in energy below 8 eV an absolute resonance integral that can be considered as useful for further normalization of ^{235}U fission cross-sections is:

$$\int_{7.8 \text{ eV}}^{11 \text{ eV}} \sigma_f(E) dE$$

because it contains a large resonance (high counting-rate) and a relatively large timing error (± 0.5 eV) does not considerably affect this integral because of the small cross-sections at the limits of the integral.

Preliminary results on these experiments were presented at the "Neutron Cross-Section and Technology Conference" at Washington. These measurements were

* Research fellow, NFWO University of Gent and SCK-CEN, Mol

repeated and considerably improved by using solid state detectors with much less scattering material. Also much better statistical accuracy was reached especially between resonances. These new data are analyzed and an extensive report on the methods used and the obtained results is in preparation.

1.5.2. $^{6}\text{Li}/^{10}\text{B}(\text{n},\alpha)$ -Cross Section Ratio

E. Migneco, J. Theobald, J. Wartena

The four Si surface barrier detectors in the arrangement described in the last annual report have shown serious paralysis effects over the range of interest (1 keV to 100 keV).

A detailed study of the γ -flash effects yielded that there is no hope for a successful application of the detector in this Linac-experiment.

A new approach consists in the use of a grid ionisation chamber, a prototype of which has been constructed.

From this chamber three signals will be extracted

- a timing signal from the collector
- an amplitude signal from the collector
- an amplitude signal from the grid, containing information on the direction of the α -particle tracks.

The last signal will be used for the correction of the timing signal and for the determination of the useful acceptance angle of the detector.

The detector has a poor efficiency for the detection of ^{7}Li particles from the $^{10}\text{B}+\text{n} \rightarrow ^{7}\text{Li}+\alpha$ reaction because of their low energy and is unable to detect the ^{3}H particles from the $^{6}\text{Li}+\text{n} \rightarrow ^{3}\text{H}+\alpha$ reaction because of their low specific ionisation.

Feasibility calculations indicate that such a detector is able to give a time resolution of about 100 nsec, an acceptance angle of 20% and an energy resolution of 75 keV for the α -particles.

The large acceptance angle allows to use a flight-path of 30 m. A similar dummy chamber will make it possible to reduce the γ -flash effects by suitable subtraction of the signals.

A camera obscura for γ -rays was installed in order to check the true position of the γ -flash source. The photographic pictures showed that this γ -source was shifted by 4 cm with respect to the "point 0", the point where the neutron source was assumed. Theoretical calculations indicate that also the neutron source has a shift of not less than 3 cm in the same direction. As a consequence of these investigations an adjustable target is being installed.

1.5.3. Reference Values for Neutron Cross Section Measurements

H. Moret, K. Gubernator

A critical evaluation of existing data of interest for the use of $^{10}\text{B}(n,\alpha)$ and $^{10}\text{B}(n,\alpha\gamma)$ as a standard cross section for neutron measurements was made and published as a EUR-report (isotopic composition, several cross sections and branching ratio (21).

1.6. Miscellaneous

1.6.1. Analysis of Nd-Resonances

E. Migneco, J. Theobald, H. Weigmann

Combined analysis of capture- and scattering data on Nd-resonances has yielded information on resonance parameters which is given in table IV. Multiple scattering and self-screening corrections have been applied for the scattering data. The lead cross-section $\sigma = 10.7$ eV has been used for the normalization; the capture data have been analysed with the GACA program (F.H. Fröhner and E. Haddad, Nucl. Phys. 71 (1965) 129). For the isotopic assignment of the

Table IV: Nd resonances

E_{res} (eV)	Isotope	$\frac{2g\Gamma_n\Gamma_\lambda}{\Gamma}$ (meV)	$2g\Gamma_n$ (meV)	Γ_γ (meV)	Type of data	Remarks
4.33			0.99 ± 0.08		c	
42.28			270 ± 15	67 ± 6*	c,s	
54.99	143	$\frac{\Gamma_n \Gamma_\lambda}{\Gamma} = 14.4 \pm 1.2$	42 ± 2.5	72 ± 10	c,s	
78.33	150		$\Gamma_n = 18 \pm 2.5$		c	for Γ_n used $\Gamma_\gamma = 70 \pm 20$
85.10	145	11.8 ± 1.0	14.5 ± 1.5		c	for Γ_n used $\Gamma_\gamma = 70 \pm 20$
95.54	145		5.2 ± 0.6		c	
101.34	145		90 ± 7	69 ± 10*	c,s	
102.86	145	23 ± 2		70 ± 10	c	for Γ_γ used $2g\Gamma_n = 38 \pm 6$ of ref.1)
126.5	143	67 ± 5		83 ± 7*	c	for Γ_γ used $2g\Gamma_n = 350 \pm 35$ "
134.6	143	29 ± 2			c	"
146.2	145	15.6 ± 1.4	20 ± 3		c	for Γ_n used $\Gamma_\gamma = 70 \pm 20$
150.5	145	12.4 ± 1.3	15 ± 2		c	for Γ_n used $\Gamma_\gamma = 70 \pm 20$
154.4	148			70 ± 8	c	with $\Gamma_n \approx 2.10^3$
157.9	143			68 ± 8*	c	with $2g\Gamma_n \approx 800$
178.4	143		438 ± 30	72 ± 7*	c,s	
185.4	143		1130 ± 70	82 ± 8*	c,s	
240.8	145	34 ± 3			c	
257.4	145	37 ± 3			c	
273.3	145		150 ± 12	61 ± 8*	c,s	
284.9	148		$\Gamma_n = 1980 \pm 100$	58 ± 6	c,s	
304.5	143/145					unresolved doublet
322.6	143		88 ± 9	87 ± 19	c,s	
443.5	143/145	44 ± 4				unresolved doublet

¹⁾ G. Bianchi, H. Colmin, C. Corge, V.D. Huynh, J. Julien, J. Morgenstern, F. Netter, M. Vastel, J. de Physique 24, 997 and 999 (1963)

Table IV: Nd resonances (contd.)

E_{res} (eV)	Isotope	$\frac{2g\Gamma_n T_\lambda}{\Gamma}$ (meV)	$2g\Gamma_n$ (meV)	Γ_γ (meV)	type of data	Remarks
462.1	145		410 \pm 40	58 \pm 6*	c,s	
484.3	145/150					unresolved doublet
494.7	145	51 \pm 6	225 \pm 50	66 \pm 15	c,s	
503.2	143/145					unresolved doublet
520.5	143	59 \pm 6	205 \pm 40	82 \pm 18	c,s	
538.8	145	52 \pm 6	460 \pm 100	62 \pm 10	c,s	
552.3	143	42 \pm 4			c	
565.7	145	54 \pm 6			c	

resonances the results have been used of E.N. Karzhavina et al. (Yaderna-ya Fizika 8 (1968) 639).

For all resonances of the odd isotopes $g = \frac{1}{2}$ has been applied. The error due to this assumption is not included in the errors listed. It is most important for the Γ_γ values marked by an asterix. In these cases the figures in the table approximately represent $2g\Gamma_\gamma$. The Γ_γ values obtained are in general at the lower limit of the errors of Γ_γ values quoted in BNL 325 II B and in agreement with the data of Karzhavina.

The following mean values are obtained:

Isotope	$\langle \Gamma_\gamma \rangle$ meV	number of resonances
143	76 \pm 7	7
145	63 \pm 6	7
148	62 \pm 6	2

The Γ_n values also agree with the results of Karzhavina except in some cases around the big resonance at 374 eV of Nd-144, where our values are probably too small. This concerns the resonances at 284.9, 322.6 and 462.1 eV.

Measurements on separated isotopes are planned.

1.6.2. Interpretation of Subthreshold Fission Cross Sections

H. Weigmann

A paper has been submitted to "Zeitschrift für Physik" (9), the abstract of which is as follows: The structure recently observed (3) in the subthreshold fission cross section of ^{240}Pu is interpreted as being due to intermediate states of the fissioning nucleus associated with the second minimum of the potential energy as a function of deformation postulated by Strutinsky.

(V.M. Strutinsky, Nucl. Phys. 195, 420 (1967)).

This subject was also discussed in an invited contribution to the 1968 Gordon Research Conference on Nuclear Chemistry, New London, N.H., U.S.A. (10).

1.6.3. Ratios of the binary-to-ternary fission Cross-Sections of ^{235}U in the Resonance Region ($E < 21$ eV)

A. Deruytter, C. Wagemans**

Two new series of measurements of the ratio of binary-to-ternary fission for ^{235}U were made in this energy range. In the preliminary analysis of the results we make the ratio of the surface of the resonances in the fission run and in the ternary α -run. These results show fluctuations from resonance to resonance outside the statistical error. However, definite conclusions with respect to a spin-dependence cannot be made due to the limited statistical accuracy. These measurements will now be repeated with the new "high power"-Linac target, and with an increased detector geometry factor.

1.6.4. Spin Assignment of Neutron Resonances of Stable Nuclides

C. Coceva***, F. Corbi***, P. Giacobbe***,
M. Stefanon,*** G. Carraro

The application of the spin assignment method, based on the multiplicity of the capture gamma rays, to odd-proton nuclei has given positive results in the case of ^{165}Ho . A total of 63 resonances of ^{165}Ho , from 150 eV to 540 eV, have been analysed. A spin-effect index of 0.14 was obtained. In most cases the spin could be assigned unambiguously. Experimental data were taken also from 3 eV to 150 eV, and in this energy range 27 reso-

** Research fellow, University of Gent

*** CNEN, Italy

nances are under analysis. The analysis of the experimental data of ^{115}In showed that our method of spin assignment cannot be applied because the statistical assumption on which the method is based is not valid for this isotope. Further work on this point is under way.

1.6.5. Resonance neutrons capture γ -rays spectra

C. Coceva⁺, F. Corvi⁺, P. Giacobbe⁺, M. Stefanon⁺, and G. Carraro⁺⁺.

To increase the storage capacity of the 4096-channel Laben analyser a modification was performed which allows the use of 8192 channels having 999 maximum capacity. The memory can be divided in 8 groups of 1024 channels or 16 groups of 512 channels. By the use of a special time programmer each group collects the γ -ray spectrum corresponding to a given time-of-flight interval (and hence to a given neutron resonance) whose width and position can be chosen as desired.

Measurements of the high energy capture spectra in ^{105}Pd resonances are continuing. The main difficulty is the extremely low peak counting rate, due to the low values of the partial radiation widths involved.

Spectra belonging to 11 different resonances were collected:

fifteen γ -ray transitions going to low-lying states with excitation energy less than 3 MeV were detected. At least six of them have certainly $M1$ character. The energy values are in agreement with the thermal neutron data of Groshev.

⁺ CNEN, Italy

⁺⁺ CBNM, Euratom

2. Van de Graaff Accelerator

2.1. Cross-Sections for Neutron Induced Threshold Reactions

H. Liskien, A. Paulsen

Measurement and data evaluation for the excitation function of the reaction $^{93}\text{Nb}(n, 2n)^{92}\text{Nb}$ between threshold and 20 MeV have been finished. Neutrons from the reactions $^{14}\text{C}(\text{d}, \text{n})$, $^{15}\text{N}(\text{d}, \text{n})$ and $\text{T}(\text{d}, \text{n})$ were used for this activation measurement. Corresponding measurements on ^{103}Rh had to be stopped due to the presence of ^{102}Rh ($T_{1/2} = 210$ d) in the rhodium samples.

The 1967 supplement sheets for the compilation EUR 119.e Vol. 2 were printed and distributed. The 1968 supplement sheets Vol. 1 were prepared for printing.

2.2. Precise Determination of Neutron Fluxes

H. Liskien, A. Paulsen

1 MeV neutron fluxes were produced via the $\text{T}(\text{p}, \text{n})^3\text{He}$ reaction and determined by counting the associated ^3He -particles under 30° with respect to the proton bombardment direction. Targets of 0.2 mg/cm^2 T-Ti on 1.1 mg/cm^2 Al foils were used. An electro-static field was applied to reduce the background produced by the Coulomb-scattered protons and other charged particles. The result of this method was compared with those from a recoil proton telescope and from a methane-filled proportional counter. Agreement within 2% was found for all three methods (11).

Corresponding measurements for 0.5 MeV neutron energy are in preparation. The ^3He particles will be detected under 20° and the targets will have only 0.3 mg/cm^2 Al backings. The telescope counter will be replaced by a recoil proton counter with collimator (modified Perlow counter). Extensive and accurate efficiency calculations for this counter using the computer program CALCOLEFF were performed (12).

Associated particle counting for 2 MeV neutrons from the D(d,n)³He reaction was successful. However, due to the strongly forward-peaked angular distribution of this reaction a cross-check with other methods was up to now impossible. But the D(d,n)³He reaction could be used for comparisons between the telescope and the proportional counter at 2.5 MeV neutron energy. All results agreed within \pm 2%.

2.3. Scattering Measurements

M. Coppola, H.H. Knitter

2.3.1. ⁷Li

Differential elastic and inelastic neutron scattering cross-sections of ⁷Li in the energy range between 1.0 and 2.3 MeV were reported at the 1968 Washington Conference (13), and then issued as EUR. Report (14).

2.3.2. ²³⁹Pu (energy range 190 to 380 keV)

The "low threshold" neutron detector was used in conjunction with the time-of-flight spectrometer for the measurements of neutron differential elastic scattering cross-sections of ²³⁹Pu in the energy region between 190 and 380 keV. Calculations of neutron flux attenuations and multiple scattering in the employed samples have been performed. Fully corrected differential cross-section values are now available. A comparison of the experimental results with those of optical model calculations is in progress.

2.3.3. ²³⁹Pu (energy range 1.5 to 5.5 MeV)

Neutron scattering measurement on ²³⁹Pu were extended to this energy interval, using the multicontroller system already described. Neutron scattering angular distributions have been measured at 1.5, 1.9, 2.3, 4.0,

4.5, 5.0 and 5.5 MeV. Neutrons up to 2.3 MeV were produced through the $T(p,n)^3He$ -reaction, using a solid Ti-T target. From 4.0 to 5.5 MeV the neutrons yielded from the $D(d,n)^3He$ -reaction were used and a deuterium gas target was employed in order to increase the primary neutron flux. Corrections to be applied to the experimental results are in progress. So far, neutron flux attenuation calculations have been completed for all energies, and multiple scattering corrections only for the 1.5 and 1.9 MeV angular distributions. Final results should soon be available.

2.3.4. Carbon

Since the total cross section of carbon is a smooth monotonic function of neutron energy below 2.0, and since neutrons are only elastically scattered from carbon in the same energy range, the differential neutron scattering cross-section of carbon is very well suited as standard cross-section in this region. For this reason an accurate determination of the differential elastic scattering cross-sections of carbon from a few hundreds keV up to 2 MeV was desired. Measurements were started during the year 1968, and so far neutron angular distributions have been measured, in steps of 50 keV, in the energy interval from 0.8 to 2.0 MeV. It is planned to extend these measurements down to about 0.5 MeV. At each energy data were collected in the angle interval between 20° and 150° , in steps of 10° . So far only uncorrected differential cross sections have been derived from the available experimental results, but correction calculations have been started.

2.3.5. Theoretical Calculations on Si

A paper on the theoretical interpretation of neutron

scattering measurement results on silicon has been published (15).

2.3.6. Computer Evaluation of Differential Cross-sections

A program for the calculation of differential cross-sections starting directly from experimental data recorded on magnetic tape has been written for the IBM 1800 computer of CBNM. This program also includes the possibility of performing least squares fit of the evaluated experimental results with a Legendre polynomial expansion, and to plot the experimental results together with the curve resulting from the fit.

2.3.7. Three-dimensional plot

A program making a three-dimensional plot of differential cross-section curves has been written in order to allow a very compact display of many results at once.

2.3.8. Theoretical Calculations of Neutron Cross-sections Using an Optical Model

The program ELIESE I was brought into operation in connection with the IBM 7090 computer at CETIS-Ispra, to calculate elastic and inelastic neutron scattering cross-sections of the nuclides now under experimental study. In a second step the same program was combined with a general least squares fit program in order to perform the routine search of optical model parameters providing the best fit with the experimental results.

3. Data Handling

3.1. Data Handling Equipment

A. De Keyser, H. Horstman

3.1.1. Computer Operation

The provisionally installed IBM 1401 computer has been replaced by the IBM 1800 data acquisition and control system in April, 1968. During a standard test time of six weeks the IBM 1800 software and hardware had turned out to be very reliable.

In August the IBM 1800 computer has been connected on-line to the data acquisition station with the highest data rate at the linear accelerator. The data acquisition and the transfer to the computer are completely controlled by the computer via an interface unit. Data reduction is performed on-line (16).

Programs for the analysis of neutron cross section data for interesting physical parameters have been executed off-line on the IBM 1800 computer as time-sharing work or via the tele-processing system IBM 7702 on the IBM 7090 and the IBM 360/65 computer of CETIS.

3.1.2. Analyser Computer Interface

A prototype of an analyser computer interface unit (17) has been constructed and thoroughly tested by means of special computer test programs. The interface unit supervises the data accumulation in a multi-channel analyser and directs the data transfer to the computer and vice versa under control of the computer. Computer control is initiated by interrupt signals from the interface unit. All data transports are made in 16 bit words at a rate of 20 Kc in data channel

operation with external synchronisation. The interface prototype has been put into operation (cf. 3.1.1.) in August. Six more interface units are being constructed.

3.1.3. Data Acquisition Station for Multi-Parameter Analysis

The use of a small data processor and controller online with the IBM 1800 for the acquisition and reduction of nuclear data from multi-parameter experiments has been studied in detail.

3.2. Data Analysis and Programming

3.2.1. Reduction and Analysis of Neutron Cross Section Data

M.G. Cao

The programs for the reduction of fission and scattering cross section data have been rewritten for the IBM 1800 computer. ^{233}U (0.018 eV - 2 keV) and ^{235}U (0.01 eV - 24 eV) fission data and Nd (100 eV - 600 eV) scattering data have been processed.

The programs of Adler and Adler (University of Illinois) for the multilevel analysis of fission and total cross section data have been rewritten in FORTRAN IV for the IBM 1800 and the IBM 7090. Several program modifications have been made and a convergence criterion for non-linear cases has been introduced.

A set of IBM 1800 FORTRAN IV programs has been written, which calculate and plot correlograms on the basis of the theory of Egelstaff, starting from the experimental cross section or from a cross section calculated as superposition of a constant mean value and a periodic or quasi-periodic fluctuation composed of several Gaussians.

Several modifications to program ELIESE-1 (JAERI-1096) have been made in order to be used for least

squares fits of differential elastic neutron scattering cross sections by means of optical model and Hauser-Feshbach calculations.

3.2.2. Monte Carlo Calculations of Neutron Capture and Neutron Moderation Times

M.G. Cao, C. Cervini

An IBM 1800 Monte Carlo program has been written which performs the calculations of a) energy, time and space dependence of neutron capture, and b) of the neutron moderation time. The program can be used for homogeneous and heterogeneous slabs and cylinders. The effect of impurities is considered. This program is an extended version of an earlier IBM 7090 program.

3.2.3. Multiple Scattering Corrections for Elastic and Inelastic Neutron Scattering Cross Section Data

H. Horstmann, H. Schmid

A report about the tests of program MAGGIE (AWRE Aldermaston) has been completed (18). Formal modifications, corrections concerning the score calculations, and additional calculations for a) the corrections of the measured inelastic neutron peaks for contamination by multiple elastic scatter and b) the shape correction of inelastic angular distributions are described. In addition to this the report contains descriptions and listings of all MAGGIE routines and several flow diagrams.

3.2.4. Calculation of Differential Neutron Scattering Cross Sections

M. Mancino, C. Cervini

An IBM 1800 FORTRAN IV program has been written which calculates the differential cross sections

from the experimental angular distributions, performs a least square fit of the cross section with Legendre polynomials, and provides for plotting of the results on the Calcomp plotter.

3.2.5. Efficiency Calculations for Proton Recoil Counters

G. Nastri

An IBM 7090 FORTRAN program for efficiency calculations of a proton recoil counter with a perforated filter as collimator has been written (12). Complicated integrations have been performed in order to calculate the efficiency for a homogeneous neutron beam and an isotropic neutron point source. A first double integration gives the open solid angles, and a second integration over the reaction volume results in the efficiencies.

3.2.6. Reduction of Total Cross Section Data

G. Nastri

An earlier set of IBM 7090 programs for reduction of total cross section data has been rewritten in a modified version for the IBM 1800. The programs calculate dead-time corrections of data collected with the accordion system, least squares fits of sample-out runs, background corrections, transmission and cross section values with the corresponding errors. The reduced data can be used by the programs for resonance parameter analysis.

3.2.7. Miscellaneous Data Analysis Programs

M.G. Cao, C. Cervini, M. Mancino, G. Nastri, and H. Schmid

Several programs for miscellaneous data analysis problems have been written: Error propagation calculations, detector response fluctuations, convolution problems, calculation of fission widths,

partial integration of spectra, transformations of angular distributions, various plots of experimental data, isotopic analysis, various least squares fits of cross section and other data, normalization of experimental data, etc.

3.3. System Analysis and Programming

H. Horstmann, H. Schmid

3.3.1. IBM 1800 Programs for On-Line Data Acquisition and Reduction

H. Horstmann

Interrupt programs for the control of the data transfer between a multi-channel analyser and the computer and vice versa have been written in ASSEMBLER language. These routines perform a detailed check of the incoming analyser data on a retry basis. In case of errors the analyser operator is informed by typewriter messages while the computer program automatically decides about the continuation or termination of the data collection. Correct data are stored on disk to be used later on for analysis. Total cross section data are reduced on-line by a special interrupt routine.

3.3.2. An IBM 1800 Program Package for On-Line and Off-Line Operation of a Calcomp Plotter

H. Schmid

A set of plotter routines has been written in ASSEMBLER language. Data stored as arrays or calculated by a user-written subroutine can be plotted with linear and/or logarithmic scales. The plotter can be operated off-line by the Calcomp 570 magnetic tape unit, on-line by the IBM 1800 computer like a slow input/output device or on-line by the IBM 1800 in time-sharing according to the principles of multiprogramming (20).

PUBLICATIONS ON NEUTRON DATA (Chapters 1, 2, 3)

- (1) KOLAR, W., BÖCKHOFF, K.H.: Resonance parameters of Pu-240. Part I: Neutron widths, J. Nucl. Energy 22, 299 (1968)
- (1a) KOLAR, W., BÖCKHOFF, K.H.: Final results on the neutron total cross section of Pu-240. Conf. on Neutron Cross Sections and Technology, Washington, March 1968
- (2) WEIGMANN, H., SCHMID, H.: Resonance parameters of Pu-240. Part II: Radiative widths, J. Nucl. Energy 22, 317 (1968)
- (3) MIGNECO, E., THEOBALD, J.: Resonance grouping structure in neutron induced subthreshold fission of Pu-240, Nucl. Phys. A 112, 603 (1968)
- (4) CAO, M.G., MIGNECO, E., THEOBALD, J., WARTENA, J., WINTER, J., Fission cross section measurements on U-235, J. Nucl. Energy 22, 211 (1968)
- (5) CAO, M.G., MIGNECO, E., THEOBALD, J.P., Autocorrelation effects in the neutron fission cross section of ^{235}U , Phys. Letters 27B, N° 7, 409 (1968)
- (6) MIGNECO, E., THEOBALD, J., MERLA, M.: A spark chamber fission fragment detector, EUR.4077.e (1968)
- (7) WEIGMANN, H., WINTER, J., Neutron radiative capture in Cu, Zeitschrift f. Physik 213, 411 (1968)
- (8) WINTER, J., Topics in the design of a two parameter system for the measurement of spectra of neutron capture resonances with Ge(Li) detectors, Int. Symposium on Nuclear Electronics, Versailles, Sept. 1968
- (9) WEIGMANN, H.: An interpretation of the structure of subthreshold fission cross section of Pu-240, Zeitschr. f. Physik 214, 7 (1968)

- (10) WEIGMANN, H., Intermediate structure in subthreshold fission cross sections, Gordon Research Conf. on Nucl. Chemistry, N. London, N. Hampshire, USA, June 17-21, 1968
- (11) PAULSEN, A., LISKIEN, H., Determination of 1 MeV neutron fluxes from the $T(p,n)He^3$ reaction by the associated particle method, Nucl. Instr. Meth., in press.
- (12) LISKIEN, H., NASTRI, G., PAULSEN, A., Efficiency calculations for a recoil proton counter with collimator, Nucl. Instr. Meth., 67, 133 (1969)
- (13) KNITTER, H., COPPOLA, M., Fast neutron scattering from 7Li , Sec. Conf. on Neutron Cross Sections and Technology, Washington, 1968
- (14) KNITTER, H., COPPOLA, M., Measurements on Neutron Scattering from 7Li , EUR.3903.e (1968)
- (15) COPPOLA, M., KNITTER, H., A study of levels in the highly excited ^{29}Si nucleus, Z. für Phys. 213, 185-191 (1968)
- (16) HORSTMANN, H., Use of an IBM 1800 System for Acquisition and Analysis of Nuclear Data at an Electron Linear Accelerator, Annual Meeting of the European Region of COMMON, Rotterdam, Sept. 1968
- (17) DE KEYSER, A., DE JONGE, S., VAN DER VEEN, T., TER MEER, P., Analyser Computer Interface, Conf. on Nucl. Electronics, Versailles, 1968
- (18) HORSTMANN, H., SCHMID, H., Modifications of Program MAGGIE (AWRE Aldermaston), report for the ENEA Computer Program Library
- (19) SCHMID, H., CLAESSENS, H., IBM 1800 Utility Programs for Magnetic Tapes and Tele-Processing Input/output, EUR.4263.e (1969)

- (20) SCHMID, H., An IBM 1800 Program Package for On-Line and Off-Line Operation of a Calcomp Digital Incremental Plotter, Annual Meeting of the European Region of COMMON, Rotterdam, Sept. 1968, EUR.4225.e, (1969)
- (21) GUBERNATOR, K., MORET, H., Evaluation of the $^{10}\text{B}(n,\alpha)$ cross section and branching ratio, EUR.3950.e (1968)

F. Radionuclides

F.1. Standardization

F.1.1. International Intercomparison of Threshold Detectors organised by the CBNM

R. Vaninbroukx

The measurements of about 300 detectors from 15 reactors were finished and a first report has been submitted to the Euratom Dosimetry Working Group. A final report, containing calculated fluxes and spectral indices, is in preparation; first standards have been distributed.

F.1.2. Low Energy γ -Standards

W. Bambynek, E. De Roost, H. Hansen, A. Spernol, W. van der Eijk, R. Vaninbroukx

An extended program for the preparation of 0.2-0.5% accurate γ -standards with energies between a few keV and a few hundred keV has been continued.

The necessary accurate redeterminations of decay schemes have been continued and new counting equipment has been constructed. First standards have been prepared of ^{137}Cs , ^{241}Am , ^{181}W , ^{109}Cd , ^{203}Hg and ^{139}Ce , but the obtained accuracy was still worse than 1 to 3%. It will be improved constantly in the future.

F.1.3. International Intercalibrations

E. De Roost, E. Funck*, W. van der Eijk, R. Vaninbroukx, A. Spernol

In order to help to solve the discrepancies found for the mean numbers of neutrons emitted in ^{252}Cf fission, a ^{56}Mn intercalibration was organized by

* Euratom Research fellow

the NPL Teddington. CBNM took part and complete agreement with other laboratories was obtained. Two chapters were written for the BIPM report on the international intercalibration of ^{54}Mn (1).

4.1.4. ANS-Meeting Contributions

A. Spernol

An invited paper on the activities of the radio-nuclides laboratory was contributed to the international American Nuclear Society meeting in Washington (2).

4.2. Assistance to other Laboratories

4.2.1. Monitoring of ^{241}Pu

A. Spernol, R. Vaninbroukx

The investigations on the best measuring methods for the low energy β -emitter ^{241}Pu have been finished. A coincidence counter with a thin plastic detector gave very satisfactory results for all kinds of solid sources and the proposed liquid scintillation method for liquid samples (3).

4.2.2. Measurements and Standards for other Laboratories

About 60 different special activity standards have been supplied to other laboratories in and outside the CBNM. More than 100 measurements with different methods were made for chemistry and sample preparation, especially on Pu, U and Eu samples. Burn-up studies and several special measurements were performed for laboratories outside the CBNM.

4.3. Improvement and Development of Counting Methods

4.3.1. Improvements in $4\pi\beta-\gamma$ Counting

E. De Roost, E. Funck, A. Spernol, W. van der Eijk

In order to be able to use shorter dead and coincidence resolution times in $4\pi\beta-\gamma$ counting and,

thus, stronger sources, afterpulses caused by photons must completely be eliminated. This problem has thoroughly been investigated and it was shown that with cylindrical counters with short anode-cathode distances dead times as short as 1 μ s can be used. All our 4π counters for coincidence work were therefore changed according to the measured optimum conditions.

A second improvement was reached by optimum choice of the cut-off energy in the β -channel. This is possible, because the γ -efficiency of the β -counter depends rather strongly on this cut-off energy. This was not recognized before, but our extended measurements on the γ -efficiency of the β -counters, which still are continued, showed this dependence quite clearly (4).

3.2. New instruments

An anti-Compton counting apparatus is under construction. A central Ge(Li) crystal of about 1 cm^3 volume will be surrounded by two 6" $\varnothing \times 3"$ height NaI crystals. The instrument could also be used as a pair spectrometer.

4. Determination of Nuclear Constants

4.1. Fluorescence Yields

W. Bambynek

The determination of the fluorescence yield of Cu after ^{65}Zn electron capture decay has been finished (5). Excellent agreement was obtained between the two different methods used for the X-ray counting. The result 0.436 ± 0.003 agrees well with other recent measurements. Investigations on ^{85}Sr are in progress and on ^{88}Y in preparation.

4.4.2. Decay of ^{137}Cs

H. Hansen, G. Löwenthal⁺, A. Spernol, W. van der Eijk,
R. Vaninbroukx

The measurements on the beta branching and the conversion coefficient, the two key constants in the ^{137}Cs decay, have been finished (6). The ratio of emitted electrons plus β -rays to emitted γ -rays has been determined to $(1.289 \pm 0.2)\%$. The K-conversion coefficient to 0.0916 ± 0.0004 and the $K/(L + ..)$ conversion ratio to 4.41 ± 0.04 . From these data the intensity of the ground state β -transition can be determined to $(5.4. \pm 0.3)\%$ and the total conversion coefficient to 0.1124 ± 0.0005 .

4.4.3. Decay of ^{58}Co

W. Bambynek, E. De Roost, E. Funck⁺)

Co-58 sources were prepared by evaporation and electro-deposition and measured with many different methods. First results on all branches of the decay were reported to an international conference at Debrecen (7).

4.4.4. Decay of ^7Be

E. De Roost, M. Mutterer⁺, A. Spernol,
W. van der Eijk, R. Vaninbroukx

The preparatory work for the measurement of the branching in the ^7Be decay has been finished.

The equipments for source preparation by fused electrolysis and by evaporation have been installed and first sources were prepared. The theoretical studies of the expected disturbing effects were continued. Measurements on the dependence of the half-life on the chemical state, and on the branching ratio were started.

⁺ EURATOM Research fellow

4.4.5. Conversion Coefficients

H. Hansen, S. Hellström ⁺), G. Maillé ⁺)

Triple coincidence measurements of the conversion coefficient in ^{139}Ce decay are nearly finished.

Measurements on $^{87\text{m}}\text{Sr}$, ^{170}Tm and $^{119\text{m}}\text{Sn}$ are in preparation, as is also an extended investigation by at least 3 different methods on ^{203}Hg . Some theoretical studies on penetration effects in conversion have been performed and will be continued.

4.4.6. Half Lives of the Uranium Isotopes

A. Spernol

About 20 sources were measured in low geometry counters under different conditions (geometry, detectors, cover foils) for the half-life determination of ^{233}U , ^{234}U and ^{235}U . While the first series of a few half-life measurements showed a standard deviation of better than 0.1%, the second series was much worse. A new series of measurements under improved conditions is in progress.

4.4.7. Decay of ^{170}Tm

H. Hansen, S. Hellström

The intensity of the EC-branch in the ^{170}Tm -decay has been determined using our high resolution Si(Li) spectrometer (8).

4.4.8. Microcalorimetry and Half-Life of ^{204}Tl

G. Bortels

The measurements have been finished. A half-life of (3.77 ± 0.02) years (standard error 0.003 y on 61 measurements) was found for the ^{204}Tl metal and a slightly less accurate value within the error limits of the first for a nitrate. These results

⁺) Euratom Research Fellow

agree very well with a similar measurement at Mound Laboratory, but is 1-2% lower than recent results from counting methods (9).

4.4.9. Various Investigations

A β -spectrometer investigation on the number of continuous electrons emitted in the decay of ^{7}Be proved, that it can be neglected for investigations of the γ -efficiency of β -counters, if the β -cut-off-energy is above 100 eV. A short measurement of the number of K-X-rays in the ^{54}Mn decay in dependence of the chemical form of the radioactive source showed that this dependence is very small, if it exists. The measurements have to be repeated under more favorable conditions.

The total number of γ -rays in the ^{56}Mn decay has been determined to $(142 \pm 1)\%$, in disagreement with presently accepted values.

The intensity of a γ -ray in the ^{147}Pm decay, which is presently regarded as a pure β -decay, is under investigation.

Our investigations on the ^{60}Co -decay were recently published (10).

Publications on Radionuclides (Chapter 4)

- (1) WEISS, H.M.: (ed.) Compte rendu de la comparaison internationale d'une solution de ^{54}Mn , BIPM, 30 Oct. 1968.
- (2) SPERNOL, A.: Some Aspects of Radioactivity Standardization at the CBNM of EURATOM, Invited paper to the ANS meeting, Washington 1968, Trans. Am. Nucl. Soc. 11, 465 (1968).
- (3) DENECKE, B., SPERNOL, A., VANINBROUKX, R.: Monitoring of Pu-241, Int. J. appl. Rad. Isotopes 19, 812, 1968
- (4) DE ROOST, E., FUNCK, E., SPERNOL, A.: Improvements in $4\pi\beta-\gamma$ Coincidence Counting, Int. J. appl. Rad. Isotopes, in press
- (5) BAMBYNEK, W., REHER, D.: Precise Determination of the $P_{K^0 K^-}$ -Value and the Fluorescence Yield α_K of Cu after Electron Capture Decay of ^{65}Zn , Z. Physik 214, 374, 1968
- (6) HANSEN, H., LOWENTHAL, G., SPERNOL, A., VAN DER EIJK, W., VANINBROUKX, R.: The Beta Branching Ratio and Conversion Coefficients in the ^{137}Cs Decay, Z. Physik 218, 25, 1969
- (7) BAMBYNEK, W., DE ROOST, E., FUNCK, E.: On the Decay of ^{58}Co , Proceedings of the conference on the electron capture and higher order processes in nuclear decays, Debrecen 1968
- (8) HANSEN, H., HELLSTRÖM, S.: On the EC-Branch in the ^{170}Tm decay, submitted for publication
- (9) BORTELS, G.: Microcalorimetric Determination of the Half-Life of ^{204}Tl , Int.J.appl.Rad.Isotopes, in press
- (10) HANSEN, H., SPERNOL, A.: Some Investigations on the Decay of ^{60}Co , Z. Physik 209, 111, 1968

5. Mass Spectrometry

5.1. Isotopic Analysis of Solids

P.J. De Bièvre, G.H. Debus

5.1.1. Isotope Standards

5.1.1.1. Boron

The absolute determination of the Boron Isotope Standard has been presented at the 16th Annual Conference on Mass Spectrometry and Allied Topics in Pittsburgh (USA) (1) and published (2).

At our request other laboratories determined the absolute isotopic composition against their own synthetic isotope mixtures. The results are:

	10B/11B	atom ratio
CBNM	0.24726	+ 0.00032
KAPL	0.24734	+ 0.00050*
NBS 1st	0.24730	+ 0.00025*
2nd	0.24732	+ 0.00025*
NBL 1st	0.24733	+ 0.00050*
2nd	0.24738	+ 0.00050*

* private communication from Dietz (KAPL), Shields (NBS) and Finley (NBL).

Standard Boron samples have been distributed to several European and U.S. Laboratories.

5.1.1.2. Lithium

P. De Bièvre, J. Pauwels*

A method for the chemical determination of Li, to assay ⁶Li and ⁷Li solutions for the preparation of isotope mixtures, is available.

* Research Fellow, University of Gent.

Four techniques, i.e. titration against benzoic acid, titration against HCl (and Ag), gravimetry of Li_2CO_3 and gravimetry of Li_2SO_4 agree within 0.02% (3). Synthetic isotope mixtures have been prepared at the 2% - 7% - 7.5% - 8% - 20% - 50% - 80% and 92.5% ^{6}Li level.

Mass spectrometric measurements with a 0.2% reproducibility have been performed.

5.1.2. Absolute Isotopic Analyses

5.1.2.1. Pure Boron layers

The isotopic definition of very small amounts of evaporated metallic Boron Samples ($\sim 40 \mu\text{g}$) has been continued successfully. The relative accuracy on the ^{10}B content has been improved from 0.25% to 0.15%, thus reducing considerably the contribution of the isotopic analysis to the uncertainty of the absolute ^{10}B content in evaporated Boron layers.

Three layers have been certified to 0.25%, and 9 layers have been certified to an accuracy of 0.15%.

5.1.2.2. Umpire Qualification Program

The measurements to qualify for isotopic analysis of Uranyl-nitrate and UF_6 (converted to nitrate) have been achieved with reproducibilities of 0.1%.

5.1.2.3. Isotopic Analyses

(Only analyses yielding a certificate are mentioned; standards, calibration and procedure runs are not included).

	Requests			Analyses			Tot.	Requests pending 1968
	Pending 1967	1968	Total	Per- formed	Can- celled	Re- fused		
External	56	159	215	149	2	15	166	49
BCMN	66	93	159	108	-	9	117	42
Total	122	252	374	257*	2	24	383	91

* in 1967 a total of 221 analyses were performed.

5.1.3. Isotopic Dilution

Quantitative determinations by isotope dilution have been performed on Pu : ~ 10 ug/g solutions were defined to \leq 3% accuracy. 1%, 20 ppm and 2 ppm Eu in Al/Eu alloys have been determined to 1.5% accuracy.

5.2. Analysis of gases

T. Babeliowsky, G.H. Debus

5.2.1. Correlation of Density and D₂O Content of Heavy Water

The density of two waters from "Eidgen. Institut für Reaktorforschung "Würenlingen, Switzerland, has been determined. Corrections were applied for the heavy oxygen and the H-content given by this institute. The obtained values for d₂₅²⁵ (D₂O) (1.10776 and 1.10778 g/ml) are to be compared with our previously determined density of 1.10780 g/ml. The literature value is 1.10772 g/ml.

5.2.2. International Heavy Water Program

The results obtained on our reference water in Sweden is 99.877 mole % D₂O. This value is much higher than the results obtained previously in Canada (99.818 mole %) and at the CBNM (99.836 mole %).

The sample will be remeasured and then sent to other laboratories.

5.2.3. Normalization of Oxygen Isotopic Content of D₂O

A glass apparatus to normalize the oxygen isotopic content of 15 ml D₂O samples at 80°C by exchange with a CO₂ stream, was built and tested during 20 runs. The density difference before and after normalization reproduces to within 6×10^{-6} g/ml. The contamination will be determined by D/H mass spectrometric analysis.

5.2.4. Measurement of D₂O Content by Infrared Absorption

Preliminary measurements of the HDO absorption at 3400 cm⁻¹ have been done on a Perkin Elmer grating spectrometer at the University of Leuven. A program (for IBM 1800 and CALCOMP PLOTTER) has been written to compare transmission curves for two different heavy waters with known difference of the HDO concentration. This should lead to the zero concentration transmission curve and to the determination of the absolute HDO concentrations. Contamination effects are still appreciable.

Publication on Mass Spectrometry (Chapter 5)

- (1) DE BIEVRE, P.J., DEBUS, G.H.: 16th Annual Conference on Mass Spectrometry and Allied Topics, ASTM-E14, Pittsburg U.S.A., May 1968
- (2) DE BIEVRE, P.J., DEBUS, G.H.: Absolute Isotope Ratio Determination of a Natural Boron Standard, Intern. J. of Mass Spectrometry and Ion Physics, February 1969
- (3) PAUWELS, J., LAUER, K.F., LE DUIGOU, Y., DE BIEVRE, P., DEBUS, G.H.: Anal. Chim. Acta 43 211 (1968)

6. Sample Preparation and Assaying

6.1. Samples delivered

G.H. Debus, K.F. Lauer, H. Moret, J. Van Audenhove

204 new requests for samples were received in 1968 which is a slight increase compared to 1967 (197 requests).

A total of 1209 samples covering 136 orders were carried out. The statistical information concerning the different applicants and the preparation techniques used is given in Table V. From the 136 orders carried out, 33.8% were covering Euratom needs, 61.1% concerned activities in different European laboratories and 5.1% supported projects outside the Community. Compared to the figures of 1967 (see Progress Report 1967) the following points may be indicated:

1. the number of requests from the different European laboratories increased considerably
2. the total number of orders carried out increased, but the number of samples decreased. This is due to the fact that in the field of alloys, used for detectors, there is a marked tendency to apply for bulk materials (sheets and wires) rather than for the more costly large series of well defined samples
3. the BCMN programs (e.g. measurements of half life time of uranium and plutonium isotopes, different cross sections of ^{10}B , ^{241}Pu and ^{241}Am) take the major capacity of the preparation techniques vacuum evaporation and chemical techniques.

Table V: Samples delivered

6.2. Development

6.2.1. Metallurgy

J. Van Audenhove

6.2.1.1. Spark Emission Machining

Spark erosion conditions, electrode materials and shapes have been determined for the machining of Ge-crystals.

6.2.1.2. Purification and Crystallization of Amorphous

$^{10}_{\text{B}}$ powder

The total amount of impurities (except C and Si) has been reduced from more than 13000 ppm to less than 2700 ppm and a crystalline material is obtained by electron beam melting of pressed and sintered compacts.

The following other methods are under investigation:

- vertical zone-refining by high frequency induction heating of isostatic pressed and sintered rods
- vertical zone refining by electron bombardment of isostatic pressed and sintered rods.

6.2.1.3. Evaporation by Induction Heating

The ultra-high vacuum high frequency levitation facility here developed has been patented in 12 countries. A commercial firm will build this equipment under license for the semi-conductor industry. Results (1) concerning the evaporation of metals and semi-conductors in ultra high vacuum by induction heating has been presented at the "Colloque international sur les applications des sciences et techniques du vide aux revêtements et états de surface" at Dijon (15-19 October).

6.2.1.4. Quantitative Alloying

Quantitative preparation methods for alloys with practically all metals and semi-conductors as base material have been developed. The homogeneity control is under investigation.

It has been proven by isotope dilution and by analytical chemistry that the preparation of Al-20 ppm Eu is possible with a quantitativity, reproducibility and homogeneity of 1.5%.

6.2.2. Chemical Preparation Methods

K.F. Lauer, V. Verdingh

6.2.1.1. ^{242}Am and ^{241}Pu Program

In view of the preparation of series of ^{241}Am and ^{241}Pu samples for σ_{nT} and $\sigma_{n,f}$ measurements at the LINAC, a study of the most suitable method for the preparation, canning and handling of samples of these highly active substances was made.

Settling techniques proved to be the best method for the preparation of oxide samples.

Uranium oxide was used as a dummy. With this compound dummy samples were prepared which meet the requirements set for final samples (X-ray controls were performed).

Packing, sealing and handling of the samples was studied in close collaboration with the workshop.

Different canning methods will be used for the ^{241}Am and ^{241}Pu samples.

The preliminary studies for the preparation of the samples are concluded. Some construction modifications of the canning apparatus are still to be done.

6.2.2.2. Molybdenum Isotopic Samples

Settling and pressing techniques were used for the preparation of molybdenum samples (100 mg/cm^2 - 600 mg/cm^2).

First experiments were made with molybdenumoxide.

A slightly modified technique is used for the preparation of metallic Mo powder samples.

A vacuum canning and sealing device was constructed. Yield and recovery were studied in order to restrict losses to a minimum.

The preparation of isotopic samples will be started.

6.2.3. Evaporation Techniques

H. Moret, H.L. Eschbach, G. Müschenborn

6.2.3.1. Boron Reference Samples

In connection with the high precision requested for the definition of mass of the boron reference layers it proved to be necessary to examine different minor effects which might influence the reliability of the mass determinations. To this end a series of systematic measurements has been started beginning with the weighing under vacuum of a gold coated quartz disk after different thermal treatments. It could be shown that after bakeout with oven and quartz disk at elevated temperatures reproducible mass readings can be made as long as the temperature of the oven is kept constant. In cooling down, however, a significant change corresponding to a decrease in mass of several micrograms was observed regularly. After passing through a minimum mass, readings increase again approaching a constant value after about 26 hours. Although the principle of substitution which is applied in the uhv balance, should exclude errors in mass determination due to slow changes in temperature, there is evidence that the initial decrease in mass readings is caused by the variation of the temperature gradient during the cooling period. These measurements were carried out both before and after deposition of a thin boron layer. In all cases similar curves resulted. An analysis of the results shows that under existing conditions an accuracy on the mass determination of boron layers of better than 2 μg is hardly feasible. Major improvement can be expected by evaporating and weighing under uhv conditions with a thermally shielded balance.

6.2.3.2. Uranium Reference

As a consequence of 12 experiments to evaporate metallic uranium by electron bombardment it was concluded that the deposition of very pure and rather thick uranium layers is extremely time consuming and cumbersome. It was therefore decided to change the existing uhv unit and to incorporate the necessary facilities for levitation evaporation. Most of the required changes have already been carried out and a series of small changes of metallic uranium (between 0.5 and 2 g each) have been prepared and degassed by electron beam melting in ultra-high vacuum. First tests with levitation evaporation can be started as soon as a suitable high frequency feedthrough is available.

6.2.3.3. Other Samples

The different types of miniature evaporation sources developed for use with small amounts of expensive material are being employed frequently. A paper discussing the different constructions and their applications has been accepted for publication (2).

Publications on Sample Preparation and Assaying (Chapter 6)

- (1) VAN AUDENHOVE, J., JOYEUX, J., PARENTH, M.: Evaporation metals and semi-conductors in ultra-high vacuum by induction heating, Supplement to "Le Vide" N° 136 (1968)
- (2) ESCHBACH, H.L., GRILLOT, A.: Construction et caractéristiques de sources miniatures d'évaporation.